UNIVERSITY OF TURIN

DOCTORAL SCHOOL

PHD PROGRAMME IN
AGRICULTURAL, FOREST AND FOOD SCIENCES

CYCLE: XXXVI

MODELLING CLIMATE CHANGE AND LAND USE CHANGE EFFECTS ON THE COMPOSITION AND DISTRIBUTION OF MOUNTAIN FORESTS

Nicolò Anselmetto

Supervisor:
Prof. Matteo Garbarino

Cycle Coordinator:
Prof. Domenico Bosco

YEARS
2021; 2022; 2023

Acknowledgments

I write, erase, rewrite
Erase again, and then
A poppy blooms.
Katsushika Hokusai

Thanks to all those who watched the poppies bloom while I wrote, rewrote, and erased, not just during my PhD period. Thanks to all my friends for their support and help in good times and bad. I am especially grateful to my family and Alessia, all my successes are yours too. Thanks to my colleagues at DISAFA for giving feedback on my research and making office days more fun. Thanks to Matthew Betts and his lab in Corvallis and to all the people I met in Oregon for giving me such good memories of those six months. Thanks to Prof. Aitor Ameztegui, Romain Bertrand, and Raffaella Marzano for their work as evaluators and committee members. Finally, I would like to thank my supervisor, Prof. Matteo Garbarino, for the opportunity to do research. His constant support and passion helped me to carry research in the best way possible.

To all the poppies that will bloom in the future.

Abstract

Environmental changes affect forest landscapes by altering the structure, composition, and distribution of their communities. These ongoing changes, referred to as “global change”, mainly consist of alterations in land use and climate. Post-abandonment natural reforestation is the main land-use change over the last century in the European Alps. Nonetheless, the region is expected to experience a shift toward a climate-change dominated stage. Climate change acts at several levels on the various components of a forest ecosystem by shifting species distribution and phenology and changing forest composition and structure. Indeed, land abandonment and the consequent natural reforestation may provide microrefugia by buffering thermal extremes, which are the main causes of species dieback.

Landscape ecology provides useful tools and perspectives for the analysis of ecological effects of global environmental changes. In particular, the spatial nature of the discipline may provide useful insights into the relationship between spatial and temporal patterns and underlying ecological processes. Ecological models, such as species distribution models and land-use/land-cover change models, are fundamental tools for researchers to transfer knowledge and quantitative assessments of landscape modification to planners and policy makers. Nevertheless, particular attention should be paid to spatial and temporal scales (i.e., extent and resolution) for providing the right level of analysis for different purposes.

This thesis aims at investigating the effects of global change in mountain forest ecosystems through spatial ecological models by focusing on the role of spatial and temporal scales.

We first examined the implications of post-abandonment natural reforestation in the European Alps at different scales through a systematic review and meta-analysis. We assessed the socioecological drivers of natural reforestation patterns

at different scales and discussed planning and management implications. Population density, road density, and the job sectors of workers were the variables most highly correlated with reforestation at the municipality scale. South-facing slopes of dry landscapes within remote municipalities had the greatest reforestation rate. We concluded by advocating for a dynamic harmonised geodatabase to capture the nonlinearity of past dynamics and forecast future trends.

In a second paper, we analyzed past and future landscape patterns of a subalpine watershed of the Alps. Using a high temporal resolution and dividing the landscape into two elevational belts, we tried to disentangle past land-use and climate signals through transition matrices and landscape metrics. By integrating deep learning and Markov chain models, we forecast short-term (2050) and long-term (2100) future Business as Usual scenarios. We observed a dominant gap-filling through secondary successions in the lower part of the landscape, and an increasing rate through time of primary successions on unvegetated soil in the upper part. Future predictions suggested a saturation of open areas in the lower part of the watershed and stronger forest gain at upper elevations. Through a good spatial and temporal resolution, we highlighted the increasing role of climate change over the last years and on future forest dynamics.

In the third and fourth paper, we dealt with species distribution models with the lens of spatial and temporal scales. In particular, in the third research paper we compared accuracy and reliability of current and future scenarios of climate change for tree species in the North-western Italy according to different species data (i.e., forest inventory) and climate predictors. We showed that fine models, built on local data species and predictors (i.e., regional climate models) may result in higher accuracy for current predictions. However, careful attention should be paid for future assessments because fine models may suffer from niche truncation, excluding possible suitable areas for a species.

Lastly, in the fourth chapter, we trained landscape-scale species distribution models for several bird species along a gradient of temporal resolution. We

observed the greatest accuracy from dynamic models trained with a finer temporal resolution accounting for interannual variations and dynamism in species responses. In particular, migratory species showed higher model performance and similarity between spatial predictions than sedentary and partially migratory species. Still, long-living species with bigger body size showed no- to little- improvements in using dynamic approaches rather than static ones.

In the conclusion section, the relevance of this multiscale approach for landscape and quantitative ecology and applications in forest landscape planning and restoration and in biodiversity conservation and monitoring were discussed, and limitations and future directions were highlighted.

Table of Contents

Chapter 1

Introduction

1.1 Land-use change

Forests cover 4.06 billion ha, corresponding to 31% of the global land area. They provide countless ecosystem services to humanity and host more than 80% of terrestrial plants and animals, acting as sanctums of biodiversity (FAO & UNEP, 2020; FAO, 2022). Forests cover more than 40% of global mountain areas and are characterized by strong environmental gradients. Their conservation is a priority for both researchers and managers. Mountain ecosystems around the world are particularly sensitive to global environmental changes, specifically to climate and land-use changes (Rodman et al., 2019; Smith et al., 2022). Nevertheless, disentangling the role of climate and land use changes – the two main components of these changes – is challenging, especially in areas where a centennial or millennial exploitation was followed by a long period of land abandonment (Gehrig-Fasel et al., 2007; Martin et al., 2013; Malfasi & Cannone, 2020).

There are many examples of processes that are controlled by both land-use and climate changes. For instance, wildfires are key factors in shaping landscape structure and driving species distribution, and their regime has been altered worldwide in the last decades (Pausas & Fernández-Muñoz, 2012; Heidari et al., 2021; Buma et al., 2022). The characteristics of wildfire regimes (e.g., severity, occurrence, frequency, intensity) are driven by both climatic factors and landscape structure (Pausas & Fernández-Muñoz, 2012; Seidl et al., 2017; Mantero et al., 2020). While climate change extends the duration of the fire season and increases the frequency of dry years, it cannot explain the whole complexity of global fire-regime changes (Rodman et al., 2019; Pausas & Keeley, 2021). For examples, land abandonment leads to fuel build-up and homogenization of forest landscape structure (Mantero et al., 2020; Stritih et al.,

2021). Species distribution is another example of synergistic interplay between climate and land-use changes. Even if a conspicuous body of literature focuses on the species response to climate change (e.g., Newbold et al., 2020; Smith et al., 2022), land-use changes such as forest fragmentation or degradation have a major impact on the distribution of many different taxa (Krauss et al., 2010; Marjakangas et al., 2020; Betts et al., 2022).

Land-use change is defined as the process by which humans alter the natural landscape structure with respect to how a land is used. Changes in land use affect land-surface properties and the provision of ecosystem services. They alter Earth's biogeochemical cycles contributing to climate change as a feedback mechanism (Foley, 2005; Song et al., 2018). Social and cultural transformations are the leading causes of land-use change globally (Crawford et al., 2022). Two main divergent but correlated trends emerge when considering major global patterns. Usually, land-use changes emphasize the functional and economic role of land for human activities through agricultural expansion, but land abandonment is another major process that reduces the economic value of the land. Generally speaking, while tropical mountains are facing deforestation and agricultural expansion (Peters et al., 2019), post-abandonment natural reforestation is the main land-use change in high-income countries of the Northern Hemisphere (MacDonald et al., 2000; Martinuzzi et al., 2015; Plieninger et al., 2016). Indeed, major changes in the job sectors of workers and improvement of socio-economic conditions in high-income countries led to rural-urban migration and abandonment of marginal areas, triggering compensating changes in trade flows and indirectly affecting land use in other countries (Lambin & Meyfroidt, 2011). At the landscape scale, topography, microclimate, road availability, and population become fundamental drivers of reforestation (Garbarino et al., 2020; Gelabert et al., 2022). Therefore, land abandonment can happen also in areas of the world where agricultural expansion is the main driver (e.g., Latin America, Africa, and tropical Asia; Crawford et al., 2022).

The complexity of post-abandonment natural reforestation processes affects both the temporal and spatial scale of analysis. Land abandonment in marginal agricultural landscapes of European mountains is a long-term dynamic, since remote areas with steep slopes and harsh edaphic conditions have been abandoned since the 19th century (MacDonald et al., 2000; Mietkiewicz et al., 2017; Gelabert et al., 2022). Therefore, its analysis requires a proper temporal extent (> 50/100 years). Moreover, given the strong influence of land-use legacies and the fine-scale patchiness of secondary successions, a fine spatial resolution is needed to capture the heterogeneity of the new post-modern landscapes (Antrop, 2005). Aerial photographs are historical data sources that meet these requirements and, if complemented with historical maps such as the Habsburg cadastral land register and the Napoleonic cadastre, can depict the spatial structure of the landscapes back to the 1800s (Garbarino et al., 2020; Hohensinner et al., 2021).

1.2 Climate, microclimate, and forests

Human activity has altered the global climate circulation system through greenhouse gas emissions and changes in land use and land cover (Calvin et al., 2023). The effects of climate change on forest ecosystems are manifold. The main consequence of climate change is global warming, with a mean increase in global temperature in the 2011-2020 decade of +1.1° C above the reference 1850-1900 period (Calvin et al., 2023). However, global warming is not a homogeneous process across biomes, and land surface showed a higher increase in temperature (mean = +1.59° C) than the oceans (+0.88° C) (Calvin et al., 2023). For instance, mountain forest ecosystems in the Alps are considered hotspots of change and are expected to experience accelerated warming, increase in thermal and precipitation extremes, and reduction of snow precipitation below 2000 m (Gobiet et al., 2014; Gobiet & Kotlarski, 2020). Thermal exposure is one of the main ecological consequences of climate change (Hartmann et al., 2022; Pigot et al., 2023). It is expected that the area of each species' geographical range at risk of thermal exposure will expand abruptly, even in a single decade for most of the

species (Pigot et al., 2023). Resilience mechanisms to overcome these risks comprise species movement and evolutionary adaptation. Indeed, the timing and rapidity of these abrupt changes may overwhelm the ecological and evolutionary processes that generally provide resilience to species and ecosystems under more gradual environmental changes (Chen et al., 2011; Vitasse et al., 2021; Smith et al., 2022). Even if shifts in elevation (Lenoir et al., 2008; Vitasse et al., 2021; Noce et al., 2023) and phenology (Richardson et al., 2013; Vitasse et al., 2021, 2022) have been observed in response to climate change, species struggle to cope with the warming pace (Bertrand et al., 2011; Alexander et al., 2018; Pörtner et al., 2022).

Most of the changes in climate are measured in terms of macroclimate, defined as climate conditions interpolated in space and time from weather stations at ~2.0 m above ground, in free-air conditions (Lembrechts, Lenoir, et al., 2019; De Frenne et al., 2021; Haesen et al., 2021). The derived macroclimate data used in ecological assessment usually have a coarse grid resolutions of 1 km or more, like WorldClim (Fick & Hijmans, 2017) or CHELSA (Karger et al., 2017). Nonetheless, species experience climatic conditions at a finer scale, that can be defined as microclimate. Microclimate conditions can differ substantially from those depicted by macroclimate interpolations in the aforementioned datasets, and clear climatic gradients observed at coarse spatial resolution result in microclimate heterogeneity because of topography, soil, and vegetation influence (Dobrowski, 2011; De Frenne et al., 2021; Haesen et al., 2021). Forests act as a thermal buffer system, with higher minimum and lower maximum temperatures, since shading, transpiration, and mechanical constraints moderates extreme temperatures (Frey et al., 2016; Wolf et al., 2021; Gril et al., 2023). It has been proven that considering macroclimate within ecological modeling and climate change assessment leads to an overestimation of range shifts in response to climate change (Scheffers et al., 2014; Haesen et al., 2023; Maclean & Early, 2023). Indeed, microclimate, far from being a brand new topic in ecology, is currently experiencing a renewed interest in forest landscape ecology nowadays

(Lenoir et al., 2017; Lembrechts, Nijs, et al., 2019; De Frenne et al., 2021; Haesen et al., 2021, 2023).

As previously highlighted, abandoned rural landscapes in high-income areas of the world are currently dominated by land-use change and its legacies (Gehrig-Fasel et al., 2007; Ameztegui et al., 2016). Nevertheless, they are expected to shift soon to a stage where climate change will be the most important factor (Martin et al., 2013). To clearly assess the interplay between these two main drivers and reconstruct land-use legacies and climate change consequences is fundamental in mountain forests. Since forests help to slow the rate of climate change by removing carbon dioxide from the atmosphere, post-abandonment natural reforestation offers an opportunity for climate change mitigation (Navarro & Pereira, 2012; Massenberg et al., 2023).

1.3 Beyond trees: forests as ecosystems and communities

In addressing the various treats and challenges of global environmental change on forests, it is important to remember that forests are not just a mere collection of trees and plants, but a network of different populations that together form a biological community. Therefore, when addressing the impacts of global change on mountain forests, the effects of these changes on different taxa should be considered if the goal is to conserve or restore biodiversity (Barbet-Masin & Jetz, 2015; Visconti et al., 2015). It is well known that biodiversity is a main component of ecological resilience (Arnoldi et al., 2018), defined as the ability of a system to maintain its functions, structures and feedbacks in the face of disturbances (Albrich et al., 2020). As resilient forest ecosystems are key to management and restoration practices, it is crucial to study the effects of climate and land use changes (e.g. land abandonment) on communities (Komatsu et al., 2019; Albrich et al., 2020).

Birds are among the most studied taxa in ecology and ecological modeling (Bonnet et al., 2002; Ducatez & Lefebvre, 2014; Zurell et al., 2022). Research on birds spans decades and even centuries, and new technologies such as

bioacoustics and computer vision are advancing bird ecology in recent years (e.g., Wang et al., 2023; Michielsen et al., 2024). The amount of comprehensive data on this taxon allows for large meta-taxonomic analyses to tackle important questions in ecology and conservation with high statistical power (Ducatez & Lefebvrem 2014). There are two reasons why comprehensive ecological research on birds is useful for global change studies. Because of their fundamental role in these ecosystems, the conservation and restoration of birds is key to increasing the resilience of forests. Therefore, monitoring the effects of global change on this taxon can help to mitigate such changes (Conroy et al., 2011). Second, due to their highly mobility, birds are usually able to respond to climate change, and the lag in species' response to change in climate (i.e., climatic debt *sensu* Devictor et al., 2012) is a valuable indicator of forest ecosystem health; therefore, birds act as bioindicators (Samraoui et al., 2011; Lopez et al., 2023; Anderle et al., 2024).

The distribution of birds – like that of all species – is mainly determined by environmental factors (also called environmental envelopes or environmental filters), species interactions, dispersal ability, and disturbance (Cunningham & Johnson, 2006; Sales et al., 2021; Bhagwat et al., 2024). The interaction between these components defines the ecological niche of a species (Sales et al., 2021). Environmental abiotic factors act at different scales to determine the occurrence and abundance of a species in a given location (Pearce-Higgins et al., 2015; Trautmann, 2018). Climatic patterns are important both at a continental or regional scales, by defining biomes and elevation belts, and at the landscape or local scales through meso- and microclimates (Betts et al., 2022). Climate change has been affecting several bird species by altering their range (Viterbi et al., 2020; Vitasse et al., 2021; Antão et al., 2022), phenology (Møller et al., 2008; Vitasse et al., 2021; Bates et al., 2023), and survival (Trautmann, 2018; Cannone et al., 2023), thus significantly altering the inter- and intraspecific relationships of a species (Ahola et al., 2007; Pearce-Higgins et al., 2015). In the temperate mountains of the northern hemisphere, land abandonment and climate change are shifting forests upwards (Ameztegui et al., 2016; Malfasi & Cannone, 2020;

Vitasse et al., 2021). This process creates novel forests, usually at early successional stages, where birds can find new favorable habitats. Indeed, although general patterns of bird distribution are strongly influenced by the interaction between climate and land-use changes, forest, and landscape characteristics mediate local responses to environmental change (Northrup et al., 2019; Rigo et al., 2024). Forest structure defines the spatial and physical template in which individuals and populations live (Bouvet et al., 2016; Rigo et al., 2024). Bird communities are closely linked to the characteristics of the forest environment. For instance, the presence of trees suitable for cavity production is a fundamental requirement for primary nesters such as woodpeckers (Pakkala et al., 2024; Rigo et al., 2024). Consequently, tree cavities are an essential requirement for the reproduction and survival of secondary cavity nesters (Baroni et al., 2020, 2021). Microclimate integration has been shown to be fundamental for investigating population and individuals distribution patterns at the landscape scale (Kim et al., 2022). Therefore, the ability to provide reliable and robust model predictions of bird distributions can aid global change ecology research by improving their conservation.

1.4 A landscape ecology's perspective

1.4.1 Scales in ecology

Given the strong spatial and temporal nature of environmental global changes, landscape-scale approaches are usually well suited for their analysis (Verburg et al., 2013). One of the main aim of landscape ecology is to infer and generalize processes while looking at spatial and temporal patterns (Naveh & Lieberman, 2013). Nonetheless, exceptions, context dependencies, methodological issues, and limitations make this inference hard to make (Turner et al., 2001; Verburg et al., 2013). In this sense, the concept of "scale" (i.e., the spatial or temporal dimensions of an object or process) is a cornerstone in landscape ecology (Turner et al., 2001). Starting from the 1980s, ecologists realized that a single scale could not be universally defined to solve all ecological problems. Therefore, comparing

(i.e., multi-scale approach) or integrating (i.e., cross-scale approach) different spatial and temporal scales is a common approach in landscape ecology (Betts et al., 2006; Behrens et al., 2019). It has been said that "scale is the lens that focuses ecological relationships" (McGarigal et al., 2016), and organisms act at multiple scales when selecting habitats and developing responses to environmental changes. Ecologists need to transfer quantitative measurements and predictions at both broad (e.g., regional, continental) and fine (e.g., landscape) scales to inform practitioners on spatial reserve prioritization and ecological restoration (Guisan et al., 2013; Wan et al., 2017).

1.4.2 Ecological models

Rapid environmental changes and their ecological consequences call for an adequate understanding of past, current, and future dynamics of forest ecosystems and landscapes (Guisan et al., 2013; Albrich et al., 2020; McDowell et al., 2020). For this purpose, several spatial ecological models have been developed to quantify and infer different ecological processes. These models allow to generate and test hypotheses about the interaction of spatial (and temporal) patterns and ecological processes (Turner et al., 2001; Zurell et al., 2022). Models are usually classified into process-based and correlative approaches. Another important distinction can be made between static approaches, depicting equilibrium states and predicting stationarity, and dynamic approaches that simulate time-dependent changes in the state of a system (Lantman et al., 2011; Dormann et al., 2012; Zurell et al., 2022). For instance, many process-based landscape models have been developed to predict past and future changes from a mechanistic perspective (e.g., Mladenoff, 2004; Scheller et al., 2007; Seidl et al., 2012).

Land-use and land-cover models are spatial models that play a pivotal role in exploring future trajectories of land change, stress past dynamics, and plan sustainable land restoration strategies (Wolff et al., 2018; Verburg et al., 2019). Many algorithms and approaches can be adopted in land-use change modeling. Amidst the variety of developed models, statistical models (e.g., FRAGSTATS, McGarigal & Marks, 1995; CLUE, Veldkamp & Fresco, 1996), agent-based

models (e.g., Parker et al., 2001), cellular automata models (e.g., Environment Explorer, de Nijs et al., 2004), and Markov chain models (e.g., Tattoni et al., 2011; Al-Shaar et al., 2021) are the most common. Many applications integrate a land-use change quantification through simple and flexible Markov chains and a spatial allocation based on cellular automata, deep learning, or machine learning (Noszczyk, 2019). The scenarios resulting from this approach are usually called "Business as Usual", since they are based on the continuation of current land-use practices and policies. Nonetheless, researchers and policy makers are also interested in alternative scenarios of land use based on political and social scenarios (i.e., socio-economic models). The main limitations of these models are the scarce validation of their prediction uncertainty and the limited representation of underlying social processes (Verburg et al., 2019).

Species distribution models (SDMs) are correlative models that establish a relationship between the presence or abundance of a species to a suite of several socio-ecological covariates such as climate, soil, topography (Franklin, 1995; Guisan & Zimmermann, 2000; Zurell et al., 2022). Nowadays, SDMs are the most common predictive tools for assessing potential range shifts of tree species under different environmental change scenarios (Guisan et al., 2013; Zurell et al., 2020, 2022). SDMs have been extensively used at several spatial and temporal scales on many plant and animal species worldwide (Newbold, 2018; Newbold et al., 2020; Maréchaux et al., 2021). Broad-extent and coarse-resolution models, primarily associated with climatic predictors, are more prevalent than local-extent and fine-resolution models, both in terms of spatial and temporal characteristics (Araújo et al., 2019).

Since no right models for all ecological purposes exist, many tools can be integrated within a common framework to emphasize their strengths and limit their weaknesses (Mas et al., 2014; Mateo et al., 2019). Moreover, testing and comparing different spatial and temporal scales of models and their input variables may lead to a better representation of real patterns and to better

understanding underlying ecological processes (Behrens et al., 2019; Zurell et al., 2022; Moudrý et al., 2023).

1.5 Thesis objectives and outline

The objective of this PhD thesis is to comprehensively analyze the impacts of global environmental changes, specifically land-use change and climate change, on mountain forest ecosystems. The analytical approaches stress the role of spatial ecological models across different spatial and temporal resolution and extent. The thesis is framed around four main objectives, corresponding to four different research chapters, as illustrated in Figure 1.1:

(i) **Investigating post-abandonment natural reforestation in the European Alps (Chapter 2)**: this chapter aims to explore the spatial and temporal scales of post-abandonment natural reforestation in the European Alps, examining its primary drivers and patterns.

(ii) **Analyzing past land-use changes and predicting future scenarios in a subalpine watershed of the Alps (Chapter 3)**: this chapter aims to assess past land-use changes and to predict future scenarios under a Business-as-Usual framework, emphasizing the role of temporal resolution of remote sensing-derived cover maps.

(iii) **Assessing spatial scale in correlative species distribution models in the Western Alps (Chapter 4)**: this chapter aims to evaluate the impact of spatial scale on the accuracy and reliability of correlative species distribution models for tree species within an administrative region of the Western Alps.

(iv) **Assessing temporal resolution in landscape-scale species distribution models in the North-western US (Chapter 5)**: this chapters aims to compare the accuracy and reliability of landscape-scale correlative SDMs across a gradient of temporal resolution in a mountain watershed in North-western US.

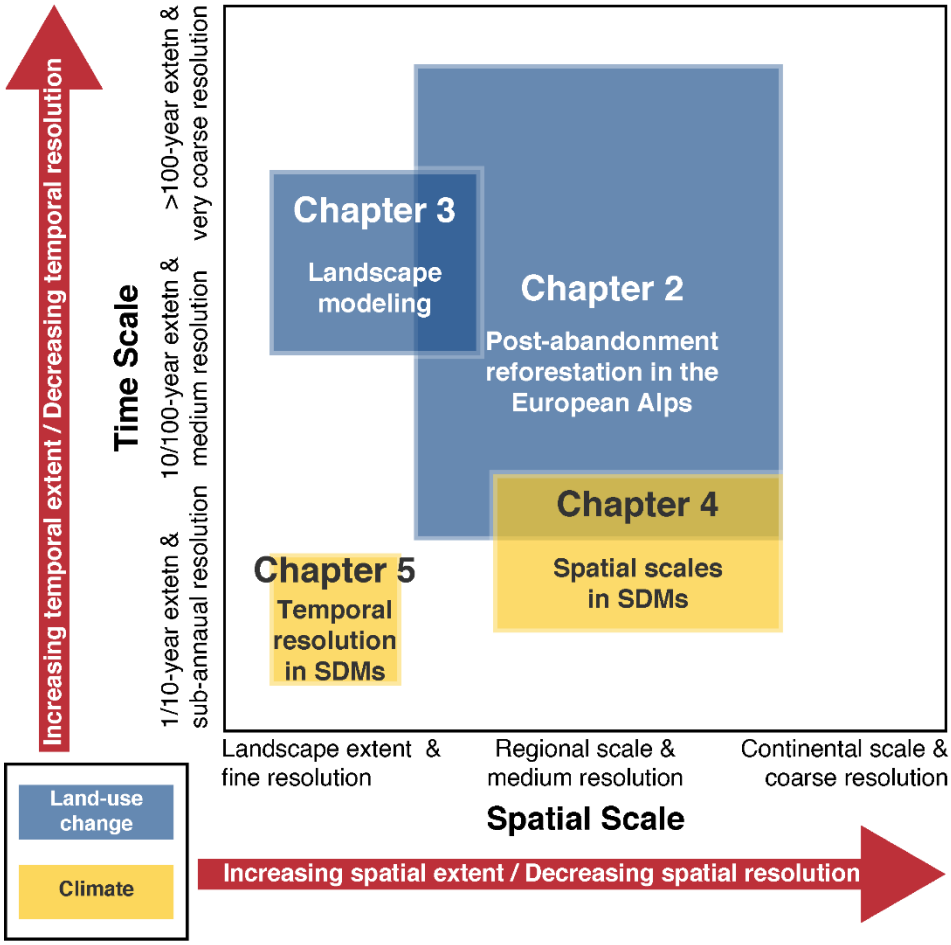

FIGURE 1.1. Conceptual framework of the four research papers in this thesis along a gradient of spatial (x axis) and temporal (y axis) scale. Examples of reference extent and resolution along the gradients are indicated in the axes. Rectangular shapes indicate the different research chapters, and the main analysis/objective is reported within the rectangles.

The thesis consists of seven chapters: introduction (Chapter 1), research chapters (Chapters 2 to 5), a general discussion (Chapter 6), and conclusions (Chapter 7). Research chapters are organized as standalone research papers. Chapter 2 has been accepted for publication, Chapter 3 has been published, and Chapters 4 and 5 have been submitted for publication. Chapter 2 "*Global change in the European Alps: a century of post-abandonment natural reforestation at the landscape scale*" aims at investigating the spatial and temporal scales of analysis of post-abandonment natural reforestation and its main driver in the European Alps.

Chapter 3 "*Land use modeling predicts divergent patterns of change between upper and lower elevations in a subalpine watershed of the Alps*" analyzes the interplay of past and future land-use and climate changes in a subalpine watershed of the European Alps through aerial images and land cover classification. Chapter 4 "*Local forest inventory data improve species distribution model predictions*" deals with the spatial scales of species data (i.e., forest inventories) and predictors (i.e., climate data) in regional-scale species distribution models by comparing fine- vs. coarse-scale models. Chapter 5 "*Long-term data and temporal dynamic frameworks can improve landscape-scale species distribution models*" focuses on the role of temporal resolution of species data (i.e., bird count) and predictors (i.e., microclimate) on the accuracy and prediction of landscape-scale species distribution models. Chapter 6 "General discussion" provides a section for linking research works and discuss the contribution of this thesis to global change literature, particularly the landscape ecology discipline.

References

Ahola, M. P., Laaksonen, T., Eeva, T., & Lehikoinen, E. (2007). Climate change can alter competitive relationships between resident and migratory birds. *Journal of Animal Ecology*, 1045-1052.

Albrich, K., Rammer, W., Turner, M. G., Ratajczak, Z., Braziunas, K. H., Hansen, W. D., & Seidl, R. (2020). Simulating forest resilience: A review. *Global Ecology and Biogeography*, *29*(12), 2082–2096.

Alexander, J. M., Chalmandrier, L., Lenoir, J., Burgess, T. I., Essl, F., Haider, S., Kueffer, C., McDougall, K., Milbau, A., Nuñez, M. A., Pauchard, A., Rabitsch, W., Rew, L. J., Sanders, N. J., & Pellissier, L. (2018). Lags in the response of mountain plant communities to climate change. *Global Change Biology*, *24*(2), 563–579.

Al-Shaar, W., Nehme, N., & Adjizian Gérard, J. (2021). The Applicability of the Extended Markov Chain Model to the Land Use Dynamics in Lebanon. *Arabian Journal for Science and Engineering*, *46*(1), 495–508. Scopus.

Ameztegui, A., Coll, L., Brotons, L., & Ninot, J. M. (2016). Land-use legacies rather than climate change are driving the recent upward shift of the mountain tree line in the Pyrenees. *Global Ecology and Biogeography*, *25*(3), 263–273.

Anderle, M., Brambilla, M., Angelini, L., Guariento, E., Paniccia, C., Plunger, J., ... & Hilpold, A. (2024). Efficiency of birds as bioindicators for other taxa in mountain farmlands. *Ecological Indicators*, 158, 111569.

Antão, L. H., Weigel, B., Strona, G., Hällfors, M., Kaarlejärvi, E., Dallas, T., ... & Laine, A. L. (2022). Climate change reshuffles northern species within their niches. *Nature Climate Change*, 12(6), 587-592.

Antrop, M. (2005). Why landscapes of the past are important for the future. *Landscape and Urban Planning*, *70*(1–2), 21–34.

Araújo, M. B., Anderson, R. P., Barbosa, A. M., Beale, C. M., Dormann, C. F., Early, R., Garcia, R. A., Guisan, A., Maiorano, L., Naimi, B., O'Hara, R. B., Zimmermann, N. E., & Rahbek, C. (2019). Standards for distribution models in biodiversity assessments. *Science Advances*, *5*(1), eaat4858.

Arnoldi, J. F., Bideault, A., Loreau, M., & Haegeman, B. (2018). How ecosystems recover from pulse perturbations: A theory of short-to long-term responses. *Journal of theoretical biology*, 436, 79-92.

Baroni, D., Korpimäki, E., Selonen, V., & Laaksonen, T. (2020). Tree cavity abundance and beyond: nesting and food storing sites of the pygmy owl in managed boreal forests. *Forest Ecology and Management*, 460, 117818.

Baroni, D., Masoero, G., Korpimäki, E., Morosinotto, C., & Laaksonen, T. (2021). Habitat choice of a secondary cavity user indicates higher avoidance of disturbed habitat during breeding than during food-hoarding. *Forest Ecology and Management*, 483, 118925.

Bates, J. M., Fidino, M., Nowak-Boyd, L., Strausberger, B. M., Schmidt, K. A., & Whelan, C. J. (2023). Climate change affects bird nesting phenology: Comparing contemporary field and historical museum nesting records. *Journal of Animal Ecology*, 92(2), 263-272.

Behrens, T., Viscarra Rossel, R. A., Kerry, R., MacMillan, R., Schmidt, K., Lee, J., Scholten, T., & Zhu, A.-X. (2019). The relevant range of scales for multi-scale contextual spatial modelling. *Scientific Reports*, *9*(1).

Bertrand, R., Lenoir, J., Piedallu, C., Riofrío-Dillon, G., de Ruffray, P., Vidal, C., Pierrat, J.-C., & Gégout, J.-C. (2011). Changes in plant community composition lag behind climate warming in lowland forests. *Nature*, *479*(7374).

Betts, M. G., Diamond, A. W., Forbes, G. J., Villard, M.-A., & Gunn, J. S. (2006). The importance of spatial autocorrelation, extent and resolution in predicting forest bird occurrence. *Ecological Modelling*, *191*(2), 197–224.

Betts, M. G., Yang, Z., Hadley, A. S., Smith, A. C., Rousseau, J. S., Northrup, J. M., Nocera, J. J., Gorelick, N., & Gerber, B. D. (2022). Forest degradation drives widespread avian habitat and population declines. *Nature Ecology & Evolution*, *6*(6).

Bhagwat, T., Kuemmerle, T., Soofi, M., Donald, P. F., Hölzel, N., Salemgareev, A., ... & Kamp, J. (2024). A novel, post-Soviet fire disturbance regime drives bird diversity and abundance on the Eurasian steppe. *Global Change Biology*, 30(1), e17026.

Bonnet, X., Shine, R., & Lourdais, O. (2002). Taxonomic chauvinism. *Trends in Ecology & Evolution*, 17(1), 1-3.

Bouvet, A., Paillet, Y., Archaux, F., Tillon, L., Denis, P., Gilg, O., & Gosselin, F. (2016). Effects of forest structure, management and landscape on bird and bat communities. *Environmental conservation*, 43(2), 148-160.

Buma, B., Hayes, K., Weiss, S., & Lucash, M. (2022). Short-interval fires increasing in the Alaskan boreal forest as fire self-regulation decays across forest types. *Scientific Reports*, *12*(1), 4901.

Calvin, K., Dasgupta, D., Krinner, G., Mukherji, A., Thorne, P. W., Trisos, C., Romero, J., Aldunce, P., Barrett, K., Blanco, G., Cheung, W. W. L., Connors, S., Denton, F., Diongue-Niang, A., Dodman, D., Garschagen, M., Geden, O., Hayward, B., Jones, C., … Péan, C. (2023). *IPCC, 2023: Climate Change 2023: Synthesis Report. Contribution of Working Groups I, II and III to the Sixth Assessment Report of the Intergovernmental Panel on Climate Change [Core Writing Team, H. Lee and J. Romero (eds.)]. IPCC, Geneva, Switzerland.* (First). Intergovernmental Panel on Climate Change (IPCC).

Canonne, C., Bernard-Laurent, A., Souchay, G., Perrot, C., & Besnard, A. (2023). Contrasted impacts of weather conditions in species sensitive to both survival and fecundity: A montane bird case study. *Ecology*, 104(2), e3932.

Chen, I.-C., Hill, J. K., Ohlemüller, R., Roy, D. B., & Thomas, C. D. (2011). Rapid Range Shifts of Species Associated with High Levels of Climate Warming. *Science*, *333*(6045), 1024–1026.

Conroy, M. J., Runge, M. C., Nichols, J. D., Stodola, K. W., & Cooper, R. J. (2011). Conservation in the face of climate change: the roles of alternative models, monitoring, and adaptation in confronting and reducing uncertainty. *Biological Conservation*, 144(4), 1204-1213.

Crawford, C. L., Yin, H., Radeloff, V. C., & Wilcove, D. S. (2022). Rural land abandonment is too ephemeral to provide major benefits for biodiversity and climate. *Science Advances*, *8*(21), eabm8999.

Cunningham, M. A., & Johnson, D. H. (2006). Proximate and landscape factors influence grassland bird distributions. *Ecological Applications*, 16(3), 1062-1075.

De Frenne, P., Lenoir, J., Luoto, M., Scheffers, B. R., Zellweger, F., Aalto, J., Ashcroft, M. B., Christiansen, D. M., Decocq, G., De Pauw, K., Govaert, S., Greiser, C., Gril, E., Hampe, A., Jucker, T., Klinges, D. H., Koelemeijer, I. A., Lembrechts, J. J., Marrec, R., … Hylander, K. (2021). Forest microclimates and climate change: Importance, drivers and future research agenda. *Global Change Biology*, *27*(11), 2279–2297.

de Nijs, T. C. M., de Niet, R., & Crommentuijn, L. (2004). Constructing land-use maps of the Netherlands in 2030. *Journal of Environmental Management*, 72(1–2), 35–42.

Devictor, V., Van Swaay, C., Brereton, T., Brotons, L., Chamberlain, D., Heliölä, J., ... & Jiguet, F. (2012). Differences in the climatic debts of birds and butterflies at a continental scale. *Nature climate change*, 2(2), 121-124.

Dobrowski, S. Z. (2011). A climatic basis for microrefugia: The influence of terrain on climate: A CLIMATIC BASIS FOR MICROREFUGIA. *Global Change Biology*, *17*(2), 1022–1035.

Dormann, C. F., Schymanski, S. J., Cabral, J., Chuine, I., Graham, C., Hartig, F., Kearney, M., Morin, X., Römermann, C., Schröder, B., & Singer, A. (2012). Correlation and process in species distribution models: Bridging a dichotomy. *Journal of Biogeography*, *39*(12), 2119–2131.

Ducatez, S., & Lefebvre, L. (2014). Patterns of research effort in birds. *PLoS One*, 9(2), e89955.

FAO. (2022). *The State of the World's Forests 2022. Forest pathways for green recovery and building inclusive, resilient and sustainable economies*. Rome, FAO.

FAO, & UNEP. (2020). *The State of the World's Forests 2020. Forests, biodiversity and people*. Rome.

Fick, S. E., & Hijmans, R. J. (2017). WorldClim 2: New 1-km spatial resolution climate surfaces for global land areas. *International Journal of Climatology*, *37*(12), 4302–4315.

Foley, J. A. (2005). Global Consequences of Land Use. *Science*, *309*(5734), 570–574.

Franklin, J. (1995). Predictive vegetation mapping: Geographic modelling of biospatial patterns in relation to environmental gradients. *Progress in Physical Geography: Earth and Environment*, *19*(4), 474–499.

Frey, S. J. K., Hadley, A. S., Johnson, S. L., Schulze, M., Jones, J. A., & Betts, M. G. (2016). Spatial models reveal the microclimatic buffering capacity of old-growth forests. *Science Advances*, *2*(4), e1501392.

Garbarino, M., Morresi, D., Urbinati, C., Malandra, F., Motta, R., Sibona, E. M., Vitali, A., & Weisberg, P. J. (2020). Contrasting land use legacy effects on forest landscape dynamics in the Italian Alps and the Apennines. *Landscape Ecology*.

Gehrig-Fasel, J., Guisan, A., & Zimmermann, N. E. (2007). Tree line shifts in the Swiss Alps: Climate change or land abandonment? *Journal of Vegetation Science*, *18*(4), 571–582.

Gelabert, P. J., Rodrigues, M., Vidal-Macua, J. J., Ameztegui, A., & Vega-Garcia, C. (2022). Spatially explicit modeling of the probability of land abandonment in the Spanish Pyrenees. *Landscape and Urban Planning*, *226*, 104487.

Gobiet, A., & Kotlarski, S. (2020). Future Climate Change in the European Alps. In *Oxford Research Encyclopedia of Climate Science*.

Gobiet, A., Kotlarski, S., Beniston, M., Heinrich, G., Rajczak, J., & Stoffel, M. (2014). 21st century climate change in the European Alps—A review. *Science of The Total Environment*, *493*, 1138–1151.

Gril, E., Laslier, M., Gallet-Moron, E., Durrieu, S., Spicher, F., Le Roux, V., Brasseur, B., Haesen, S., Van Meerbeek, K., Decocq, G., Marrec, R., & Lenoir, J. (2023). Using airborne LiDAR to map forest microclimate temperature buffering or amplification. *Remote Sensing of Environment*, *298*, 113820.

Guisan, A., Tingley, R., Baumgartner, J. B., Naujokaitis-Lewis, I., Sutcliffe, P. R., Tulloch, A. I. T., Regan, T. J., Brotons, L., McDonald-Madden, E., Mantyka-Pringle, C., Martin, T. G., Rhodes, J. R., Maggini, R., Setterfield, S. A., Elith, J., Schwartz, M. W., Wintle, B. A., Broennimann, O., Austin, M., … Buckley, Y. M. (2013). Predicting species distributions for conservation decisions. *Ecology Letters*, *16*(12), 1424–1435.

Guisan, A., & Zimmermann, N. E. (2000). Predictive habitat distribution models in ecology. *Ecological Modelling*, *135*(2), 147–186.

Haesen, S., Lembrechts, J. J., De Frenne, P., Lenoir, J., Aalto, J., Ashcroft, M. B., Kopecký, M., Luoto, M., Maclean, I., Nijs, I., Niittynen, P., Van Den Hoogen, J., Arriga, N., Brůna, J., Buchmann, N., Čiliak, M., Collalti, A., De Lombaerde, E., Descombes, P., … Van Meerbeek, K. (2021). ForestTemp – Sub-canopy microclimate temperatures of European forests. *Global Change Biology*, *27*(23), 6307–6319.

Haesen, S., Lenoir, J., Gril, E., De Frenne, P., Lembrechts, J. J., Kopecký, M., Macek, M., Man, M., Wild, J., & Van Meerbeek, K. (2023). Microclimate reveals the true thermal niche of forest plant species. *Ecology Letters*, ele.14312.

Hartmann, H., Bastos, A., Das, A. J., Esquivel-Muelbert, A., Hammond, W. M., Martínez-Vilalta, J., McDowell, N. G., Powers, J. S., Pugh, T. A. M., Ruthrof, K. X., & Allen, C. D. (2022). Climate Change Risks to Global Forest Health: Emergence of Unexpected Events of Elevated Tree Mortality Worldwide. *Annual Review of Plant Biology*, *73*(1), 673–702.

Heidari, H., Arabi, M., & Warziniack, T. (2021). Effects of Climate Change on Natural-Caused Fire Activity in Western U.S. National Forests. *Atmosphere*, *12*(8), 981.

Hohensinner, S., Atzler, U., Fischer, A., Schwaizer, G., & Helfricht, K. (2021). Tracing the Long-Term Evolution of Land Cover in an Alpine Valley 1820–2015 in the Light of Climate, Glacier and Land Use Changes. *Frontiers in Environmental Science*, *9*, 683397.

Karger, D. N., Conrad, O., Böhner, J., Kawohl, T., Kreft, H., Soria-Auza, R. W., Zimmermann, N. E., Linder, H. P., & Kessler, M. (2017). Climatologies at high resolution for the earth's land surface areas. *Scientific Data*, *4*(1)

Kim, H., McComb, B. C., Frey, S. J., Bell, D. M., & Betts, M. G. (2022). Forest microclimate and composition mediate long-term trends of breeding bird populations. *Global Change Biology*, 28(21), 6180-6193.

Komatsu, K. J., Avolio, M. L., Lemoine, N. P., Isbell, F., Grman, E., Houseman, G. R., ... & Zhang, Y. (2019). Global change effects on plant communities are magnified by time and the number of global change factors imposed. *Proceedings of the National Academy of Sciences*, 116(36), 17867-17873.

Krauss, J., Bommarco, R., Guardiola, M., Heikkinen, R. K., Helm, A., Kuussaari, M., Lindborg, R., Öckinger, E., Pärtel, M., Pino, J., Pöyry, J., Raatikainen, K. M., Sang, A., Stefanescu, C., Teder, T., Zobel, M., & Steffan-Dewenter, I. (2010). Habitat fragmentation causes immediate and time-delayed biodiversity loss at different trophic levels. *Ecology Letters*, *13*(5), 597–605.

Lambin, E. F., & Meyfroidt, P. (2011). Global land use change, economic globalization, and the looming land scarcity. *Proceedings of the National Academy of Sciences*, 108(9), 3465-3472.

Lantman JVS, Verburg PH, Bregt A, Geertman S. 2011. Core principles and concepts in land-use modelling: a literature review. In: Koomen E, Borsboom-Van Beurden J, Eds. *LandUse Modelling in Planning Practice*, London: Springer. pp 35–57.

Lembrechts, J. J., Lenoir, J., Roth, N., Hattab, T., Milbau, A., Haider, S., Pellissier, L., Pauchard, A., Ratier Backes, A., Dimarco, R. D., Nuñez, M. A., Aalto, J., & Nijs, I. (2019). Comparing temperature data sources for use in species distribution models: From in-situ logging to remote sensing. *Global Ecology and Biogeography*, *28*(11), 1578–1596. Scopus.

Lembrechts, J. J., Nijs, I., & Lenoir, J. (2019). Incorporating microclimate into species distribution models. *Ecography*, *42*(7), 1267–1279.

Lenoir, J., Gégout, J. C., Marquet, P. A., Ruffray, P. de, & Brisse, H. (2008). A Significant Upward Shift in Plant Species Optimum Elevation During the 20th Century. *Science*, *320*(5884), 1768–1771.

Lenoir, J., Hattab, T., & Pierre, G. (2017). Climatic microrefugia under anthropogenic climate change: Implications for species redistribution. *Ecography*, *40*(2), 253–266.

Lopez, D., Fonda, F., Monti, F., & Dal Zotto, M. (2023). Density Estimates and Habitat Preferences of Two Sympatric Bird Species as Potential Bioindicators of Tropical Forest Alterations. *Diversity*, 15(2), 208.

MacDonald, D., Crabtree, J. R., Wiesinger, G., Dax, T., Stamou, N., Fleury, P., Gutierrez Lazpita, J., & Gibon, A. (2000). Agricultural abandonment in mountain areas of Europe: Environmental consequences and policy response. *Journal of Environmental Management*, *59*(1), 47–69.

Maclean, I. M. D., & Early, R. (2023). Macroclimate data overestimate range shifts of plants in response to climate change. *Nature Climate Change*.

Malfasi, F., & Cannone, N. (2020). Climate Warming Persistence Triggered Tree Ingression After Shrub Encroachment in a High Alpine Tundra. *Ecosystems*, *23*(8), 1657–1675.

Mantero, G., Morresi, D., Marzano, R., Motta, R., Mladenoff, D. J., & Garbarino, M. (2020). The influence of land abandonment on forest disturbance regimes: A global review. *Landscape Ecology*, *35*(12), 2723–2744.

Maréchaux, I., Langerwisch, F., Huth, A., Bugmann, H., Morin, X., Reyer, C. P. O., Seidl, R., Collalti, A., Paula, M. D. de, Fischer, R., Gutsch, M., Lexer, M. J., Lischke, H., Rammig, A., Rödig, E., Sakschewski, B., Taubert, F., Thonicke, K., Vacchiano, G., & Bohn, F. J. (s.d.). Tackling unresolved questions in forest ecology: The past and future role of simulation models. *Ecology and Evolution*.

Marjakangas, E.-L., Abrego, N., Grøtan, V., de Lima, R. A. F., Bello, C., Bovendorp, R. S., Culot, L., Hasui, É., Lima, F., Muylaert, R. L., Niebuhr, B. B., Oliveira, A. A., Pereira, L. A., Prado, P. I., Stevens, R. D., Vancine, M. H., Ribeiro, M. C., Galetti, M., & Ovaskainen, O. (2020). Fragmented tropical forests lose mutualistic plant–animal interactions. *Diversity and Distributions*, *26*(2), 154–168.

Martin, Y., Van Dyck, H., Dendoncker, N., & Titeux, N. (2013). Testing instead of assuming the importance of land use change scenarios to model species distributions under climate change. *Global Ecology and Biogeography*, *22*(11), 1204–1216.

Martinuzzi, S., Gavier-Pizarro, G. I., Lugo, A. E., & Radeloff, V. C. (2015). Future Land-Use Changes and the Potential for Novelty in Ecosystems of the United States. *Ecosystems*, *18*(8), 1332–1342.

Mas, J.-F., Kolb, M., Paegelow, M., Camacho Olmedo, M. T., & Houet, T. (2014). Inductive pattern-based land use/cover change models: A comparison of four software packages. *Environmental Modelling & Software*, *51*, 94–111.

Massenberg, J. R., Schiller, J., & Schröter-Schlaack, C. (2023). Towards a holistic approach to rewilding in cultural landscapes. *People and Nature*, *5*(1), 45–56.

Mateo, R. G., Gastón, A., Aroca-Fernández, M. J., Broennimann, O., Guisan, A., Saura, S., & García-Viñas, J. I. (2019). Hierarchical species distribution models in support of vegetation conservation at the landscape scale. *Journal of Vegetation Science*, *30*(2), 386–396.

McDowell, N. G., Allen, C. D., Anderson-Teixeira, K., Aukema, B. H., Bond-Lamberty, B., Chini, L., Clark, J. S., Dietze, M., Grossiord, C., Hanbury-Brown, A., Hurtt, G. C., Jackson, R. B., Johnson, D. J., Kueppers, L., Lichstein, J. W., Ogle, K., Poulter, B., Pugh, T. A. M., Seidl, R., … Xu, C. (2020). Pervasive shifts in forest dynamics in a changing world. *Science*.

McGarigal, K., & Marks., B. J. (1995). *FRAGSTATS: Spatial pattern analysis program for quantifying landscape structure*. Portland, OR: US, Department of Agriculture, Forest Service, Pacific Northwest Research Station-PNW-GTR–351.

McGarigal, K., Wan, H. Y., Zeller, K. A., Timm, B. C., & Cushman, S. A. (2016). Multi-scale habitat selection modeling: A review and outlook. *Landscape Ecology*, 31(6), 1161–1175.

Michielsen, R. J., Żmihorski, M., Pärt, T., Walesiak, M., & Mikusiński, G. (2024). Seasonal patterns of habitat use of resident birds in Białowieża Forest and its links to post-disturbance management. *Forest Ecology and Management*, 554, 121669.

Mietkiewicz, N., Kulakowski, D., Rogan, J., & Bebi, P. (2017). Long-term change in sub-alpine forest cover, tree line and species composition in the Swiss Alps. *Journal of Vegetation Science*, *28*(5), 951–964.

Mladenoff, D. J. (2004). LANDIS and forest landscape models. *Ecological modelling*, 180(1), 7-19.

Møller, A. P., Rubolini, D., & Lehikoinen, E. (2008). Populations of migratory bird species that did not show a phenological response to climate change are declining. *Proceedings of the National Academy of Sciences*, 105(42), 16195-16200.

Moudrý, V., Keil, P., Gábor, L., Lecours, V., Zarzo-Arias, A., Barták, V., Malavasi, M., Rocchini, D., Torresani, M., Gdulová, K., Grattarola, F., Leroy, F., Marchetto, E., Thouverai, E., Prošek, J., Wild, J., & Šímová, P. (2023). Scale mismatches between predictor and response variables in species distribution modelling: A review of practices for appropriate grain selection. *Progress in Physical Geography: Earth and Environment*, *47*(3), 467–482.

Navarro, L. M., & Pereira, H. M. (2012). Rewilding Abandoned Landscapes in Europe. *Ecosystems*, *15*(6), 900–912.

Naveh, Z., & Lieberman, A. S. (2013). *Landscape ecology: theory and application*. Springer Science & Business Media.

Newbold, T. (2018). Future effects of climate and land-use change on terrestrial vertebrate community diversity under different scenarios. *Proceedings of the Royal Society B: Biological Sciences*, *285*(1881), 20180792.

Newbold, T., Oppenheimer, P., Etard, A., & Williams, J. J. (2020). Tropical and Mediterranean biodiversity is disproportionately sensitive to land-use and climate change. *Nature Ecology & Evolution*, 4(12).

Noce, S., Cipriano, C., & Santini, M. (2023). Altitudinal shifting of major forest tree species in Italian mountains under climate change. *Frontiers in Forests and Global Change*, 6, 1250651.

Northrup, J. M., Rivers, J. W., Yang, Z., & Betts, M. G. (2019). Synergistic effects of climate and land-use change influence broad-scale avian population declines. *Global Change Biology*, 25(5), 1561-1575.

Noszczyk, T. (2019). A review of approaches to land use changes modeling. *Human and Ecological Risk Assessment: An International Journal*, *25*(6), 1377–1405.

Pakkala, T., Peltonen, A., Lindberg, H., Hjältén, J., & Kouki, J. (2024). The intensity of forest management affects the nest cavity production of woodpeckers and tits in mature boreal forests. *European Journal of Forest Research*, 1-18.

Parker, D. C., Berger, T., & Manson, S. M. (2001). *Agent-based models of land-use and land-cover change. Adaptive agents, intelligence and emergent human organization: Capturing complexity through agent-based modelling*. Irvine, CA: LUCC International Project Office.

Pausas, J. G., & Fernández-Muñoz, S. (2012). Fire regime changes in the Western Mediterranean Basin: From fuel-limited to drought-driven fire regime. *Climatic Change*, *110*(1), 215–226.

Pausas, J. G., & Keeley, J. E. (2021). Wildfires and global change. *Frontiers in Ecology and the Environment*, fee.2359.

Pearce-Higgins, J. W., Eglington, S. M., Martay, B., & Chamberlain, D. E. (2015). Drivers of climate change impacts on bird communities. *Journal of Animal Ecology*, 84(4), 943-954.

Peters, M. K., Hemp, A., Appelhans, T., Becker, J. N., Behler, C., Classen, A., Detsch, F., Ensslin, A., Ferger, S. W., Frederiksen, S. B., Gebert, F., Gerschlauer, F., Gütlein, A., Helbig-Bonitz, M., Hemp, C., Kindeketa, W. J., Kühnel, A., Mayr,

A. V., Mwangomo, E., … Steffan-Dewenter, I. (2019). Climate–land-use interactions shape tropical mountain biodiversity and ecosystem functions. *Nature*, *568*(7750), Articolo 7750.

Pigot, A. L., Merow, C., Wilson, A., & Trisos, C. H. (2023). Abrupt expansion of climate change risks for species globally. *Nature Ecology & Evolution*.

Plieninger, T., Draux, H., Fagerholm, N., Bieling, C., Bürgi, M., Kizos, T., Kuemmerle, T., Primdahl, J., & Verburg, P. H. (2016). The driving forces of landscape change in Europe: A systematic review of the evidence. *Land Use Policy*, 57, 204–214.

Pörtner, H. O., Roberts, D. C., Adams, H., Adler, C., Aldunce, P., Ali, E., ... & Fischlin, A. (2022). *Climate change 2022: Impacts, adaptation and vulnerability.* IPCC Sixth Assessment Report.

Richardson, A. D., Keenan, T. F., Migliavacca, M., Ryu, Y., Sonnentag, O., & Toomey, M. (2013). Climate change, phenology, and phenological control of vegetation feedbacks to the climate system. *Agricultural and Forest Meteorology*, 169, 156–173.

Rigo, F., Paniccia, C., Anderle, M., Chianucci, F., Obojes, N., Tappeiner, U., ... & Mina, M. (2024). Relating forest structural characteristics to bat and bird diversity in the Italian Alps. *Forest Ecology and Management*, 554, 121673.

Rodman, K. C., Veblen, T. T., Saraceni, S., & Chapman, T. B. (2019). Wildfire activity and land use drove 20th-century changes in forest cover in the Colorado front range. *Ecosphere*, 10(2), e02594.

Sales, L. P., Hayward, M. W., & Loyola, R. (2021). What do you mean by "niche"? Modern ecological theories are not coherent on rhetoric about the niche concept. *Acta Oecologica*, 110, 103701.

Samraoui, F., Alfarhan, A. H., Al-Rasheid, K. A., & Samraoui, B. (2011). An appraisal of the status and distribution of waterbirds of Algeria: indicators of global changes?. *Ardeola*, 58(1), 137-163.

Scheffers, B. R., Edwards, D. P., Diesmos, A., Williams, S. E., & Evans, T. A. (2014). Microhabitats reduce animal's exposure to climate extremes. *Global Change Biology*, 20(2), 495–503.

Scheller, R. M., Domingo, J. B., Sturtevant, B. R., Williams, J. S., Rudy, A., Gustafson, E. J., & Mladenoff, D. J. (2007). *Design, development, and application of*

LANDIS-II, a spatial landscape simulation model with flexible temporal and spatial resolution. ecological modelling, 201(3-4), 409-419.

Seidl, R., Rammer, W., Scheller, R. M., & Spies, T. A. (2012). An individual-based process model to simulate landscape-scale forest ecosystem dynamics. *Ecological Modelling*, 231, 87-100.

Seidl, R., Thom, D., Kautz, M., Martin-Benito, D., Peltoniemi, M., Vacchiano, G., Wild, J., Ascoli, D., Petr, M., Honkaniemi, J., Lexer, M. J., Trotsiuk, V., Mairota, P., Svoboda, M., Fabrika, M., Nagel, T. A., & Reyer, C. P. O. (2017). Forest disturbances under climate change. *Nature Climate Change*, 7(6), Articolo 6.

Smith, T., Traxl, D., & Boers, N. (2022). Empirical evidence for recent global shifts in vegetation resilience. *Nature Climate Change*, 12(5), 477–484.

Song, X.-P., Hansen, M. C., Stehman, S. V., Potapov, P. V., Tyukavina, A., Vermote, E. F., & Townshend, J. R. (2018). Global land change from 1982 to 2016. *Nature*, 560(7720).

Stritih, A., Senf, C., Seidl, R., Grêt-Regamey, A., & Bebi, P. (2021). The impact of land-use legacies and recent management on natural disturbance susceptibility in mountain forests. *Forest Ecology and Management*, 484.

Tattoni, C., Ciolli, M., & Ferretti, F. (2011). The Fate of Priority Areas for Conservation in Protected Areas: A Fine-Scale Markov Chain Approach. *Environmental Management*, *47*(2), 263–278.

Trautmann, S. (2018). *Climate change impacts on bird species*. Bird Species: How They Arise, Modify and Vanish, 217-234.

Turner, M. G., Gardner, R. H., O'neill, R. V., & O'Neill, R. V. (2001). *Landscape ecology in theory and practice* (Vol. 401). Springer New York.

Veldkamp, A., & Fresco, L. O. (1996). CLUE: A conceptual model to study the conversion of land use and its effects. *Ecological Modelling*, 85(2–3), 253–270.

Verburg, P. H., Alexander, P., Evans, T., Magliocca, N. R., Malek, Z., Rounsevell, M. D., & van Vliet, J. (2019). Beyond land cover change: Towards a new generation of land use models. *Current Opinion in Environmental Sustainability*, 38, 77–85.

Verburg, P. H., van Asselen, S., van der Zanden, E. H., & Stehfest, E. (2013). The representation of landscapes in global scale assessments of environmental change. *Landscape Ecology*, 28(6), 1067–1080.

Visconti, P., Bakkenes, M., Baisero, D., Brooks, T., Butchart, S. H., Joppa, L., ... & Rondinini, C. (2016). Projecting global biodiversity indicators under future development scenarios. *Conservation Letters*, 9(1), 5-13.

Vitasse, Y., Baumgarten, F., Zohner, C. M., Rutishauser, T., Pietragalla, B., Gehrig, R., Dai, J., Wang, H., Aono, Y., & Sparks, T. H. (2022). The great acceleration of plant phenological shifts. *Nature Climate Change*, 12(4), Articolo 4.

Vitasse, Y., Ursenbacher, S., Klein, G., Bohnenstengel, T., Chittaro, Y., Delestrade, A., Monnerat, C., Rebetez, M., Rixen, C., Strebel, N., Schmidt, B. R., Wipf, S., Wohlgemuth, T., Yoccoz, N. G., & Lenoir, J. (2021). Phenological and elevational shifts of plants, animals and fungi under climate change in the European Alps. *Biological Reviews*, 96(n/a), 1816–1835.

Viterbi, R., Cerrato, C., Bionda, R., & Provenzale, A. (2020). Effects of temperature rise on multi-taxa distributions in mountain ecosystems. *Diversity*, 12(6), 210.

Wan, J. Z., Wang, C. J., & Yu, F. H. (2017). Spatial conservation prioritization for dominant tree species of Chinese forest communities under climate change. *Climatic Change*, 144, 303-316.

Wang, L., Clayton, M., & Rossberg, A. G. (2023). Drone audition for bioacoustic monitoring. *Methods in Ecology and Evolution*, 14(12), 3068-3082.

Wolf, C., Bell, D. M., Kim, H., Nelson, M. P., Schulze, M., & Betts, M. G. (2021). Temporal consistency of undercanopy thermal refugia in old-growth forest. *Agricultural and Forest Meteorology*, 307, 108520.

Wolff, S., Schrammeijer, E. A., Schulp, C. J. E., & Verburg, P. H. (2018). Meeting global land restoration and protection targets: What would the world look like in 2050? *Global Environmental Change*, 52, 259–272.

Zurell, D., Franklin, J., König, C., Bouchet, P. J., Dormann, C. F., Elith, J., Fandos, G., Feng, X., Guillera-Arroita, G., Guisan, A., Lahoz-Monfort, J. J., Leitão, P. J., Park, D. S., Peterson, A. T., Rapacciuolo, G., Schmatz, D. R., Schröder, B., Serra-Diaz, J. M., Thuiller, W., … Merow, C. (2020). A standard protocol for reporting species distribution models. *Ecography*, 43(9), 1261–1277.

Zurell, D., König, C., Malchow, A., Kapitza, S., Bocedi, G., Travis, J., & Fandos, G. (2022). Spatially explicit models for decision-making in animal conservation and restoration. *Ecography*, 2022(4), ecog.05787.

Chapter 2

Global change in the European Alps: a century of post-abandonment natural reforestation at the landscape scale

Nicolò Anselmetto, Peter J. Weisberg, Matteo Garbarino

This chapter has been published open access in the *Landscape and Urban Planning* journal: Anselmetto, N., Weisberg, P. J., & Garbarino, M. (2024). Global change in the European Alps: A century of post-abandonment natural reforestation at the landscape scale. Landscape and Urban Planning, 243, 104973. https://doi.org/10.1016/j.landurbplan.2023.104973

Abstract

Natural reforestation is one of the dominant processes in marginal mountain areas of the Northern hemisphere. There is a globally relevant need to predict where and when natural reforestation is likely to occur and what the ecological and social effects might be. We conducted a systematic review and meta-analysis of land use/land cover change (LULCC) case studies investigating spatial patterns of post-abandonment natural reforestation in the European Alps. We selected the Alps as representative of global change effects on forests due to their history of LULCC since the 19th century and. Our aim was to identify the most important socioecological influences on reforestation and discuss implications for planners and managers. At the regional scale, we summarised the spatiotemporal distribution and methodological approaches of the case studies. At the municipality scale, we explored the relationships between reforestation rate and socio-economic variables using multivariate statistics. At the landscape scale, we

assessed climate, topographic, and socio-economic drivers on reforestation using Random Forest regression. We observed a lack of studies in the northeastern region of the Alps. Population density, road density, and the proportion of workers employed in industrial vs. agricultural job sectors were the variables most highly correlated with reforestation. Reforestation rate was greatest in south-facing slopes of dry landscapes within remote and sparsely populated municipalities. We advocate for a dynamic harmonised LULCC geodatabase to capture the nonlinearity of past LULCC in training both correlative and process-based models for landscape planning.

Keywords: Alps, land abandonment, land cover change, land use, mountain landscapes, natural reforestation.

Highlights

- European Alps have a long history of LULCC research spanning 150 years.
- The spatial distribution of LULCC studies is heterogeneous across the Alps.
- Reforestation was greatest in remote and sparsely populated municipalities.
- Reforestation was higher in south-facing slopes of dry marginal landscapes.
- A dynamic harmonised LULCC database is needed to analyse post-abandonment trends.

2.1 Introduction

Human action has been a dominant force shaping Earth systems for millennia, affecting the ecological structure of landscapes and the provision of ecosystem services (Ellis et al., 2013; Lewis & Maslin, 2015). During the Anthropocene, land use/land cover change (LULCC) and climate change has affected forest ecosystems by dampening species diversity and distribution, increasing tree mortality, and altering disturbance regimes (e.g., Seidl et al., 2017; Mantero et al., 2020; McDowell et al., 2020). To date, LULCC is considered to be the most important global change component in affecting terrestrial ecosystems, despite

predictions that in the future climate change will equal or surpass the role of LULCC (Oliver & Morecroft, 2014; Newbold, 2018). While tropical deforestation in areas where forests are increasingly being converted to agricultural lands is of great global concern (FAO, 2020; Fagan et al., 2022), the post-abandonment natural reforestation of former agricultural lands also represents a major land use change of global importance (Meli et al., 2017; Ward, 2019). Despite local post-abandonment reforestation may occur in areas where the dominant LULCC processes at the regional scale are deforestation, urbanisation, and agricultural land expansion (e.g., Latin America, Africa, and tropical Asia; Crawford et al., 2022; Díaz et al., 2011), land abandonment is usually associated with high-income countries in the Northern hemisphere (e.g., Ramankutty et al. (2010) and Martinuzzi et al. (2015) for the US; MacDonald et al. (2000) and Plieninger et al. (2016) for Europe; Uchida et al. (2018) for Japan).

The European Alps (hereafter, Alps) are paradigmatic in this sense; human settlements in the Alps became particularly important at the end of the Würm glaciation (i.e., 12 000 before present), with an increase of population starting from the Neolithic and Bronze Age (i.e., 8000 to 3000 BP) (Carcaillet, 1998; Favilli et al., 2010). During that period, evidence shows how slash-and-burn practices were largely adopted across the Alps to create open areas for pastures and agriculture (e.g., Carcaillet, 1998; Tinner et al., 2005; Carcaillet et al., 2009). Since then, Alpine landscapes have been modified by the exploitation of forests for timber and fuelwood, grazing, mining practices, and maintenance of agricultural land (Mietkiewicz et al., 2017). In the last millennium, societal changes and consequent land use are associated with historical shifts in climate (e.g., Medieval Optimum and Little Ice Age; Büntgen et al., 2016). The industrial revolution of the 19th century led to an intense exodus from the marginal valleys of the Alps towards urban and industrial centres, resulting in widespread natural reforestation following agricultural abandonment (MacDonald et al., 2000; Mietkiewicz et al., 2017; Gelabert et al., 2022) and shaping new post-modern landscapes (Antrop, 2005). Nevertheless, patterns of abandonment may vary

locally, with an intensification of agriculture in districts with more favourable environments, greater productivity, and closer connections to transportation corridors and population centres, but an enduring abandonment of environmentally harsh and remote areas (MacDonald et al., 2000; Egarter Vigl et al., 2016). Therefore, even as the area used for agriculture has declined over time, the intensity of use has increased in the remaining agricultural areas. For example, livestock numbers in the Alpine countries have declined by 16% over the last 60 years, but the density of livestock (LAU ha^{-1}) has increased by 6% over the same period (-22% and +10% respectively for Europe as a whole) (FAOSTAT, 2022).

Following agricultural abandonment in the Alps, secondary succession has led to a natural reforestation of areas that had been converted to croplands and pastures for millennia. At lower elevations, secondary succession consisted of in-filling of non-forest patches such as abandoned meadows, grasslands, and arable lands (Garbarino et al., 2020). At the treeline ecotone, LULCC is considered the most important factor determining treeline position and change in areas with a prolonged history of agriculture or resource exploitation (Gehrig-Fasel et al., 2007; Garbarino et al., 2020; Anselmetto et al., 2021). Social and cultural transformations are the leading drivers of land use change at the global scale (Crawford et al., 2022), but topography, microclimate, road availability, and population become fundamental drivers of reforestation at the landscape scale (Garbarino et al., 2020; Gelabert et al., 2022). The synergic effect of social and ecological conditions can be difficult to disentangle, as is also true for the interplay between land use legacies and climate change (Gehrig-Fasel et al., 2007; Ameztegui et al., 2016; Anselmetto et al., 2021).

Post-abandonment natural reforestation can provide a restoration opportunity to establish trajectories towards ecologically functional landscapes (Navarro & Pereira, 2012; Plieninger et al., 2016), but this must be weighed against the threats for reduced biodiversity, increased risk of natural disturbances associated with closed-canopy forests, and potentially diminished cultural values. From a conservation point of view, large carnivores and old-growth specialist birds have

been favoured by the widespread natural reforestation of mountain ecosystems of the Alps (Chapron et al., 2014; Bani et al., 2019; Davoli et al., 2022). However, many plant and animal species associated with historical anthropic disturbances benefit from the presence of forest edges and semi-natural landscapes (Bani et al., 2019; Betts et al., 2019). Moreover, many landscapes experiencing post-abandonment reforestation are particularly sensitive to natural disturbances, given the permeability of continuous forest cover associated with land abandonment (Mantero et al., 2020). For instance, many large wildfires struck the Western Italian Alps in 2017, affecting around 10 000 ha (Morresi et al., 2022). Finally, post-abandonment reforestation dampens aesthetic and cultural functionalities of the so-called anthromes (anthropic biomes) (Halada et al., 2011; Egarter Vigl et al., 2016; Schirpke et al., 2021). Most of these abandoned landscapes, such as the larch wood pastures and terraced landscapes of the Alps – but also Satoyama in Japan and dehesa systems in the Iberic peninsula – are considered cultural landscapes, and concern over their conservation is increasing all over the world (Fischer et al., 2012; Perino et al., 2019).

The complexity of natural reforestation processes and their socioecological outcomes demands proper analytical scales to quantify and model spatial and temporal patterns of change (Garbarino & Weisberg, 2020). Ecosystem functioning and recovery and the socio-economic conditions of land abandonment are key factors when choosing tools and scales. For instance, land abandonment is only a temporary condition in some regions of the world (Crawford et al., 2022), but it can be permanent or long lasting in many others, such as the Alps (MacDonald et al., 2000; Plieninger et al., 2016). In these long-lasting abandoned ecosystems, natural vegetation recovery and reforestation have been ongoing over past decades to centuries, and land use legacies are still driving trajectories of change (McDowell et al., 2020). Given strong local influences of land use legacies and the fine-scale patchiness of secondary successional processes (i.e., in-filling of small, grass-dominated patches by woody species), fine spatial and at least decadal temporal resolutions are needed to capture their

heterogeneity (Orlandi et al., 2016; Meli et al., 2017). The Alps have been the subject of numerous landscape ecological investigations of LULCC. However, many case studies from this region report inferences developed from inconsistent remote sensing data sources and analytical approaches, lacking a common and harmonised approach.

Based on this gap of knowledge and with the intention of providing a consistent framework for analysis, the overall aim of our study was to conduct a systematic literature review and meta-analysis of natural reforestation across the Alps over a range of scales from landscapes to large municipalities. Specifically, our objectives were (a) to collect methodological and spatiotemporal information on natural reforestation research across the region, (b) to analyse the relationship between socio-economic variables and forest gain at the municipality scale, (c) to explore and quantify influences of climate, topography, and anthropogenic drivers on natural reforestation processes at the landscape scale, (d) to discuss future directions in managing post-abandonment natural reforestation from a landscape planning perspective.

2.2 Materials and methods

2.2.1 Study area

The Alps extend over 1200 km from southeastern France to northwestern Austria (Alpine Convention, 2018), showing significant topographic variability comprising extensive lowlands, steep valleys, and mountain peaks rising above 4800 m a.s.l. The Alps host more than one-third of European flora, with several endemic taxa (Fauquette et al., 2018). Oak forests (*Quercus spp.*) dominate at lower elevations, silver fir (*Abies alba* Mill.) and beech (*Fagus sylvatica* L.) are associated with mesic regions, and Scots pine (*Pinus sylvestris* L.) with xeric slopes of the montane belt. European larch (*Larix decidua* Mill.), Norway spruce (*Picea abies* (L.) H. Karst.), and Stone pine (*Pinus cembra* L.) dominate the subalpine belt. Mean annual temperatures range from less than 0° to 10°. Annual precipitation in the region ranges from 400 to 3000 mm, with topographic effects

acting at different spatial scales (Isotta et al., 2014). Climate change is already affecting the region and is expected to increase summer and winter temperatures and alter precipitation regimes (Pörtner et al., 2022). Because of their long land use history and excellent availability of long-term data, the Alps are a perfect study system for investigating the phenomenon of post-abandonment natural reforestation.

2.2.2 Systematic review

The workflow of this study consisted of two main phases (Figure 2.1): (i) a systematic review of the scientific literature to retrieve data on LULCC dynamics of diverse case study landscapes within the Alps (location, scale of analysis, methodology), and (ii) a meta-analysis of the selected case studies to quantify the influences of several key socioecological drivers on forest gain. To conduct our literature review, we searched the main scientific literature databases (Scopus, ISI Web of Science, and PubMed) on 10 February 2022. The search query as applied in Scopus was TITLE-ABS-KEY (("land use" OR “land-use” OR "land cover" OR “land-cover” OR "land abandonment" OR “landscape change”) AND forest* AND (alps OR "alp* region")). After combining the publications obtained from Scopus, WoS, and PubMed, our systematic review identified 458 unique articles. The first screening of titles and abstracts was used to remove duplicates and select only those landscapes located within the Alps. The remaining articles were then thoroughly read to ensure that inclusion criteria were met. We chose only case study landscapes that (i) analysed LULCC changes through a polygon-based change detection, (ii) included forested areas, and (iii) had a spatial extent smaller than 200 000 ha. As a result, we obtained a total of 42 relevant articles for the meta-analysis (Table A2.1, Appendix A of Supplementary Materials).

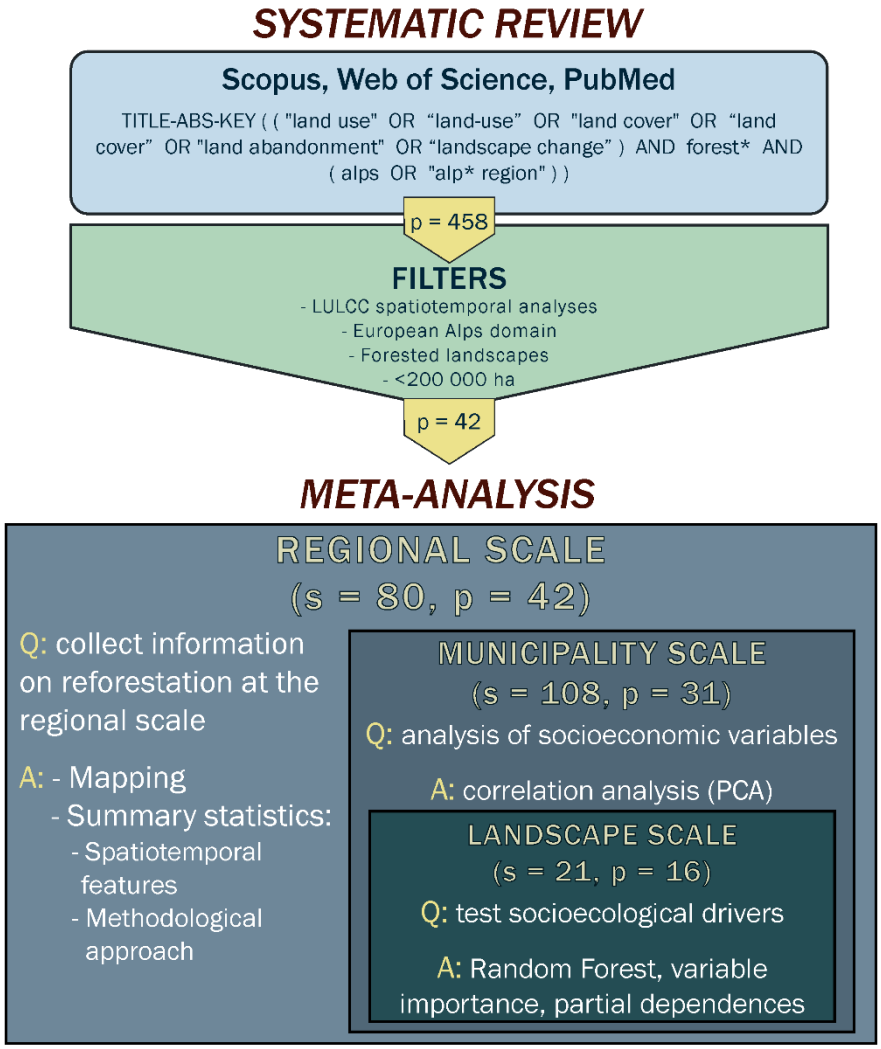

Figure 2.1. Conceptual workflow of the study from the systematic literature review to the meta-analysis. Q = scientific questions/objectives associated with each scale of analysis; A = analytical tools associated with each scale of analysis; p = number of papers in each methodological step; s = number of sites analysed in the present study for each scale (i.e., case studies at the regional scale, municipalities at the municipality scale, and landscapes at the landscape scale).

2.2.3 Scales of Analysis

From the selected articles, we derived a set of unique case studies. A single research article may have analysed multiple sites; also, the same site may have been investigated in several articles. In the latter case, we selected the study with

the longest temporal extent. We analysed several aspects of reforestation across three spatial scales (Figure 2.1). At the regional scale (reg) we included spatially defined case studies located within the Alpine Convention Perimeter (sites = 80) for which the forest gain was not reported in the articles. We used this scale to summarise methodological approaches and spatiotemporal characteristics of the studies across the entire region. As a reference, we used the Nomenclature of Territorial Units for Statistics (NUTS, 2021).

The municipality scale (mun) consisted of spatially defined studies reporting forest change. We selected observed annual forest gain per site (% of increase $year^{-1}$) as our measure of reforestation since it was the only forest gain variable common to all the studies. We derived this information either directly from the articles' main text and supplementary materials or by calculating it from absolute or relative values whenever feasible. We assumed that, in the Alpine region, the forest gain over the last 100 years has been mostly related to post-abandonment natural reforestation (hereafter, reforestation) and climate change, with novel afforestation due to plantation forestry playing only a minor role (Gehrig-Fasel et al., 2007; Tasser et al., 2007, 2017; Garbarino et al., 2020). We chose relative over absolute increase because larger landscapes tended to be in close proximity. Had we used the absolute increase as our measure, our findings would have been biased towards large-area studies and therefore would have over-emphasized only a subset of the overall Alpine region. At this scale, we selected only landscapes that could be attributed to a municipality (108 municipalities) according to Local Administrative Units (LAU) level 1 (LAU, 2021).

The landscape scale (lan) included landscape studies from which it was possible to derive precise spatial attributes such as geographic position and surface area (s = 21). Nevertheless, since few authors showed the land cover maps they used in their research, we made the simplifying assumption that study landscapes were circular in shape. We determined a circular buffer around the centroid of each landscape, with radius length calculated such that buffered areas would match the

study area extents reported in the literature and the centroid represented the coordinates provided by the authors.

2.2.4 Socio-ecological predictors

We selected a set of socio-economic, topographic, climate, and vegetation variables that we tested with respect to forest gain rate at the municipality and landscape scales (Table 2.1, Appendix B of Supplementary Materials). Ecological and socio-economic constraints can be considered the two main drivers of post-abandonment reforestation (Garbarino et al., 2020; Gelabert et al., 2022). We compared the observed forest gain as synthesized from the articles in our meta-analysis to the recent forest cover change rate derived from satellite remote sensing using the Corine Land Cover (CLC; European Commission, 1994) for the period 2000–2018. The CLC has been widely applied for mapping habitats, assessing biodiversity, analysing landscape fragmentation and developing future land use scenarios (e.g., Lehsten et al., 2015). Nevertheless, the CLC has performed poorly in estimating agricultural abandonment and quantification of forest expansion, especially related to small patches (i.e., < 5 ha) processes (Kuemmerle et al., 2016; Pazúr & Bolliger, 2017; Lieskovský & Lieskovská, 2021). Our aim was to assess our long-term fine scale dataset derived from discrete study site locations against this widely used medium resolution wall-to-wall dataset. We excluded 1990 CLC to include Switzerland, for which data are unavailable for the first year of analysis (Appendix B of Supplementary Materials). At the landscape scale we explored more general patterns by adopting a series of ecological drivers at 1-km spatial resolution and socio-economic variables. We selected this coarse spatial resolution due to the exploratory objective of our study and the uncertainty in attributing spatial position to the landscapes.

TABLE 2.1. Socioecological predictors used in the study, divided by category. Job sectors are classified as primary (i.e., agricultural/natural resource), secondary (i.e., manufacturing), and tertiary (i.e., service).

Category	Variable	Data source	Spatial resolution	Data level
Socio-economic -Population-	Population density (1961, 1971, 1981, 1991, 2001, 2011, 2020)	Eurostat	Municipality	lv2 lv3
	Population change (1961-2020)	Eurostat	Municipality	lv2 lv3
	Population rate of change (1961-2020)	Eurostat	Municipality	lv2 lv3
Socio-economic -Agriculture-	Job sectors employment (primary, secondary, tertiary)	Alpine Convention atlas	Municipality	lv2
	Relative change in number of farms (1990-2000)	Alpine Convention atlas	Municipality	lv2
Socio-economic -Remoteness-	Tourism density	OSM	Municipality	lv2
	Road density (primary, secondary, tertiary)	OSM	Municipality	lv2
	Cost of movement (min, mean, max)	OSM + MERIT DEM	1 km	lv3
	Distance from cities (min, mean, max)	OSM	1 km	lv3
	Distance from towns (min, mean, max)	OSM	1 km	lv3
Topography	Elevation (mean, standard deviation)	MERIT DEM	1 km	lv3
	Slope (mean, standard deviation)	MERIT DEM	1 km	lv3
	Topographic position index (mean, standard deviation)	MERIT DEM	1 km	lv3
	Heat load index (mean, standard deviation)	MERIT DEM	1 km	lv3
Climate -Mean values-	Precipitation (annual, summer, winter)	CHELSA timeseries	1 km	lv3

	(median, standard deviation)			
	Mean temperature (annual, summer, winter) (median, standard deviation)	CHELSA timeseries	1 km	lv3
	Minimum temperature (annual, summer, winter) (median, standard deviation)	CHELSA timeseries	1 km	lv3
	Maximum temperature (annual, summer, winter) (median, standard deviation)	CHELSA timeseries	1 km	lv3
Climate -Slope of change-	Slope of precipitation change (1979-2013)	CHELSA timeseries	1 km	lv3
	Slope of mean temperature change (1979-2013)	CHELSA timeseries	1 km	lv3
	Slope of minimum temperature change (1979-2013)	CHELSA timeseries	1 km	lv3
	Slope of maximum temperature change (1979-2013)	CHELSA timeseries	1 km	lv3
Vegetation	Forest cover change (2000-2018)	Corine Land Cover	Municipality	lv2

We analysed municipality and landscape scales separately because there were few articles in our database that provided sufficient spatial precision to allow for a fine-scale analysis of topographic and climate predictors (landscape scale). Nevertheless, we did not want to lose information about the case studies where values of forest gain were provided, but the spatial positioning was not precise (municipality scale). For this reason, we used the latter to analyse broad socio-economic drivers and the differences between forest gain values in the articles and forest gain reported by the CLC.

2.5 Statistical analysis

At the municipality scale (mun), we analysed the multivariate correlation between observed forest gain, socio-economic conditions, and satellite-derived forest gain through Principal Component Analysis (PCA). We transformed the data to meet normality assumptions either through logarithmic or square-root transformations.

At the landscape scale (lan), we created a Random Forest (RF) regression model using principal components of socio-ecological drivers as predictors and the annual forest gain (% year^{-1}) as the response variable. Due to the *p>n problem* of machine learning, related to a low number of rows, we reduced the feature dimensionality through PCA prior to fitting RF models. We performed a PCA for each group of environmental drivers: socio-economic (Table B2.1 Supplementary Materials), climate (Tables B2.2, B2.3 Supplementary Materials), and topographic (Table B2.4 Supplementary Materials), considering statistically significant principal components (PCs) that accounted for 75% of the variability. We measured statistical significance using p-values derived from a Monte Carlo permutation test on 10 000 runs with randomized data. We adopted a nested fivefold repeated spatial cross-validation to tune the RF model and evaluate its performance (Lovelace et al., 2019). For tuning hyperparameters (number of variables tried at each split, number of trees, minimum node size, and sample fraction), we developed an optimization algorithm based on a random search within a search space using 50 steps. To evaluate the models and select the model of best fit, an outer 3-fold cross-validation resampling strategy was used. Mean absolute error (MAE), mean squared error (MSE), and root-mean-square error (RMSE) were estimated by averaging the values obtained from the resulting 300 models. We assessed variable importance of the RF model using the permutation method (Breiman, 2001). We ran a second RF regression using the main variables associated with the most influential PCs to derive partial dependence plots (Goldstein et al., 2015) on the marginal effect of each variable on the annual forest gain rate.

PCA was conducted in PC-Ord v7.08 (McCune & Mefford, 1999). All other analyses were conducted in R version 4.1.2 (R Core Team, 2021). See Table B2.5 in Supplementary Materials for R packages used in the analyses.

2.3 Results

2.3.1 Spatiotemporal characteristics of case studies

We retrieved 42 papers that met our inclusion criteria. We observed an increasing trend of publication until 2020, with more than 50% of publications occurring between 2007 and 2017. The topic is strongly multidisciplinary, with multiple research objectives including ecosystem services evaluation (e.g., Schirpke et al., 2013), natural disturbances risk analysis (e.g., Zgheib et al., 2020), land use change (e.g., Tasser et al., 2017), species distribution modelling (e.g., Carlson et al., 2014a), and assessment of reforestation drivers (e.g., Garbarino et al., 2020). We chose 80 eligible case studies according to our requirements (Figure 2.2). The total extent covered by the 80 sites was 9257 km^2, corresponding to 5.17% of the whole Alpine region surface area (~ 179 014 km^2) and the mean distance between each landscape was 210.71 km. The case studies belonged to 6 different countries (Austria, France, Germany, Italy, Slovenia, Switzerland), 25 different provinces (NUTS level 3), with Italy emerging as the most represented country (s = 48, 60% of the total). We observed 17 provinces with more than one case study, with Trento (s = 16) and Bolzano-Bozen (s = 14) being the most studied. In addition to having the greatest number of study landscapes, Italy had the largest landscapes in terms of mean surface area. However, Austrian and French studies investigated LULCC with a longer temporal extent and a finer temporal resolution, often integrating historical maps (Figure 2.3a). On average, we observed a comparable number of land cover classes within countries. Countries were similar in the numbers and types of case study characteristics used (Figure 2.3a).

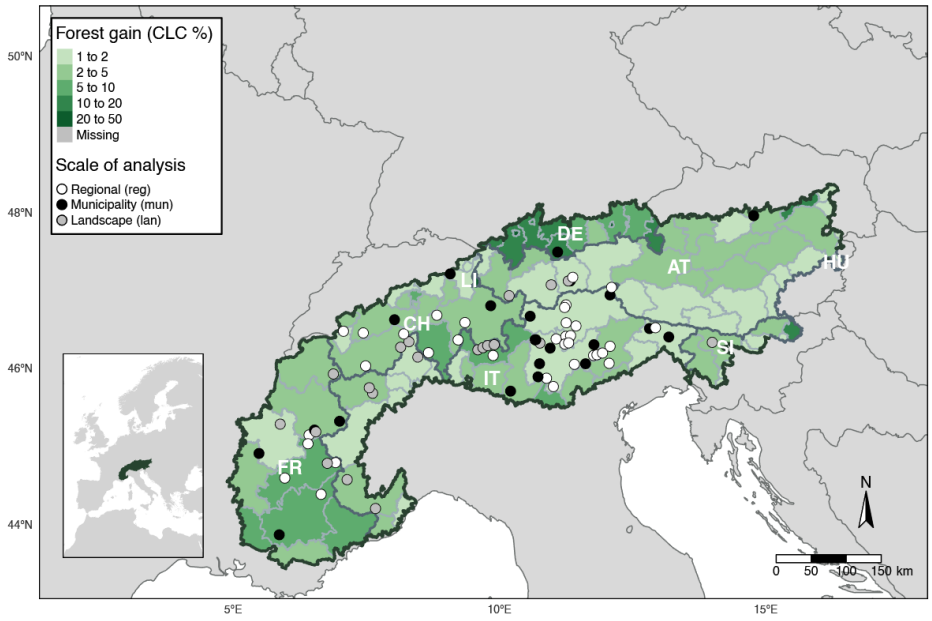

FIGURE 2.2. Location of the case studies within the Alpine region (Alpine convention perimeter). Point symbol shading indicates the analytical scale. Green polygon shading shows the forest gain at NUTS lv3 derived from Corine Land Cover for the period 2000-2018. The inset map shows the location of the European Alps within Europe. AT = Austria, CH = Switzerland, DE = Germany, FR = France, IT = Italy, LI = Liechtenstein, SI = Slovenia.

The largest site was Gemona (Italy; 114 800 ha), the smallest was Längenfeld (Austria; 100 ha) (Figure 2.3b). Most of the studies derived forest gain data from both historical maps and aerial photos. Historical maps included the Siegfried map (Topographic Atlas of Switzerland), the Hasburgic map, and the Napoleonic cadastral map. Temporal extent (last year – first year) ranged from 12 years (Agordino, Italy) to 195 years (Waidhofen, Austria), with a mean value of 103 years and a standard deviation of 54 years (Figure 2.3c). Regarding the temporal resolution, most studies (n = 25) adopted 2 or 4 different maps to analyse forest cover dynamics, with a maximum of 8 different time steps observed and an average value of 3.5 ± 1.5 (Figure 2.3d). Most studies (n = 14) examined 5 land cover classes, with a minimum of 2, a maximum of 21, and a mean of 5.8 ± 3.0 (Figure 2.3e).

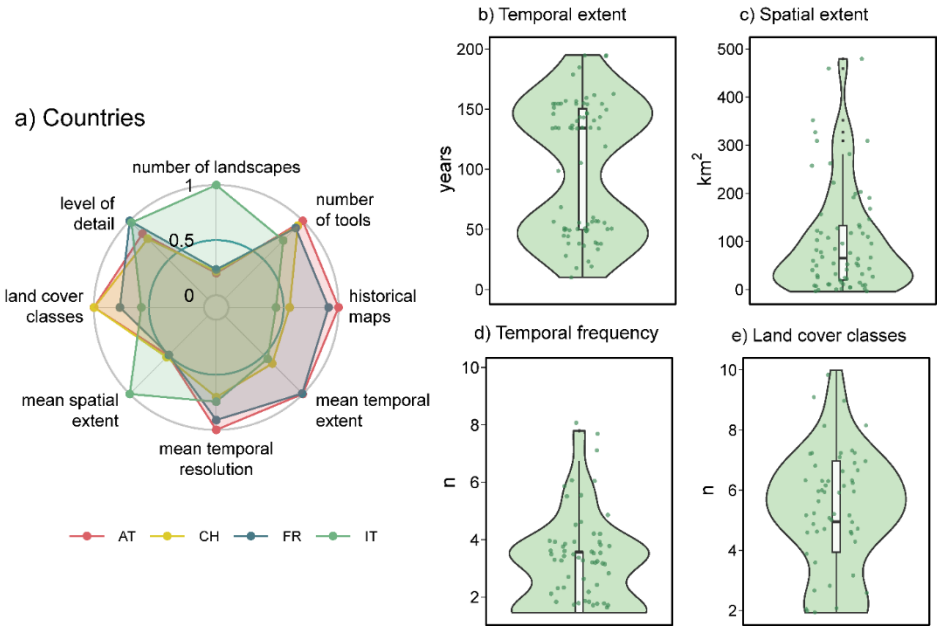

FIGURE 2.3. Summary of case study characteristics (s = 80). (a) Radar plot on nine variables grouped by country (number of tools = number of different data sources and tools used to derive land cover information, historical maps = number of studies using historical maps, land cover classes = number of analysed land cover classes, level of detail = level of details about reforestation and spatial positioning provided for the study sites). Sources of land cover information. Violin plots and box plots display frequency distributions, median, and interquantile range for the (b) spatial extent of the landscapes; (c) temporal extent of the studies; (d) temporal frequency; (e) number of land cover classes.

2.3.2 Socio-economic drivers at the municipality scale

We analysed the relationship between observed forest gain and a set of socio-economic drivers at the municipality scale through principal component analysis. The first and second components accounted for 34.4 and 16.3% of the total variation, respectively, while the third component accounted for the 14.8% (Figure 2.4, Figure C2.1 and Table C2.1 Supplementary Materials). The first PC axis was strongly associated with long-term (i.e., more than 60 years) dynamics such as the observed forest gain (negative association) and population (1961, 2020) and road density (positive association). The second component was mostly associated with recent dynamics such as job sectors (positive association with

agricultural/natural resource and manufacturing sectors employees, negative association with the service sector employees), recent forest change through CLC, and recent farm change. Sites that experienced a higher forest gain were likely to have had lower population both in 1961 and 2020 and to have more workers in the agricultural/natural resource sector. Manufacturing sector employees (Pearson's r = – 0.29), agricultural/natural resource sector employees (r = 0.27), road density (r = – 0.28), and population density in 1961 (r = – 0.26) emerged as the most correlated variables to the observed forest gain. Forest gain derived from CLC analysis of the last 20 years (2000-2018) appeared to be uncorrelated (perpendicular) to the observed forest gain rate (r = – 0.03) (Figure 2.4).

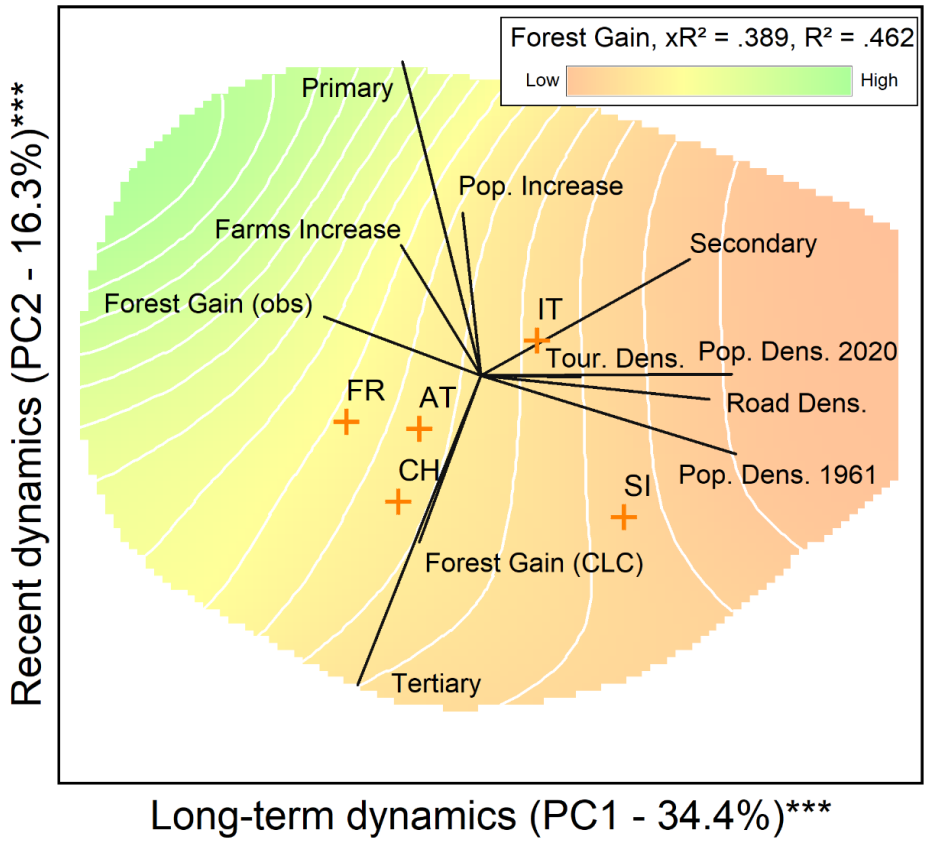

FIGURE 2.4. Results of the principal component analysis at the municipality scale (s = 108). PC1 vs PC2. Principal components were significant (p < 0.001, Monte Carlo permutation test on 10 000

runs with randomized data). Country centroids are shown as orange crosses: AT = Austria, CH = Switzerland, FR = France, IT = Italy, SI = Slovenia. Forest gain gradient is represented as a 3D response surface and contour lines obtained through non-parametric regression against PC1 and PC2 scores. Flexibility was optimized according to the highest cross-validated fit (xR^2).

2.3.3 Socio-ecological drivers at the landscape scale

Prior to fitting the landscape-scale RF regression model, we reduced the number of variables through a principal component analysis, retrieving 8 principal components (Appendix B and Figure C2.2 Supplementary Materials). The climate PC associated with precipitation (Precipitation) was the most important in explaining forest gain, followed by human related variables (Remoteness and Population), and topography (especially the second PC, Topography_2). Climate change proved unimportant for predicting the forest gain rate (Figure 2.5a). Due to the small number of observations at this scale (s = 21), errors calculated through the 300 iterations are quite noticeable (Figure C2.3 Supplementary Materials). From the second RF regression model, we calculated partial-dependence plots for the main drivers of each of the four most important PCs. In particular, we assessed annual median precipitation (Precipitation; Figure 2.5b), minimum distance from towns (Remoteness; Figure 2.5c), population density of 1961 (Population; Figure 2.5d), and mean heat load index (Topography_2; Figure 2.5e). Forest gain rate was generally higher in landscapes with lower annual precipitation and population density, more than 50 km from towns, and on south-facing slopes.

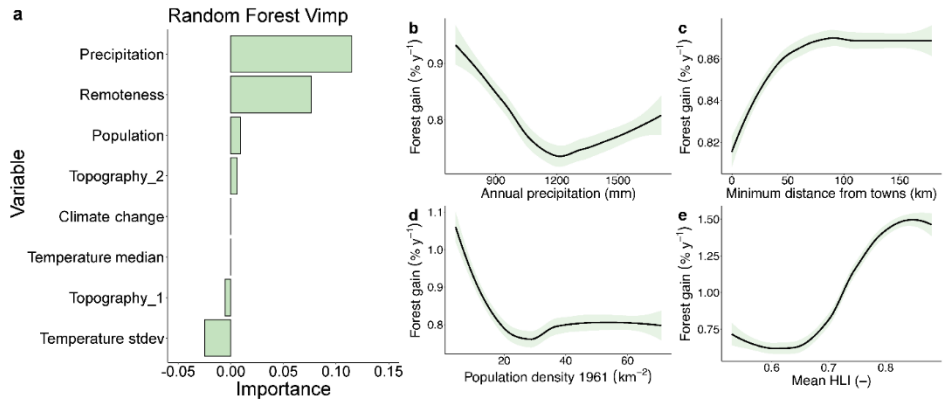

FIGURE 2.5. Results of the RF regressions at the landscape scale (s = 21). (a) Variable importance of the RF regression on the principal components; partial dependence plots on (b) annual precipitation, (c) minimum distance from towns, (d) population density of 1961, (e) mean HLI.

2.4 Discussion

2.4.1 Reforestation rate and pattern across the Alps

Post-abandonment natural reforestation is a widespread phenomenon in many countries of the Northern hemisphere (Ellis et al., 2013; Haddaway et al., 2014; Crawford et al., 2022). The Alps provides an excellent study region for investigating this global phenomenon due to its long history of land use followed by more than one century of abandonment (MacDonald et al., 2000; Mietkiewicz et al., 2017). In our literature review, we observed a good availability of spatiotemporal forest cover data for the Alps. The case studies utilized covered a surface area of more than 5% of the Alpine Convention area, and inclusion of grey literature studies would most likely have encompassed a greater area. High research interest in spatial analysis of reforestation has resulted in a multidisciplinary set of analytical perspectives and methods for us to synthesize in our review. We observed an unbalanced spatial density and location of case studies, probably due to the magnitude and perception of human action (Haddaway et al., 2014), with the Western Alps showing the highest density of studies. It is possible that the increased concern regarding post-abandonment reforestation and its ecological and economic effects have been greater in the

Western rather than in the Eastern Alps because depopulation and rural exodus took place earlier in the Western sector (Batzing et al., 1996). For instance, Tasser et al. (2017) reported the twenty years between 1960 and 1980 as the most relevant period of land abandonment for the Stubai Valley (AT), consistent with the twenty years indicated by Krausmann et al. (2003) for all of Austria (1950-1970). Furthermore, the Slovenian Julian Alps experienced land abandonment after 1945, only a half-century after the less favourable land was tilled at the beginning of the 20th century (Andrič et al., 2010). Conversely, in the Western Alps the industrial sector had already begun to supersede agriculture by the second half of the 19th century (Batzing et al., 1996; Farvacque et al., 2019).

Given the generally long-time frames since land abandonment has occurred within the region, it is not surprising that we observed an average temporal extent of around a century from among the case studies. This time span may be particularly relevant for studies of post-abandonment reforestation, since the mean time required by passive restoration to recover biogeochemical functions has been measured globally as 35.5 ± 33.1 years, depending on factors such as ecosystem resilience, the type and intensity of land use legacy, and local edaphic conditions (Meli et al., 2017). Therefore, satellite remote sensing timeseries (e.g., Landsat) and derived products (e.g., Corine Land Cover , CLC), spanning the last 30-40 years and lacking in fine spatial resolution, provide only a partial insight into this global process. Historical maps and aerial photos are fundamental tools to assess ecological responses to past land abandonment, given their longer temporal extent and finer (i.e., 1-10m) spatial resolution (Garbarino et al., 2020). The first aerial photos emerged around World War II, and thus correspond well with the timing of abandonment in many landscapes. On historical aerial photos, cultural landscapes are often recognizable by the presence of patches of pasture enclosed in a forest matrix (Orlandi et al., 2016). The spatial mosaic of cultural landscapes is generally characterized by an interspersion of small patches with several ecological functions and structures. For this reason, they are often described as hotspots of ecosystem services worldwide (e.g., larch wood pastures

in Austrian landscapes; Schirpke et al., 2013). Since post-abandonment reforestation usually consists of in-filling of these non-forested patches, a fine spatial resolution is crucial to monitor the loss of ecotones and the spatial simplification of a landscape.

Another important temporal feature to consider is the temporal resolution (i.e., the frequency of temporal observations for a given landscape). Even if satellite-based products have a higher temporal resolution (i.e., weeks/days), decadal land cover maps derived from aerial photos have the potential to inform managers and planners (Schneeberger et al., 2007; Carlson et al., 2014b) by capturing the nonlinearity of past LULCCs for more accurate prediction of future change scenarios (Carlson et al., 2014a). For instance, a series of aerial photos led to improved accuracy of future Business as Usual LULCC scenarios, by disentangling land use change- and climate change-dominated periods (Anselmetto et al., 2021). Also, correlations between temporal trade-offs of ecosystem services and the spatial arrangement of the landscape can be detected using multiple time steps of aerial photography (Egarter Vigl et al., 2016).

2.4.2 Drivers of reforestation across spatial scales

Land abandonment is associated with regional socio-economic processes, but it also depends on conditions particular to a given landscape (i.e., climate, topography, infrastructures) that increase cultivation costs (Ameztegui et al., 2016; Crawford et al., 2022). On average, forest area increased at a net rate of +0.64% $year^{-1}$ across the case studies. This value was higher than the one described by Bebi et al. (2017) for the entire Alps (+0.37% $year^{-1}$ from 1930) and the average annual rate of change reported by FAO (2020) for Europe (+0.29% $year^{-1}$ from 1990 - 2020). At the municipality scale (mun), road and population density in 1961 had a strong negative correlation with forest gain. A sparse road network influences the cultivation cost, and marginal areas with weak infrastructure are the first to be abandoned (MacDonald et al., 2000; Ren et al., 2019). These abandonment patterns have been defined in the Forest Transition Theory (Mather, 1992; Díaz et al., 2011). Sometimes, good road infrastructure

and increase in population lead to recultivation of abandoned areas (Crawford et al., 2022). We found a weak correlation between satellite-derived forest gain (2000-2018) and observed forest gain in the last century. This confirms our hypothesis that long-lasting human exploited areas that experienced a centennial land abandonment (i.e., Alps, Japanese *Satoyama* landscapes, or Spanish *dehesa*), characterised by a complex interspersion of patches, should be evaluated with a longer temporal extent and finer spatial resolution. Recent satellite-derived products suffer from a temporal mismatch between the diachronic analysis period and the duration of secondary successional processes.

The proportion of workers employed in the primary (i.e., agriculture and forestry) and secondary sector (i.e., industry) were respectively positively and negatively correlated to forest gain. This contradicts other findings that showed how national increase of workers in the off-forest sectors (i.e., secondary and tertiary) displaces land use outside borders, leading to an off-set of deforestation in other countries of the world and promoting reforestation (Pendrill et al., 2019). Employment data used in the study were taken for the year 2000, representing a momentary condition in a dynamic process. Moreover, mountain municipalities often occupy both the bottom part of a valley and its slopes, and the depopulation dynamics of a single farm, village, or slope could have affected reforestation rate more than depopulation when considered at the scale of the entire municipality. Nevertheless, analyses at the municipality scale are useful for landscape planning and decision systems in view of the increasing debate on wildness versus wilderness and passive restoration management (e.g., Meli et al., 2017; Ward, 2019; Schulte to Bühne et al., 2022).

Very few studies, from our literature review, provided spatially explicit data to perform exhaustive meta-analysis at the landscape scale (lan) because land cover maps were often an intermediate product of the analysis. Therefore, we used the annual forest gain rate as a proxy for landscape scale forest dynamics. Given the different time span of observations, the low number of landscapes, and the inability to accurately locate the case studies, our results offer a partial insight

into global change effects on forest dynamics. Nevertheless, our results highlighted agriculturally unfavourable areas as hotspots of post-abandonment reforestation. In particular, sites characterized by a lower precipitation were more likely to experience intense forest gain, probably because landscapes with harsher ecological conditions and lower productivity are prone to be abandoned first, thus leading to a longer process of natural reforestation (MacDonald et al., 2000; Garbarino et al., 2020). It is interesting to note the increase of forest gain with an annual precipitation higher than 1200 mm. This high reforestation rate associated to a high primary production might occur in relatively high-elevation areas (hence, higher primary production) that had been agriculturally marginal by virtue of stony soils, colder temperatures, or shorter growing seasons. Human variables emerged as the second (i.e., remoteness) and third (i.e., population) most important driver, with higher forest gain in remote areas of low population that are also far from towns. Regarding topographical features, higher values of forest gain associated with high heat load values indicate a suitability for reforestation of southern slopes, where croplands and pasture had been concentrated in the past (Garbarino et al., 2020).

Climate change was one of the least important variables in the RF model. This supports the hypothesis that broad scale dynamics such as reforestation and forest gain are still mostly driven by land abandonment rather than climate change, even if a shift towards climatic-driven changes is expected (Martin et al., 2013; Ameztegui et al., 2016; Anselmetto et al., 2021). Global change affects abandoned mountain areas generating divergent processes of vegetation dynamics, with an in-filling of abandoned open areas at lower elevations, but with fragmentation of open areas and tree encroachment in the upper elevations (Gehrig-Fasel et al., 2007; Kulakowski et al., 2011; Anselmetto et al., 2021). In the lower mountain elevations, the rate of woodland expansion is gradually decelerating due to saturation of available space (Campagnaro et al., 2017). Above the treeline, active shrub and tree encroachment on semi-natural and natural alpine grasslands and unvegetated areas are likely due to warmer

conditions during the growing season related to climate change (Bani et al., 2019; Choler et al., 2021).

2.4.3 Methodological insights: a plea for consistency

Natural rewilding of landscapes with a long history of intensive human land use may create novel ecosystem conditions that require adequate monitoring, planning, and management to provide the services demanded by the society (Ward, 2019; Schulte to Bühne et al., 2022). Hence, there is a relevant need to quantify and predict where and when reforestation is likely to occur, and at what rate. Despite the availability of numerous case studies in the Alps, we observed the absence of a common protocol to analyse post-abandonment reforestation. Some papers encompassed more than one landscape (e.g., Zimmermann et al., 2010; Egarter Vigl et al., 2016; Tattoni et al., 2017; Garbarino et al., 2020) and integrated data from different previous studies, but without a regional scale approach. For this reason, we highlight the need for a harmonised geodatabase produced through a common land cover classification. We believe that a harmonised and dynamic land use change geodatabase encompassing an entire mountain region could serve as an accurate foundation for answering to several socioecological questions with global implication.

Landscape planning requires a profound knowledge of the land use history to assess forest ecosystem resilience and trajectories of change (Garbarino et al., 2020; McDowell et al., 2020). For instance, it would be useful for species distribution models to integrate dynamic scenarios of LULCC, characterized by fine spatial resolution and long temporal extent, with alternative climate scenarios (Martin et al., 2013; Carlson et al., 2014a). Policy decisions may benefit from a multi-scale assessment of reforestation (Schulte to Bühne et al., 2022). Regionally, an in-depth analysis of reforestation suitability can be used to quantify wall-to-wall reforestation probability or ecosystem services provision maps using logistic regressions with models trained on long-term data at the landscape scale (e.g., Díaz et al., 2011; Pellissier et al., 2012; Gelabert et al., 2022). This information may be integrated at the landscape scale, where

reconstructing past dynamics of change may improve resources allocation and contrast land use legacies and climate change (Holl & Aide, 2011; Garbarino et al., 2020). A common LULCC dataset for the Alps can provide a monitoring tool for mountain ecosystem services such as cultural values, carbon sequestration, hydrologic regime, protection from natural disturbances, biodiversity, and conservation. Being able to reconstruct the history of LULCC and predict future scenarios of post-abandonment reforestation in mountain regions can drive the choice between passive restoration (i.e., rewilding) and active restoration of semi-natural ecosystems such as grasslands and agroforestry systems (Navarro & Pereira, 2012).

2.5 Conclusions

Abandoned rural landscapes in high incomes areas of the world such as the European Alps are expected to face a shift from land use change- to climate change-dominated stages (Martin et al., 2013). Indeed, assessing the long-term history of change and its land use legacy on forest dynamics should be the first step to plan future resilient landscapes (Beller et al., 2020; Garbarino & Weisberg, 2020). We observed several case studies across the Alps dealing with post-abandonment natural reforestation with the potential to fulfil this aim. The multidisciplinary nature of this topic is represented by studies which utilized disparate data sources and quantitative tools (e.g., historical maps, aerial photos, GIS environment) and research objectives (e.g., quantification of forest gain, driver of reforestation, future forecasting, analysis of multiple ecosystem services). Many studies have encompassed more than 100 years of change using a fine spatial resolution (i.e., 1-10 m) and with the potential to have a sufficient temporal resolution (i.e., 10-20 years). The importance of anthropic drivers for post-abandonment natural reforestation appeared both at the municipality and landscape scale. Population density, both in the past and currently, and the remoteness (i.e., road availability, distance to cities) of the municipalities and landscapes clearly emerged from our analyses, outdoing the role of climate change-related variables. In particular, reforestation rate was greatest in south-

facing slopes of dry landscapes within remote and sparsely populated municipalities.

We advocate for a dynamic harmonised LULCC geodatabases integrating landscape case studies across the entire mountain region. Despite the high availability of data for the Alpine region, a comprehensive fine scale analysis across the entire region is still lacking. Therefore, there is a need to incorporate case studies from the grey literature and new landscapes where the density of available data seems scarce. We believe such a database can provide the foundation for predicting future trajectories of change both within the same region (e.g., Gelabert et al., 2022) and in other mountain regions where post-abandonment natural reforestation is a more recent process (i.e., China, India; Ren et al., 2019).

Acknowledgments

We thank ARPA Piemonte and CINECA for funding N.A. PhD program through the Highlander Project co-financed by the Connecting European Facility Programme of the European Union under Grant agreement n° INEA/CEF/ICT/A2018/1815462.

References

Alpine Convention. Alpine Convention Perimeter (2018). https://www.atlas.alpconv.org/layers/geonode_data:geonode:Alpine_Convention_Perimeter_2018_v2

Ameztegui, A., Coll, L., Brotons, L., & Ninot, J. M. (2016). Land-use legacies rather than climate change are driving the recent upward shift of the mountain tree line in the Pyrenees. *Global Ecology and Biogeography*, 25(3), 263–273.

Andrič, M., Martinčič, A., Štular, B., Petek, F., & Goslar, T. (2010). Land-use changes in the Alps (Slovenia) in the fifteenth, nineteenth and twentieth centuries AD: A comparative study of the pollen record and historical data. *The Holocene*, 20(7), 1023–1037.

Anselmetto, N., Sibona, E. M., Meloni, F., Gagliardi, L., Bocca, M., & Garbarino, M. (2021). Land Use Modeling Predicts Divergent Patterns of Change Between

Upper and Lower Elevations in a Subalpine Watershed of the Alps. *Ecosystems*, 1-16.

Antrop, M. (2005). Why landscapes of the past are important for the future. *Landscape and Urban Planning*, 70(1–2), 21–34.

Bani, L., Luppi, M., Rocchia, E., Dondina, O., & Orioli, V. (2019). Winners and losers: How the elevational range of breeding birds on Alps has varied over the past four decades due to climate and habitat changes. *Ecology and Evolution*, 9(3), 1289–1305.

Barbet-Massin, M., & Jetz, W. (2015). The effect of range changes on the functional turnover, structure and diversity of bird assemblages under future climate scenarios. *Global Change Biology*, 21(8), 2917-2928.

Batzing, W., Perlik, M., & Dekleva, M. (1996). Urbanization and Depopulation in the Alps. *Mountain Research and Development*, 16(4), 335.

Bebi, P., Seidl, R., Motta, R., Fuhr, M., Firm, D., Krumm, F., … & Kulakowski, D. (2017). Changes of forest cover and disturbance regimes in the mountain forests of the Alps. *Forest Ecology and Management*, 388:43–56.

Beller, E. E., McClenachan, L., Zavaleta, E. S., & Larsen, L. G. (2020). Past forward: Recommendations from historical ecology for ecosystem management. *Global Ecology and Conservation*, 21, e00836.

Betts, M. G., Wolf, C., Pfeifer, M., Banks-Leite, C., Arroyo-Rodríguez, V., Ribeiro, D. B., … & Ewers, R. M. (2019). Extinction filters mediate the global effects of habitat fragmentation on animals. *Science*.

Breiman, L. (2001). Random Forests. *Machine Learning*, 45(1), 5–32.

Büntgen, U., Myglan, V. S., Ljungqvist, F. C., McCormick, M., Di Cosmo, N., Sigl, M., …& Kirdyanov, A. V. (2016). Cooling and societal change during the Late Antique Little Ice Age from 536 to around 660 AD. *Nature Geoscience*, 9(3), 231–236.

Campagnaro, T., Frate, L., Carranza, M. L., & Sitzia, T. (2017). Multi-scale analysis of alpine landscapes with different intensities of abandonment reveals similar spatial pattern changes: Implications for habitat conservation. *Ecological Indicators*, 74, 147–159.

Carcaillet, C. (1998). A spatially precise study of Holocene fire history, climate and human impact within the Maurienne valley, North French Alps. *Journal of ecology*, 86(3), 384-396.

Carcaillet, C., Ali, A.A., Blarquez, O., Genries, A., Mourier, B. & Bremond, L. (2009) Spatial variability of fire history in subalpine forests: from natural to cultural regimes. *Ecoscience*, 16, 1–12.

Carlson, B. Z., Georges, D., Rabatel, A., Randin, C. F., Renaud, J., Delestrade, A., … & Thuiller, W. (2014a). Accounting for tree line shift, glacier retreat and primary succession in mountain plant distribution models. *Diversity and Distributions*, 20(12), 1379–1391.

Carlson, B. Z., Renaud, J., Biron, P. E., & Choler, P. (2014b). Long-term modeling of the forest–grassland ecotone in the French Alps: Implications for land management and conservation. *Ecological Applications*, 24(5), 1213–1225.

Chapron, G., Kaczensky, P., Linnell, J. D. C., Von Arx, M., Huber, D., Andrén, H., … & Boitani, L. (2014). Recovery of large carnivores in Europe's modern human-dominated landscapes. *Science*, 346(6216), 1517–1519.

Choler, P., Bayle, A., Carlson, B. Z., Randin, C., Filippa, G., & Cremonese, E. (2021). The tempo of greening in the European Alps: Spatial variations on a common theme. *Global Change Biology*, 27(21), 5614–5628.

Crawford, C. L., Yin, H., Radeloff, V. C., & Wilcove, D. S. (2022). Rural land abandonment is too ephemeral to provide major benefits for biodiversity and climate. *Science Advances*, 8(21), eabm8999.

Davoli, M., Ghoddousi, A., Sabatini, F. M., Fabbri, E., Caniglia, R., & Kuemmerle, T. (2022). Changing patterns of conflict between humans, carnivores and crop-raiding prey as large carnivores recolonize human-dominated landscapes. *Biological Conservation*, 269, 109553.

Díaz, G. I., Nahuelhual, L., Echeverría, C., & Marín, S. (2011). Drivers of land abandonment in Southern Chile and implications for landscape planning. *Landscape and Urban Planning*, 99(3–4), 207–217.

Egarter Vigl, L., Schirpke, U., Tasser, E., & Tappeiner, U. (2016). Linking long-term landscape dynamics to the multiple interactions among ecosystem services in the European Alps. *Landscape Ecology*, 31(9), 1903–1918.

Ellis, E. C., Kaplan, J. O., Fuller, D. Q., Vavrus, S., Goldewijk, K. K., & Verburg, P. H. (2013). Used planet: A global history. *Proceedings of the National Academy of Sciences*, 110(20), 7978–7985.

European Commission (1994). Directorate-General for the Information Society and Media, Directorate-General for Environment. *Corine land cover : Guide technique*, Publications Office.

Fagan, M. E., Kim, D. H., Settle, W., Ferry, L., Drew, J., Carlson, H., ... & Ordway, E. M. (2022). The expansion of tree plantations across tropical biomes. *Nature Sustainability*, 5(8), 681-688.

FAO (2020). *Global Forest Resources Assessment 2020: Main report*. Rome.

FAOSTAT (2022). FAO. https://www.fao.org/faostat/en/

Farvacque, M., Lopez-Saez, J., Corona, C., Toe, D., Bourrier, F., & Eckert, N. (2019). How is rockfall risk impacted by land-use and land-cover changes? Insights from the French Alps. *Global and Planetary Change*, 174, 138–152.

Fauquette, S., Suc, J. P., Médail, F., Muller, S. D., Jiménez-Moreno, G., Bertini, A., ... & De Beaulieu, J. L. (2018). The Alps: a geological, climatic and human perspective on vegetation history and modern plant diversity. *Mountains, climate and biodiversity*, 413-428.

Favilli, F., Cherubini, P., Collenberg, M., Egli, M., Sartori, G., Schoch, W., & Haeberli, W. (2010). Charcoal fragments of Alpine soils as an indicator of landscape evolution during the Holocene in Val di Sole (Trentino, Italy). *The Holocene*, 20(1), 67-79.

Fischer, J., Hartel, T., & Kuemmerle, T. (2012). Conservation policy in traditional farming landscapes: Conserving traditional farming landscapes. *Conservation Letters*, 5(3), 167–175.

Garbarino, M., Morresi, D., Urbinati, C., Malandra, F., Motta, R., Sibona, E. M., … & Weisberg, P. J. (2020). Contrasting land use legacy effects on forest landscape dynamics in the Italian Alps and the Apennines. *Landscape Ecology*, 35, 2679-2694.

Garbarino, M., & Weisberg, P. J. (2020). Land-use legacies and forest change. *Landscape Ecology*, 35(12), 2641-2644.

Gehrig-Fasel, J., Guisan, A., & Zimmermann, N. E. (2007). Tree line shifts in the Swiss Alps: climate change or land abandonment? *Journal of vegetation science*, 18(4), 571-582.

Gelabert, P. J., Rodrigues, M., Vidal-Macua, J. J., Ameztegui, A., & Vega-Garcia, C. (2022). Spatially explicit modeling of the probability of land abandonment in the Spanish Pyrenees. *Landscape and Urban Planning*, 226, 104487.

Goldstein A, Kapelner A, Bleich J, Pitkin E (2015) Peeking inside the black box: visualizing statistical learning with plots of individual conditional expectation. *Journal of Computational and Graphical Statistics*, 24, 44–65.

Haddaway, N. R., Styles, D., & Pullin, A. S. (2014). Evidence on the environmental impacts of farmland abandonment in high altitude/mountain regions: A systematic map. *Environmental Evidence*, 3(1), 17.

Halada, L., Evans, D., Romão, C., & Petersen, J. E. (2011). Which habitats of European importance depend on agricultural practices? *Biodiversity and Conservation*, 20(11), 2365–2378.

Holl, K. D., & Aide, T. M. (2011). When and where to actively restore ecosystems? *Forest Ecology and Management*, 261(10), 1558–1563.

Isotta, F. A., Frei, C., Weilguni, V., Perčec Tadić, M., Lassègues, P., Rudolf, B., … & Vertačnik, G. (2014). The climate of daily precipitation in the Alps: Development and analysis of a high-resolution grid dataset from pan-Alpine rain-gauge data. *International Journal of Climatology*, 34(5), 1657–1675.

Krausmann, F., Haberl, H., Schulz, N. B., Erb, K.-H., Darge, E., & Gaube, V. (2003). Land-use change and socio-economic metabolism in Austria—Part I: Driving forces of land-use change: 1950–1995. *Land Use Policy*, 20(1), 1–20.

Kuemmerle, T., Levers, C., Erb, K., Estel, S., Jepsen, M. R., Müller, D., ... & Reenberg, A. (2016). Hotspots of land use change in Europe. *Environmental research letters*, 11(6), 064020.

Kulakowski, D., Bebi, P., & Rixen, C. (2011). The interacting effects of land use change, climate change and suppression of natural disturbances on landscape forest structure in the Swiss Alps. *Oikos*, 120(2), 216–225.

LAU. (2021) Local Administrative Units. EUROSTAT. https://ec.europa.eu/eurostat/web/nuts/local-administrative-units

Lehsten, V., Sykes, M. T., Scott, A. V., Tzanopoulos, J., Kallimanis, A., Mazaris, A., ... & Vogiatzakis, I. (2015). Disentangling the effects of land-use change, climate and CO2 on projected future European habitat types. *Global Ecology and Biogeography*, 24(6), 653-663.

Lewis, S. L., & Maslin, M. A. (2015). Defining the Anthropocene. *Nature*, 519(7542), 171–180.

Lieskovský, J., & Lieskovská, D. (2021). Cropland abandonment in Slovakia: Analysis and comparison of different data sources. *Land*, 10(4), 334.

Lovelace, R., Nowosad, J., & Muenchow, J. (2019) *Geocomputation with R*. Chapman and Hall/CRC, Boca Raton, ISBN 978-11-3830-451-2

MacDonald, D., Crabtree, J. R., Wiesinger, G., Dax, T., Stamou, N., Fleury, P ... & Gibon, A. (2000). Agricultural abandonment in mountain areas of Europe: Environmental consequences and policy response. *Journal of Environmental Management*, 59(1), 47–69.

Mantero, G., Morresi, D., Marzano, R., Motta, R., Mladenoff, D. J., & Garbarino, M. (2020). The influence of land abandonment on forest disturbance regimes: A global review. *Landscape Ecology*, 35(12), 2723–2744.

Martin, Y., Van Dyck, H., Dendoncker, N., & Titeux, N. (2013). Testing instead of assuming the importance of land use change scenarios to model species distributions under climate change. *Global Ecology and Biogeography*, 22(11), 1204–1216.

Martinuzzi, S., Gavier-Pizarro, G. I., Lugo, A. E., & Radeloff, V. C. (2015). Future Land-Use Changes and the Potential for Novelty in Ecosystems of the United States. *Ecosystems*, 18(8), 1332–1342.

Mather, A. S. (1992). The forest transition. *Area*, 367-379.

McCune, B., & Mefford, M.J. (1999). *PC-ORD. Multivariate analysis of ecological data, Vers. 7. User's Guide*. Corvallis, Oregon: MjM Software Design.

McDowell, N. G., Allen, C. D., Anderson-Teixeira, K., Aukema, B. H., Bond-Lamberty, B., Chini, L., … & Xu, C. (2020). Pervasive shifts in forest dynamics in a changing world. *Science*.

Meli, P., Holl, K. D., Benayas, J. M. R., Jones, H. P., Jones, P. C., Montoya, D., & Mateos, D. M. (2017). A global review of past land use, climate, and active vs. Passive restoration effects on forest recovery. *PLOS ONE*, 12(2), e0171368.

Mietkiewicz, N., Kulakowski, D., Rogan, J., & Bebi, P. (2017). Long-term change in sub-alpine forest cover, tree line and species composition in the Swiss Alps. *Journal of Vegetation Science*, 28(5), 951–964.

Morresi, D., Marzano, R., Lingua, E., Motta, R., & Garbarino, M. (2022). Mapping burn severity in the western Italian Alps through phenologically coherent reflectance composites derived from Sentinel-2 imagery. *Remote Sensing of Environment*, 269, 112800.

Navarro, L. M., & Pereira, H. M. (2012). Rewilding Abandoned Landscapes in Europe. *Ecosystems*, 15(6), 900–912.

Newbold, T. (2018). Future effects of climate and land-use change on terrestrial vertebrate community diversity under different scenarios. *Proceedings of the Royal Society B*, 285(1881), 20180792

NUTS. (2021) Nomenclature of Territorial Units for Statistics. EUROSTAT. https://ec.europa.eu/eurostat/web/nuts/nuts-maps

Oliver, T. H., & Morecroft, M. D. (2014). Interactions between climate change and land use change on biodiversity: attribution problems, risks, and opportunities. *Wiley Interdisciplinary Reviews: Climate Change*, 5(3), 317-335

Orlandi, S., Probo, M., Sitzia, T., Trentanovi, G., Garbarino, M., Lombardi, G., & Lonati, M. (2016). Environmental and land use determinants of grassland patch diversity in the western and eastern Alps under agro-pastoral abandonment. *Biodiversity and Conservation*, 25(2), 275–293.

Pazúr, R., & Bolliger, J. (2017). Land changes in Slovakia: Past processes and future directions. *Applied Geography*, 85, 163-175.

Pellissier, L., Anzini, M., Maiorano, L., Dubuis, A., Pottier, J., Vittoz, P., & Guisan, A. (2013). Spatial predictions of land-use transitions and associated threats to biodiversity: The case of forest regrowth in mountain grasslands. *Applied Vegetation Science*, 16(2), 227-236.

Pendrill, F., Persson, U. M., Godar, J., & Kastner, T. (2019). Deforestation displaced: Trade in forest-risk commodities and the prospects for a global forest transition. *Environmental Research Letters*, 14(5), 055003.

Perino, A., Pereira, H. M., Navarro, L. M., Fernández, N., Bullock, J. M., Ceauşu, S., C … & Wheeler, H. C. (2019). Rewilding complex ecosystems. *Science*, 364(6438), eaav5570.

Plieninger, T., Draux, H., Fagerholm, N., Bieling, C., Bürgi, M., Kizos, T., … & Verburg, P. H. (2016). The driving forces of landscape change in Europe: A systematic review of the evidence. *Land Use Policy*, 57, 204–214.

Pörtner, H. O., Roberts, D. C., Adams, H., Adler, C., Aldunce, P., Ali, E., ... & Fischlin, A. (2022). Climate change 2022: Impacts, adaptation and vulnerability. *IPCC Sixth Assessment Report*.

R Core Team (2021). *R: A language and environment for statistical computing*. R Foundation for Statistical Computing, Vienna, Austria.

Ramankutty, N., Heller, E., & Rhemtulla, J. (2010). Prevailing Myths About Agricultural Abandonment and Forest Regrowth in the United States. *Annals of the Association of American Geographers*, 100(3), 502–512.

Ren, C., Chen, L., Wang, Z., Zhang, B., Xi, Y., & Lu, C. (2019). Spatio–Temporal Changes of Forests in Northeast China: Insights from Landsat Images and Geospatial Analysis. *Forests*, 10(11), 937.

Schirpke, U., Leitinger, G., Tasser, E., Schermer, M., Steinbacher, M., & Tappeiner, U. (2013). Multiple ecosystem services of a changing Alpine landscape: Past, present and future. *International Journal of Biodiversity Science, Ecosystem Services & Management*, 9(2), 123–135.

Schirpke, U., Zoderer, B. M., Tappeiner, U., & Tasser, E. (2021). Effects of past landscape changes on aesthetic landscape values in the European Alps. *Landscape and Urban Planning*, 212, 104109.

Schneeberger, N., Bürgi, M., & Kienast, P. D. F. (2007). Rates of landscape change at the northern fringe of the Swiss Alps: Historical and recent tendencies. *Landscape and Urban Planning*, 80(1), 127–136.

Schulte to Bühne, H., Pettorelli, N., & Hoffmann, M. (2022). The policy consequences of defining rewilding. *Ambio*, 51(1), 93–102.

Seidl, R., Thom, D., Kautz, M., Martin-Benito, D., Peltoniemi, M., Vacchiano, G., … & Reyer, C. P. O. (2017). Forest disturbances under climate change. *Nature Climate Change*, 7(6), 395–402.

Tasser, E., Leitinger, G., & Tappeiner, U. (2017). Climate change versus land-use change—What affects the mountain landscapes more? *Land Use Policy*, 60, 60–72.

Tasser, E., Walde, J., Tappeiner, U., Teutsch, A., & Noggler, W. (2007). Land-use changes and natural reforestation in the Eastern Central Alps. *Agriculture, Ecosystems & Environment*, 118(1-4), 115-129.

Tattoni, C., Ianni, E., Geneletti, D., Zatelli, P., & Ciolli, M. (2017). Landscape changes, traditional ecological knowledge and future scenarios in the Alps: A holistic ecological approach. *Science of The Total Environment*, 579, 27–36.

Tinner, W., Conedera, M., Ammann, B., Lotter, A.F., 2005. Fire ecology north and south of the Alps since the last ice age. *The Holocene* 15, 1214–1226.

Uchida, K., Koyanagi, T. F., Matsumura, T., & Koyama, A. (2018). Patterns of plant diversity loss and species turnover resulting from land abandonment and

intensification in semi-natural grasslands. *Journal of Environmental Management*, 218, 622–629.

Ward, K. (2019). For wilderness or wildness? Decolonising rewilding. In N. Pettorelli, S. M. Durant, & J. T. du Toit (A c. Di), *Rewilding* (1st ed., pp. 34–54). Cambridge University Press.

Zgheib, T., Giacona, F., Granet-Abisset, A. M., Morin, S., & Eckert, N. (2020). One and a half century of avalanche risk to settlements in the upper Maurienne valley inferred from land cover and socio-environmental changes. *Global Environmental Change*, 65, 102149.

Zimmermann, P., Tasser, E., Leitinger, G., & Tappeiner, U. (2010). Effects of land-use and land-cover pattern on landscape-scale biodiversity in the European Alps. *Agriculture, Ecosystems & Environment*, 139(1), 13–22.

Supplementary Materials

Appendix A2 – European Alps LUC studies Database (EALUC)

TABLE A2.1. Alpine LUC studies database. References follow the table. AT = Austria, CH = Switzerland, DE = Germany, FR = France, IT = Italy, LI = Liechtenstein, SI = Slovenia. As source maps we report all sources of geospatial information listed by the papers; AP = Aerial photos, CM = Cadastral maps, HM = Historical maps, Sat = Satellite, TM = Topographic maps, TP = Terrestrial photos. In cases where papers report results for more than one landscape, first and last year refer to the oldest and the newest observations within all the landscapes. In cases where papers report results for more than one landscape, mean values of temporal extent, temporal frequency and spatial extent are reported. If the study analyses one landscape, values refer to the features of that landscape. Spatial resolution was reported only if provided in meters, not as a nominal scale.

PAPER	YEAR	JOURNAL	COUNTRIES	SOURCE MAPS	TEMPORAL MEAN EXTENT(years)	MEAN SPATIAL EXTENT(ha)	UPPER LEVEL OF ANALYSIS
Andrič et al.	2010	The Holocene	SI	HM, CM	179	8180	lv1,2,3
Anselmetto et al.	2021	Ecosystems	IT	AP	52	5500	lv1,2,3
Carlson et al.	2014a	Diversity and Distribution	FR	AP	56	12 200	lv1,2,3
Carlson et al.	2014b	Ecological Applications	FR	AP	61	15 000	lv1,2
Dalla Valle et al.	2009	Mountain Research and Development	IT	AP	12	65 916	lv1

Didier [1]	2001	Forest Ecology and Management	FR	HM, AP	86	5320	lv1,2,3
Egarter Vigl et al.	2016	Landscape Ecology	AT, CH, FR, IT	HM, AP	155	20 467	lv1,2
Fedrigotti et al.	2016	Global NEST Journal	IT	HM, AP	152	~ 20 000	lv1,2
Garbarino et al.	2006	IUFRO Landscape Ecology Conference	IT	AP	46	~ 4000	lv1,2,3
Garbarino et al.	2011	European Journal of Forest Research	IT	AP	42	1137	lv1,2,3
Garbarino et al.	2013	Landscape Ecology	IT	AP	44	3250	lv1,2,3
Garbarino et al.	2014	Journal of Mountain Science	IT	AP	46	4150	lv1,2,3
Garbarino et al.	2020	Landscape Ecology	IT	AP	54	1261	lv1,2,3
Gellrich et al.	2008	Agricultural Systems	CH	AP	41	6300	lv1
Hohensinner et al.	2021	Frontiers in Environmental Science	AT	HM, AP, Sat	195	5430	lv1,2,3
Knevels et al. [2]	2020	Mitteilungen der Österreichischen Geographischen Gesellschaft	AT	HM, AP	195	NA	lv1,2
Kulakowski et al.	2011	Oikos	CH	AP	46	4500	lv1,2
Lieskovský & Bürgi [3]	2018	Regional Environmental Change	CH	HM, AP	137	12 610	lv1
Lopez-Saez et al.	2016	Science of The Total Environment	FR	HM, AP	163	403.5	lv1,2,3
Mainieri et al.	2020	Anthropocene	FR	HM, AP	188	135	lv1,2,3
Malek et al.	2014	Land	IT	TM, AP	21	114 800	lv1,2
Marage & Brun [4]	2007	Acta Botanica Gallica	FR	HM, AP	185	5700	lv1
Mietkiewicz et al.	2017	Journal of Vegetation Science	CH	HM, AP, TP	100	28 400	lv1,2
Niedertscheider et al. [5]	2017	Ecosystems	AT	HM	138	25 000	lv1,2
Orlandi et al.	2016	Biodiversity and Conservation	IT	AP	55	4078	lv1,2,3
Pellissier et al.	2013	Applied Vegetation Science	CH	AP, plots	25	NA	lv1
Piégay & Salvador	1997	Global Ecology and Biogeography Letters	FR	HM, AP	160	NA	lv1
Ranzi et al.	2002	Hydrology and Earth System Sciences	IT	AP	40	31 108	lv1,2
Schirpke et al.	2012	Ecological Informatics	AT, CH, DE, FR, IT	AP	27	17 333	lv1,2
Schirpke et al.	2013	Journal of Biodiversity Science, Ecosystem Services & Management	AT	HM, AP	57	510	lv1,2,3
Sitzia & Trentanovi	2011	Biodiversity and Conservation	IT	HM, AP	147	16 000	lv1
Tappeiner et al.	2008	Ecosystems	AT	HM, AP	142	13 849	lv1,2
Tasser et al. [6]	2007	Agriculture, Ecosystems and Environment	AT, IT	HM, AP	157	22 923	lv1

Tasser et al.	2009	Landscape Ecology	IT	HM, AP	135	5272	lv1
Tasser et al.	2017	Land Use Policy	AT	HM, AP	150	26 500	lv1,2
Tattoni et al.	2010	IForest - Biogeosciences and Forestry	IT	HM, AP	147	19 400	lv1,2
Tattoni et al. [7]	2017	Science of The Total Environment	IT	HM, AP	75	7681	lv1,2,3
Vogel & Conedera	2020	Plant, Soil and Environment	CH	AP, TM	NA	NA	lv1
Wallentin et al.	2008	Ecological Modelling	AT	AP, LiDAR	52	100	lv1,2,3
Zgheib et al.	2020	Global Environmental Change	FR	HM, AP	157	30 900	lv1,2
Zgheib et al.	2022	Regional Environmental Change	FR	HM, AP	159	21 633	lv1
Zimmermann et al.	2010	Agriculture, Ecosystems and Environment	AT, CH, DE, FR, IT	HM, AP	NA	19 575	lv1,2

Footnotes:
[1] This study comprises a regional case study and a landscape case study.
[2] This article is in German.
[3] European study with six different case studies. In our study we considered the case study number 4 in Lenk (CH).
[4] This article is in French.
[5] Spatial maps reported in this study derived from *Patek M (2013) Waldentwicklung und Biomassenvera¨nderung in Neustift im Stubaital in Tirol seit 1834. Diploma thesis, University of Vienna.*
[6] We considered the four municipalities and not the landscape case study because it used a different methodology (permanent plots).
[7] This study analysed several landscapes from both peer-reviewed and grey literature (degree thesis, technical reports).

Appendix A – References.

Andrič, M., Martinčič, A., Štular, B., Petek, F., & Goslar, T. (2010). Land-use changes in the Alps (Slovenia) in the fifteenth, nineteenth and twentieth centuries AD: A comparative study of the pollen record and historical data. *The Holocene*, 20(7), 1023–1037.

Anselmetto, N., Sibona, E. M., Meloni, F., Gagliardi, L., Bocca, M., & Garbarino, M. (2021). Land Use Modeling Predicts Divergent Patterns of Change Between Upper and Lower Elevations in a Subalpine Watershed of the Alps. *Ecosystems*.

Carlson, B. Z., Georges, D., Rabatel, A., Randin, C. F., Renaud, J., Delestrade, A., … & Thuiller, W. (2014a). Accounting for tree line shift, glacier retreat and primary succession in mountain plant distribution models. *Diversity and Distributions*, 20(12), 1379–1391.

Carlson, B. Z., Renaud, J., Biron, P. E., & Choler, P. (2014b). Long-term modeling of the forest–grassland ecotone in the French Alps: Implications for land management and conservation. *Ecological Applications*, 24(5), 1213–1225.

Dalla Valle, E., Lamedica, S., Pilli, R., & Anfodillo, T. (2009). Land Use Change and Forest Carbon Sink Assessment in an Alpine Mountain Area of the Veneto Region (Northeast Italy). *Mountain Research and Development*, 29(2), 161–168.

Didier, L. (2001). Invasion patterns of European larch and Swiss stone pine in subalpine pastures in the French Alps. *Forest Ecology and Management*, 145(1–2), 67–77.

Egarter Vigl, L., Schirpke, U., Tasser, E., & Tappeiner, U. (2016). Linking long-term landscape dynamics to the multiple interactions among ecosystem services in the European Alps. *Landscape Ecology*, 31(9), 1903–1918.

Fedrigotti, C., Aschonitis, V., & Fano, E.A. (2016). Effects of forest expansion and land abandonment on ecosystem services of alpine environments: case study in Ledro valley (Italy) for the period 1859-2011. *Global NEST Journal*, 18(4), 875–884.

Garbarino, M., Lingua, E., Martinez Subirà, M., & Motta, R. (2011). The larch wood pasture: Structure and dynamics of a cultural landscape. *European Journal of Forest Research*, 130(4), 491–502.

Garbarino, M., Lingua, E., Vacchiano, G., & Motta, R. (2006). Scots Pine forests in the NW Italian Alps. What has changed in the last 50 years? *IUFRO Landscape Ecology Conference*, Locorotondo, Bari (IT).

Garbarino, M., Lingua, E., Weisberg, P. J., Bottero, A., Meloni, F., & Motta, R. (2013). Land-use history and topographic gradients as driving factors of subalpine Larix decidua forests. *Landscape Ecology*, 28(5), 805–817.

Garbarino, M., Morresi, D., Urbinati, C., Malandra, F., Motta, R., Sibona, E. M., … & Weisberg, P. J. (2020). Contrasting land use legacy effects on forest landscape dynamics in the Italian Alps and the Apennines. *Landscape Ecology*.

Garbarino, M., Sibona, E., Lingua, E., & Motta, R. (2014). Decline of traditional landscape in a protected area of the southwestern Alps: The fate of enclosed pasture patches in the land mosaic shift. *Journal of Mountain Science*, 11(2), 544–554.

Gellrich, M., Baur, P., Robinson, B. H., & Bebi, P. (2008). Combining classification tree analyses with interviews to study why sub-alpine grasslands sometimes revert to forest: A case study from the Swiss Alps. *Agricultural Systems*, 96(1), 124–138.

Hohensinner, S., Atzler, U., Fischer, A., Schwaizer, G., & Helfricht, K. (2021). Tracing the Long-Term Evolution of Land Cover in an Alpine Valley 1820–2015 in the Light of Climate, Glacier and Land Use Changes. *Frontiers in Environmental Science*, 9, 683397.

Knevels, R., Brenning, A., Gingrich, S., Gruber, E., Lechner, T., Leopold, P … & Plutzar, C. (2021). Kulturlandschaft im Wandel: Ein indikatorenbasierter Rückblick bis in das 19. Jahrhundert. Fallstudie anhand der Gemeinden Waidhofen/Ybbs und Paldau. *Mitteilungen der Österreichischen Geographischen Gesellschaft*, 1, 255–285. (in German)

Kulakowski, D., Bebi, P., & Rixen, C. (2011). The interacting effects of land use change, climate change and suppression of natural disturbances on landscape forest structure in the Swiss Alps. *Oikos*, 120(2), 216–225.

Lieskovský, J., & Bürgi, M. (2018). Persistence in cultural landscapes: A pan-European analysis. *Regional Environmental Change*, 18(1), 175–187.

Lopez-Saez, J., Corona, C., Eckert, N., Stoffel, M., Bourrier, F., & Berger, F. (2016). Impacts of land-use and land-cover changes on rockfall propagation: Insights from the Grenoble conurbation. *Science of The Total Environment*, 547, 345–355.

Mainieri, R., Favillier, A., Lopez-Saez, J., Eckert, N., Zgheib, T., Morel, P., … & Corona, C. (2020). Impacts of land-cover changes on snow avalanche activity in the French Alps. *Anthropocene*, 30, 100244.

Malek, Ž., Scolobig, A., & Schröter, D. (2014). Understanding Land Cover Changes in the Italian Alps and Romanian Carpathians Combining Remote Sensing and Stakeholder Interviews. *Land*, 3(1), 52–73.

Marage, D., & Brun, J.-J. (2007). Relation entre productivité et richesse spécifique du tapis herbacé au cours d'une succession écologique dans les Alpes du Sud françaises. *Acta Botanica Gallica*, 154(2), 275–292. (in French)

Mietkiewicz, N., Kulakowski, D., Rogan, J., & Bebi, P. (2017). Long-term change in sub-alpine forest cover, tree line and species composition in the Swiss Alps. *Journal of Vegetation Science*, 28(5), 951–964.

Niedertscheider, M., Tasser, E., Patek, M., Rüdisser, J., Tappeiner, U., & Erb, K.-H. (2017). Influence of Land-Use Intensification on Vegetation C-Stocks in an Alpine Valley from 1865 to 2003. *Ecosystems*, 20(8), 1391–1406.

Orlandi, S., Probo, M., Sitzia, T., Trentanovi, G., Garbarino, M., Lombardi, G., & Lonati, M. (2016). Environmental and land use determinants of grassland patch diversity in the western and eastern Alps under agro-pastoral abandonment. *Biodiversity and Conservation*, 25(2), 275–293.

Pellissier, L., Anzini, M., Maiorano, L., Dubuis, A., Pottier, J., Vittoz, P., & Guisan, A. (2013). Spatial predictions of land-use transitions and associated threats to biodiversity: The case of forest regrowth in mountain grasslands. *Applied Vegetation Science*, 16(2), 227-236.

Piégay, H., & Salvador, P.-G. (1997). Contemporary Floodplain Forest Evolution along the Middle Ubaye River, Southern Alps, France. *Global Ecology and Biogeography Letters*, 6(5), 397.

Ranzi, R., Bochicchio, M., & Bacchi, B. (2002). Effects on floods of recent afforestation and urbanisation in the Mella River (Italian Alps). *Hydrology and Earth System Sciences*, 6(2), 239–254.

Schirpke, U., Leitinger, G., Tappeiner, U., & Tasser, E. (2012). SPA-LUCC: Developing land-use/cover scenarios in mountain landscapes. *Ecological Informatics*, 12, 68-76.

Schirpke, U., Leitinger, G., Tasser, E., Schermer, M., Steinbacher, M., & Tappeiner, U. (2013). Multiple ecosystem services of a changing Alpine landscape: Past, present and future. *International Journal of Biodiversity Science, Ecosystem Services & Management*, 9(2), 123–135.

Sitzia, T., & Trentanovi, G. (2011). Maggengo meadow patches enclosed by forests in the Italian Alps: evidence of landscape legacy on plant diversity. *Biodiversity and Conservation*, 20(5), 945-961.

Tappeiner, U., Tasser, E., Leitinger, G., Cernusca, A., & Tappeiner, G. (2008). Effects of Historical and Likely Future Scenarios of Land Use on Above- and Belowground Vegetation Carbon Stocks of an Alpine Valley. *Ecosystems*, 11(8), 1383–1400.

Tasser, E., Leitinger, G., & Tappeiner, U. (2017). Climate change versus land-use change—What affects the mountain landscapes more? *Land Use Policy*, 60, 60–72.

Tasser, E., Ruffini, F. V., & Tappeiner, U. (2009). An integrative approach for analysing landscape dynamics in diverse cultivated and natural mountain areas. *Landscape Ecology*, 24(5), 611–628.

Tasser, E., Walde, J., Tappeiner, U., Teutsch, A., & Noggler, W. (2007). Land-use changes and natural reforestation in the Eastern Central Alps. *Agriculture, Ecosystems and Environment*, 118(1–4), 115–129. Scopus.

Tattoni, C., Ciolli, M., Ferretti, F., & Cantiani, M. (2010). Monitoring spatial and temporal pattern of Paneveggio forest (northern Italy) from 1859 to 2006. *IForest - Biogeosciences and Forestry*, 3(3), 72–80.

Tattoni, C., Ianni, E., Geneletti, D., Zatelli, P., & Ciolli, M. (2017). Landscape changes, traditional ecological knowledge and future scenarios in the Alps: A holistic ecological approach. *Science of The Total Environment*, 579, 27–36.

Vogel, S., & Conedera, M. (2020). Effects of land use-induced vegetation and topography changes on soil chemistry in the Southern Alps (Ticino, Switzerland). *Plant, Soil and Environment*, 66(2), 73–80.

Wallentin, G., Tappeiner, U., Strobl, J., & Tasser, E. (2008). Understanding alpine tree line dynamics: An individual-based model. *Ecological Modelling*, 218(3–4), 235–246.

Zgheib, T., Giacona, F., Granet-Abisset, A.-M., Morin, S., & Eckert, N. (2020). One and a half century of avalanche risk to settlements in the upper Maurienne valley inferred from land cover and socio-environmental changes. *Global Environmental Change*, 65, 102149.

Zgheib, T., Giacona, F., Granet-Abisset, A.-M., Morin, S., Lavigne, A., & Eckert, N. (2022). Spatio-temporal variability of avalanche risk in the French Alps. *Regional Environmental Change*, 22(1), 8.

Zimmermann, P., Tasser, E., Leitinger, G., & Tappeiner, U. (2010). Effects of land-use and land-cover pattern on landscape-scale biodiversity in the European Alps. *Agriculture, Ecosystems & Environment*, 139(1), 13–22.

Refinement on socio-ecological predictors

At the municipality scale, we calculated relative annual CLC-derived forest gain by subtracting the final forest cover of 2018 from the initial forest cover of 2000, relativised to the 2000 cover, and divided by the temporal extent of 18 years.

Among the socio-economic drivers at the municipality scale, we obtained population data from Eurostat data for the years 1961, 1971, 1981, 1991, 2001, 2011, and 2020 (https://ec.europa.eu/eurostat/web/nuts/local-administrative-units). We then derived population density, change, and rate of change. We obtained information on employment by job sector (primary, secondary, tertiary) and relative change in number of farms (1990-2000) from Alpine Convention atlas (https://www.atlas.alpconv.org/). At the municipality scale, road density was integrated as an indicator of landscape connectivity and remoteness. At the landscape scale, we used this road dataset along with a digital elevation model (DEM) to compute cost of movement (Alberti, 2019). We used Open Street Map (OSM) as reference data, considering primary, secondary, and tertiary roads. From OSM, we also derived cities (i.e. the largest settlement or settlements within a territory, including national, state and provincial capitals, and other major conurbations) and towns) above 800 m a.s.l (available at https://wiki.openstreetmap.org/wiki/Key:place#Populated_settlements,_urban). We defined towns as important urban centres, between a village and a city in size and having a good range of shops and facilities which are used by people from nearby villages. From these two point-datasets we derived continuous maps through a variable-bandwidth smoothing kernel interpolation as a proxy for remoteness and the possible past magnitude of rural exodus (Davis & Baddeley, 2018).

We calculated several topographic variables from the MERIT DEM (Yamazaki et al., 2017) at 3sec spatial resolution resampled at 1 km. Specifically, we derived the elevation, slope, heat load index (HLI) or the incident radiation of the sun

according to the aspect (McCune et al., 2002), and topographic position index (TPI), indicating the position of a focal cell relative to its neighbours.

We obtained climate variables from the CHELSA v1.2 timeseries from 1979 to 2013 at 30 arc sec spatial resolution (Karger et al., 2017, 2018), using the median and standard deviation of seasonal (winter and summer) and annual values related to annual precipitation and minimum, mean, and maximum temperatures. Moreover, we also calculated the slope of linear models developed from the four timeseries as a proxy of climate change.

All R packages used in the analysis are listed in Table B2.5.

TABLE B2.1. Summary of the Principal Component Analysis for socio-economic variables at the landscape scale (lan). Loadings scaled to unit length. The most correlated variables to each principal component (1-6) are highlighted in the table (green for positive correlation, orange for negative one). Grey cells refer to PCs that were not used in the analyses. P-values, Eigenvalue and % of explained variation are reported. Movecost = cost of movement (Alberti, 2019); Cities = distance from cities (Padgham et al., 2017); Towns = distance from towns (Padgham et al., 2017); Pop. dens. = population density.

Variable	PC1	PC2	PC3	PC4	PC5	PC6
Movecost min	0.186	-0.222	0.083	0.542	0.204	0.358
Movecost mean	0.202	**-0.257**	0.048	0.489	-0.052	0.092
Movecost max	0.194	**-0.255**	0.068	0.387	-0.409	-0.516
Cities min	0.132	**-0.271**	-0.452	-0.096	0.193	-0.028
Cities mean	0.125	**-0.277**	-0.457	-0.108	0.139	-0.046
Cities max	0.119	**-0.282**	-0.458	-0.117	0.088	-0.070
Towns min	0.001	**0.385**	-0.317	0.238	-0.078	0.095
Towns mean	0.000	**0.382**	-0.326	0.229	-0.105	0.106
Towns max	-0.001	**0.378**	-0.335	0.220	-0.135	0.113
Pop. dens. 1961	**-0.263**	-0.204	-0.112	-0.074	-0.484	0.164
Pop. dens. 1971	**-0.278**	-0.175	-0.117	-0.043	-0.458	0.084
Pop. dens. 1981	**-0.313**	-0.139	-0.068	0.052	-0.186	0.103
Pop. dens. 1991	**-0.322**	-0.110	-0.025	0.106	0.062	0.103
Pop. dens. 2001	**-0.322**	-0.097	-0.014	0.116	0.147	0.067
Pop. dens. 2011	**-0.323**	-0.096	-0.018	0.107	0.141	0.026
Pop. dens. 2020	**-0.323**	-0.091	-0.016	0.113	0.151	0.032
Pop. dens. change	**-0.314**	-0.047	0.016	0.163	0.343	-0.014
Pop. change rate	**-0.285**	0.146	-0.110	0.199	0.158	-0.704
p-value	*0.001*	*0.001*	0.234	1.000	1.000	1.000
Eigenvalue	8.890	4.660	2.28	1.33	0.63	0.13
% of variance	49.4	25.9	12.69	7.38	3.5	0.71

TABLE B2.2. Summary of the Principal Component Analysis for climate variables at the landscape scale (lan). Loadings scaled to unit length. The most correlated variables to each principal component (1-6) are highlighted in the table (green for positive correlation, orange for negative one). Grey cells refer to PCs that were not used in the analyses. P-values, Eigenvalue and % of explained variation are reported. P = precipitation, Tmean = mean temperature, Tmin = minimum temperature, Tmax = maximum temperature.

Variable	PC1	PC2	PC3	PC4	PC5	PC6
Annual P median	-0.080	0.104	**0.496**	0.010	-0.023	0.032
Annual P st.dev.	-0.100	0.025	**0.419**	0.367	0.111	-0.152
Summer P median	-0.087	**0.266**	**0.323**	0.101	-0.204	0.412
Summer P st.dev.	-0.071	0.101	**0.369**	0.485	0.009	-0.226
Winter P median	-0.035	-0.023	**0.353**	-0.550	0.244	-0.021
Winter P st.dev.	-0.073	-0.107	**0.368**	-0.461	-0.130	0.256
Annual Tmean median	**0.268**	-0.137	0.061	0.066	0.032	0.118
Annual Tmean st.dev.	0.236	0.197	0.002	-0.048	-0.445	-0.095
Summer Tmean median	**0.270**	-0.132	0.051	0.074	0.014	0.099
Summer Tmean st.dev.	0.224	0.229	0.079	-0.088	0.205	-0.251
Winter Tmean median	**0.259**	-0.170	0.069	0.052	0.056	0.085
Winter Tmean st.dev.	0.113	**0.380**	-0.079	0.045	0.188	0.145
Annual Tmin median	**0.263**	-0.152	0.069	0.075	0.012	0.124
Annual Tmin st.dev.	0.164	**0.304**	-0.046	-0.007	-0.439	0.232
Summer Tmin median	**0.264**	-0.147	0.057	0.087	-0.013	0.145
Summer Tmin st.dev.	0.240	0.141	0.097	-0.144	-0.002	-0.439
Winter Tmin median	**0.253**	-0.183	0.090	0.041	0.070	0.065
Winter Tmin st.dev.	0.135	**0.366**	-0.044	0.001	-0.109	0.101
Annual Tmax median	**0.273**	-0.117	0.052	0.062	0.034	0.109
Annual Tmax st.dev.	**0.254**	0.102	0.037	-0.141	-0.213	-0.376
Summer Tmax median	**0.273**	-0.115	0.054	0.051	0.051	0.035
Summer Tmax st.dev.	0.204	**0.273**	0.041	-0.123	0.263	-0.096
Winter Tmax median	**0.262**	-0.164	0.052	0.048	0.057	0.109
Winter Tmax st.dev.	0.068	**0.363**	-0.117	0.041	0.509	0.305
p-value	*0.001*	*0.001*	*0.001*	1.000	1.000	1.000
Eigenvalue	12.12	5.44	3.40	1.66	0.51	0.46
% of variance	50.51	22.66	14.16	6.91	2.13	1.93

TABLE B2.3. Summary of the Principal Component Analysis for climate change variables at the landscape scale (lan). Loadings scaled to unit length. The most correlated variables to each principal component (1-6) are highlighted in the table (green for positive correlation, orange for negative one). Grey cells refer to PCs that were not used in the analyses. P-values, Eigenvalue and % of explained variation are reported. P = precipitation, Tmean = mean temperature, Tmin = minimum temperature, Tmax = maximum temperature.

Variable	PC1	PC2	PC3	PC4	PC5	PC6
Annual P slope	-0.214	0.472	-0.194	-0.399	-0.092	0.198
Summer P slope	-0.108	0.352	-0.622	-0.016	0.552	0.065
Winter P slope	-0.175	0.395	0.414	-0.506	-0.230	0.112
Annual Tmean slope	**-0.354**	-0.168	-0.028	0.133	-0.094	0.401
Summer Tmean slope	**-0.338**	0.215	0.067	0.291	-0.067	-0.309
Winter Tmean slope	**-0.309**	-0.327	-0.052	-0.303	0.120	-0.214
Annual Tmin slope	**-0.328**	-0.214	-0.223	0.007	-0.368	0.210
Summer Tmin slope	**-0.355**	0.106	-0.101	0.211	-0.103	-0.352
Winter Tmin slope	**-0.279**	-0.329	-0.321	-0.246	-0.216	-0.179
Annual Tmax slope	**-0.328**	-0.078	0.231	0.276	0.281	0.584
Summer Tmax slope	**-0.296**	0.305	0.226	0.347	-0.026	-0.244
Winter Tmax slope	**-0.264**	-0.229	0.359	-0.299	0.579	-0.203
p-value	*0.001*	0.100	0.999	1.000	1.000	1.000
Eigenvalue	7.090	2.24	1.29	0.71	0.45	0.19
% of variance	59.08	18.64	10.79	5.94	3.76	1.54

TABLE B2.4. Summary of the Principal Component Analysis for selected topographic variables at the landscape scale (lan). Loadings scaled to unit length. The most correlated variables to each principal component (1-6) are highlighted in the table (green for positive correlation, orange for negative one). Grey cells refer to PCs that were not used in the analyses. P-values, Eigenvalue and % of explained variation are reported.

Variable	PC1	PC2	PC3	PC4	PC5	PC6
Elevation st.dev. mean	-0.239	**-0.295**	0.071	0.083	0.068	0.155
Elevation st.dev. min	**-0.293**	-0.084	0.204	-0.048	0.057	0.031
Elevation st.dev. max	-0.239	0.221	0.339	-0.110	0.187	0.021
HLI median min	0.076	**-0.317**	0.460	-0.217	0.227	-0.535
HLI st.dev. min	-0.231	-0.228	-0.344	0.023	-0.064	-0.009
HLI st.dev. mean	**-0.281**	0.008	-0.319	0.010	-0.192	-0.240
HLI st.dev. max	-0.201	**0.290**	-0.247	-0.005	-0.280	-0.387
Slope median min	-0.234	**-0.280**	0.018	-0.014	0.205	0.163
Slope median mean	**-0.297**	-0.060	-0.031	-0.196	0.076	-0.216
Slope median max	**-0.255**	0.207	-0.052	-0.395	-0.099	-0.153
Slope st.dev. min	**-0.254**	-0.246	-0.132	0.103	-0.010	0.099
Slope st.dev. mean	**-0.298**	-0.062	0.049	0.151	-0.123	0.030
Slope st.dev. max	-0.194	**0.277**	0.290	0.253	-0.207	0.389
TPI median min	0.142	**-0.304**	0.002	-0.674	-0.463	0.334
TPI median max	-0.100	**0.336**	-0.300	-0.388	0.621	0.263
TPI st.dev. min	**-0.255**	**-0.263**	-0.051	0.042	0.097	0.161
TPI st.dev. mean	**-0.301**	0.010	0.184	0.022	-0.018	-0.085
TPI st.dev. max	-0.194	**0.284**	0.334	-0.180	-0.249	0.089
p-value	*0.001*	*0.001*	1.000	1.000	1.000	1.000
Eigenvalue	10.21	4.47	1.44	0.58	0.35	0.32
% of variance	56.71	24.85	7.97	3.23	1.95	1.78

TABLE B2.5. List of R packages used in the analysis with citations.

Package name	Version	Citation	Purpose
corrplot	v0.92	Wei & Simko, 2017	Creation of correlograms
iml	v0.11.0	Molnar et al., 2018	Variable importance and variable effects
mlr3	v0.13.3	Lang et al., 2019	Random Forest regression and accuracy evaluation (lv3)
movecost	v1.3	Alberti, 2019	Computation of cost of movement
osmdata	v0.1.9	Padgham et al., 2017	Download Open Street Map data
sf	v0.9-8	Pebesma, 2018	Manipulation of spatial vector data
spatstat	v2.1-0	Baddeley et al., 2015	Computation of variable-bandwidth smoothing kernel interpolation
terra	v1.5-21	Hijmans, 2022	Manipulation of spatial raster data
tidyverse	v1.3.1	Wickham et al., 2019	Manipulation of data
tmap	v3.3-2	Tennekes, 2018	Creation of maps

Appendix B – References.

Alberti, G. (2019). movecost: An R package for calculating accumulated slope-dependent anisotropic cost-surfaces and least-cost paths. *SoftwareX*, 10, 100331.

Baddeley, A., Rubak, E., & Turner, R. (2015). *Spatial Point Patterns: Methodology and Applications with R*. Chapman and Hall/CRC Press. http://www.crcpress.com/Spatial-Point-Patterns-Methodology-and-Applications-with-R/Baddeley-Rubak-Turner/9781482210200/

Davies, T.M. and Baddeley, A. (2018) Fast computation of spatially adaptive kernel estimates. *Statistics and Computing*, 28(4), 937-956.

Hijmans, R.J. (2022). terra: Spatial Data Analysis. R package version 1.5-21. https://CRAN.R-project.org/package=terra

Karger, D. N., Conrad, O., Böhner, J., Kawohl, T., Kreft, H., Soria-Auza, R. W., … Kessler, M. (2017). Climatologies at high resolution for the earth's land surface areas. *Scientific Data*, 4(1), 170122.

Karger, D.N. et al. (2018), Data from: Climatologies at high resolution for the earth's land surface areas, *Dryad*, Dataset.

Lang, M., Binder, M., Richter, J., Schratz, P., Pfisterer, F., Coors, S., … Bischl, B. (2019). mlr3: A modern object-oriented machine learning framework in R. *Journal of Open Source Software*, 4(44), 1903.

McCune, B., J.B. Grace, and D.L. Urban. (2002). *Analysis of ecological communities*. OR: Gleneden Beach.

Molnar, C., Bischl, B., & Casalicchio, G. (2018). "iml: An R package for Interpretable Machine Learning." *Journal of Open Source Software*, 3(26), 786.

Padgham, M., Rudis, B., Lovelace, R., Salmon, M. (2017). Osmdata. *Journal of Open Source Software*, 2(14).

Pebesma, E. (2018). Simple Features for R: Standardized Support for Spatial Vector Data. *The R Journal*, 10(1), 439–446.

Tennekes M (2018). tmap: Thematic Maps in R. *Journal of Statistical Software*, 84(6), 1–39.

Wei, T., & Simko, V. (2017). *R package "corrplot": Visualization of a Correlation Matrix*. https://github.com/taiyun/corrplot

Wickham et al., (2019). Welcome to the tidyverse. *Journal of Open Source Software*, 4(43), 1686.

Yamazaki D., D. Ikeshima, R. Tawatari, T. Yamaguchi, F. O'Loughlin, J.C. Neal, … P.D. Bates. (2017). A high accuracy map of global terrain elevations. *Geophysical Research Letters*, vol.44, pp.5844-5853.

Appendix C2 – Supporting Information on Results

TABLE C2.1. Summary of the Principal Component Analysis at the municipality scale (mun). Loadings scaled to unit length. The most correlated variables to each principal component (1-6) are highlighted in the table (green for positive correlation, orange for negative one). Grey cells refer to PCs that were not used in the analyses. P-values, Eigenvalue and % of explained variation are reported.

Variable	PC1	PC2	PC3	PC4	PC5	PC6
forest gain (obs)	-0.292	0.110	0.085	0.550	-0.299	-0.127
farms change	-0.148	0.242	0.503	-0.203	0.239	0.702
primary	-0.146	0.584	-0.151	-0.332	0.023	-0.170
secondary	0.388	0.215	-0.216	0.252	0.251	-0.002
tertiary	-0.228	-0.575	0.260	-0.078	-0.242	0.042
tourism density	0.185	-0.002	0.488	-0.443	0.053	-0.601
road density	0.424	-0.045	0.198	0.071	-0.180	0.040
forest gain (CLC)	-0.114	-0.310	0.022	0.193	0.832	-0.161
population density 61	0.474	-0.145	-0.056	-0.049	-0.052	0.170
population density 20	0.465	0.003	0.199	0.170	-0.030	0.089
population change	-0.034	0.303	0.531	0.455	0.037	-0.186
p-value	*0.001*	*0.001*	*0.001*	0.963	0.994	1.000
Eigenvalue	3.79	1.79	1.63	1.08	0.96	0.55
% of variance	34.45	16.29	14.78	9.83	8.72	4.95

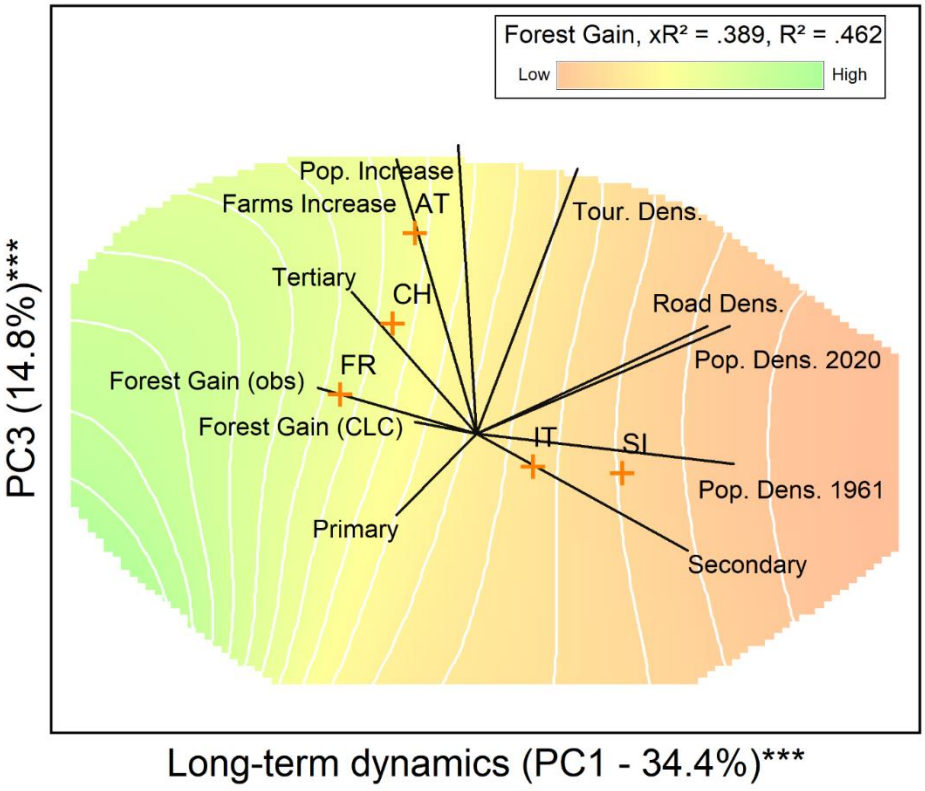

FIGURE C2.1. Results of the principal component analysis at the municipality scale (n = 108). PC1 vs PC3. Principal components were significant ($p < 0.05$, Monte Carlo permutation test on 10 000 runs with randomized data). AT = Austria, CH = Switzerland, FR = France, IT = Italy, SI = Slovenia.

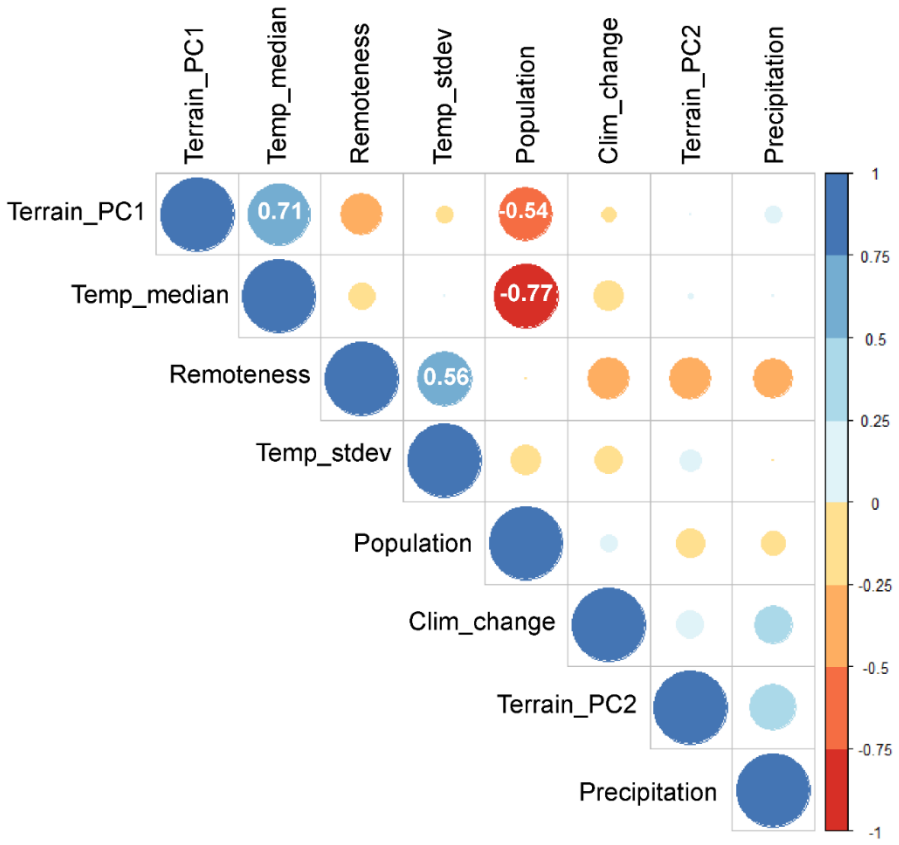

FIGURE C2.2. Correlogram for the 8 environmental variables used as predictors in the RF regression. Positive and negative correlation values higher than 0.5 are reported in the figure.

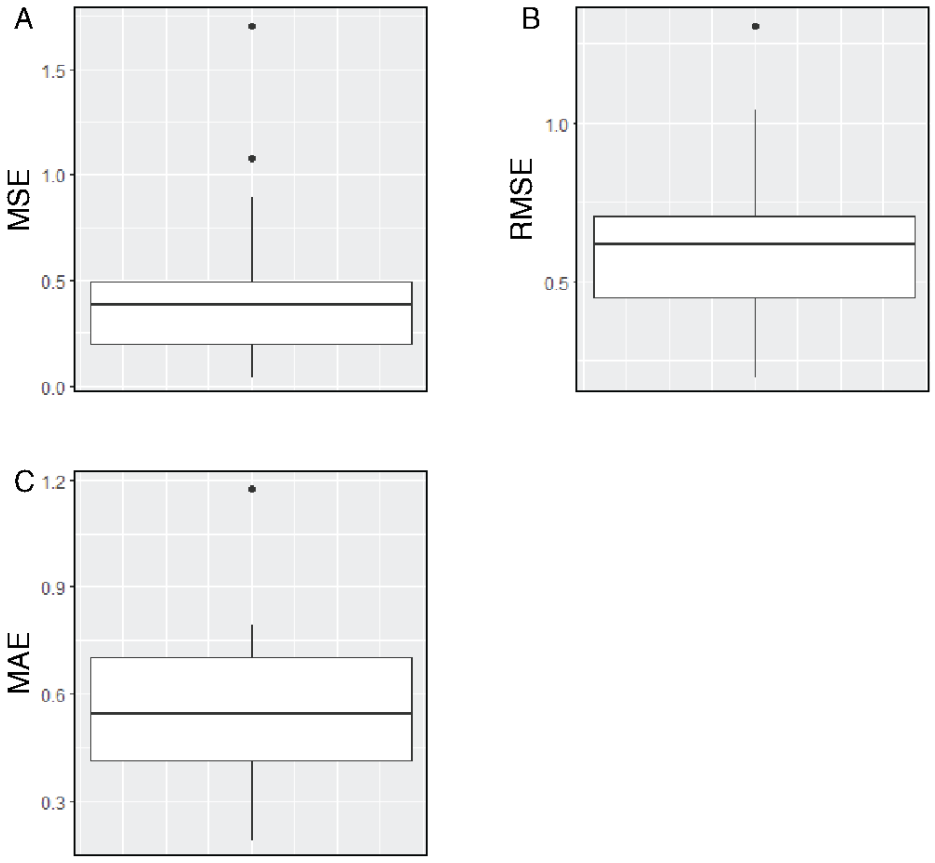

FIGURE C2.3. Accuracy results (root mean squared errors) of Random Forest regression on Principal Components at the landscape scale (lan). Results of 300 models created through nested spatial cross-validation.

Chapter 3

Land use modeling predicts divergent patterns of change between upper and lower elevations in a subalpine watershed of the Alps

Nicolò Anselmetto, Emanuele Marco Sibona, Fabio Meloni, Luca Gagliardi, Massimo Bocca, Matteo Garbarino

This chapter has been published open access in the *Ecosystems* journal: Anselmetto, N., Sibona, E. M., Meloni, F., Gagliardi, L., Bocca, M., & Garbarino, M. (2021). Land use modeling predicts divergent patterns of change between upper and lower elevations in a subalpine watershed of the Alps. *Ecosystems*, 1-16. https://doi.org/10.1007/s10021-021-00716-7

Abstract

The synergic influence of land use and climate change on future forest dynamics is hard to disentangle, especially in human-dominated forest ecosystems. Forest gain in mountain ecosystems often creates different spatial–temporal patterns between upper and lower elevation belts. We analyzed land cover dynamics over the past 50 years and predicted Business as Usual future changes on an inner subalpine watershed by using land cover maps, derived from five aerial images, and several topographic, ecological, and anthropogenic predictors. We analyzed historical landscape patterns through transition matrices and landscape metrics and predicted future forest ecosystem change by integrating multi-layer perceptron and Markov chain models for short-term (2050) and long-term (2100) timespans. Below the maximum timberline elevation of the year 1965, the dominant forest dynamic was a gap-filling process through secondary succession at the expense of open areas leading to an increase of landscape homogeneity. At upper elevations, the main observed dynamic was the colonization of unvegetated soil through primary succession and timberline upward shift, with an increasing

speed over the last years. Future predictions suggest a saturation of open areas in the lower part of the watershed and stronger forest gain at upper elevations. Our research suggests an increasing role of climate change over the last years and on future forest dynamics at a landscape scale.

Keywords: land use change modeling, land abandonment, natural park, alpine forest, multilayer perceptron, Markov chain.

Highlights

- Alpine forest gain shows two different landscape patterns depending on the elevation.
- Primary successions at upper elevations are increasing due to climate change.
- Future LUC scenarios suggest an expansion of dense forests mostly at upper elevations.

3.1 Introduction

Mountain ecosystems and populations around the world are increasingly affected by the combination of changes in climate and land use (Bugmann et al., 2007; Lasanta et al., 2017). Tropical mountains, for instance, are facing expansion and intensification of agriculture and an over-exploitation of natural resources (Peters et al., 2019). In contrast, temperate mountain forest dynamics, especially in Europe, are controlled by land-abandonment processes (Chauchard et al., 2007) that, along with gradual effects of climate change, are expected to modify landscape structures and ecosystem services supply in the future (Van der Sluis et al., 2019). Nevertheless, it is hard to disentangle the role of climate and land use changes (hereafter, CC and LUC), since they influence in synergy, especially in highly exploited landscapes (Clavero et al., 2011).

At lower elevations, LUC plays the most relevant role through secondary successions represented by in-filling of open areas and forest gaps at the expense of abandoned meadows, grasslands and arable lands (Gautam et al., 2004;

Garbarino et al., 2014; Malandra et al., 2019). The loss of these areas is strongly related to the abandonment of marginal areas during the twentieth century and to the decline of traditional land uses and practices (Chauchard et al., 2007; Tattoni et al., 2017).

In the upper part of mountain watersheds, the limit of tree distribution, that is, the treeline, is one of the most studied ecotones where the role of long-term CC can be assessed since it is mainly limited by heat availability (Körner, 2015; Fajardo et al., 2019). However, other environmental variables such as soil and topography also proved to be important treeline drivers (Holtmeier & Broll, 2020). Several studies have shown evidence of wood encroachment on upper grasslands (Barros et al., 2017; Malfasi & Cannone, 2020) and of treeline upward shift in different ecosystems around the world (Fang et al., 2009; Elliott, 2011; Ameztegui et al., 2016). Land abandonment effect is often highlighted as the main driver of the treeline upward shift, but it is expected to be equalized by the CC, which will become the most important in future years (Gehrig-Fasel et al., 2007).

Vegetation maps and aerial photographs are fundamental historical data sources for the comprehension of past dynamics and future trajectories of forests. These spatially explicit datasets are useful for LUC detection and can be used to assess the contribution of climate and land use on forest gain (Cousins et al., 2015; Filippa et al., 2019; Ridding et al., 2020). A long time-series dataset with a fine temporal resolution is a crucial aspect for setting observed current changes in a comprehensive historical context in order to produce more realistic future predictions of a process that is highly variable and nonlinear (Becker et al., 2007; Tattoni et al., 2017).

Many approaches and classification methods can be adopted in LUC forecast modeling. Six types of models exist (*sensu* Lantman et al., 2011): (i) agent-based; (ii) artificial neuron networks (ANNs); (iii) cellular automata (CA); (iv) economics-based; (v) Markov chains (MCs); and (vi) statistical. Since there is not a 'right model' for all ecological purposes, different tools can be integrated in a single framework to boost their strengths and minimize their weaknesses

(Mas et al., 2014). Another important decision that must be made in forecast modeling is the one between scenario-based simulation models and Business as Usual (BaU) ones. BaU models base their predictions according to the continuation of current land use practices and policies. BaU models are data-driven tools that permit to: (i) forecast landscape trajectories according to past situations and (ii) stress past dynamics. There are two model types that can be considered adequate to carry out this task: Markov chains (MCs) and artificial neuron networks (ANNs). MCs are widely used to model both anthropogenic and natural or semi-natural LUC at different spatiotemporal scales (Muller & Middleton, 1994; Tattoni et al., 2011; Al-Shaar et al., 2021). MCs forecasts are based on previous changes and on the assumption of the persistence of historical dynamics, thus they are reliable tools for BaU scenarios. Their main strengths are simplicity and flexibility and the ability to describe complex and lengthy processes of land use dynamics as simple transition probabilities (Lantman et al., 2011; Iacono et al., 2015). However, these models are not spatially explicit (Noszczyk, 2019), and because of these aspects they are often combined with other models such as ANNs and CAs (Tattoni et al., 2011; Ozturk, 2015).

ANNs are machine learning algorithms built around several layers of interconnected neurons, similar to human brains (Noszczyk, 2019). Therefore, they can recognize patterns and facilitate the development of irregular relationships between past and future LUC (Lantman et al., 2011). ANNs are usually connected to suitability maps, expressions of transition potential from one state of the system to another. Their principal limitations are the ‘black box’ approach and the time required to build them. They have different applications on LUC modeling like urban growth, natural trends, habitat loss (for example, Gontier et al., 2010; Tattoni et al., 2011; Fattah et al., 2021). Though the interaction between MCs and ANNs has been thoroughly analyzed, few studies use more than two or three land cover maps (that is, time steps) to predict future dynamics, oversimplifying the complexity of LUC over time.

In this study, we analyzed past dynamics and future trajectories of LUC using five land cover maps and a nonlinear BaU modeling approach to test our three hypotheses on an inner subalpine watershed: (i) post-abandonment forest gain at lower and upper elevations shows different landscape patterns; (ii) primary successions at higher elevations are becoming more important in the last decades due to increasing climate change and decreasing land abandonment effects; (iii) forest canopy closure at lower elevations and the availability of open areas at the treeline ecotone will favor a stronger forest gain at higher elevations. We had the opportunity to test our hypotheses at the Mont Avic Natural Park, Aosta valley (hereafter, MA), a human-dominated forest ecosystem with a history of intense forest exploitation and a relatively low agro-pastoral impact.

3.2 Materials and methods

3.2.1 Study Area

MA is located on the southwest part of Aosta Valley, a mountainous autonomous region in northwestern Italy. The Natural Park covers more than 5800 ha and contains Chalamy and Champorcher valleys. It was created in 1989 to protect natural resources in the upper part of the valleys, where high value landscapes had not been strongly modified by humans because of their rough terrain. For this reason, the main human disturbance is not livestock grazing as in many other alpine valleys, but forest cutting for mining activities (Mont Avic, 2018). The climate is Alpine, with annual average temperatures ranging from 1 to 3 °C and precipitations (800–1200 mm year-1) mainly concentrated in autumn and spring (Tiberti et al., 2019). The valleys belong to the 'Mont Avic Ophiolitic Complex', and the prevailing lithology is serpentine (D'Amico et al., 2008). Deciduous trees such as beech *Fagus sylvatica* L., chestnut *Castanea sativa* Mill., downy oak *Quercus pubescens* Willd. and birch *Betula pendula* Roth prevail below 1100 m a.s.l. and are sporadic over 1500 m a.s.l. Three coniferous forest species (*Larix decidua* Mill., *Pinus sylvestris* L. and *Pinus mugo* Turra subsp. *uncinata*)

dominate the landscape in the upper montane and subalpine zones (1100–2000 m a.s.l.).

The study area (about 5500 ha and with an elevation gradient between 500 and 2600 m a.s.l.) contains only the Chalamy watershed and some neighboring areas and lies on four different elevation zones: lowland (500–800 m a.s.l.), montane (801–1500 m a.s.l.), subalpine (1501–2200 m a.s.l.) and alpine (2201–2600 m a.s.l.) (Figure 3.1).

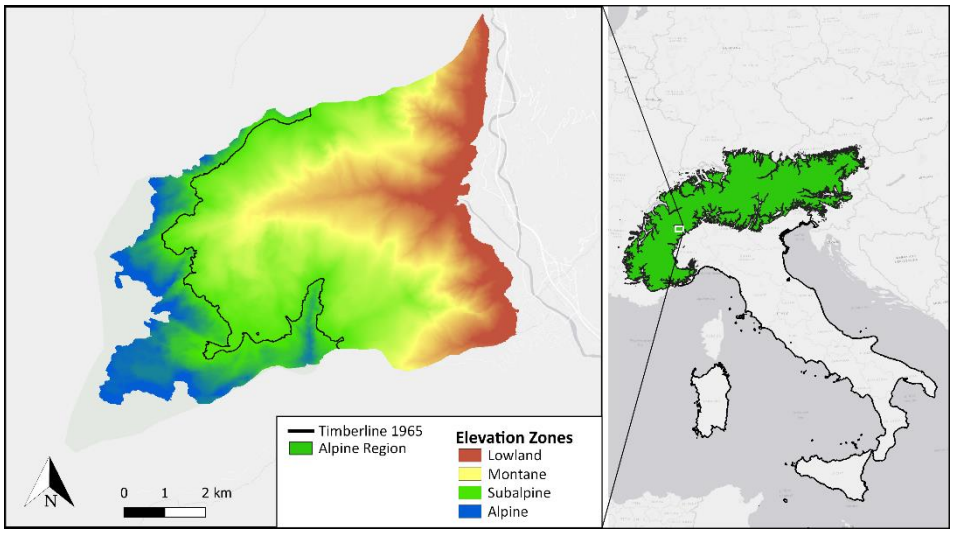

FIGURE 3.1. Study area location on the Italian Alps and elevation zones. The black line indicates the elevation threshold based on dense forest treeline in 1965.

Elevations above 2600 m a.s.l. were excluded from analyses because conditions are considered unfavorable for plant species; in this way, the analyses were limited to the vegetated areas, reducing the weight of unvegetated soil (Garbarino et al., 2020). For the analysis of trends and successions, three areas were chosen: (i) the full study area (5478 ha), (ii) the upper elevations (1230 ha) and (iii) lower elevations (4248 ha). The threshold between upper and lower areas was determined based on the maximum elevation of the dense forests in the oldest available aerial image (that is, 1965), corresponding to a medium elevation of 2182 m a.s.l.

3.2.2 Image Analysis and Environmental Predictors

Historical forest dynamics were evaluated by using land cover maps obtained from the classification of five aerial images spanning 52 years (Table S3.1 Supplementary Materials). Historical aerial photographs were orthorectified and segmented. A supervised classification based on an initial set of polygons was then performed, and lastly a manual classification of residual unclassified polygons (Garbarino et al., 2020). Five land cover classes (LCCs) were considered: dense forest (FO), sparse forest (SF), grassland (GR), urban surface (UR) and unvegetated (UV). The land cover class 'dense forest' includes high (‡ 80%) canopy cover stands; the 'sparse forest' class represents lower (< 80%) canopy cover stands and shrublands, which have a similar spectral signature and pixel texture and are therefore hard to separate in this landscape. The unvegetated class is a residual class that includes rocks, bare soil, gravel, sand and water. Urban surfaces were not considered in further analyses because our main goal was to explore natural forest dynamics, independent of the marginal expansion of human settlements in the lower part of the valley. Among the maps, overall accuracy (OA) ranged from 78% (1988) to 92% (2017) with a Cohen's Kappa coefficient between 0.71 and 0.89, respectively (Table S3.1 Supplementary Materials).

Several environmental predictors of land use change (Table 3.1) were produced such as topographic variables (elevation, aspect, slope, heat load index (HLI), topographic wetness index (TWI), topographic position index (TPI), terrain ruggedness index (TRI), roughness, curvature), anthropogenic variables (cost of movement, Euclidean distance to buildings and roads), the distance from preexisting forest and sparse forest edges and the likelihood of class transitions. The choice of predictors was based on a preliminary literature search and expert knowledge (for example, Rutherford et al., 2008; Dubovyk et al., 2011; Garbarino et al., 2020). A neighborhood size of 8 was used for all the GIS variables computed at the neighborhood level. We derived the accumulated cost of movement through Tobler's hiking on-path function using slope and buildings

from Open Street Map as starting points. The cost was expressed as hours required for the movement. Almost all the predictors were produced in R environment: Cost of movement was implemented with the movecost package (Alberti, 2019), the heat load index was calculated with the spatialEco package (Evans, 2020), and the topographic wetness index was calculated according to Beven's classical topmodel with the dynatopmodel package (Metcalfe et al., 2018). The likelihood of transitions was calculated in the TerrSet environment (Eastman, 2016).

TABLE 3.1. *Environmental Predictors Used in the Study with the Unit, Description and Source*

Predictor Name	Tipology	Unit	Description	Source
Elevation	Topographic	m	Elevation above sine level	DTM
Aspect cosine	Topographic	-1 to +1	Easterness (aspect relative to west)	DTM
Aspect sine	Topographic	-1 to +1	Northerness (aspect relative to south)	DTM
Slope	Topographic	°	Proxy for diffuse solar radiation and growth limitations	DTM
Curvature	Topographic	-	Rate of change of slope	DTM
Roughness	Topographic	m	The largest inter-cell difference of a central pixel and its surrounding cell	DTM
Heat Load Index	Topographic	0 to 1	Incident radiation of sun according to the aspect; McCune and Grace 2002	DTM

Topographic Wetness Index	Topographic	-	Proxy for the moisture accumulation and availability	DTM
Topographic Position Index	Topographic	-	Index of the position of a cell according to the neighbors	DTM
Terrain Ruggedness Index	Topographic	-	Amount of elevation difference between adjacent cells of a DEM; Riley et al., 1999	DTM
Euclidean distance from buildings	Anthropogenic	m	Proxy for the accessibility of the site	OSM
Euclidean distance from roads	Anthropogenic	m	Proxy for the accessibility of the site	OSM
Cost of movement	Anthropogenic	h	Proxy for the accessibility of the site that considers buildings and orography according to the Tobler's hiking function	OSM + DTM
Distance from pre-existing forests	Ecological	m	Proxy for land abandonment dynamics and seed sources	Land Cover
Distance from pre-existing sparse forests	Ecological	m	Proxy for land abandonment dynamics and seed sources	Land Cover
Likelihood of class transitions	Ecological	0 to 1	Likelihood of class transitions	Land Cover

		according to past observations; computed in TerrSet

3.2.3 Historical Landscape Pattern Analysis

The historical patterns were evaluated looking at both quantity and allocation of changes. The quantification was assessed in the R environment by producing 10 transition matrices regarding all the possible combinations between land cover maps. This procedure was conducted for the full landscape and the upper and lower parts of the landscape (Table S2 Supplementary Materials). The qualitative and spatial dynamics were assessed with landscape metrics, produced with the R package landscapemetrics (Hesselbarth et al., 2019). These two analyses allowed a more comprehensive insight into the nature of ecological successions. We considered four landscape metrics for the comparison between higher and lower elevations: edge density, patch density, contagion and Shannon's evenness index. The Shannon's evenness index was preferred over diversity indices because it does not include the richness, which is a meaningless variable in our landscape since the number of classes does not change over the years.

3.2.4 Landscape Pattern Forecast

Future changes were predicted for both short (that is, 2050) and long-term (that is, 2100) predictions using a GIS modeling approach in TerrSet environment within the panel 'Land Change Modeler' (LCM), conveniently implemented with other TerrSet tools. This framework joins two separate models: MC and multi-layer perceptron (MLP) (Figure 3.2).

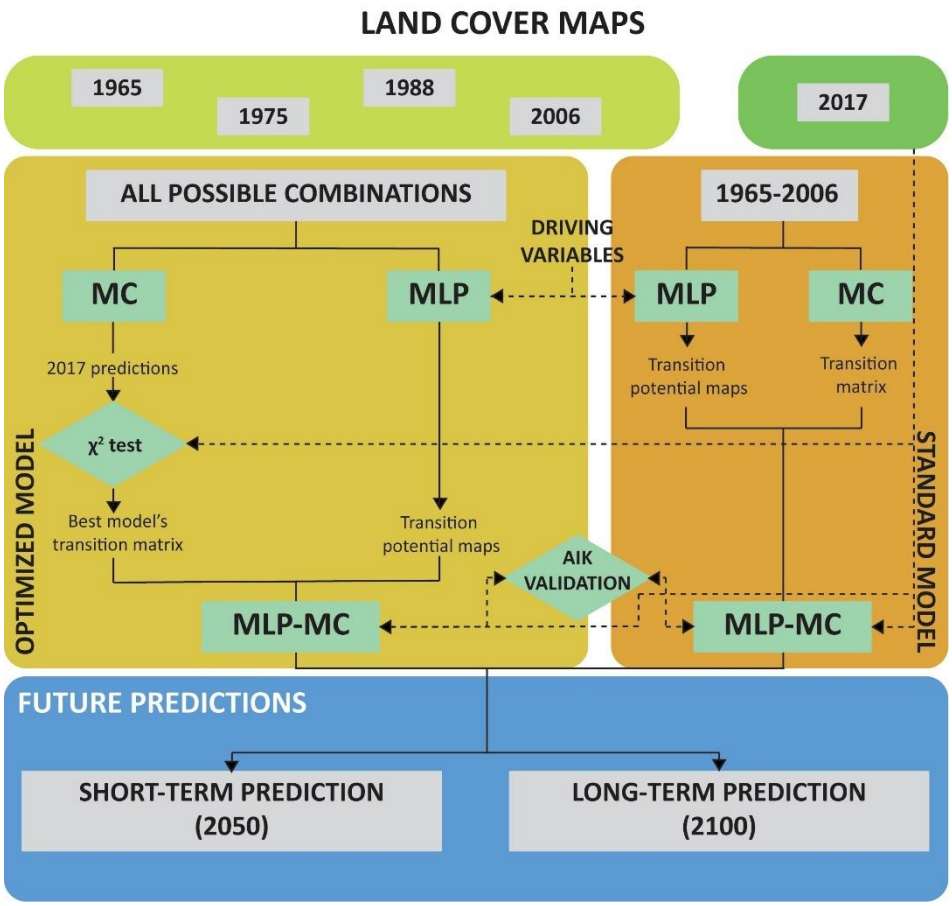

FIGURE 3.2. Conceptual workflow of the LCM model adopted at Mont Avic. A combination of MC (Markov chain) and MLP (multi-layer perceptron) models.

First, a 'transition probability matrix' was produced through the use of MC model that expresses the likelihood of change from one state to another in a consecutive way, by providing two distinct land cover maps (Jokar Arsanjani et al., 2013). A MC is a system of elements that pass through one state to another over a discrete time space (Balzter 2000) consistent with the Markov property:

$$P(X_{t+1} = i_{s+1} | X_t = i_s, X_{t-1} = i_{s-1}, \ldots, X_0 = i_0) = P(X_{t+1} = i_{s+1} | X_t = i_s) \qquad (3.1)$$

For all times t = 1,2,3,... and for all states $s = s_0, s_1, \ldots, s_t, s$. Accordingly, X_{t+1} depends upon X_t, but it does not depend upon $X_{t-1}, \ldots, X_1, X_0$. The transition

probability matrix P reports the probability that each land cover type would be found after a certain number of time units for k states:

$$P = \begin{pmatrix} p_{11} & \cdots & p_{1k} \\ \cdots & \cdots & \cdots \\ p_{k1} & \cdots & p_{kk} \end{pmatrix} \quad (3.2)$$

where p_{ij} are calculated according to Eq. (3.1).

An assumption to the original MC formulation is the time homogeneity between observations. If time intervals are not equal, different estimation techniques are available (see Takada et al., 2010 for the implementation of yearly matrices).

Second, a spatially explicit model was trained to produce a suitability map that describes the likelihood of change among the different cells. For this study, we applied a MLP model, one of the most common types of ANN (Sangermano et al., 2012) that consists of an input layer, one or more hidden layers and an output layer, where every neuron in each hidden layer is connected to other neighboring layers' neurons (Ozturk, 2015). MLP is a non-parametric algorithm; thus, it allows multicollinearity and meaningless variables to be excluded.

The model consists of a series of submodels that represents specific transitions. For this study, only the main dense forest dynamics, that is, the transitions from SF, GR and UV to FO, were considered when training MLP. Model parameterization is a crucial part of the process and requires adjusting especially the start learning rate and the hidden layer nodes in order to produce the highest accuracy (Eastman et al., 2005). The explanatory variables in the submodels can be both static and dynamic. Static variables do not change over time, while dynamic variables are recalculated during the prediction. In this study, we considered all the variables as static except for the distance from forest and sparse forest areas. It is common in landscape ecology studies (Mishra, 2016; Ozturk, 2015) to consider distance from buildings and roads as dynamic variables, but since the area did not show great urbanization, these variables were counted as fixed. The MLP model also applies a Jackknife test to measure the relevance of each variable in driving the changes.

The joining of the two models (MLP-MC) allows for the change allocation prediction according to the amount of change (MC model) and the potential for change (MLP model). A common experimental approach is to predict future cover classes based on the oldest and newest land cover maps (for example, Al-Shaar et al., 2021; Mirici, 2018). In this research, we compared this standard model (hereafter, SM; 1965 as a starting date for the calibration period) with an optimized model (OM) that considered the ability in predicting future land cover for the year 2017. To do this, all possible combinations between maps before 2017 were tested to extract all the change detection matrices (Markov chain's probability transition matrices and area matrices) of LU change (Table S3.3 Supplementary Materials). Note the numbers in this table refer to probabilities of change according to MC, and consequent areas, while the numbers in Table S3.2 Supplementary Materials are observed transitions in the past. By using the 'Markov' tool of TerrSet, the probability transition matrices were calculated considering the classification accuracy as a measure of uncertainty called proportional error, which in this study was based on the mean of the OAs of the calibration periods. We then validated these MCs by comparing observed and predicted land cover values for 2017 using Pearson's Chisquare test according to the Eq. (3.3):

$$X^2 = \sum_{i=1}^{n} \frac{(O_i - E_i)^2}{E_i} \tag{3.3}$$

where n = 4 (FO, SF, GR and UV classes were considered); O_i is the observed value of land cover; E_i is the expected one obtained from the MC model. The initial state chosen for this OM was the one with the lowest Pearson's Chi-square in respect of the 2017 prediction.

We predicted the 2017 land cover map according to the SM and the OM with reference to 2006 to validate the results (Verburg et al., 2004). The process was conducted with the TerrSet tool 'Validate', which provides an assessment of the spatial prediction according to four components of the kappa index of agreement

(KIA): Kstandard, Kno, Klocation and Klocationstrata (Table S3.4 Supplementary Materials). The combination of these four kappa indices allows the overall success rate to be assessed and to understand the strength factors of the prediction (that is, allocation and quantity).

Once this MLP-MC validation had been performed, two BaU predictions were assessed for both the SM (1965–2017 calibration period) and OM (initial state selected according to Pearson's ChiSquare results and final state as 2017), one for the short-term (2050) and one for the long-term timespan (2100). The two models were also averaged to evaluate mean trends. The transition potential matrices obtained with the MC were applied to all the LCCs (Table S3.3 Supplementary Materials). The future allocation (MLP-MC model) considered only the major transition (all-to-FO) to obtain superior results (Ozturk, 2015) and to gather just future forest dynamics. Three class metrics (edge density, patch density, mean core area) based on FO class were performed to compare past and future dynamics.

3.3 Results

3.3.1 Historical Landscape Pattern

Historical landscape dynamics were measured with quantitative and spatial metrics, according to transition matrices and landscape metrics. Figure 3.3 shows the evolution of the five LCCs area from 1965 to 2017 on the total landscape. The most important trend is the expansion of dense forest, from 1778 ha in 1965 to 2978 ha in 2017, corresponding to an increase at a rate of + 1.3% $year^{-1}$. The biggest loss was experienced by unvegetated areas, more than 36% of their surface and a decrease at a rate of –0.7% $year^{-1}$ (from 1876 to 1194 ha). According to the Producer's Accuracy, the most uncertain class is SF, while other classes are relatively accurate.

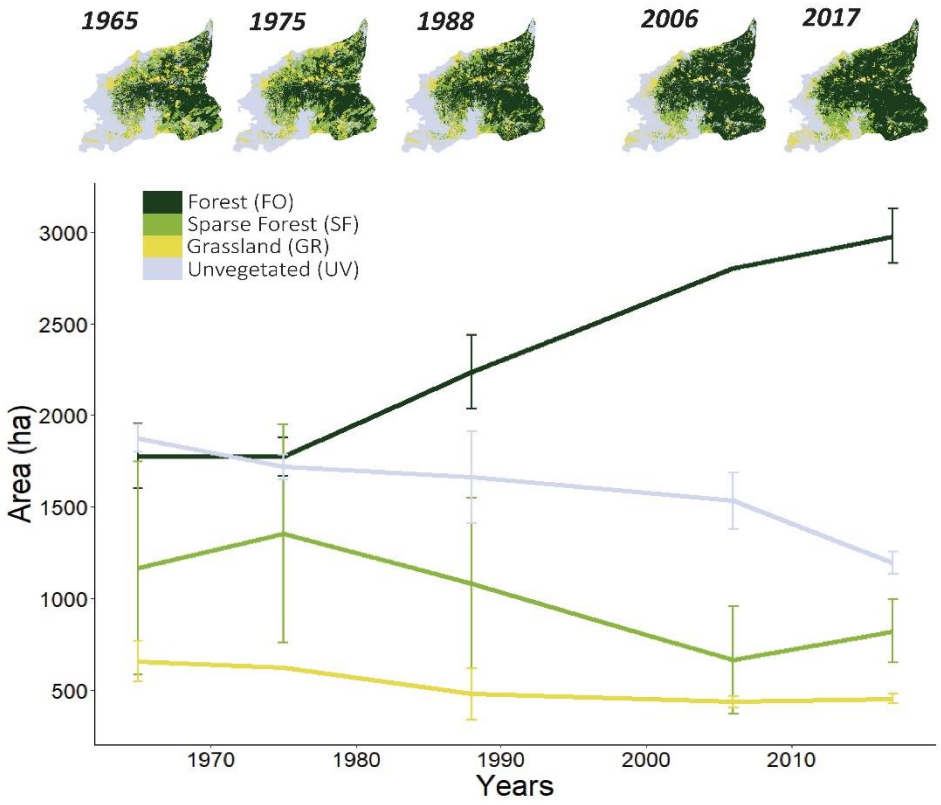

FIGURE 3.3. Historical land cover maps (1965, 1975, 1988, 2006, 2017) and area of each land cover class over time. Urban class was removed from the analysis. The error bars represent the Producer's Accuracy of the different classes (Table S1 Supplementary Materials).

Temporal (Figure 3.3) and spatial (Figure 3.4) LUC patterns at MA emerged as being not linear. FO increase between 1975 and 2006 was constant (+ 2.0% year-1 in the period 1975–1988 and + 1.5% year-1 between 1988 and 2006), while it decreased in the last 11 years (+ 0.6% year-1). SF decreased between 1975 and 2006, but showed an improvement in the last 11 years (2006–2017), with an increase rate of + 2.1% year^{-1}.

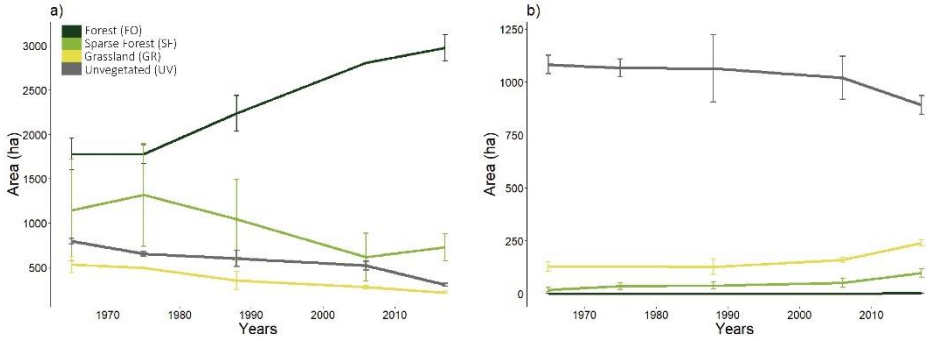

FIGURE 3.4. Land cover classes area for the lower (a) and upper (b) elevations at MA from 1965 to 2017. The error bar represents the Producer's Accuracy of different classes (Table S1 Supplementary Materials).

At lower elevations, the decreasing trend of edge density, patch density and Shannon evenness and the increase of the contagion index suggest a simplification of spatial pattern due to the forest gain (Table 3.2). In the upper part of the landscape, the most relevant class over the period remains UV, thus facing a decrease at a rate of –0.4% year^{-1} in the 50 years (from 1082 ha in 1965 to 891 ha in 2017). SF and GR increased over the period with a rate of + 7.8% year^{-1} and + 1.6% year^{-1}, respectively (Figure 3.4b). Looking at the transition matrices (Table S3.2 Supplementary Materials), UV contributed to increasing especially the GR (168 ha exchanged between 1965 and 2017) and then SF (46 ha). Landscape metrics (Table 3.2) indicate an opposite trend with respect to the lower elevations, corresponding to fragmentation and plant colonization of UV areas. Biggest changes—represented in Figure S3.4 and Table 3.2—were experienced in the last years, especially from 2006 to 2017; UV surface decreased at a rate of –1.1% year^{-1} in this period, more than nine time faster than the previous 40 years –0.14% year^{-1}, Shannon evenness increase in this period (+ 3.4% year^{-1}) was more than ten times higher with respect to the previous period (+ 0.3% year^{-1}).

TABLE 3.2. Landscape Metrics for Past Classes in the Upper (above 2182 m a.s.l.) and Lower (below 2182 m a.s.l.) Parts of the Landscape and Trend Over Time.

	LANDSCAPE METRICS							
	Edge Density (m ha^{-1})		**Contagion (%)**		**Patch Density (N 100ha^{-1})**		**Shannon Evenness (-)**	
Years	**Low**	**High**	**Low**	**High**	**Low**	**High**	**Low**	**High**
1965	372.0	76.5	39.1	79.4	155.0	29.6	0.81	0.30
1975	387.0	108.0	39.5	75.8	146.0	41.5	0.80	0.33
1988	365.0	96.1	43.6	76.1	130.0	29.9	0.74	0.34
2006	285.0	165.0	51.8	73.6	131.0	72.9	0.64	0.35
2017	197.0	189.0	59.2	65.5	82.4	63.3	0.57	0.48
TREND	↘	↗	↗	↘	↘	↗	↘	↗

3.3.2 Model Outcomes

The Pearson's Chi-square analyses show that the highest predictive power for 2017 projection was the one obtained from the 1975–2006 period, with a value of 40.1. Thus, we selected 1975 as the initial state for the OM. The mean accuracy of MLP models was about 60% (Table S3.4 Supplementary Materials). All the kappa values for the 2017 validation (1965–2006 and 1975–2006 calibration periods) are greater than 0.80, reaching 0.88 peaks for *Klocation* and *Klocationstrata* in the SM (Table S3.4 Supplementary Materials). Predictions can thus be considered strong, and both the optimized and standard MLP-MC models can be applied to predict future dynamics.

Figure 3.5 shows the relative importance of the most relevant driving variables common to all the MLP models (distance from FO, the likelihood of class transitions, the cost of movement and the TWI) according to the Jackknife test of MLP models. These four driving factors contribute to more than 99.8% of the total accuracy. There are little differences between the models regarding the driving variables explanatory power, and the relevance order is the same.

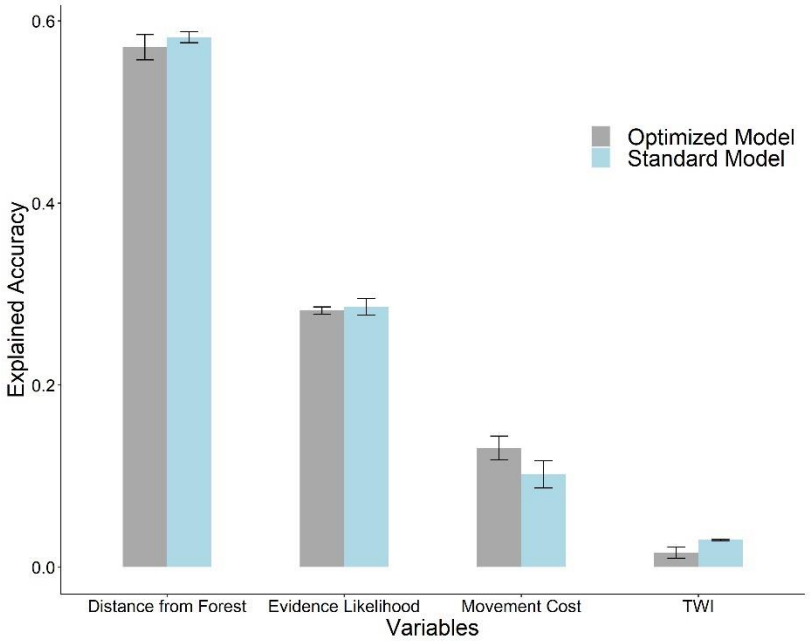

FIGURE 3.5. Drivers' relevance corresponding to the amount of accuracy gained by including the variable in the model according to backward stepwise constant forcing based on the mean of standard (1965–2006 and 1965–2017) and optimized (1975–2006 and 1975–2017) models. The error bars represent the standard deviation.

3.3.3 Landscape Pattern Forecast

Predicted forest gain is higher for the OM (19752017 calibration period) than the SM (1965–2017) (Figure 3.6). Initial FO expansion (2017–2050) shows an increase at a rate of + 0.29% y^{-1} and + 0.16% y^{-1}, respectively, for the OM (3258 ha in 2050) and SM (3139 ha). Between 2050 and 2100, the OM's trend remains quite constant (+ 0.33% y^{-1}, 3802 ha), while it increases for the SM (+ 0.33% y^{-1}, 3674 ha). SF class shows an initial growth until 2050 for the two models, then

a decrease related to FO transitions, confirmed by the mirrored behavior of FO and SF transitions and by the potential matrices (Table S3.3 Supplementary Materials), which reflects a great inclination of SF classes toward FO. UV, the second biggest class in 2017, will be outclassed by SF before 2050. GR cover was predicted as decreasing in a similar way according to the two models: about –0.30% y^{-1} for the period 2017–2050, about –0.55% y^{-1} for the period 2050–2100.

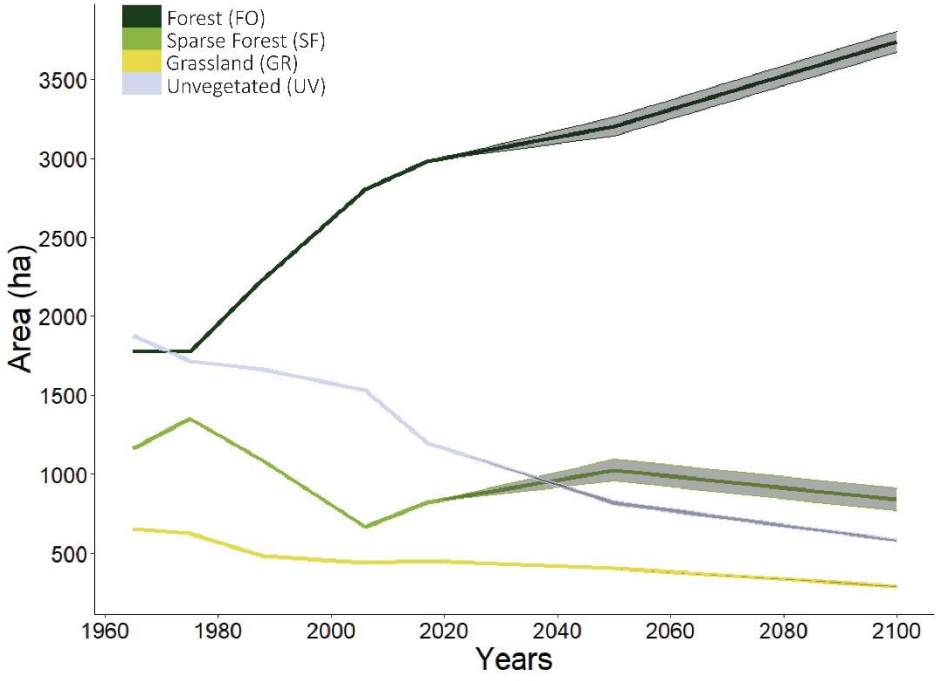

FIGURE 3.6. Observed and predicted land cover with Markov chain model based on standard model (1965–2017 calibration period) and optimized model (1975–2017 calibration period). The geometric line represents the mean between the two models; the geometric ribbon represents the range described by the two models.

Dense forest gain was forecast toward upper elevations, especially in the long-term prediction (Figure 3.7). Class metrics relative to the dense forest stands reflect different future forest dynamics at lower and upper elevations (Table 3.3). Below the timberline, edge density and patch density were predicted to decrease between 1965 and 2100 (–50% and –80%, respectively), while mean core area was forecast to increase tenfold over the years. Edge density and patch density

showed a divergent trend in the upper part of the landscape, while mean core area showed an increase where in 1965 there were no dense forests.

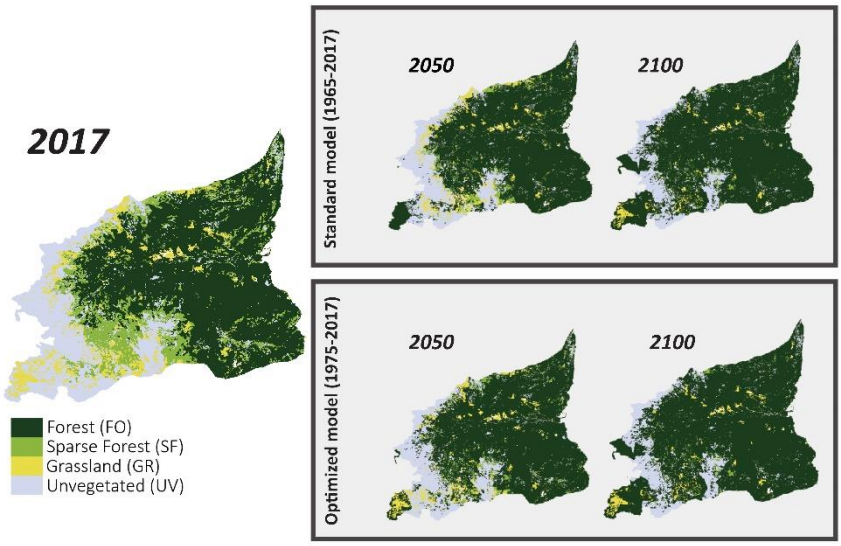

FIGURE 3.7. Land cover predictions for future scenarios (2050, 2100) based on the standard model (calibration period 19652017) and on the optimized model (calibration period 1975–2017).

TABLE 3.3. Metrics for the Class Dense Forest (FO) for Past and Future.

	FOREST METRICS																	
Years	***Edge Density (m ha^{-1})***						***Patch Density (N 100ha^{-1})***						***Mean Core Area (ha)***					
	Low			***High***			***Low***			***High***			***Low***			***High***		
	Mean	***Opt***	***Std***	***Mean***	***Opt***	***Std***	***Mean***	***Opt***	***Std***	***Mean***	***Opt***	***Std***	***Mean***	***Opt***	***Std***	***Mean***	***Opt***	***Std***
1965	*212.0*	*-*	*-*	*0.02*	*-*	*-*	*20.30*	*-*	*-*	*0.08*	*-*	*-*	*1.42*	*-*	*-*	*0.00*	*-*	*-*
1975	*201.0*	*-*	*-*	*0.27*	*-*	*-*	*17.80*	*-*	*-*	*0.33*	*-*	*-*	*1.65*	*-*	*-*	*0.00*	*-*	*-*
1988	*237.0*	*-*	*-*	*0.02*	*-*	*-*	*11.60*	*-*	*-*	*0.08*	*-*	*-*	*3.27*	*-*	*-*	*0.00*	*-*	*-*
2006	*182.0*	*-*	*-*	*0.41*	*-*	*-*	*6.10*	*-*	*-*	*0.24*	*-*	*-*	*8.81*	*-*	*-*	*0.02*	*-*	*-*
2017	*136.0*	*-*	*-*	*1.54*	*-*	*-*	*7.20*	*-*	*-*	*1.13*	*-*	*-*	*8.49*	*-*	*-*	*0.05*	*-*	*-*

2050	*123.0*	*127.0*	*119.0*	*24.90*	*32.70*	*17.10*	*6.10*	*6.39*	*5.80*	*6.88*	*9.46*	*4.29*	*9.17*	*8.71*	*9.62*	*0.38*	*0.18*	*0.58*
2100	*108.5*	*101.0*	*116.0*	*34.25*	*38.60*	*29.90*	*4.00*	*3.15*	*4.84*	*5.30*	*5.84*	*4.75*	*15.85*	*19.60*	*12.10*	*1.65*	*1.25*	*2.04*
TREND	↘			↗			↘			↗			↗			↗		

3.4 Discussion

3.4.1 Historical Landscape Pattern

Forest gain following land abandonment is a common dynamic in temperate mountain areas (Kamada & Nakagoshi, 1997; Gautam et al., 2004; Benayas et al., 2007). Considering dense (FO) and sparse (SF) forest classes together, we observed an overall increase at a rate of + 0.56% year^{-1} (1965–2017 period) that is similar to the mean value recently observed by Garbarino et al., (2020) for other landscapes of the Alps and Apennines (+ 0.60% year^{-1}) and to the reforestation rate of temperate areas reported by Sitzia et al. (2010) of 0.59 ± 0.30% year^{-1}. The FO class alone shows a higher past overall increase (+ 1.30% year^{-1}). The length of time since abandonment affects forest density; thus, the value we observed highlights an important role of land abandonment (Tasser et al., 2007; Orlandi et al., 2016).

We observed a divergent pattern of change between lower and upper elevation in our study area. Landscape metrics and transition matrices display an increase of homogeneity at lower elevations due to the expansion of dense forests led especially by gap-filling processes to the detriment of sparse forests (SF) and grasslands (GR) (Tables 3.2, S3.2 Supplementary Materials). The increase of dense forests started in 1975, while between 1965 and 1975 their amount remained quite stable, and the SF class increased from 1164 to 1353 ha (Figure 3.3). Looking at the transition matrices, these starting dynamics seem to be linked to a mutual exchange of surface between the two land classes (SF/FO). The observed pattern may be explained by the slowness of initial forestation processes and the occurrence of the final stage of forest use and rural economy. However, the limited SF class accuracy could have led to an overestimation of the transition from SF to FO and vice versa. The forest gain appears to recede in the last years (1990–2020) maybe due to a saturation of available open areas. The faster decline of edge density and patch density at lower elevations between 2006 and 2017 is

associated to the intensification of canopy cover closure. This process is probably favored by longer vegetation periods with warmer spring temperatures and by land use legacies (Richardson et al., 2013; Filippa et al., 2019). In contrast, the upper elevations appear to be more fragmented, as demonstrated by the increase of Shannon's evenness and edge density, and a decrease of contagion index. This was due to the encroachment of unvegetated soil by grasslands, and woody vegetation (88% of the total upper area was occupied by unvegetated soil in 1965, 71% in 2017), where the role of land use is expected to be lower (Figure 3.4b). The general timberline upward shift in MA study area for FO categories was measured as + 2.3 m $year^{-1}$ (maximum dense forest elevation of 2182 m a.s.l. in 1965, 2302 m a.s.l. in 2017). These results are comparable to the treeline migration (+ 2.0–3.0 m $year^{-1}$) described in many European mountain areas (Walther et al., 2005; Lenoir et al., 2008; Ameztegui et al., 2016; Leonelli et al., 2016). Treelines in the Canadian Rocky Mountains showed a similar behavior (that is, treeline advance and tree density increase), but the upward shift rate was lower (Trant et al., 2020). The transition from unvegetated to vegetated classes (primary succession) increased in magnitude in the last decade (+ 15.9 ha $year^{-1}$), compared to the previous period (+ 2.7 ha $year^{-1}$). The acceleration of primary succession processes at MA may reflect the leading role of the CC, which is probably equaling the relevance of LUC and is expected to become the dominant driver of change, especially at upper elevations (Gehrig-Fasel et al., 2007; Filippa et al., 2019). A particular case of transition in the upper part is the expansion of sparse forests and shrubs, which highlights a fast woody intrusion in the subalpine and alpine zone. The SF class increase is due to the transition from unvegetated soil (46 ha), which can be considered a primary succession, and from grassland (37 ha), a secondary succession (Table S3.2 Supplementary Materials). Mountain areas with past heavy exploitation followed by abandonment typically show a similar pattern, with gap-filling processes at lower elevations (Malandra et al., 2019), and an upward shift of treeline and woody encroachment at upper elevations (Harsch et al., 2009; Malfasi & Cannone, 2020).

Historical land use legacies on forest structure and landscape patterns is a well-known process (Garbarino & Weisberg, 2020). New forests that developed in the last 50 years through encroachment on grasslands and meadows show a higher proportion of larch among seedlings, young, and dominant trees layers, whereas mountain pines dominate forest patches developed on unvegetated areas (primary succession).

3.4.2 Landscape Pattern Forecast

Our land cover change models predict a future change that is consistent with the historical one. Gap-filling dynamics will be dominant at lower elevations and a fragmentation will continue in the upper part of the catchment (Table 3.3). However, the overall forest gain and the expansion of FO class alone are predicted to slow down in the future (2017–2100) according to the two models at a mean rate of + 0.31% $year^{-1}$ (Figure 3.6). These predictions are considered realistic because of a reduction of space availability for forest gain at lower elevations and the slow processes at the timberline ecotone. Moreover, future predictions tend to allocate forest gain at upper elevations more than to the detriment of grasslands located in the lower portion; this may be explained by the present utilization of these meadows that do not persuade the MLP-MC model to forecast future forest gap-filling in these areas (Figure 3.7). A decrease in forest edge and patch densities is predicted by our models. Mean core area, instead, shows different behaviors, with a regular increasing trend for the standard model and a higher increase for the optimized model that suggests strong future gap-filling dynamics causing a further saturation of available open habitats.

At upper elevations, the density of forest patches is predicted to follow two different future patterns: a linear expansion of trees (standard model) and a rapid expansion of small patches followed by a decrease in the number of patches (optimized model), maybe due to a closure of the patches. Since the two models differed only for the starting period, the amount of dense forests of 1965 and 1975 influences the future forest gain prediction.

According to long-term future predictions, sparse forests will be replaced by dense ones in our study area (Figure 3.7, Table S3.3 Supplementary Materials). However, it is important to consider that the prevailing serpentine lithology of the catchment limits soil fertility and subsequently slows down the growth and establishment of trees (Kim & Shim, 2008). Nevertheless, the increase in extreme drought frequency due to CC may counteract the expensive dynamics of forest, leading to different and complex treeline dynamics, ignored by models like MLP-MC (Allen et al., 2010). Other extreme events, such as wildfires, heavy rains with potential of landslides, insect disturbances and their interaction, are expected to increase in frequency and intensity according to climate and LU changes and may dampen future predictions reliability (Barros et al., 2017; Seidl et al., 2017).

3.4.3 Models Discussion: MC, MLP-MC and Driving Factors

LUC historical patterns show a nonlinear trend in our study area, so we adopted a non–linear modeling approach to make predictions. Assessment of future dynamics based on past land use data proved to be a useful tool not only for predicting future trends, but also for amplifying and better understanding past dynamics, especially with a fine temporal resolution. Still, forest landscape ecological forecasting studies often lack a common design and rely on a few maps or low time frequency. Our methodological approach based on the selection of the initial stage with the Pearson's Chi-square highlights that land use dynamics between 1965 and 1975 were different from the recent ones. Furthermore, by looking at general trends it is possible to notice that the slope of transition remains constant from 1975 to 2006 for almost all LCCs. This means that the OM focuses on the most relevant degree of change.

The distance from preexisting forest edges is the most important driver for the forest cover change (Figure 3.5). The proximity to closed canopy affects seed recruitment and creates favorable microsites for forest gain in different forest ecosystems (for example, Günter et al., 2007; Garbarino et al., 2020).

The second driving variable according to its relevance is the evidence likelihood, which represents the future transition probability based on past observations. Another important driver appears to be the cost of movement according to the Tobler hiking function that joins anthropogenic and topographic aspects to determine the accessibility of land for human activities and is thus a proxy for site remoteness that is strictly related to historical human legacies such as harvesting and pasturing.

Prediction of forest landscape changes through historical aerial images and environmental driving variables can be important to satisfy the increasing request of future LUC scenarios to guide decision making (Guan et al., 2008; Tattoni et al., 2011; Stürck & Verburg, 2017). With this study, park managers can understand future trajectories of forests under BaU scenarios. Our predictions confirm the hypothesis under which climate change and land abandonment promote gap-filling dynamics at lower elevations and woody encroachment at upper elevations, leading to an overall loss of open habitats (Barros et al., 2017). This may cause different cascading effects such as loss of biodiversity, increased risk of fire ignition and propagation due to landscape uniformity and fuel buildup, and the loss of cultural landscapes and management techniques (Lasanta et al., 2017; Mantero et al., 2020). In European mountains, the loss of a-diversity caused by the decline of open habitats is mostly related to least concern species with low vagility, while the past forest gain led to an enrichment in forest specialist birds and mammals (Guliherme & Pereira, 2013; Martínez-Abraín et al., 2020).

3.5 Conclusions

Our data provide evidence of divergent land use change dynamics between lower and upper elevations in a subalpine watershed of the Alps over the last 50 years. Secondary succession gap-filling processes dominate at lower elevations, whereas primary successions and treeline advancement are stronger at upper elevations and have accelerated in recent years. Climate and land use change effects are difficult to disentangle, but our predictions suggest that the influence

of climate will be stronger than land use legacies on future upper elevation forest dynamics. Our results are in line with other studies in mountain watersheds and represent a possibility of a BaU forecasting approach in alpine ecosystems. One caveat to this approach is the assumption that socioeconomic conditions will endure in the future. It is important to remark that different land use scenarios might arise unpredictably because of changes in agricultural and forestry policies (for example, the European Union's Common Agricultural Policy, CAP). In some mountain regions, recent pastoral promotion is leading to an increase in domestic density and traditional land uses (Lasanta et al., 2016).

However, it is rather difficult that an abrupt change in socioeconomic patterns will occur in a remote and marginal area such as MA, where the soil conditions have always been a limitation for pastoral practices as a consequence of the toxic and unfertile serpentine lithology (D'Amico et al., 2008). Long fine-resolution time series allowed a good evaluation of past dynamics on a subalpine watershed and led to the evidence of the role of climate change at upper elevations. We believe that this approach should be applied to reconstruct time series of land use change over a wide range of mountain forest ecosystems. As shown in this study, a higher number of LC maps over the years can be crucial to assess the role of climate change and land abandonment in alpine landscapes and to predict future dynamics. Moreover, the application of a nonlinear model along with different LC maps allowed a thorough model calibration, avoiding the traditional approach in which the adopted calibration period is given by the oldest and newest land cover classification. The relatively low agro-pastoral activity at Mont Avic and the high classification accuracy of the unvegetated class are important to emphasize the role of climate-driven primary successions. The main limitation of our work is the low accuracy of the SF class, which includes both rare woody areas and shrubs, which can lead to some mistakes in the accuracy assessment and future projection. Climate change is expected to be the most relevant process in the near future, overcoming LUC in alpine forests and our results suggest that it is likely that forest gain at upper elevations will increase in the future, with

consequences on habitat composition, biodiversity, natural disturbance regime and forest management.

Acknowledgements

We thank the Mont Avic Natural Park for funding this research through the Interreg V-A Italy/ Switzerland 2014/2020 Project N.622393 MINERALP and for logistic support during the field surveys. We thank Alison M.N. Garside for the language revision and three reviewers for their comments on an earlier version of this manuscript.

Data availability

Data are available at https://figshare.com/articles/dataset/Past_1965-2017_and_future_2050_2100_land_cover_raster_data_of_Mont_Avic_NW_Alps_/1 6718737

References

Alberti, G. (2019). movecost: An R package for calculating accumulated slope-dependent anisotropic cost-surfaces and least-cost paths. *SoftwareX*, 10, 100331.

Allen, C. D., Macalady, A. K., Chenchouni, H., Bachelet, D., McDowell, N., Vennetier, M., ... & Cobb, N. (2010). A global overview of drought and heat-induced tree mortality reveals emerging climate change risks for forests. *Forest ecology and management*, 259(4), 660-684.

Al-Shaar, W., Nehme, N., & Adjizian Gérard, J. (2021). The applicability of the extended markov chain model to the land use dynamics in Lebanon. *Arabian Journal for Science and Engineering*, 46, 495-508.

Ameztegui, A., Coll, L., Brotons, L., & Ninot, J. M. (2016). Land-use legacies rather than climate change are driving the recent upward shift of the mountain tree line in the P yrenees. *Global Ecology and Biogeography*, 25(3), 263-273.

Balzter, H. (2000). Markov chain models for vegetation dynamics. *Ecological modelling*, 126(2-3), 139-154.

Barros, C., Gueguen, M., Douzet, R., Carboni, M., Boulangeat, I., Zimmermann, N. E., ... & Thuiller, W. (2017). Extreme climate events counteract the effects of

climate and land-use changes in A lpine tree lines. *Journal of Applied Ecology*, 54(1), 39-50.

Becker, A., Körner, C., Brun, J. J., Guisan, A., & Tappeiner, U. (2007). Ecological and land use studies along elevational gradients. *Mountain Research and Development*, 27(1), 58-65.

Benayas, J. M., Martins, A., Nicolau, J. M., & Schulz, J. J. (2007). Abandonment of agricultural land: an overview of drivers and consequences. *CAB reviews: Perspectives in Agriculture, Veterinary Science, Nutrition and Natural Resources* 2.57:1–14.

Bugmann, H., Gurung, A. B., Ewert, F., Haeberli, W., Guisan, A., Fagre, D., & Kääb, A. (2007). Modeling the biophysical impacts of global change in mountain biosphere reserves. *Mountain Research and Development*, 27(1), 66-77.

Chauchard, S., Carcaillet, C., & Guibal, F. (2007). Patterns of land-use abandonment control tree-recruitment and forest dynamics in Mediterranean mountains. *Ecosystems*, 10(6), 936-948.

Clavero, M., Villero, D., & Brotons, L. (2011). Climate change or land use dynamics: do we know what climate change indicators indicate? *PLoS One*, 6(4), e18581.

Cousins, S. A., Auffret, A. G., Lindgren, J., & Tränk, L. (2015). Regional-scale land-cover change during the 20th century and its consequences for biodiversity. *Ambio*, 44, 17-27.

D'Amico, M., Julitta, F., Previtali, F., & Cantelli, D. (2008). Podzolization over ophiolitic materials in the western Alps (Natural Park of Mont Avic, Aosta Valley, Italy). *Geoderma*, 146(1-2), 129-137.

Dubovyk, O., Sliuzas, R., & Flacke, J. (2011). Spatio-temporal modelling of informal settlement development in Sancaktepe district, Istanbul, Turkey. *ISPRS Journal of Photogrammetry and Remote Sensing*, 66(2), 235-246.

Eastman, J. R., Van Fossen, M. E., & Solarzano, L. A. (2005). Transition potential modeling for land cover change. *GIS, spatial analysis and modeling*, 17, 357-386.

Eastman, J.R. (2016). *TerrSet Geospatial Monitoring and Modeling System–Manual*. Clark University.

Elliott, G. P. (2011). Influences of 20th-century warming at the upper tree line contingent on local-scale interactions: Evidence from a latitudinal gradient in the Rocky Mountains, USA. *Global Ecology and Biogeography*, 20(1), 46-57.

Evans, J. S. (2020). *SpatialEco. r Package Version 1.3-6*. R Package version, 1.

Fajardo, A., Gazol, A., Mayr, C., & Camarero, J. J. (2019). Recent decadal drought reverts warming-triggered growth enhancement in contrasting climates in the southern Andes tree line. *Journal of Biogeography*, 46(7), 1367-1379.

Fang, K., Gou, X., Chen, F., Peng, J., D'Arrigo, R., Wright, W., & Li, M. H. (2009). Response of regional tree-line forests to climate change: evidence from the northeastern Tibetan Plateau. *Trees*, 23, 1321-1329.

Fattah, M. A., Morshed, S. R., & Morshed, S. Y. (2021). Multi-layer perceptron-Markov chain-based artificial neural network for modelling future land-specific carbon emission pattern and its influences on surface temperature. *SN Applied Sciences*, 3, 1-22.

Filippa, G., Cremonese, E., Galvagno, M., Isabellon, M., Bayle, A., Choler, P., ... & Migliavacca, M. (2019). Climatic drivers of greening trends in the Alps. *Remote Sensing*, 11(21), 2527.

Garbarino, M., Morresi, D., Urbinati, C., Malandra, F., Motta, R., Sibona, E. M., ... & Weisberg, P. J. (2020). Contrasting land use legacy effects on forest landscape dynamics in the Italian Alps and the Apennines. *Landscape Ecology*, 35, 2679-2694.

Garbarino, M., Sibona, E., Lingua, E., & Motta, R. (2014). Decline of traditional landscape in a protected area of the southwestern Alps: the fate of enclosed pasture patches in the land mosaic shift. *Journal of Mountain Science*, 11, 544-554.

Garbarino, M., & Weisberg, P. J. (2020). Land-use legacies and forest change. *Landscape Ecology*, 35(12), 2641-2644.

Gautam, A. P., Shivakoti, G. P., & Webb, E. L. (2004). Forest cover change, physiography, local economy, and institutions in a mountain watershed in Nepal. *Environmental management*, 33, 48-61.

Gehrig-Fasel, J., Guisan, A., & Zimmermann, N. E. (2007). Tree line shifts in the Swiss Alps: climate change or land abandonment?. *Journal of vegetation science*, 18(4), 571-582.

Gontier, M., Mörtberg, U., & Balfors, B. (2010). Comparing GIS-based habitat models for applications in EIA and SEA. *Environmental Impact Assessment Review*, 30(1), 8-18.

Guan, D., Gao, W., Watari, K., & Fukahori, H. (2008). Land use change of Kitakyushu based on landscape ecology and Markov model. *Journal of Geographical Sciences*, 18, 455-468.

Guilherme, J. L., & Miguel Pereira, H. (2013). Adaptation of bird communities to farmland abandonment in a mountain landscape. *PloS one*, 8(9), e73619.

Günter, S., Weber, M., Erreis, R., & Aguirre, N. (2007). Influence of distance to forest edges on natural regeneration of abandoned pastures: a case study in the tropical mountain rain forest of Southern Ecuador. *European Journal of Forest Research*, 126, 67-75.

Harsch, M. A., Hulme, P. E., McGlone, M. S., & Duncan, R. P. (2009). Are treelines advancing? A global meta-analysis of treeline response to climate warming. *Ecology Letters*, 12(10), 1040-1049.

Hesselbarth, M. H., Sciaini, M., With, K. A., Wiegand, K., & Nowosad, J. (2019). landscapemetrics: an open-source R tool to calculate landscape metrics. *Ecography*, 42(10), 1648-1657.

Holtmeier, F. K., & Broll, G. (2019). Treeline research—From the roots of the past to present time. A review. *Forests*, 11(1), 38.

Iacono, M., Levinson, D., El-Geneidy, A., & Wasfi, R. (2015). A Markov chain model of land use change. *TeMA Journal of Land Use, Mobility and Environment*, 8(3), 263-276.

Arsanjani, J. J., Helbich, M., Kainz, W., & Boloorani, A. D. (2013). Integration of logistic regression, Markov chain and cellular automata models to simulate urban expansion. *International Journal of Applied Earth Observation and Geoinformation*, 21, 265-275.

Kamada, M., & Nakagoshi, N. (1997). Influence of cultural factors on landscapes of mountainous farm villages in western Japan. *Landscape and Urban Planning*, 37(1-2), 85-90.

Kim, J. M., & Shim, J. K. (2008). Toxic effects of serpentine soils on plant growth. *Journal of Ecology and Environment*, 31(4), 327-331.

Körner, C. (2015). Paradigm shift in plant growth control. *Current opinion in plant biology*, 25, 107-114.

Lantman, J.V.S., Verburg, P. H., Bregt, A., & Geertman, S. (2011). Core principles and concepts in land-use modelling: A literature review. *Land-use modelling in planning practice*, 35-57.

Lasanta, T., Nadal-Romero, E., Errea, P., & Arnáez, J. (2016). The effect of landscape conservation measures in changing landscape patterns: a case study in Mediterranean mountains. *Land Degradation & Development*, 27(2), 373-386.

Lasanta, T., Arnáez, J., Pascual, N., Ruiz-Flaño, P., Errea, M. P., & Lana-Renault, N. (2017). Space–time process and drivers of land abandonment in Europe. *CATENA*, 149, 810-823.

Lenoir, J., Gégout, J. C., Marquet, P. A., de Ruffray, P., & Brisse, H. (2008). A significant upward shift in plant species optimum elevation during the 20th century. *Science*, 320(5884), 1768-1771.

Leonelli, G., Masseroli, A., & Pelfini, M. (2016). The influence of topographic variables on treeline trees under different environmental conditions. *Physical Geography*, 37(1), 56-72.

Malandra, F., Vitali, A., Urbinati, C., Weisberg, P. J., & Garbarino, M. (2019). Patterns and drivers of forest landscape change in the Apennines range, Italy. *Regional Environmental Change*, 19, 1973-1985.

Malfasi, F., & Cannone, N. (2020). Climate warming persistence triggered tree ingression after shrub encroachment in a high alpine tundra. *Ecosystems*, 23, 1657-1675.

Mantero, G., Morresi, D., Marzano, R., Motta, R., Mladenoff, D. J., & Garbarino, M. (2020). The influence of land abandonment on forest disturbance regimes: a global review. *Landscape Ecology*, 35, 2723-2744.

Mas, J. F., Kolb, M., Paegelow, M., Olmedo, M. T. C., & Houet, T. (2014). Inductive pattern-based land use/cover change models: A comparison of four software packages. *Environmental Modelling & Software*, 51, 94-111.

Martínez-Abraín, A., Jiménez, J., Jiménez, I., Ferrer, X., Llaneza, L., Ferrer, M., ... & Oro, D. (2020). Ecological consequences of human depopulation of rural areas on wildlife: A unifying perspective. *Biological Conservation*, 252, 108860.

Metcalfe, P., Beven, K., Freer, J., Metcalfe, M. P., & deSolve, I. (2018). Package 'dynatopmodel'.

Ersoy Mirici, M., Berberoglu, S., Akın Tanrıöver, A., & Satir, O. (2018). Land use/cover change modelling in a mediterranean rural landscape using multi-layer perceptron and markov chain (mlp-mc). *Applied Ecology and Environmental Research*.

Mishra, V. N., & Rai, P. K. (2016). A remote sensing aided multi-layer perceptron-Markov chain analysis for land use and land cover change prediction in Patna district (Bihar), India. *Arabian Journal of Geosciences*, 9, 1-18.

Mont Avic. (2018). *Parco Naturale Mont Avic – Dichiarazione Ambientale 2018–2020*.

Muller, M. R., & Middleton, J. (1994). A Markov model of land-use change dynamics in the Niagara Region, Ontario, Canada. *Landscape Ecology*, 9, 151-157.

Noszczyk, T. (2018). A review of approaches to land use changes modeling. *Human and Ecological Risk Assessment: An International Journal*.

Orlandi, S., Probo, M., Sitzia, T., Trentanovi, G., Garbarino, M., Lombardi, G., & Lonati, M. (2016). Environmental and land use determinants of grassland patch diversity in the western and eastern Alps under agro-pastoral abandonment. *Biodiversity and Conservation*, 25, 275-293.

Ozturk, D. (2015). Urban growth simulation of Atakum (Samsun, Turkey) using cellular automata-Markov chain and multi-layer perceptron-Markov chain models. *Remote Sensing*, 7(5), 5918-5950.

Peters, M. K., Hemp, A., Appelhans, T., Becker, J. N., Behler, C., Classen, A., ... & Steffan-Dewenter, I. (2019). Climate–land-use interactions shape tropical mountain biodiversity and ecosystem functions. *Nature*, 568(7750), 88-92.

Richardson, A. D., Keenan, T. F., Migliavacca, M., Ryu, Y., Sonnentag, O., & Toomey, M. (2013). Climate change, phenology, and phenological control of vegetation feedbacks to the climate system. *Agricultural and Forest Meteorology*, 169, 156-173.

Ridding, L. E., Newton, A. C., Redhead, J. W., Watson, S. C., Rowland, C. S., & Bullock, J. M. (2020). Modelling historical landscape changes. *Landscape Ecology*, 35, 2695-2712.

Rutherford, G. N., Bebi, P., Edwards, P. J., & Zimmermann, N. E. (2008). Assessing land-use statistics to model land cover change in a mountainous landscape in the European Alps. *Ecological Modelling*, 212(3-4), 460-471.

Sangermano, F., Toledano, J., & Eastman, J. R. (2012). Land cover change in the Bolivian Amazon and its implications for REDD+ and endemic biodiversity. *Landscape Ecology*, 27, 571-584.

Seidl, R., Thom, D., Kautz, M., Martin-Benito, D., Peltoniemi, M., Vacchiano, G., ... & Reyer, C. P. (2017). Forest disturbances under climate change. *Nature Climate Change*, 7(6), 395-402.

Sitzia, T., Semenzato, P., & Trentanovi, G. (2010). Natural reforestation is changing spatial patterns of rural mountain and hill landscapes: A global overview. *Forest Ecology and Management*, 259(8), 1354-1362.

Stürck, J., & Verburg, P. H. (2017). Multifunctionality at what scale? A landscape multifunctionality assessment for the European Union under conditions of land use change. *Landscape Ecology*, 32, 481-500.

Takada, T., Miyamoto, A., & Hasegawa, S. F. (2010). Derivation of a yearly transition probability matrix for land-use dynamics and its applications. *Landscape Ecology*, 25, 561-572.

Tasser, E., Walde, J., Tappeiner, U., Teutsch, A., & Noggler, W. (2007). Land-use changes and natural reforestation in the Eastern Central Alps. *Agriculture, Ecosystems & Environment*, 118(1-4), 115-129.

Tattoni, C., Ciolli, M., & Ferretti, F. (2011). The fate of priority areas for conservation in protected areas: a fine-scale Markov chain approach. *Environmental Management*, 47, 263-278.

Tattoni, C., Ianni, E., Geneletti, D., Zatelli, P., & Ciolli, M. (2017). Landscape changes, traditional ecological knowledge and future scenarios in the Alps: A holistic ecological approach. *Science of the Total Environment*, 579, 27-36.

Tiberti, R., Buscaglia, F., Armodi, M., Callieri, C., Ribelli, F., Rogora, M., ... & Bocca, M. (2020). Mountain lakes of Mont Avic Natural Park: Ecological features and conservation issues. *Journal of Limnology*, 79(1).

Trant, A., Higgs, E., & Starzomski, B. M. (2020). A century of high elevation ecosystem change in the Canadian Rocky Mountains. *Scientific Reports*, 10(1), 9698.

Van der Sluis, T., Pedroli, B., Frederiksen, P., Kristensen, S. B., Busck, A. G., Pavlis, V., & Cosor, G. L. (2019). The impact of European landscape transitions on the provision of landscape services: an explorative study using six cases of rural land change. *Landscape Ecology*, 34, 307-323.

Verburg, P. H., Schot, P. P., Dijst, M. J., & Veldkamp, A. (2004). Land use change modelling: current practice and research priorities. *GeoJournal*, 61, 309-324.

Walther, G. R., Beißner, S., & Burga, C. A. (2005). Trends in the upward shift of alpine plants. *Journal of Vegetation Science*, 16(5), 541-548.

Supplementary Materials

TABLE S3.1. Description (source and color) and accuracy of the five aerial images used to produce land cover maps.

1965		
Image Description	**Rossi S.r.l**	**B/W**
Class	**PA%**	**UA%**
FO	90	82
SF	50	86
GR	83	75
UR	100	100
UV	96	80
OA%	81	
K	0.75	

1975		
Image Description	**GCR S.p.a.**	**Color**
Class	**PA%**	**UA%**
FO	94	86
SF	56	91
GR	100	82
UR	43	100
UV	96	83
OA%	85	
K	0.80	

1988		
Image Description	**GCR S.p.a.**	**B/W**
Class	**PA%**	**UA%**
FO	91	81
SF	57	72
GR	71	88
UR	100	80
UV	85	71
OA%	78	
K	0.71	

2006

Image Description	AGEA	Color
Class	**PA%**	**UA%**
FO	100	94
SF	56	90
GR	93	88
UR	100	100
UV	90	82
OA%	90	
K	0.86	

2017

Image Description	GeoEye-1	Color
Class	**PA%**	**UA%**
FO	95	93
SF	79	83
GR	94	94
UR	100	100
UV	95	95
OA%	92	
K	0.89	

TABLE S3.2. Transition Matrices regarding all the possible combinations between land cover maps for the overall landscape and the lower and upper elevations.

OVERALL LANDSCAPE

TRANSITIONS FROM 1965

		1975					
		FO	**SF**	**GR**	**UR**	**UV**	**tot**
1965	**FO**	1412.45	293.68	27.19	2.70	41.73	**1777.75**
	SF	258.97	729.46	79.68	1.57	94.34	**1164.02**
	GR	47.23	119.76	437.35	1.41	51.88	**657.63**
	UR	0.40	0.41	0.73	2.32	0.33	**4.19**
	UV	55.84	209.75	78.05	1.05	1529.92	**1874.61**
	tot	**1774.89**	**1353.06**	**623.00**	**9.05**	**1718.20**	**5478.20**

		1988					
		FO	**SF**	**GR**	**UR**	**UV**	**tot**
1965	**FO**	1521.53	204.26	13.37	6.11	32.4	**1777.67**
	SF	513.95	523.65	42.43	2.63	80.12	**1162.78**
	GR	103.98	148.97	347	4.14	53.15	**657.24**
	UR	0.61	0.53	0.82	2.04	0.19	**4.19**
	UV	96.44	203.76	75.65	1.38	1497.17	**1874.40**
	tot	**2236.51**	**1081.17**	**479.27**	**16.30**	**1663.03**	**5476.28**

TRANSITIONS FROM 1975

		1988					
		FO	**SF**	**GR**	**UR**	**UV**	**tot**
1975	**FO**	1570.68	165.27	11.29	3.64	23.96	**1774.84**
	SF	544.30	642.66	48.18	3.06	113.51	**1351.71**
	GR	72.26	132.17	359.56	3.77	54.92	**622.68**
	UR	1.38	1.40	1.13	4.37	0.77	**9.05**
	UV	47.97	139.80	59.11	1.46	1469.88	**1718.22**
	tot	**2236.59**	**1081.30**	**479.27**	**16.30**	**1663.04**	**5476.50**

		2006					
		FO	**SF**	**GR**	**UR**	**UV**	**tot**
1965	**FO**	1625.28	90.00	11.30	11.95	39.22	**1777.75**
	SF	785.98	265.24	29.98	4.36	78.46	**1164.02**
	GR	193.33	121.92	255.38	15.18	71.82	**657.63**
	UR	0.88	0.10	0.15	3.04	0.02	**4.19**
	UV	198.10	187.79	138.08	3.88	1346.76	**1874.61**
	tot	**2803.57**	**665.05**	**434.89**	**38.41**	**1536.28**	**5478.20**

		2006					
		FO	**SF**	**GR**	**UR**	**UV**	**tot**
1975	**FO**	1634.65	85.99	11.62	8.85	33.80	**1774.91**
	SF	869.83	322.86	39.68	6.68	114.11	**1353.16**
	GR	161.39	113.41	255.61	13.92	78.74	**623.07**
	UR	2.66	0.35	0.12	5.40	0.52	**9.05**
	UV	135.26	142.43	127.86	3.56	1309.11	**1718.22**
	tot	**2803.79**	**665.04**	**434.89**	**38.41**	**1536.28**	**5478.41**

		2017					
		FO	**SF**	**GR**	**UR**	**UV**	**tot**
1965	**FO**	1668.41	82.64	7.94	8.31	10.45	**1777.75**
	SF	854.32	267.63	17.93	2.99	21.15	**1164.02**
	GR	226.12	178.01	209.64	12.10	31.76	**657.63**
	UR	0.99	0.08	0.21	2.86	0.05	**4.19**
	UV	226.91	296.31	218.35	2.07	1130.97	**1874.61**
	tot	**2976.75**	**824.67**	**454.07**	**28.33**	**1194.38**	**5478.20**

		2017					
		FO	**SF**	**GR**	**UR**	**UV**	**tot**
1975	**FO**	1687.11	66.06	7.24	5.4	9.1	**1774.91**
	SF	946.82	341.77	24.43	4.34	35.81	**1353.17**
	GR	191.3	173.29	214.42	11.78	32.28	**623.07**
	UR	3.33	0.68	0.36	4.45	0.23	**9.05**
	UV	148.38	242.9	207.62	2.36	1116.96	**1718.22**
	tot	**2976.94**	**824.70**	**454.07**	**28.33**	**1194.38**	**5478.42**

TRANSITIONS FROM 1988

		2006					
		FO	**SF**	**GR**	**UR**	**UV**	**tot**
1988	**FO**	2046.50	115.13	19.29	10.52	45.15	**2236.59**
	SF	587.78	335.22	42.86	6.17	109.26	**1081.29**
	GR	65.82	83.03	244.08	12.00	74.34	**479.27**
	UR	6.13	0.57	1.42	7.43	0.75	**16.30**
	UV	96.32	130.63	127.17	2.24	1306.68	**1663.04**
	tot	**2802.55**	**664.58**	**434.82**	**38.36**	**1536.18**	**5476.49**

TRANSITIONS FROM 2006

		2017					
		FO	**SF**	**GR**	**UR**	**UV**	**tot**
1988	**FO**	2108.20	99.73	11.33	6.84	10.49	**2236.59**
	SF	666.42	349.28	27.17	3.59	34.84	**1081.30**
	GR	86.25	141.79	209.51	9.59	32.13	**479.27**
	UR	6.57	1.11	1.47	6.96	0.19	**16.30**
	UV	107.85	232.58	204.58	1.30	1116.73	**1663.04**
	tot	**2975.29**	**824.49**	**454.06**	**28.28**	**1194.38**	**5476.50**

		2017					
		FO	**SF**	**GR**	**UR**	**UV**	**tot**
2006	**FO**	2574.35	185.44	16.11	5.23	22.66	**2803.79**
	SF	257.76	346.71	24.08	0.59	35.90	**665.04**
	GR	40.38	103.75	229.52	4.78	56.46	**434.89**
	UR	11.22	3.48	5.91	17.30	0.50	**38.41**
	UV	93.23	185.31	178.45	0.43	1078.86	**1536.28**
	tot	**2976.94**	**824.69**	**454.07**	**28.33**	**1194.38**	**5478.41**

LOWER ELEVATIONS

TRANSITIONS FROM 1965

		1975					
		FO	**SF**	**GR**	**UR**	**UV**	**tot**
1965	**FO**	1412.45	293.67	27.19	2.70	41.73	**1777.74**
	SF	258.95	716.42	76.31	1.57	91.40	**1144.65**
	GR	47.23	111.11	344.52	1.41	24.27	**528.54**
	UR	0.40	0.41	0.73	2.32	0.33	**4.19**
	UV	55.73	196.04	45.53	1.05	494.37	**792.72**
	tot	**1774.76**	**1317.65**	**494.28**	**9.05**	**652.10**	**4247.84**

		1988					
		FO	**SF**	**GR**	**UR**	**UV**	**tot**
1965	**FO**	1521.53	204.26	13.36	6.11	32.40	**1777.66**
	SF	513.95	510.63	38.75	2.63	77.45	**1143.41**
	GR	103.97	135.85	258.67	4.14	25.52	**528.15**

TRANSITIONS FROM 1975

		1988					
		FO	**SF**	**GR**	**UR**	**UV**	**tot**
1975	**FO**	1570.68	165.24	11.29	3.64	23.86	**1774.71**
	SF	544.30	619.08	44.12	3.06	105.74	**1316.30**
	GR	72.25	124.62	263.82	3.77	29.50	**493.96**

	UR	0.61	0.53	0.82	2.04	0.19	**4.19**
	UV	96.44	190.65	40.10	1.38	463.94	**792.51**
	tot	**2236.50**	**1041.92**	**351.70**	**16.30**	**599.50**	**4245.92**

	UR	1.38	1.40	1.13	4.37	0.77	**9.05**
	UV	47.97	131.71	31.34	1.46	439.64	**652.12**
	tot	**2236.58**	**1042.05**	**351.70**	**16.30**	**599.51**	**4246.14**

		2006					
		FO	**SF**	**GR**	**UR**	**UV**	**tot**
1965	**FO**	1625.28	89.99	11.30	11.95	39.22	**1777.74**
	SF	785.98	253.56	26.45	4.23	74.42	**1144.64**
	GR	193.33	103.86	187.39	15.05	28.91	**528.54**
	UR	0.88	0.10	0.15	3.04	0.02	**4.19**
	UV	197.73	166.46	49.80	3.81	374.92	**792.72**
	tot	**2803.20**	**613.97**	**275.09**	**38.08**	**517.49**	**4247.83**

		2006					
		FO	**SF**	**GR**	**UR**	**UV**	**tot**
1975	**FO**	1634.65	85.98	11.62	8.85	33.68	**1774.78**
	SF	869.64	304.67	34.38	6.58	102.48	**1317.75**
	GR	161.39	98.63	185.44	13.73	35.16	**494.35**
	UR	2.66	0.35	0.12	5.40	0.52	**9.05**
	UV	135.08	124.34	43.53	3.52	345.65	**652.12**
	tot	**2803.42**	**613.97**	**275.09**	**38.08**	**517.49**	**4248.05**

		2017					
		FO	**SF**	**GR**	**UR**	**UV**	**tot**
1965	**FO**	1668.41	82.63	7.94	8.31	10.45	**1777.74**
	SF	854.28	252.12	15.29	2.98	19.98	**1144.65**
	GR	224.95	141.14	140.64	11.97	9.84	**528.54**
	UR	0.99	0.08	0.21	2.86	0.05	**4.19**
	UV	226.25	250.48	50.53	2.02	263.44	**792.72**
	tot	**2974.88**	**726.45**	**214.61**	**28.14**	**303.76**	**4247.84**

		2017					
		FO	**SF**	**GR**	**UR**	**UV**	**tot**
1975	**FO**	1687.11	65.96	7.24	5.40	9.07	**1774.78**
	SF	946.41	317.09	19.25	4.34	30.67	**1317.76**
	GR	190.12	140.16	140.58	11.62	11.87	**494.35**
	UR	3.33	0.68	0.36	4.45	0.23	**9.05**
	UV	148.10	202.59	47.18	2.33	251.92	**652.12**
	tot	**2975.07**	**726.48**	**214.61**	**28.14**	**303.76**	**4248.06**

TRANSITIONS FROM 1988

		2006					
		FO	**SF**	**GR**	**UR**	**UV**	**tot**
1988	**FO**	2046.50	115.12	19.29	10.52	45.15	**2236.58**
	SF	587.51	314.70	35.90	6.02	97.91	**1042.04**
	GR	65.82	68.68	175.88	11.82	29.50	**351.70**
	UR	6.13	0.57	1.42	7.43	0.75	**16.30**
	UV	96.22	114.44	42.53	2.24	344.08	**599.51**
	tot	**2802.18**	**613.51**	**275.02**	**38.03**	**517.39**	**4246.13**

		2017					
		FO	**SF**	**GR**	**UR**	**UV**	**tot**
1988	**FO**	2108.20	99.72	11.33	6.84	10.49	**2236.58**
	SF	665.51	320.31	21.89	3.59	30.75	**1042.05**
	GR	85.51	110.02	135.57	9.40	11.20	**351.70**
	UR	6.57	1.11	1.47	6.96	0.19	**16.30**
	UV	107.63	195.11	44.34	1.30	251.13	**599.51**
	tot	**2973.42**	**726.27**	**214.60**	**28.09**	**303.76**	**4246.14**

TRANSITIONS FROM 2006

		2017					
		FO	**SF**	**GR**	**UR**	**UV**	**tot**
2006	**FO**	2574.09	185.36	16.10	5.23	22.64	**2803.42**
	SF	257.40	307.40	17.81	0.59	30.77	**613.97**
	GR	39.31	77.27	138.13	4.66	15.72	**275.09**
	UR	11.22	3.34	5.79	17.23	0.50	**38.08**
	UV	93.05	153.10	36.78	0.43	234.13	**517.49**
	tot	**2975.07**	**726.47**	**214.61**	**28.14**	**303.76**	**4248.05**

UPPER ELEVATIONS

TRANSITIONS FROM 1965

		1975					
		FO	**SF**	**GR**	**UR**	**UV**	**tot**
1965	**FO**	0.00	0.01	0.00	0.00	0.00	**0.01**
	SF	0.02	13.04	3.37	0.00	2.94	**19.37**

TRANSITIONS FROM 1975

GR	0.00	8.65	92.83	0.00	27.61	**129.09**
UR	0.00	0.00	0.00	0.00	0.00	**0.00**
UV	0.11	13.71	32.52	0.00	1035.52	**1081.86**
tot	**0.13**	**35.41**	**128.72**	**0.00**	**1066.07**	**1230.33**

		1988					
		FO	**SF**	**GR**	**UR**	**UV**	**tot**
1965	**FO**	0.00	0.00	0.01	0.00	0.00	**0.01**
	SF	0.00	13.02	3.68	0.00	2.67	**19.37**
	GR	0.01	13.12	88.33	0.00	27.63	**129.09**
	UR	0.00	0.00	0.00	0.00	0.00	**0.00**
	UV	0.00	13.11	35.55	0.00	1033.20	**1081.86**
	tot	**0.01**	**39.25**	**127.57**	**0.00**	**1063.50**	**1230.33**

		1988					
		FO	**SF**	**GR**	**UR**	**UV**	**tot**
1975	**FO**	0.00	0.03	0.00	0.00	0.10	**0.13**
	SF	0.00	23.58	4.06	0.00	7.77	**35.41**
	GR	0.01	7.55	95.74	0.00	25.42	**128.72**
	UR	0.00	0.00	0.00	0.00	0.00	**0.00**
	UV	0.00	8.09	27.77	0.00	1030.21	**1066.07**
	tot	**0.01**	**39.25**	**127.57**	**0.00**	**1063.50**	**1230.33**

		2006					
		FO	**SF**	**GR**	**UR**	**UV**	**tot**
1965	**FO**	0.00	0.01	0.00	0.00	0.00	**0.01**
	SF	0.00	11.67	3.53	0.13	4.04	**19.37**
	GR	0.00	18.06	67.99	0.13	42.91	**129.09**
	UR	0.00	0.00	0.00	0.00	0.00	**0.00**
	UV	0.37	21.33	88.28	0.07	971.81	**1081.86**
	tot	**0.37**	**51.07**	**159.80**	**0.33**	**1018.76**	**1230.33**

		2006					
		FO	**SF**	**GR**	**UR**	**UV**	**tot**
1975	**FO**	0.00	0.01	0.00	0.00	0.12	**0.13**
	SF	0.19	18.19	5.30	0.10	11.63	**35.41**
	GR	0.00	14.78	70.17	0.19	43.58	**128.72**
	UR	0.00	0.00	0.00	0.00	0.00	**0.00**
	UV	0.18	18.09	84.33	0.04	963.43	**1066.07**
	tot	**0.37**	**51.07**	**159.80**	**0.33**	**1018.76**	**1230.33**

		2017					
		FO	**SF**	**GR**	**UR**	**UV**	**tot**
1965	**FO**	0.00	0.01	0.00	0.00	0.00	**0.01**
	SF	0.04	15.51	2.64	0.01	1.17	**19.37**
	GR	1.17	36.87	69.00	0.13	21.92	**129.09**
	UR	0.00	0.00	0.00	0.00	0.00	**0.00**
	UV	0.66	45.82	167.82	0.05	867.51	**1081.86**
	tot	**1.87**	**98.21**	**239.46**	**0.19**	**890.60**	**1230.33**

		2017					
		FO	**SF**	**GR**	**UR**	**UV**	**tot**
1975	**FO**	0.00	0.10	0.00	0.00	0.03	**0.13**
	SF	0.41	24.68	5.18	0.00	5.14	**35.41**
	GR	1.18	33.13	73.84	0.16	20.41	**128.72**
	UR	0.00	0.00	0.00	0.00	0.00	**0.00**
	UV	0.28	40.30	160.44	0.03	865.02	**1066.07**
	tot	**1.87**	**98.21**	**239.46**	**0.19**	**890.60**	**1230.33**

TRANSITIONS FROM 1988

		2006					
		FO	**SF**	**GR**	**UR**	**UV**	**tot**
1988	**FO**	0.00	0.01	0.00	0.00	0.00	**0.01**
	SF	0.27	20.52	6.96	0.15	11.35	**39.25**
	GR	0.00	14.35	68.20	0.18	44.84	**127.57**
	UR	0.00	0.00	0.00	0.00	0.00	**0.00**
	UV	0.10	16.19	84.68	0.00	962.57	**1063.54**
	tot	**0.37**	**51.07**	**159.84**	**0.33**	**1018.76**	**1230.37**

		2017					
		FO	**SF**	**GR**	**UR**	**UV**	**tot**
1988	**FO**	0.00	0.01	0.00	0.00	0.00	**0.01**
	SF	0.91	28.97	5.28	0.00	4.09	**39.25**
	GR	0.74	31.77	73.94	0.19	20.93	**127.57**
	UR	0.00	0.00	0.00	0.00	0.00	**0.00**
	UV	0.22	37.46	160.24	0.00	865.58	**1063.50**
	tot	**1.87**	**98.21**	**239.46**	**0.19**	**890.60**	**1230.33**

TRANSITIONS FROM 2006

		2017					
		FO	**SF**	**GR**	**UR**	**UV**	**tot**
2006	**FO**	0.26	0.08	0.01	0.00	0.02	**0.37**
	SF	0.36	39.31	6.27	0.00	5.13	**51.07**
	GR	1.07	26.48	91.39	0.12	40.74	**159.80**
	UR	0.00	0.14	0.12	0.07	0.00	**0.33**
	UV	0.18	32.20	141.67	0.00	844.71	**1018.76**
	tot	**1.87**	**98.21**	**239.46**	**0.19**	**890.60**	**1230.33**

TABLE S3.3. Markov Chain's transition matrices for the validation period and the future prediction. Probability matrices, area matrices and proportional errors used for the 2017 LC map validation are provided too.

2017 MODELIZATION

TRANSITIONS FROM 1965 (PROBABILITIES)

1965-1975	2017 FO	SF	GR	UV	tot
FO	0.45	0.34	0.08	0.13	**1.00**
SF	0.42	0.27	0.12	0.19	**1.00**
GR	0.28	0.31	0.20	0.21	**1.00**
UV	0.20	0.27	0.12	0.41	**1.00**
tot	**1.36**	**1.19**	**0.51**	**0.94**	**4.00**

prop error = 0.16

1965-1988	2017 FO	SF	GR	UV	tot
FO	0.66	0.27	0.02	0.05	**1.00**
SF	0.59	0.27	0.05	0.09	**1.00**
GR	0.24	0.30	0.34	0.12	**1.00**
UV	0.11	0.21	0.08	0.60	**1.00**
tot	**1.60**	**1.06**	**0.48**	**0.86**	**4.00**

prop error = 0.2

1965-2006	2017 FO	SF	GR	UV	tot
FO	0.82	0.15	0.01	0.02	**1.00**
SF	0.58	0.34	0.03	0.06	**1.00**
GR	0.07	0.29	0.56	0.09	**1.00**
UV	0.00	0.14	0.09	0.77	**1.00**
tot	**1.47**	**0.91**	**0.69**	**0.93**	**4.00**

prop error = 0.14

TRANSITIONS FROM 1975 (PROBABILITIES)

1975-1988	2017 FO	SF	GR	UV	tot
FO	0.68	0.23	0.02	0.06	**1.00**
SF	0.62	0.20	0.05	0.14	**1.00**
GR	0.31	0.26	0.25	0.17	**1.00**
UV	0.14	0.18	0.08	0.60	**1.00**
tot	**1.75**	**0.87**	**0.40**	**0.97**	**4.00**

prop error = 0.17

1975-2006	2017 FO	SF	GR	UV	tot
FO	0.84	0.13	0.01	0.02	**1.00**
SF	0.56	0.34	0.03	0.07	**1.00**
GR	0.08	0.26	0.56	0.10	**1.00**
UV	0.00	0.12	0.10	0.78	**1.00**
tot	**1.48**	**0.85**	**0.70**	**0.97**	**4.00**

prop error = 0.12

TRANSITIONS FROM 1988 (PROBABILITIES)

1988-2006	2017 FO	SF	GR	UV	tot
FO	0.79	0.15	0.02	0.04	**1.00**
SF	0.52	0.35	0.04	0.10	**1.00**
GR	0.08	0.23	0.54	0.15	**1.00**
UV	0.04	0.12	0.12	0.72	**1.00**
tot	**1.43**	**0.85**	**0.71**	**1.01**	**4.00**

prop error = 0.16

TRANSITIONS FROM 1965 (AREA)

1965-1975	2017 FO	SF	GR	UV	tot
FO	796.40	605.07	142.53	230.92	**1774.91**
SF	568.88	369.33	156.39	258.26	**1352.86**
GR	177.01	192.72	124.51	129.19	**623.42**
UV	348.89	466.22	198.41	704.31	**1717.82**
tot	**1891.18**	**1633.33**	**621.83**	**1322.67**	**5469.01**

TRANSITIONS FROM 1975 (AREA)

2017

TRANSITIONS FROM 1988 (AREA)

1965-1988		FO	SF	GR	UV	tot
	FO	1481.50	609.37	43.38	101.97	**2236.22**
	SF	635.66	294.74	50.93	99.80	**1081.12**
	GR	115.87	145.45	161.94	56.14	**479.40**
	UV	178.76	351.70	133.69	998.72	**1662.87**
	tot	**2411.78**	**1401.26**	**389.94**	**1256.63**	**5459.61**

1975-1988		FO	SF	GR	UV	tot
	FO	1525.10	518.80	55.68	136.41	**2236.00**
	SF	668.20	216.46	50.49	145.97	**1081.12**
	GR	150.77	126.75	119.66	82.26	**479.44**
	UV	230.31	296.16	132.86	1003.54	**1662.87**
	tot	**2574.38**	**1158.17**	**358.70**	**1368.18**	**5459.43**

1965-2006	2017	FO	SF	GR	UV	tot
	FO	2301.05	419.44	19.07	64.21	**2803.76**
	SF	386.27	224.60	18.31	36.69	**665.88**
	GR	31.06	124.46	243.56	37.17	**436.24**
	UV	0.00	213.49	144.78	1175.28	**1533.56**
	tot	**2718.38**	**982.00**	**425.71**	**1313.35**	**5439.44**

1975-2006	2017	FO	SF	GR	UV	tot
	FO	2354.32	370.10	24.11	55.23	**2803.76**
	SF	370.03	227.80	19.98	48.08	**665.88**
	GR	36.64	112.64	244.78	42.18	**436.24**
	UV	0.00	177.76	152.14	1203.81	**1533.71**
	tot	**2760.99**	**888.29**	**441.01**	**1349.30**	**5439.59**

1988-2006	2017	FO	SF	GR	UV	tot
	FO	2213.85	425.33	52.15	112.43	**2803.76**
	SF	344.86	230.99	26.57	63.46	**665.88**
	GR	35.16	98.94	235.53	66.66	**436.29**
	UV	63.80	190.95	178.22	1100.90	**1533.86**
	tot	**2657.67**	**946.21**	**492.46**	**1343.44**	**5439.79**

2050 MODELIZATION

TRANSITIONS FROM 2017 (PROBABILITIES)

1965-2017	2050	FO	SF	GR	UV	tot
	FO	0.81	0.16	0.01	0.02	**1.00**
	SF	0.70	0.26	0.02	0.02	**1.00**
	GR	0.22	0.36	0.37	0.05	**1.00**
	UV	0.04	0.20	0.15	0.60	**1.00**
	tot	**1.78**	**0.98**	**0.56**	**0.69**	**4.00**

prop error = 0.15

TRANSITIONS FROM 2017 (PROBABILITIES)

1975-2017	2050	FO	SF	GR	UV	tot
	FO	0.84	0.13	0.01	0.02	**1.00**
	SF	0.69	0.27	0.02	0.03	**1.00**
	GR	0.25	0.33	0.37	0.05	**1.00**
	UV	0.06	0.17	0.15	0.62	**1.00**
	tot	**1.84**	**0.90**	**0.55**	**0.72**	**4.00**

prop error = 0.12

TRANSITIONS FROM 2017 (AREA)

1965-2017	2050	FO	SF	GR	UV	tot
	FO	2408.52	484.15	38.11	46.75	**2977.53**
	SF	578.65	215.18	13.98	14.72	**822.54**
	GR	100.90	162.02	168.05	22.78	**453.75**
	UV	50.74	236.89	184.83	721.53	**1193.99**
	tot	**3138.83**	**1098.23**	**404.98**	**805.77**	**5447.81**

TRANSITIONS FROM 2017 (AREA)

1975-2017	2050	FO	SF	GR	UV	tot
	FO	2510.36	383.80	38.11	45.26	**2977.53**
	SF	565.99	218.71	15.71	22.13	**822.54**
	GR	113.25	150.72	165.74	24.05	**453.75**
	UV	68.65	202.02	179.93	743.38	**1193.99**
	tot	**3258.24**	**955.26**	**399.50**	**834.81**	**5447.81**

2100 MODELIZATION

TRANSITIONS FROM 2017 (PROBABILITIES)

		2100				
		FO	**SF**	**GR**	**UV**	**tot**
1965-2017	**FO**	0.79	0.16	0.02	0.03	**1.00**
	SF	0.87	0.09	0.02	0.02	**1.00**
	GR	0.59	0.22	0.13	0.06	**1.00**
	UV	0.28	0.20	0.14	0.38	**1.00**
	tot	**2.53**	**0.68**	**0.31**	**0.48**	**4.00**

prop error = 0.15

TRANSITIONS FROM 2017 (PROBABILITIES)

		2100				
		FO	**SF**	**GR**	**UV**	**tot**
1975-2017	**FO**	0.82	0.13	0.02	0.03	**1.00**
	SF	0.87	0.09	0.02	0.03	**1.00**
	GR	0.62	0.20	0.12	0.06	**1.00**
	UV	0.30	0.18	0.14	0.39	**1.00**
	tot	**2.61**	**0.60**	**0.29**	**0.50**	**4.00**

prop error = 0.12

TRANSITIONS FROM 2017 (AREA)

		2100				
		FO	**SF**	**GR**	**UV**	**tot**
1965-2017	**FO**	2352.84	490.70	56.28	78.01	**2977.83**
	SF	715.69	77.24	12.50	17.11	**822.54**
	GR	267.37	99.86	60.43	26.09	**453.75**
	UV	337.66	239.99	164.77	451.57	**1193.99**
	tot	**3673.56**	**907.79**	**293.98**	**572.78**	**5448.11**

TRANSITIONS FROM 2017 (AREA)

		2100				
		FO	**SF**	**GR**	**UV**	**tot**
1975-2017	**FO**	2455.57	389.16	54.79	78.01	**2977.53**
	SF	711.74	72.71	14.23	23.85	**822.54**
	GR	280.71	89.06	55.17	28.72	**453.66**
	UV	354.14	216.59	162.86	460.52	**1194.11**
	tot	**3802.16**	**767.53**	**287.05**	**591.11**	**5447.84**

TABLE S3.4. KIA (Kappa Index of Agreement) obtained from the 2017 LC validation process.

		2017 validation	
Kappa values	**Description**	**Standard model (1965-2006)**	**Optimized model (1975-2006)**
Kstandard	Measure of correctly assigned proportion relating to the proportion correct by chance	0.81	0.80
Kno	Measure of correctly classified proportion relative to the expected proportion according to a simulation	0.84	0.83
Klocation	Measure of success of simulation in specify the allocation relating to the maximum possible success	0.88	0.86
Klocationstrata	Measure of the allocation success within predifined strata	0.88	0.86

Chapter 4

Local forest inventory data improve species distribution model predictions

Nicolò Anselmetto, Donato Morresi, Simona Barbarino, Nicola Loglisci, Matthew G. Betts, Matteo Garbarino

This chapter has been submitted to the *Agricultural and Forest Meteorology* journal. A preprint version is available at http://dx.doi.org/10.2139/ssrn.4696875

Abstract

The increasing role of modeling for planning forest ecosystems' conservation and restoration calls for robust assessments of response (i.e., species data such as forest inventories) and predictor (e.g., climate) variables. The aim of this study is to predict current and future probability of occurrence for different tree species comparing inventory and climate data at different spatial scales.

We built species distribution models (SDMs) for 22 tree species of Piedmont, an Alpine administrative region of north-western Italy. We compared a local forest inventory with a 250-m spatial resolution at the extent of Piedmont versus a pan-European one (EU-Forest) at 1-km resolution. We compared a regional climate model (RCM) calibrated on the Italian extent versus a commonly applied global climate dataset (CHELSA v1.2). We defined as fine scale the combination of local species data and RCM and as coarse scale the combination of EU-Forest and CHELSA. We evaluated models using spatial-block cross-validation and external validation through several metrics. We predicted the probability of occurrence for current and future under two climate scenarios.

Models built with local species data outperformed models built using broad species data. Spatial predictions were different in probability of occurrence and

binary maps for current and future scenarios. Species showed individualistic responses in terms of differences between the local and coarse models both in terms of spatial predictions and estimated magnitude of changes, especially for species with peculiar local history.

Our results highlight the importance of fine-resolution predictors in SDMs. We advocate for adequate testing of response and predictor variables within SDMs for ecologists and forest practitioners. Fine-scale models showed better performance in terms of current probability of occurrence compared to forest maps for the Piedmont region, but coarse-scale models encompass a greater portion of a species' niche and therefore grant higher transferability to novel future conditions.

Keywords: climate change, mountain forest ecosystems, regional climate models, local inventories, spatial scales, species distribution models.

Highlights

- Fine predictors and responses can improve performance of tree distribution models.
- Models trained with local forest inventories outperformed a continental dataset.
- No statistically significant differences in accuracy between climate datasets.
- Spatial mismatch between predictions, geographical range, and local forest maps.
- Differences in magnitude of future changes depended on the scale of variables.

4.1 Introduction

It is well known that forest ecosystems provide essential ecosystem services such as biodiversity conservation, food and timber production, water regulation, and carbon sequestration (Mori et al., 2017). Climate and land use changes are already

altering the distribution, abundance, and phenology of forest species at different scales (Vitasse et al., 2021) with significant consequences for the resilience of the communities that depend on these ecosystems (Forzieri et al., 2022; Smith et al., 2022). Global forest policies commonly attempt conserving forest systems as an active climate mitigation strategy (Fagan et al., 2020; Begemann et al., 2021). Therefore, understanding past, current, and future dynamics of forest ecosystems is critical for understanding and monitoring species- and ecosystems-response to climate change at different spatiotemporal scales (Guisan et al., 2013; Albrich et al., 2020; McDowell et al., 2020). Quantitative predictions lie at the heart of informed decision-making and responsible management, anticipating ecological shifts and preparing for necessary interventions such as assisted migration of animals and plants (Twardek et al., 2023) and ecological restoration (SER, 2002). Global forest governance is characterized by a complex cross-scale interaction of institutions (e.g., from the United Nations [UN] to sub-national levels), actors (e.g., public and private stakeholders), targets (e.g., biodiversity, human rights, climate crisis), and norms (Begemann et al., 2021; Sharma et al., 2023). Amidst this framework, predictive spatial modeling emerges as a powerful tool for adaptive planning and management (Zurell et al., 2022). However, ecologists and forest practitioners need reliable and informative models at both broad (regional to continental) and fine (landscape to regional) scales to allow for spatial reserve prioritization and ecological restoration (Wan et al., 2017; Buenafe et al., 2023).

Species distribution models (SDMs) are now the most common predictive tools for assessing potential range shifts of tree species under future scenarios (Franklin, 1995; Guisan et al., 2013; Zurell et al., 2020, 2022). SDMs are correlative models that establish a relationship between the presence or abundance of a species to a suite of several socio-ecological covariates. These covariates include, but are not limited to, climate data, soil features, topography, land use, and socioeconomic drivers (Franklin, 1995; Guisan et al., 2013). These models have been extensively used at several spatial and temporal scales to study the potential ecological impact of climate change on various plant and animal

species worldwide (Newbold, 2018; Maréchaux et al., 2021; Zurell et al., 2022). Broad-extent and coarse-resolution models, primarily associated with climatic predictors, are more prevalent than local-extent and fine-resolution models, which often emphasize habitat characteristics (Araújo et al., 2019). However, regardless of the scale or resolution, the accuracy and reliability of the models hinge on the source of response (i.e. species data such as ecological inventories) and predictor (e.g., climate) variables used in model calibration and validation (Bobrowski & Udo, 2017; Araújo et al., 2019; Zurell et al., 2020).

Among the main sources of species data, ecological inventories assume a pivotal role in understanding the status and trends of forest ecosystems and populations across different spatiotemporal scales (Tomppo et al., 2010; Tinkham et al., 2018). Their primary advantage lies in their statistical sampling scheme, which provides reliable information on true presences and absences at a specific extent and resolution (Pecchi et al., 2019; Ellis-Soto et al., 2021). Forest inventories, for instance, often include multiple stand attributes (e.g., basal area) that allow for a comprehensive assessment of ecosystem resources and services, and can inform decision-making for timber production, biodiversity conservation, and carbon sequestration (Tomppo et al., 2010). When it comes to climate predictors, limited-area high-resolution models (e.g., regional climate models, RCMs), serve as valuable tools for the dynamical downscaling of general circulation models (GCMs) to fine scales with very high resolution (VHR). This process offers detailed and reliable insights into the local variability of climate variables within specific local areas (Giorgi et al., 2009). Many studies have been exploring RCMs at the so-called convection-permitting, convection-resolving, convection-allowing, or kilometer-scale grid spacing (Kendon et al., 2014; Ban et al., 2014; Liu et al., 2017; Berthou et al., 2020; Fumière et al., 2020). The main characteristic of these types of simulations is the explicit resolution of deep convection at grid spacings below 4 km, without using any kind of parameterization. These studies demonstrate that kilometer-scale modeling offers significant advantages in representing climate, and the costs are justified when

focusing on local to regional scales (Ban et al., 2021). The importance of VHR climate data has been recently increasing in several fields, including climate change research, environmental monitoring, agriculture, and water resource management (Crespi et al., 2018; Mauri et al., 2022).

Robust standards for assessing the ecological reliability and statistical accuracy of distribution models are crucial given the increasing body of SDMs studies predicting current and future species distribution and habitat suitability (Araújo et al., 2019; Zurell et al., 2020). The spatial resolution and extent of predictors and response variables are particularly important when fitting and evaluating SDMs (e.g., Betts et al., 2006; Elith & Leathwick, 2009; Patiño et al., 2023). Simultaneously, the dynamical downscaling of GCMs to RCMs increase their reliability within the calibration area by pairing the synoptic scale of GCM fields and the mesoscale resolution fields simulated by RCMs (Fumière et al., 2020; Ban et al., 2021; Mauri et al., 2022). Several studies have compared modeling algorithms (e.g., Valavi et al., 2022), response variables (e.g., Waldock et al., 2022), and predictors (e.g., Lembrechts et al., 2019a; Patiño et al., 2023) in SDMs but, to our knowledge, few comparisons (e.g., Simon et al., 2023) examine different combinations of predictors and response data at different scales to model current and future probability of occurrence of species at fine scales appropriate for regional and local planning and decision making.

Therefore, the general aim of this paper was to predict current and future probability of occurrence for different tree species of Piedmont, an administrative region of the western Italian Alps, using fine-scale SDMs. We defined as fine scale the combination of species data (i.e., forest inventory) for the Piedmont region with fine spatial resolution and local extent and an RCM with a local calibration area and extent such as Italy (Figure 4.1). Our main research question was: how does the spatial scale of response (i.e., species data) and predictor variables affect prediction success and reliability in SDMs? To address this question, we compared SDM frameworks built using (i) a local forest inventory (250-m resolution at the extent of Piedmont, 25 387 km^2) versus a broad

European forest inventory (1-km resolution at the extent of the European Alp, 179 014 km^2) and (ii) a local climate dataset based on an RCM versus a widely applied climate dataset based on GCM. Our final aim was to analyze future scenarios of climate change for the main tree species of Piedmont by comparing magnitude of change estimated from the fine and coarse predictors and response. We conclude by discussing the potential applications of local species data and predictors and fine-scale approaches within SDMs in ecology and forestry.

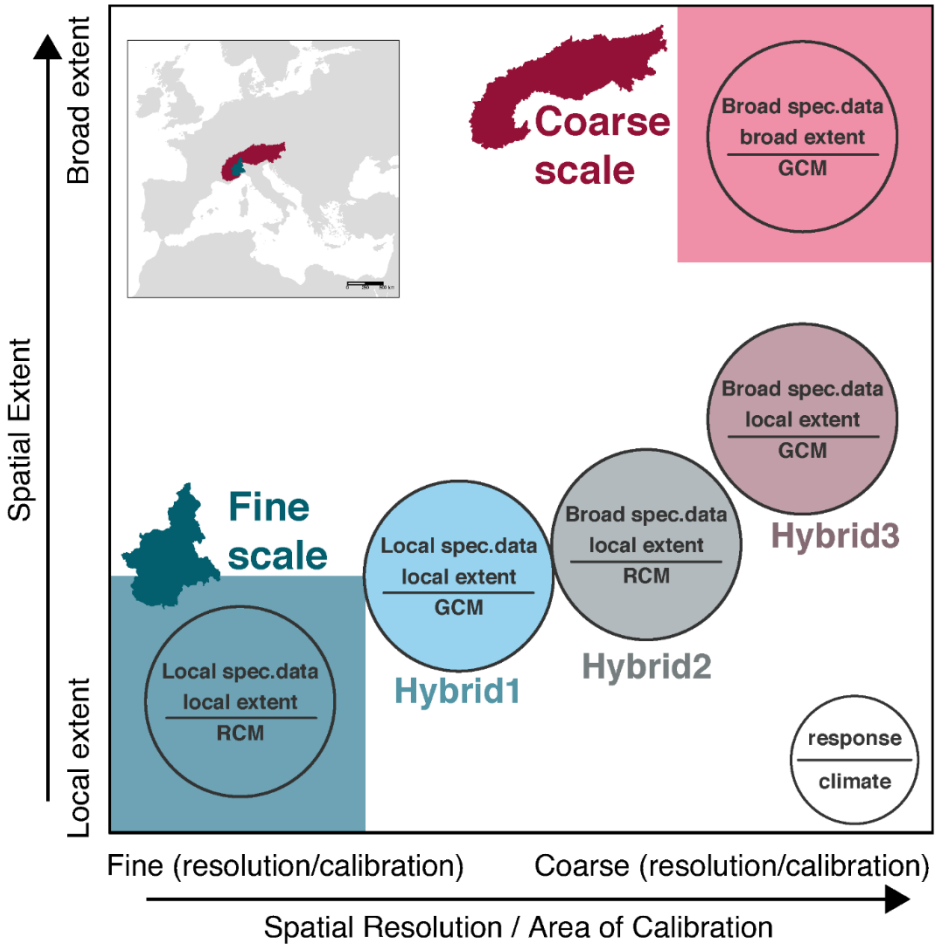

FIGURE 4.1. Combinations of response (local versus broad species data) and climate (regional climate model, RCM, versus general circulation model, GCM) data according to the spatial resolution and spatial extent (for response) and area of calibration and spatial extent (for climate). We defined as fine scale the combination of local species data (fine resolution and local [Piedmont region] extent forest inventory) and a regional climate model (fine area of calibration and local

[Italy] extent). We defined as coarse scale the combination of continental species data (coarse resolution and broad [European Alps] extent forest inventory) and a general circulation model (coarse area of calibration and broad [global] extent). We defined as hybrid scales the other combinations between response and climate data. In particular, Hybrid1 is the combination of local species data and GCM, Hybrid2 is the combination of broad species data and RCM, and Hybrid3 is the combination of broad species data at the local extent and GCM. We defined a gradient from the fine to the coarse scale and placed the hybrid combinations along it.

4.2 Materials and methods

4.2.1 Study area

Piedmont is an administrative region of north-western Italy covering 25 387 km^2 (Figure 4.2). Around 43% of its area (11 000 km2) lies in the montane belt, with two mountain regions; the western Alps and the northern Apennines. Piemonte hosts more than 1 billion trees belonging to 52 different species; its forests cover 9 770 km^2 with a forest cover of 38.5%, but in mountain areas the forest cover increases to reach 57% (6631 km^2) (Camerano et al., 2017). The main tree species in the region are the sweet chestnut (*Castanea sativa* Mill., 22% of the total forest area), European beech (*Fagus sylvatica* L., 15%), black locust (*Robinia pseudoacacia* L., 12%), and European larch (*Larix decidua* Mill., 10%) (Camerano et al., 2017). Like many areas in Europe, the millennial history of human practices in the region (e.g., logging for timber and fuelwood, mining, and creation of semi-natural ecosystems) shaped the structure and composition of its forests since the Neolithic (Mietkiewicz et al., 2017; Zanon et al., 2018). For instance, in the subalpine elevation belt of the Alps, European larch has been favored over stone pine (*Pinus cembra* L.) and other competing species because of its suitability for wood pastures; indeed, its fast growth and timber quality make it a target species for timber production while its light canopy allows forage grass to grow underneath (Garbarino et al., 2011). At lower elevations, sweet chestnut cultivation was introduced by the Romans and then expanded in Medieval times (A.D. 100 to A.D. 600) in areas naturally occupied by oak stands (*Quercus* spp.) (Conedera et al., 2004). Due to socio-economic changes that led

to land abandonment starting from the Industrial Revolution, forests are expanding to the detriment of former croplands, vineyards, and grasslands (Batzing et al., 1996; Plieninger et al., 2016; Anselmetto et al., 2024).

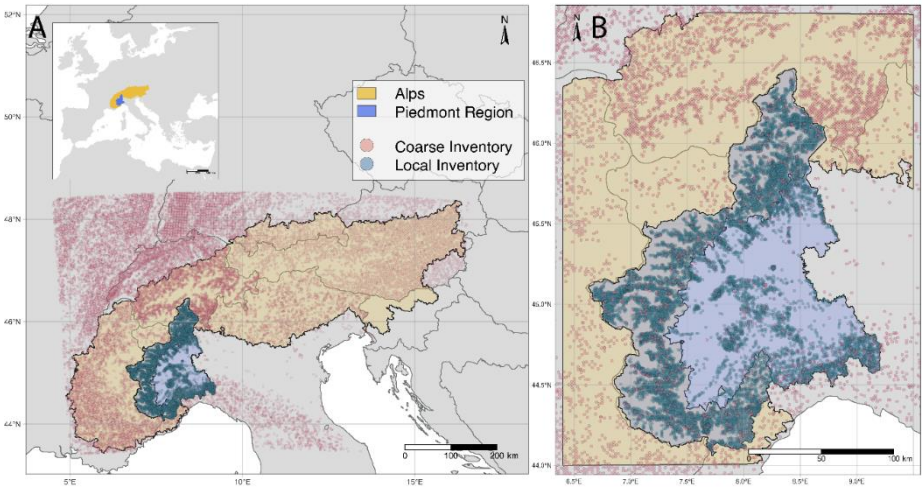

FIGURE 4.2. Maps of the (a) Alps and (b) Piedmont Region with occurrences of local inventory and the broad inventory (EU-Forest; Mauri et al., 2017).

4.2.2 SDM framework overview

Below we describe the SDM framework according to the ODMAP (Overview, Data, Model, Assessment, and Prediction) protocol for Species Distribution Models (Zurell et al., 2020; see Supplementary Material Table A.1 for further details). We assumed that the distribution of our 22 focal tree species is mostly driven by climate, topography, and soil characteristics. We know that human legacy has had a major role in current distribution, but we did not include those variables in our models due to a lack of spatially explicit data at a regional scale. We also assumed that (i) species are at (pseudo-) equilibrium with the environment (i.e., the species occupies all suitable habitats where it can disperse), (ii) inventory sampling is adequate and representative, with negligible detection errors, (iii) in forest inventories, tree individuals below a certain diameter at breast height are not recorded, and we assume that this procedure does not bias

species identification, and (v) the current distribution's delimiting factors will also form the niche of the species in the future (i.e., niche conservatism).

All the analyses were conducted in R version 4.2.3 (R Core Team, 2023) (See Supplementary Table A4.2 Supplementary Materials for R packages used in the analyses).

4.2.3 Species occurrence data

We compared a local forest inventory led by IPLA (Istituto per le Piante da Legno e l'Ambiente; Camerano et al., 2017) in the early 2000s for the Piedmont region to a broad inventory that comes from a harmonization of national forest inventories at the European scale called EU-Forest (Mauri et al., 2017). We cropped EU-Forest to the extent of the Alpine Convention Perimeter (Alpine Convention, 2018).

The local species data is a collection of forest plots from the early 2000s that was used to inform forest management plans of Piedmont Region (Piani Forestali Territoriali, PFT; Camerano et al., 2017). Plots encompass 36 species and 14 164 occurrence points at a spatial resolution of 250 m. The EU-Forest project emerged from a collaboration between JRC (Joint European Research Center) and 21 European Countries. This dataset is the result of merge and harmonization of National forest inventories and pre-existing European datasets, and it collects occurrence (presence/absence) data of 242 tree species and a total of 1 000 525 occurrence records. EU-Forest has a spatial resolution of 1 km^2 and is aligned to the European INSPIRE-compliant 1 km x 1 km grid (European Parliament, 2007). We also compared models trained with the broad species data clipped on the extent of the Piedmont Region to the broad species data at the extent of the entire Alps to evaluate the utility of broad inventories in local contexts. We did this to account for different spatial (i.e., geographical range) and ecological (i.e., niche) extents for a coarse-resolution species dataset. Our hypothesis was that coarse-resolution species data clipped to a smaller extent before model calibration will perform poorly due to niche truncation.

We selected 22 species that were common between the two datasets (Table 4.1). Both the datasets were re-projected to the coordinate reference system ETRS89 / LAEA Europe (EPSG: 3035). To overcome the uneven sampling intensity and point clustering, we applied a spatial filter to the presence points using a custom function. A distance of 500 m was considered as the minimum distance between the points, to harmonize the sampling intensity between presence and absence data.

TABLE 4.1. List of the 22 tree forest species assessed in this study and their prevalence (presence/total number of occurrences) according to the local and broad inventories for both the local (Piedmont) and broad (Alpine) extent.

Species code	**Common species name**	**Scientific species name**	**Forest type**	**Prevalence**		
				Local spec.data	**Broad spec.data Local ext.**	**Broad spec.data Broad ext.**
aa	Silver fir	*Abies alba*	Conifer	0.056	0.051	0.201
ag	Black alder	*Alnus glutinosa*	Broadleaf	0.016	0.057	0.019
ap	Sycamore	*Acer pseudoplatanus*	Broadleaf	0.087	0.102	0.086
at	Field maple	*Acer campestre*	Broadleaf	0.024	0.046	0.044
bp	European birch	*Betula pendula*	Broadleaf	0.034	0.091	0.039
cb	European hornbeam	*Carpinus betulus*	Broadleaf	0.034	0.016	0.059
cs	Sweet chestnut	*Castanea sativa*	Broadleaf	0.371	0.199	0.025
fe	European ash	*Fraxinus excelsior*	Broadleaf	0.139	0.027	0.024
fo	Manna ash	*Fraxinus ornus*	Broadleaf	0.054	0.040	0.011
fs	European beech	*Fagus sylvatica*	Broadleaf	0.246	0.080	0.135
ld	European larch	*Larix decidua*	Conifer	0.153	0.072	0.048
pa	Norway spruce	*Picea abies*	Conifer	0.064	0.011	0.124
pc	Swiss stone pine	*Pinus cembra*	Conifer	0.013	0.002	0.004
pn	Black pine	*Pinus nigra*	Conifer	0.008	0.010	0.014

ps	Scots pine	*Pinus sylvestris*	Conifer	0.067	0.022	0.032
pt	Common aspen	*Populus tremula*	Broadleaf	0.038	0.003	0.001
pv	Wild cherry	*Prunus avium*	Broadleaf	0.165	0.021	0.002
qf	Pedunculate oak	*Quercus robur*	Broadleaf	0.086	0.011	0.004
qp	Downy oak	*Quercus pubescens*	Broadleaf	0.070	0.002	0.017
qr	Sessile oak	*Quercus petraea*	Broadleaf	0.130	0.016	0.006
rp	Black locust	*Robinia pseudoacacia*	Broadleaf	0.197	0.019	0.002
su	Rowan	*Sorbus aucuparia*	Broadleaf	0.042	0.002	0.000

4.2.4 Environmental predictors for SDMs

4.2.4.1 Climate data

We tested two different climate datasets in our SDM framework (Table 4.2). First, we applied VHR (Very High Resolution) climate data from the Euro-Mediterranean Center on Climate Change (CMCC) for the Piedmont region available from the Highlander project (https://highlanderproject.eu/). The dataset was based on a dynamic downscaling of current (1989-2013) ERA5 reanalysis (Hersbach et al., 2020), originally available at ~31 km spatial resolution, to obtain a final resolution of ~1.8 km through a regional climate model called COSMO (Raffa et al., 2021). We identified this climate dataset as the local climate dataset. For the future period (2051-2070) we utilized another climate dataset developed within the Highlander project through a dynamic downscaling of CMCC-CM global model to 0.02° (~1.8 km) spatial resolution according to IPCC scenarios RCP8.5 (Raffa et al., 2023) and RCP4.5 (Raffa & Mercogliano, 2022). The dynamical downscaling makes use of the same RCM (COSMO-CLM) used for ERA5. Pre-processing on this dataset consisted of a bias-correction procedure to remove overestimation or underestimation of the model in comparison to the observed data, for every timestep (every day) and every grid

point, due to systematic errors originated (Watanabe et al., 2012). We applied a simple pixel-based additive bias correction method for temperatures and a multiplicative one for precipitation. Climate data are part of the project Highlander and are available at https://dds-dev.highlander.cineca.it/app/datasets.

The second dataset derived from CHELSA (Climate at high resolution for the Earth's land surface areas) v1.2 (Karger et al., 2017). CHELSA consists of downscaled general circulation models output temperature and precipitation estimates at a horizontal resolution of 30 arc sec (~1 km at the Alps latitude). The temperature downscaling algorithm is based on statistical downscaling of atmospheric temperatures from ERA-Interim using a temperature lapse rate based on elevation. The precipitation downscaling algorithm includes orographic predictors such as wind, valley exposition, and boundary layer height. Final data consist of monthly temperature and precipitation and derived parameters. We cropped the gridded variables at the extent of the Alps, and we identified this dataset as broad climate dataset. The future climate data derived from downscaled CMIP5 climatologies (Karger et al., 2017, 2018). We selected six different models (CESM1-CAM5, CMCC-CM, CNRM-CM5, CSIRO-Mk3.6.0, GISS-E2-H, HadGEM2-AO) based on the quality of current prediction on the Alps and Europe (Zubler et al., 2016) but also considering dissimilarities between models to capture uncertainties in modeling future climate scenarios (Knutti et al., 2013; Sanderson et al., 2015).

For each of the two climate datasets, we calculated monthly average values for the current (1989-2013) and future (2051-2070) periods and the 19 bioclimatic predictors (Hijmans et al., 2005; Table A4.3 Supplementary Materials). We considered 1989-2013 as the current since it was the common temporal extent of both local and broad climate datasets. We assessed two different future IPCC RCPs (RCP4.5 and RCP8.5) for the 2051-2070 period. Climate data were resampled through a nearest neighbor method to 250 m. That means that they operated at the native resolution (1 km and ~1.8 km for the broad and the local dataset, respectively). To test for correlation between the variables of the two

climate data sets, the centroids of every cell were extracted and examined using Pearson's correlation. To visualize geographical discordance between the two climate data sets, variables were intersected performing cell by cell subtraction of broad climate minus local climate.

4.2.4.2 Other environmental predictors

We derived topography from the Multi-Error Removed Improved-Terrain (MERIT) digital elevation model (DEM; Table 4.2). The MERIT DEM is available at 3sec spatial resolution (~90 m at the equator). This dataset derives from multiple satellite data and several filtering techniques used for the bias correction of height error components from previous spaceborne DEMs (Yamazaki et al., 2017). We derived the median and standard deviation of five topographic metrics from MERIT DEM resampled at 250 m. We calculated the elevation, slope, heat load index (HLI) or the incident radiation of the sun according to the aspect (McCune et al., 2002), topographic position index (TPI), indicating the position of a cell according to its 8 surrounding cells neighbors, and terrain ruggedness index (TRI), that expresses the amount of elevation difference between adjacent cells of a DEM (Riley et al., 1999) (Table 4.2).

We included soil pH and organic carbon content (OCC) at 250-m spatial resolution derived from SoilGrids250m (Table 4.2; Hengl et al., 2017). This dataset provides global predictions for standard numeric soil properties such as bulk density, pH, soil texture fractions, and organic carbon at different depths (0, 5, 15, 30, 60, 100 and 200 cm). The gridded maps were interpolated combining 150 000 soil profiles and 158 remote sensing-based soil covariates (e.g., MODIS land products and DEM derivatives) within random forest models and multinomial logistic regression algorithm.

TABLE 4.2. *Environmental predictors used in SDMs.*

Group	Variable	Data source	Native spatial resolution	Reference
Topography	Elevation (median)	MERIT DEM	3" (~90m)	Yamazaki et al. 2017
	Slope (median, standard deviation)	MERIT DEM	3" (~90m)	
	Heat load index (median, standard deviation)	MERIT DEM	3" (~90m)	
	Topographic position index (median, standard deviation)	MERIT DEM	3" (~90m)	
Climate	Monthly precipitation (Jan, Mar, Apr, May, Jun, Sep, Oct)	CHELSA timeseries COSMO	1 km 0.02° (~1.8km)	Karger et al. 2017, 2018 Raffa et al. 2021 Raffa et al. 2023
	Mean diurnal range	CHELSA timeseries	1 km	

	COSMO	0.02° (~1.8km)
Isothermality	CHELSA timeseries	1 km
	COSMO	0.02° (~1.8km)
Temperature seasonality	CHELSA timeseries	1 km
	COSMO	0.02° (~1.8km)
Temperature annual range	CHELSA timeseries	1 km
	COSMO	0.02° (~1.8km)
Mean temperature of	CHELSA timeseries	1 km
wettest quarter	COSMO	0.02° (~1.8km)
Mean temperature of	CHELSA timeseries	1 km
driest quarter	COSMO	0.02° (~1.8km)
Precipitation of wettest month	CHELSA timeseries	1 km
	COSMO	0.02° (~1.8km)

	Precipitation of driest month	CHELSA timeseries	1 km	
		COSMO	0.02° (~1.8km)	
	Precipitation seasonality	CHELSA timeseries	1 km	
		COSMO	0.02° (~1.8km)	
Soil	pH (0-15 cm)	SoilGrid250m	250m	Hengl et al. 2017
	Soil organic Carbon (0-15 cm)	SoilGrid250m	250m	

4.2.5 SDMs architecture, assessment, and predictions

4.2.5.1 SDM architecture

We built species distribution models using Bayesian additive regression trees (BART) through the `embarcadero` R package v1.2.0 (Carlson, 2020). BART is a machine learning modeling procedure based on an ensemble of trees, similar to boosted regression trees and random forest. In addition, BART employs a sum-of-trees model within a Bayesian framework; trees are first constrained as weak learners by priors, then updated through an iterative Bayesian backfitting Markov Chain Monte Carlo (MCMC) algorithm which generates a posteriori distribution of predicted classification probabilities instead of a single estimate (Chipman et al., 2010; Carlson, 2020). Overfitting results are lower than other similar methods, and several studies showed the better predictive power of this model compared to ensemble models with multiple algorithms (e.g., Baquero et al.,

2021; Konowalik & Nosol, 2021; Plant et al., 2021). We used BART's default settings (Table A4.1 Supplementary Materials).

We reduced the number of initial variables (Table 4.2) through a variable pre-selection based on the correlation between variables and the variance inflation factor (VIF) through the function `vifcor` of the `usdm` package (Naimi et al., 2014). The function first pairs variables with a linear correlation higher than a pre-selected threshold and excludes the one with a greater VIF. The procedure is iterated until no pair of variables with a high correlation remains. We used a Pearson's correlation of 0.9 as the threshold at which one of a correlated pair was excluded. Our aim was to avoid highly correlated variables and speed-up the computation time even if BART is considered to be robust against multicollinearity. We assessed spatial autocorrelation using automatic variograms through the R package `automap` (Hiemstra et al., 2009).

4.2.5.2 SDMs assessment

We assessed models accuracy, calibration, and realism. The former was statistically tested through internal (5-fold spatial block cross-validation) and external validation on a fully independent dataset (GBIF + LUCAS; Mauri et al., 2022). We determined the block-size dimension by constructing empirical variograms for measuring spatial autocorrelation. When the mean range of spatial autocorrelation was > 15 000 m, we used 10 000 m as block-size dimension. We retrieved several accuracy metrics such as the Area Under the receiving operator Curve (AUC), True Skill Statistic (TSS), Sensitivity, Specificity, and the F1 score. The AUC is a threshold-independent metric that shows the relationship between false-positive and true-positive rates. The TSS and F1 score are threshold-dependent accuracy metrics that depend on the sensitivity and specificity of the models. TSS values > 0.6 are considered to be useful to excellent, AUC scores > 0.8 are considered to be good to excellent. We assessed the calibration (i.e., the agreement between predicted probabilities of occurrence and observation of presence and absence) and generalizability of the models through Pearon's correlation coefficient (COR). We calculated the correlation

between the observation (presence/absence dichotomous variable) and the predictions (range of probabilities). COR is therefore a threshold-independent metric similar to AUC, but it accounts for the distance between the prediction and the observation (Elith et al., 2006). Realism was assessed from an ecological point of view through variable importance (vimp) and a visual comparison of the spatial predictions for the current time to the European geographic range of different species developed by the Joint Research Center (JRC) of the European Union (Caudullo et al., 2017) and the EU-Trees4F dataset (Mauri et al., 2022). We ran generalized linear mixed models (GLMMs) on accuracy (AUC, TSS, F1) and calibration (COR) results to test for significant differences among frameworks, species data, and climate using the species as a random effect.

4.2.5.3 SDMs predictions

The main output of the modeling consisted of predictions of relative probability of occurrence. We also derived the uncertainty based on the 5th and 95th percentile of the probability distribution obtained through the Bayesian approach. We converted continuous probability maps into binary maps for ecological assessment and quantification of species range shifts. The threshold selection for binary maps is a crucial step in species distribution mapping (Hintze et al., 2021). Therefore, we tested three different widely applied thresholds; minimum training presence (MTP, sometimes also called lowest presence threshold), 10th percentile of the predicted values (P10), and maximum of TSS (maxTSS). We chose the latter since it was the most conservative approach.

4.2.5.4 Post-processing analysis

We post-processed models output using Corine Land Cover (CLC; European Commission, 1994) to mask out unvegetated areas (i.e., urban areas, rocks, and water). We then focused on two combinations of response and predictors; we defined as fine scale the combination of local species data and local climate data (RCM) and as coarse scale the combination of the broad species data and broad climate data (CHELSA) at the extent of the Alpine region (Figure 4.1). Finally,

we assessed changes in terms of probability of occurrence of the different tree species between each one of the two future climate scenarios (RCP4.5 and RCP8.5 for 2051-2070) and the current.

4.3 Results

4.3.1 Climate data comparison

We compared the spatial distribution and seasonal trends of mean temperature (Figure 4.3a, c) and precipitation (Figure 4.3b, d) to characterize differences among the two climate datasets. The broad climate dataset was consistently hotter than the local one (min difference = 0.52 °C, mean difference = 7.28 °C, max difference = 10.04 °C; Figure 4.3a, c). Differences in temperature between these datasets tended to decrease with elevation (R^2 = 0.78, slope =-0.18 °C every 100 m of elevation gain), with average differences in the mountains (> 800 m) of 5.68 ± 1.49 °C (mean ± standard deviation) and up to 8.15 ± 0.56 °C in the flat areas of the Po Valley (Figure 4.3a). This was not as much the case for precipitation patterns (R^2 = 0.53, Figure 4.3b), that seemed to be more related to continentality. Dry continental sectors, like the inner Alps (e.g., upper Susa Valley) and Po Valley, exhibited higher values in the broad dataset, while wetter sectors such as Cuneo province (South of Piedmont) and Ossola (the Northern extremity of Piedmont) showed higher values in the local climate dataset. The seasonal trends showed consistent differences in mean monthly temperatures, where the broad dataset was hotter in every month, especially during the summer months (Figure 4.3c). Values showed similar left-skewed distributions, with lower values associated with upper elevations.

We assessed spatial and temporal trends for the two future scenarios (Figure B4.1 Supplementary Materials for RCP4.5 and Figure B4.2 Supplementary Materials for RCP8.5). We derived average values of monthly temperatures and precipitation between the six CMIP5 models included within the broad climate dataset. We observed a higher degree of similarity in temperature spatial patterns and seasonal trends (monthly local ~ monthly broad with intercept = -0.82, slope

= 1.12, and R^2 = 0.99 for RCP 4.5; intercept = -0.25, slope = 1.10, and R^2 = 0.99 for RCP 8.5), but lower correspondence for precipitation (intercept = -40.5, slope = 1.97, and R^2 = 0.40 for RCP 4.5; intercept = -41.2, slope = 1.94, and R^2 = 0.65 for RCP 8.5). The broad climate dataset was hotter than or equal to the local one during winter, especially for RCP 4.5, but colder in summer. Seasonal trends of precipitation showed differences between the two RCPs, especially for the local climate data.

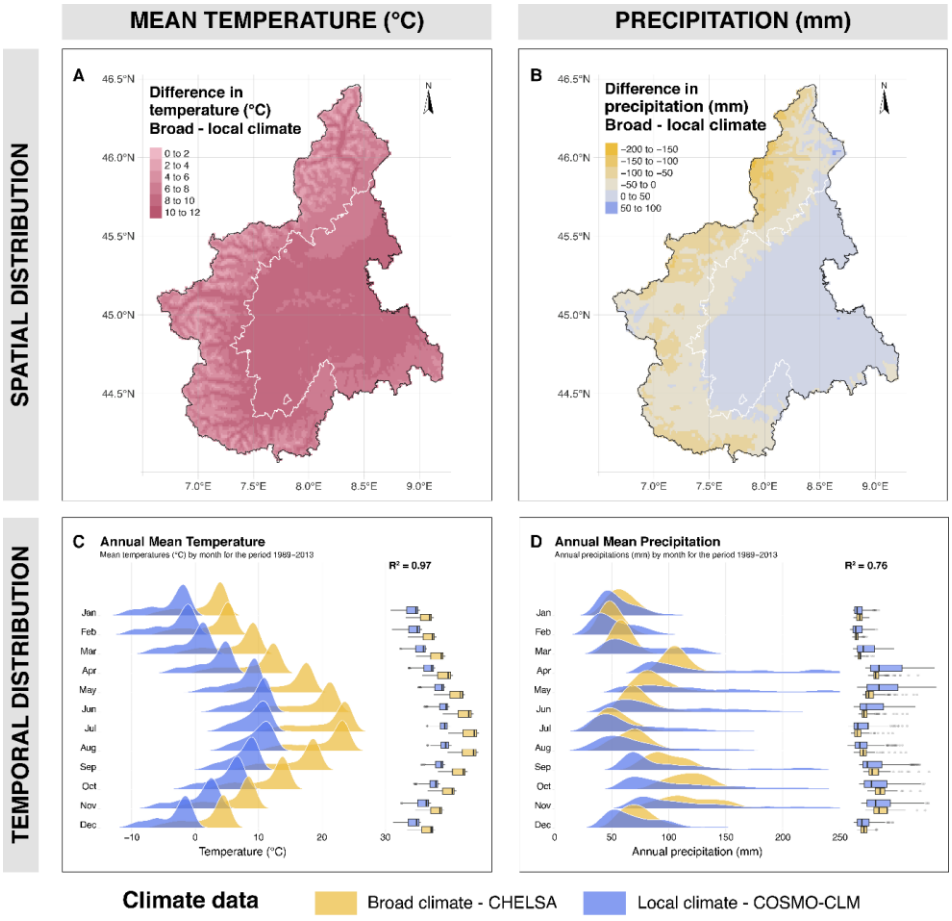

FIGURE 4.3. Spatial (a, b) and temporal (c, d) distribution of mean temperature (a, c) and precipitation (b, d) of the two climate datasets (local climate = COSMO-CLM and broad climate = CHELSA v1.2) for the period 1989-2013. The broad climate dataset was consistently hotter than the local, but with similar seasonal trends. Differences in precipitation patterns seemed to be more related to continentality.

4.3.2 Model performance and predictions

We compared model performance in terms of accuracy and calibration for different frameworks based on different responses (local species data versus broad species data) and predictors (local climate versus broad climate). Models trained with local inventories outperformed those trained with broad inventories both in terms of accuracy (AUC, F1) and calibration (COR) (Figure 4.4a, b). Most models trained with local species data had an AUC >0.8 and a TSS >0.6, showing good model performance. AUC but not F1 and COR was significantly higher for models trained with broad inventories at the broad extent than those at the local extent (Figure 4.4a, b). The only significant difference we observed when validating against an external dataset (i.e., GBIF, LUCAS) was in terms of the AUC (Figure 4.4b). We did not observe significant differences between models based on different sets of climate datasets.

The 5th and 95th percentiles were 0.58 and 0.97 for AUC (mean = 0.81, median = 0.83), 0.11 and 0.93 for TSS (mean = 0.55, median = 0.57), 0.04 and 0.70 for F1 (mean = 0.31, median = 0.29), and 0.00 and 0.67 for COR (mean = 0.31, median = 0.29). On average across the frameworks, we observed the best model performances for Swiss stone pine (AUC = 0.98, COR = 0.49), European larch (AUC = 0.93, COR = 0.67), and manna ash (AUC = 0.92, COR = 0.39), while the worst were European aspen (AUC = 0.60, 0.07), sycamore (AUC = 0.70, COR = 0.19), and field maple (AUC = 0.71, COR = 0.12), despite large differences can be observed relatively to the modeling framework. When comparing AUC (accuracy) and COR (calibration), local models outperformed broad ones especially for sessile oak (Δ AUC = 0.27 and Δ COR = 0.34), European aspen (Δ AUC = 0.21), and silver fir (Δ AUC = 0.18 and Δ COR = 0.24). Broad models significantly outperformed local ones only on black pine (Δ AUC = -0.19 and Δ COR = -0.13) and Norway spruce (Δ COR = -0.13). Details and *p-values* of generalized models for accuracy and calibration can be found in Table B4.1 Supplementary Materials.

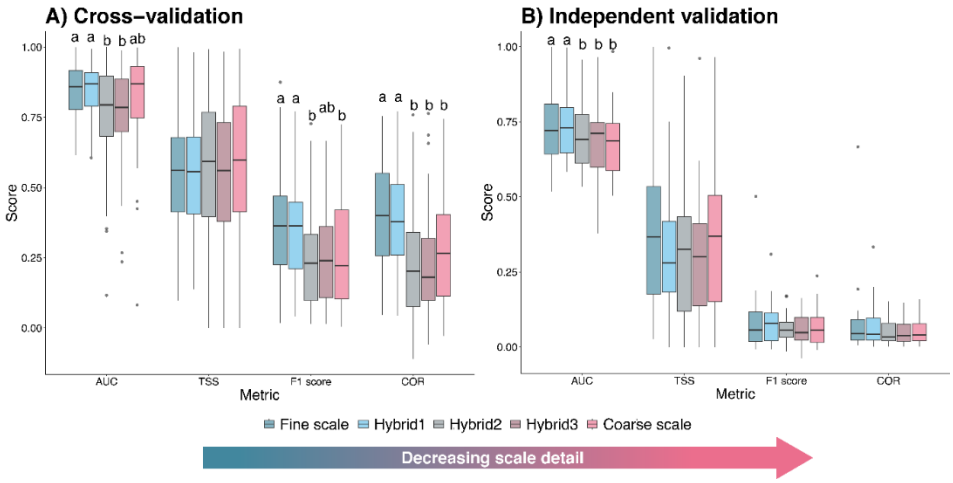

FIGURE 4.4. Validation results from (a) internal 5-fold spatial block cross-validation and (b) external validation on a fully independent dataset for accuracy (AUC, TSS, and F1 score) and calibration (COR). Letters represent the results of significant generalized linear mixed models (Table B.1 Supplementary Materials). Decreasing the scale detail (from fine to coarse with all the combinations in between) leads to a decrease in model accuracy for some accuracy and calibration metrics. Hybrid1 refers to the combination of local species data and GCM, Hybrid2 is the combination of broad species data and RCM, and Hybrid3 is the combination of broad species data at the local extent and GCM.

We assessed the ecological reliability of model outputs and we observed individualistic patterns in terms of spatial predictions (Figures 4.5 and B.4.6 to B.4.8 Supplementary Materials), variable importance (Figures B.4.9 to B.4.11 Supplementary Materials), and correlation between spatial predictions (Table B4.2 Supplementary Materials). Coarse-scale models for sweet chestnut overestimated the occurrence of the species (Figure 4.5). Patterns of over- and underestimation for European beech (Figure B4.6 Supplementary Materials), European larch (Figure B4.7 Supplementary Materials), and Scots pine (Figure B.4.8 Supplementary Materials) were more difficult to decipher. Variable importance was similar among models for species such as black alder, sweet chestnut, European larch, black pine, and downy oak (Figures B.4.9 to B.4.11 Supplementary Materials). Correlation between spatial predictions ranged between -0.01 (sessile oak, RCP 8.5) and 0.88 (European larch) with a mean value

of 0.47, a median value of 0.49, and a standard deviation of 0.22 (Table B4.2 Supplementary Materials).

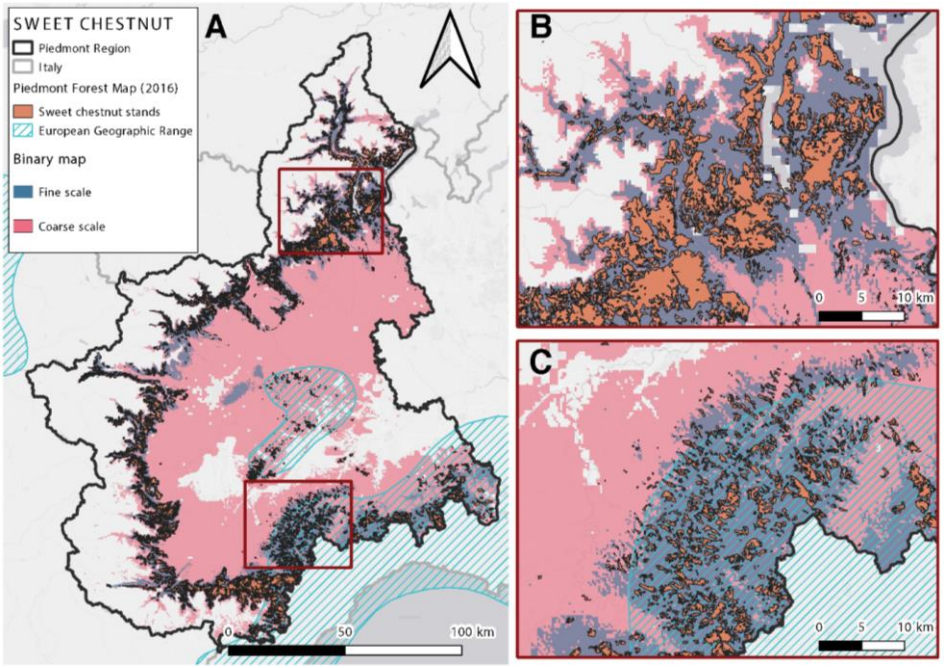

FIGURE 4.5. Comparison between the current potential suitable range of sweet chestnut Castanea sativa expressed by the two scales (Fine = local species data + local climate in blue and coarse scale = broad species data + broad climate at the extent of the Alpine region in pink). The two outputs were compared to the Piedmont Forest Map of 2016 (filtered only for the selected forest type, in orange) and the geographic range for Europe (light blue polygons) derived from Caudullo et al. (2017). Panel a) shows an overview of the entire administrative area, panels (b) and (c) show two closeups corresponding to the Northern (b) and Southern Piedmont (c). Coarse-scale models seemed to overpredict the distribution of sweet chestnut, especially compared to the main stands of the species within Piedmont.

4.3.3 Current and future probability of occurrence of tree species

The species showed individualistic responses between the fine-scale and coarse-scale models for current and future (2051-2070) both in spatial predictions (Figures 4.6, B.4.12 to B.4.14 Supplementary Materials) and estimated changes in probability of occurrence (Figures 4.7, B.4.15 Supplementary Materials). Coarse-scale models generally exhibited changes in the probability of occurrence

closer to zero, while fine-scale models showed more significant positive or negative values (Figure 4.7).

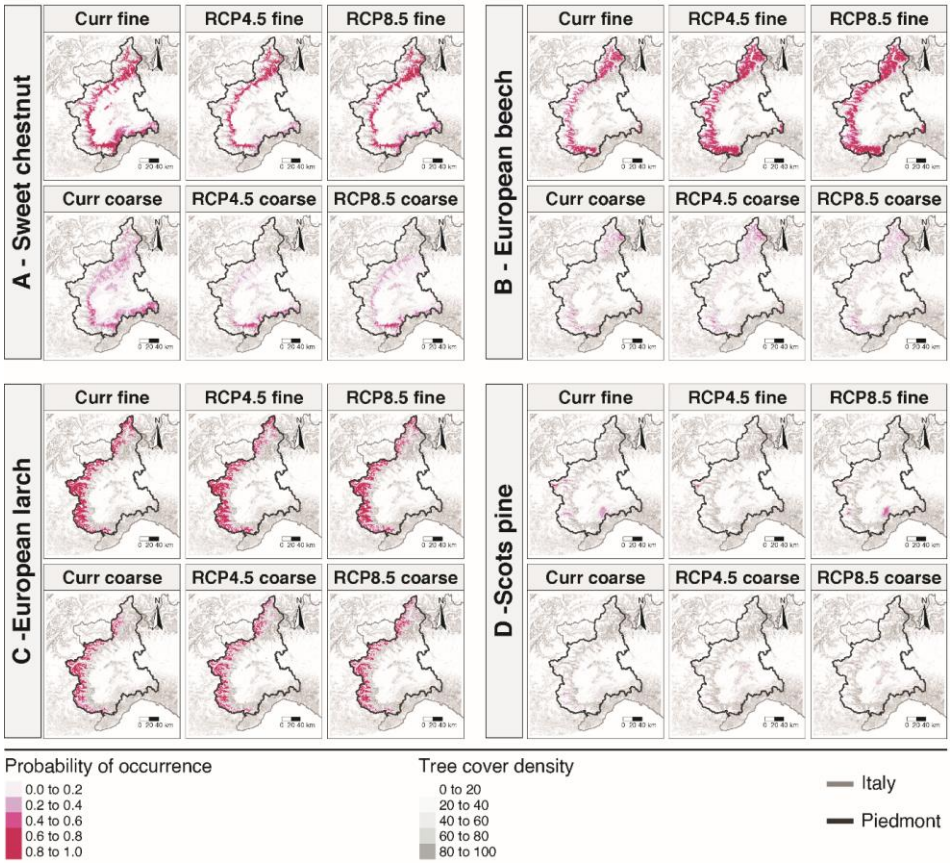

FIGURE 4.6. Probability of occurrence of four species (sweet chestnut, European beech, European larch, and Scots pine) for current and future (RCP 4.5 and RCP 8.5) scenarios for fine-scale (local species data + local climate, upper rows) and coarse-scale (broad species data + broad climate at the alpine extent, lower rows) models. Very different patterns emerged between species in terms of current and future probability of occurrence.

Sweet chestnut (Figures 4.5, 4.6a), oaks (Figure B.4.14 Supplementary Materials), and silver fir (Figure B.4.12a Supplementary Materials) showed discrepancies in terms of spatial prediction patterns between the two models, while European beech (Figure 4.6b), European larch (Figure 4.6c), and Scots pine (Figure 4.6d) displayed consistency. In terms of absolute changes in probability of occurrence, models consistently indicated decreasing probabilities for sweet

chestnut, Scots pine, and sycamore, and increasing probabilities for black alder and European hornbeam. European beech showed differing predictions, increasing in the fine-scale model and remaining stable in the coarse-scale model (Figure 4.6b). European larch and Norway spruce followed an inverse pattern, with the fine-scale models predicting a median net loss and the coarse models predicting stability or slight increase. Downy oak, the most thermophilic of the oak species, was predicted to gain probability of occurrence according to fine-scale models, while the other two species were predicted to experience a more severe net loss under RCP 4.5 than under RCP 8.5.

Among the fine-scale models, we observed the highest gain for European beech (median = +0.18 and +0.22 for RCP4.5 and RCP8.5, respectively) and sessile oak (median = +0.14 and +0.11 for RCP4.5 and RCP8.5, respectively) and the highest loss for black locust (median = -0.18 and -0.14 for RCP4.5 and RCP8.5, respectively) and sweet chestnut (median = -0.14 and -0.08 for RCP4.5 and RCP8.5, respectively). We observed the greatest differences between the frameworks for European beech, black alder, and sessile oak, while the smallest disparities were found for sweet chestnut, downy oak, and European larch.

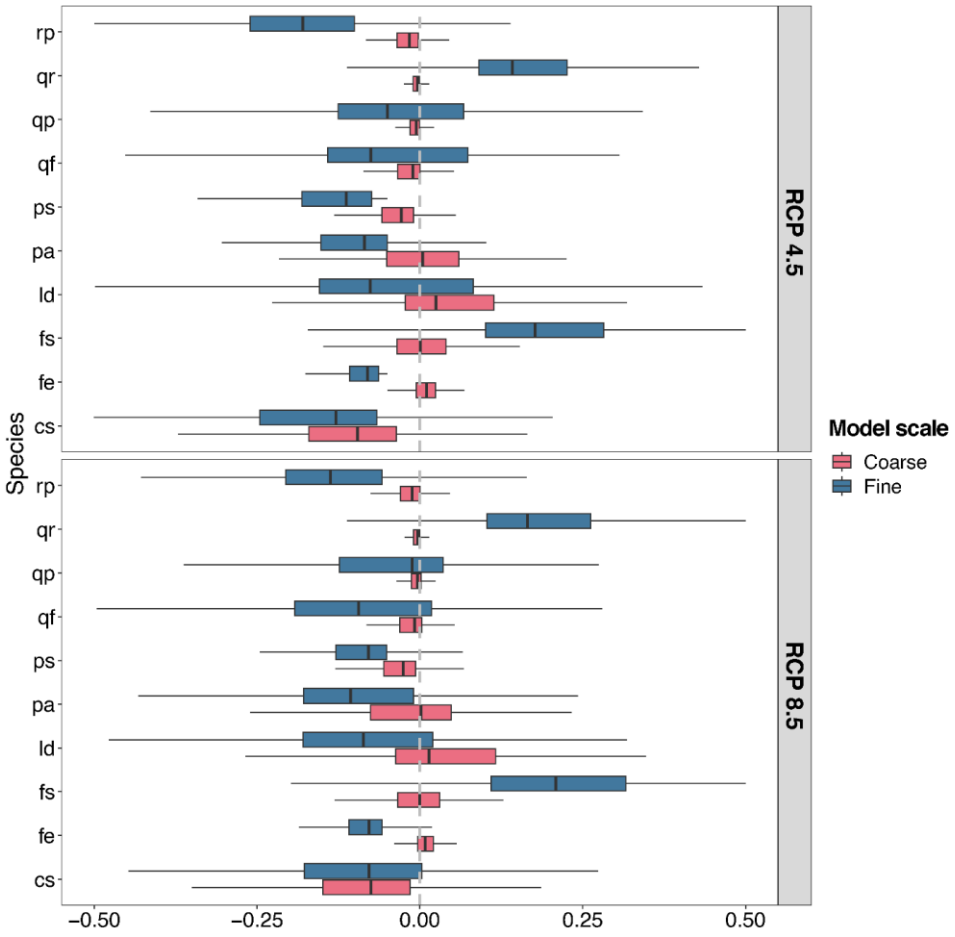

FIGURE 4.7. Boxplots representing the change in probability of occurrence of thirteen species according to the two climate scenarios (RCP 4.5 and RCP 8.5) and the input dataset (fine = local species data + local climate, coarse = broad species data + broad climate at the extent of the Alps). cs = sweet chestnut, fe = European ash, fs = European beech, ld = European larch, pa = Norway spruce, ps = Scots pine, qf = pedunculate oak, qp = downy oak, qr = sessile oak, rp = black locust. Delta between -0.05 and 0.05 were removed to enhance differences between the frameworks. Coarse-scale model predictions seemed to be closer to 0 than fine-scale ones.

4.4 Discussion

In this study, our aim was to evaluate the role of spatial scales in Species Distribution Models (SDMs) for local planning and management. Species Distribution Models (SDMs) along with future scenarios of climate and land use have the potential to be a fundamental part of spatially explicit landscape conservation and restoration for numerous species (Guisan et al., 2013; Mateo et al., 2019; Zurell et al., 2022). However, most predictive SDMs are typically conducted at coarse spatial scales (i.e., continental to global extent and kilometers resolution), which is hardly useful for reserve selection at fine scales, or in considering where to move organisms in assisted migration.

4.4.1 The role of spatial scale in SDMs

Our study demonstrates that SDMs built at different scales yield different spatial predictions and accuracies. Fine-scale models trained with local species data consistently outperformed coarse-scale and hybrid-scale models based on a broad European species data (EU-Forest inventory; Mauri et al., 2017). This was especially evident by using internal spatial-block cross-validation. Our results highlight the distinctive characteristics of different scales of response and predictor variables (Anderson & Raza, 2010; Mateo et al., 2019). Fine-scale models can better capture local conditions, benefiting from dynamically downscaled RCM climate data and finer spatial resolution of species data (i.e., inventory). Nevertheless, models fitted with species data from a partial section of a species' ecological niche can suffer from niche truncation and express truncated response curves (Sánchez-Fernández et al., 2011). Conversely, coarse-scale models, while encompassing a broader portion of the species niche, can lead to higher commission errors due to increased false positives (see for instance sweet chestnut within our study). These behaviors were especially evident when comparing future expected changes in probability of occurrence (Figures 4.7, B4.15 Supplementary Materials), where coarse-scale models predicted a

magnitude of changes in probability closer to zero and fine-scale models predicted higher negative values.

While our study found that climate data did not significantly affect model performance, the characteristics of climate data can impact spatial outcomes in terms of probability of occurrence and binary maps (Bobrowski & Udo, 2017; Patiño et al., 2023). Patiño et al. (2023) showed the potential of finer-resolution climate data in detecting warming trends and mesorefugia by comparing CHELSA with its downscaling version for Canary Islands (~100 m) even if their performance did not show significant difference. Indeed, it is recommended to account for climate uncertainty by using ensembles of multiple dissimilar regional climate models when projecting into the future (Knutti et al., 2013). For instance, a recent pan-European study on tree species distributions applied 11 different RCMs at ~10 km resolution to project future change scenarios (Mauri et al., 2022). However, in our study, we used data from a single climate model for future local climate, which can be a limitation.

The choice of scale in SDMs is a critical factor, and fine-scale models performed better in capturing local conditions in our study. Nevertheless, when fine-scale response data are not accessible, coarse-scale data can still offer valuable insights, especially for certain species. Given the absence of consistent improvement patterns across different extents of broad inventories, we recommend that researchers opt for broader extents to mitigate the risk of niche truncation in such cases, especially when predicting future conditions. Hierarchical approaches integrating variables at different scales have been proposed as a solution to address spatial mismatches in SDMs predictions (Pearson et al., 2004; Mateo et al., 2019; Simon et al., 2023). However, it is worth mentioning that hierarchical modeling has not shown consistent predictions improvement compared to common approaches, especially because of challenges in their validation (El-Gabbas & Dormann, 2018; Simon et al., 2023).

Our choice of using Bayesian Additive Regression Trees (BART) was supported by preliminary tests, which demonstrated comparable accuracy to ensemble

models, as highlighted by previous studies (e.g., Baquero et al., 2021; Konowalik & Nosol, 2021; Plant et al., 2021). We also experimented with different subsets of predictor variables (no filtering, principal components, VIF and correlation filter) and chose a variable reduction approach based on variable importance, as it offered faster computation and facilitated ecological assessment.

4.4.2 Current and future probability of occurrence of the main tree species

Our study provides insights into the reliability of different tree species' predictions under various frameworks. Comparisons with local forest maps, European geographic range (Caudullo et al., 2017), EU-Trees4F (Mauri et al., 2022), and literature revealed both consistent and divergent results. Our results corroborated existing literature (Hanewinkel et al., 2013; Dyderski et al., 2018; Mauri et al., 2022), indicating a probability increase for silver fir, particularly under the fine-scale RCP 4.5 scenario, and European beech in fine-scale models. Conversely, probability losses were observed for European larch, especially in fine-scale models, as well as for Scots pine and Norway spruce, the latter being more pronounced in the fine-scale models. Notably, many of the studies we used as reference did not mask unvegetated areas at high elevations or in urban regions. By doing that, they included as suitable areas that we expected to be not suitable in the future 50-100 years. This consideration is particularly important for montane and subalpine species such as the European larch.

Overall, many species showed different responses to the spatial scales of predictors. We discuss two examples for tree species with an important history of use within Piedmont: sweet chestnut and European larch. Our analysis of sweet chestnut exhibited significantly different spatial predictions between fine-scale and coarse-scale models, yet the extent of probability of occurrence loss remained similar. In the current scenario, the fine-scale model showed greater ecological reliability, designating hilly and low mountain regions as the most suitable habitats for the species. This aligns with local traditional silvicultural practices that have historically favored sweet chestnut in these areas due to its value in fruit, timber, and fuel wood production, a practice also observed in other Alpine

regions such as Canton Ticino, Switzerland (Conedera et al., 2004; Camerano et al., 2017). Conversely, coarse-scale models emphasized lowland areas (i.e., the Po Valley), as the most climatically suitable regions, but these models may overlook the influence of traditional land use. The anticipated future decline in the probability of occurrence can likely be attributed to the widespread expansion into areas with lower climatic suitability that were previously dominated by stands of sessile and downy oaks (Conedera et al., 2004; Camerano et al., 2017).

When comparing models for a different species, such as the European larch, we observed a different outcome. Current probability of occurrence was relatively consistent between the two modeling frameworks ($r = 0.88$), but the fine-scale model displayed greater suitability at lower elevations, particularly in the Southern and Northern sectors of the study area. In spatial predictions more than in model performance, the effect of climate data emerged. Therefore, we attributed this discrepancy to differences in climate scenarios but also to possible niche truncation. Additionally, the relative variable importance exhibited similar patterns between the frameworks, with a slightly greater emphasis on temperature in the coarse-scale model. In terms of future scenarios, both models projected a decline in the probability of occurrence at lower elevations, but the fine-scale model predicted a more substantial loss compared to the coarse-scale model. The fine-scale result is in line with results from the literature (Dyderski et al., 2018; Mauri et al, 2022), likely due to the comprehensive representation of European larch in Piedmont region, encompassing a wide array of the environmental conditions across its entire geographic range because of the historical use of the species across several altitudinal and ecological gradients (Garbarino et al., 2011).

One key limitation of our approach is the absence of accounting for dispersal constraints in future scenarios, a factor highlighted in recent research (Mauri et al., 2022).

4.4.3 SDMs as tools for local forest management

As previously discussed, SDMs can be particularly important for implementing assisted migration and ecological restoration within local reforestation plans (Wan et al., 2017; Begemann et al., 2021; Twardek et al., 2023). Advancements in forest planning should therefore account for spatial scales of response and predictive variables within predictive models, especially given the increasing research on microclimate variation based on fine-scale topography and canopy cover (Lembrechts et al., 2019b; DeFrenne, et al., 2021; Haesen et al., 2023).

We advocate for adequate testing of species data (i.e., forest inventories) and predictor variables within SDMs for forest planning and management. Fine-scale models are valuable for current predictions, particularly when local data sources and response data align with the scale of application. Moreover, in our study area, fine-scale models appeared to magnify local anthropogenic signals associated with the traditional use of sweet chestnut. This result emphasizes the difficulties in aligning meaningful spatial scales of ecological processes with available climate data, a major challenge especially in long-lasting human-dominated mountain systems such as the Alps, where human activities have profoundly altered ecosystem spatial patterns (Batzing et al., 1996; Plieninger et al., 2016; Zanon et al., 2018). Coarse-scale models, on the other hand, can be trained over broader geographic extents, covering a larger portion of a species' niche (Anderson & Raza, 2010; Sánchez-Fernández et al., 2011). We should still note that SDMs usually refer to the species level, but many adaptation strategies take place at the level of genotypes and populations, which are defined at local spatial scales. This multi-scale approach can be particularly useful in complex forest policy frameworks, where various model scales correspond to different policy levels. Indeed, multi-scale approaches can enhance the discussion with stakeholders and increase the robustness of predictions (Begemann et al., 2021; Sharma et al., 2023).

4.5 Conclusions

In this study, we explored the importance of spatial scales in Species Distribution Models (SDMs), shedding light on their core relevance in ecological research and forest management within the context of climate change. Our findings highlight the need to adopt fine scales in SDMs. Models built upon local species data (i.e., forest inventory) consistently outperformed their coarser counterparts, while high-resolution regional climate models allowed for precision in capturing local conditions, making them indispensable for current predictions, ecological assessments, and localized forest management.

Fine-scale models not only enhanced accuracy but also magnified local anthropogenic influences by emphasizing the profound impact of local traditional practices like sweet chestnut and European larch silvicultural systems. In contrast, coarse-scale models may miss these nuances, favoring climatic suitability over intricate local practices. Therefore, incorporating fine-scale data is essential when it aligns with the study's scale of application.

However, we acknowledge that fine-scale models do not come without problems. Niche truncation can occur when response data encompass only a portion of a species' ecological niche, potentially affecting future predictive accuracy. Therefore, ecologists and forest practitioners should carefully choose the scale of response data based on the study's scope and the species under investigation. In terms of climate data, while they did not significantly affect model performance, their resolution can impact the spatial outcomes of probability of occurrence and binary maps. Indeed, using fine-resolution climate data may enhance the detection of local warming trends and mesorefugia.

In the light of the ongoing climate and land use changes, SDMs have an increasingly important role in forest planning and management. Considering differences in spatial scales, integrating fine-scale models and microclimate data, and using hierarchical approaches can enhance the accuracy and reliability of species distribution models for ecologists, policymakers, and forest practitioners.

Acknowledgments

We thank Renata Pelosini, ARPA Piemonte, and CINECA for funding N.A. PhD program through the Highlander Project co-financed by the Connecting European Facility Programme of the European Union under Grant agreement n° INEA/CEF/ICT/A2018/1815462.

Data availability

Code will be made available in a Figshare repository. The EU-Forest inventory, CHELSA climate dataset, and COSMO-CLM are publicly available in their official repositories.

References

Albrich, K., Rammer, W., Turner, M. G., Ratajczak, Z., Braziunas, K. H., Hansen, W. D., & Seidl, R. (2020). Simulating forest resilience: A review. *Global Ecology and Biogeography*, 29(12), 2082–2096.

Alpine Convention. Alpine Convention Perimeter (2018). https://www.atlas.alpconv.org/layers/geonode_data:geonode:Alpine_Convention_Perimeter_2018_v2

Anderson, R. P., & Raza, A. (2010). The effect of the extent of the study region on GIS models of species geographic distributions and estimates of niche evolution: preliminary tests with montane rodents (genus Nephelomys) in Venezuela. *Journal of Biogeography*, 37(7), 1378-1393.

Anselmetto, N., Weisberg, P.J., Garbarino, M. (2024). Global change in the European Alps: a century of post-abandonment natural reforestation at the landscape scale. *Landscape and Urban Planning*.

Araújo, M. B., Anderson, R. P., Barbosa, A. M., Beale, C. M., Dormann, C. F., Early, R., Garcia, R. A., Guisan, A., Maiorano, L., Naimi, B., O'Hara, R. B., Zimmermann, N. E., & Rahbek, C. (2019). Standards for distribution models in biodiversity assessments. *Science Advances*, 5(1), eaat4858.

Ban, N., Caillaud, C., Coppola, E., Pichelli, E., Sobolowski, S., Adinolfi, M., ... & Zander, M. J. (2021). The first multi-model ensemble of regional climate simulations at

kilometer-scale resolution, part I: evaluation of precipitation. *Climate Dynamics*, 57, 275-302.

Ban, N., Schmidli, J., & Schär, C. (2014). Evaluation of the convection-resolving regional climate modeling approach in decade-long simulations. *Journal of Geophysical Research: Atmospheres*, 119(13), 7889-7907.

Baquero, R.A., Barbosa, A.M., Ayllón, D., Guerra, C., Sánchez, E., Araújo, M.B., & Nicola, G.G. (2021). Potential distributions of invasive vertebrates in the Iberian Peninsula under projected changes in climate extreme events. *Diversity and Distributions*, 27(11), 2262-2276.

Batzing, W., Perlik, M., & Dekleva, M. (1996). Urbanization and Depopulation in the Alps. *Mountain Research and Development*, 16(4), 335.

Begemann, A., Giessen, L., Roitsch, D., Roux, J.-L., Lovrić, M., Azevedo-Ramos, C., Boerner, J., Beeko, C., Cashore, B., Cerutti, P. O., De Jong, W., Fosse, L. J., Hinrichs, A., Humphreys, D., Pülzl, H., Santamaria, C., Sotirov, M., Wunder, S., & Winkel, G. (2021). Quo vadis global forest governance? A transdisciplinary delphi study. *Environmental Science & Policy*, 123, 131–141.

Berthou, S., Kendon, E. J., Chan, S. C., Ban, N., Leutwyler, D., Schär, C., & Fosser, G. (2020). Pan-European climate at convection-permitting scale: a model intercomparison study. *Climate Dynamics*, 55, 35-59.

Betts, M. G., Diamond, A. W., Forbes, G. J., Villard, M. A., & Gunn, J. S. (2006). The importance of spatial autocorrelation, extent and resolution in predicting forest bird occurrence. *Ecological Modelling*, 191(2), 197-224.

Bobrowski, M., & Udo, S. (2017). Why input matters: Selection of climate data sets for modelling the potential distribution of a treeline species in the Himalayan region. *Ecological Modelling*, 359, 92–102.

Bucklin , D. N., Basille, M., Benscoter, A. M., Brandt, L. A., Mazzotti, F. J., Romanach, S. S., ... & Watling, J. I. (2015). Comparing species distribution models constructed with different subsets of environmental predictors. *Diversity and Distributions*, 21(1), 23-35.

Buenafe, K. C. V., Dunn, D. C., Everett, J. D., Brito-Morales, I., Schoeman, D. S., Hanson, J. O., ... & Richardson, A. J. (2023). A metric-based framework for climate-smart conservation planning. *Ecological Applications*, 33(4), e2852.

Camerano, P., Giannetti, F., Terzuolo, P. G., & Guiot, E. (2017). *La Carta Forestale del Piemonte—Aggiornamento 2016*. IPLA SpA–Regione Piemonte.

Carlson, C.J. (2020) embarcadero: Species distribution modelling with Bayesian additive regression trees in r. *Methods in Ecology and Evolution*, 11(7), 850-858.

Caudullo, G., Welk, E., & San-Miguel-Ayanz, J. (2017). Chorological maps for the main European woody species. *Data in Brief*, 12, 662-666.

Chipman HA, George EI, McCulloch RE (2010). *BART: Bayesian additive regression trees.*

Conedera, M., Krebs, P., Tinner, W., Pradella, M., & Torriani, D. (2004). The cultivation of Castanea sativa (Mill.) in Europe, from its origin to its diffusion on a continental scale. *Vegetation History and Archaeobotany*, 13(3).

Crespi, A., Brunetti, M., Lentini, G., & Maugeri, M. (2018). 1961–1990 high-resolution monthly precipitation climatologies for Italy. *International Journal of Climatology*, 38(2), 878-895.

De Frenne, P., Lenoir, J., Luoto, M., Scheffers, B. R., Zellweger, F., Aalto, J., ... & Hylander, K. (2021). Forest microclimates and climate change: Importance, drivers and future research agenda. *Global Change Biology*, 27(11), 2279-2297.

Dyderski, M. K., Paź, S., Frelich, L. E., & Jagodziński, A. M. (2018). How much does climate change threaten European forest tree species distributions? *Global Change Biology*, 24(3), 1150-1163.

El-Gabbas, A., & Dormann, C. F. (2018). Wrong, but useful: regional species distribution models may not be improved by range-wide data under biased sampling. *Ecology and Evolution*, 8(4), 2196-2206.

Elith, J., H. Graham, C., P. Anderson, R., Dudík, M., Ferrier, S., Guisan, A., ... & E. Zimmermann, N. (2006). Novel methods improve prediction of species' distributions from occurrence data. *Ecography*, 29(2), 129-151.

Ellis-Soto, D., Merow, C., Amatulli, G., Parra, J. L., & Jetz, W. (2021). Continental-scale 1 km hummingbird diversity derived from fusing point records with lateral and elevational expert information. *Ecography*, 44(4), 640-652.

European Commission (1994). Directorate-General for the Information Society and Media, Directorate-General for Environment. *Corine land cover: Guide technique*. Publications Office.

European Parliament. (2007). *Directive 2007/2/EC of the European parliament and of the council of 14 march 2007 establishing an infrastructure for spatial information in the European community (INSPIRE)*. Official Journal of the European Union, 50, 1–14.

Fagan, M. E., Reid, J. L., Holland, M. B., Drew, J. G., & Zahawi, R. A. (2020). How feasible are global forest restoration commitments? *Conservation Letters*, 13(3).

Forzieri, G., Dakos, V., McDowell, N. G., Ramdane, A., & Cescatti, A. (2022). Emerging signals of declining forest resilience under climate change. *Nature*, 608(7923), 534–539.

Franklin, J. (1995). Predictive vegetation mapping: Geographic modelling of biospatial patterns in relation to environmental gradients. *Progress in Physical Geography: Earth and Environment*, 19(4), 474–499.

Fumière, Q., Déqué, M., Nuissier, O., Somot, S., Alias, A., Caillaud, C., ... & Seity, Y. (2020). Extreme rainfall in Mediterranean France during the fall: added value of the CNRM-AROME Convection-Permitting Regional Climate Model. *Climate Dynamics*, 55, 77-91.

Garbarino, M., Lingua, E., Martinez Subirà, M., & Motta, R. (2011). The larch wood pasture: Structure and dynamics of a cultural landscape. *European Journal of Forest Research*, 130(4), 491–502.

Giorgi, F., Jones, C., & Asrar, G. R. (2009). *Addressing climate information needs at the regional level: the CORDEX framework.* World Meteorological Organization (WMO) Bulletin, 58(3), 175.

Guisan, A., Tingley, R., Baumgartner, J. B., Naujokaitis-Lewis, I., Sutcliffe, P. R., Tulloch, A. I. T., Regan, T. J., Brotons, L., McDonald-Madden, E., Mantyka-Pringle, C., Martin, T. G., Rhodes, J. R., Maggini, R., Setterfield, S. A., Elith, J., Schwartz, M. W., Wintle, B. A., Broennimann, O., Austin, M., … Buckley, Y. M. (2013). Predicting species distributions for conservation decisions. *Ecology Letters*, 16(12), 1424–1435.

Haesen, S., Lenoir, J., Gril, E., De Frenne, P., Lembrechts, J. J., Kopecký, M., ... & Van Meerbeek, K. (2023). Microclimate reveals the true thermal niche of forest plant species. *Ecology Letters*.

Hanewinkel, M., Cullmann, D. A., Schelhaas, M. J., Nabuurs, G. J., & Zimmermann, N. E. (2013). Climate change may cause severe loss in the economic value of European forest land. *Nature Climate Change*, 3(3), 203-207.

Hengl, T., Mendes de Jesus, J., Heuvelink, G. B., Ruiperez Gonzalez, M., Kilibarda, M., Blagotić, A., ... & Kempen, B. (2017). SoilGrids250m: Global gridded soil information based on machine learning. *PLOS ONE*, 12(2), e0169748.

Hersbach, H., Bell, B., Berrisford, P., Hirahara, S., Horányi, A., Muñoz-Sabater, J., ... & Thépaut, J. N. (2020). The ERA5 global reanalysis. *Quarterly Journal of the Royal Meteorological Society*, 146(730), 1999-2049.

Hiemstra, P. H., Pebesma, E. J., Twenhöfel, C. J., & Heuvelink, G. B. (2009). Real-time automatic interpolation of ambient gamma dose rates from the Dutch radioactivity monitoring network. *Computers & Geosciences*, 35(8), 1711-1721.

Hijmans, R.J., Cameron, S.E., Parra, J.L., Jones, P.G., & Jarvis, A. (2005). Very high resolution interpolated climate surfaces for global land areas. *International Journal of Climatology*, 25, 1965-1978.

Hintze, F., Machado, R. B., & Bernard, E. (2021). Bioacoustics for in situ validation of species distribution modelling: An example with bats in Brazil. *PLOS ONE*, 16(10), e0248797.

Karger, D. N., Conrad, O., Böhner, J., Kawohl, T., Kreft, H., Soria-Auza, R. W., Zimmermann, N. E., Linder, H. P., & Kessler, M. (2017). Climatologies at high resolution for the earth's land surface areas. *Scientific Data*, 4(1).

Karger D.N., Conrad, O., Böhner, J., Kawohl, T., Kreft, H., Soria-Auza, R.W., Zimmermann, N.E, Linder, H.P., Kessler, M. (2018): Data from: Climatologies at high resolution for the earth's land surface areas. *Dryad digital repository*.

Kendon, E. J., Roberts, N. M., Fowler, H. J., Roberts, M. J., Chan, S. C., & Senior, C. A. (2014). Heavier summer downpours with climate change revealed by weather forecast resolution model. *Nature Climate Change*, 4(7), 570-576.

Knutti, R., Masson, D. & Gettelman, A. (2013) Climate model genealogy: Generation CMIP5 and how we got there. *Geophysical Research Letters*, 40, 1194–1199.

Konowalik, K., & Nosol, A. (2021). Evaluation metrics and validation of presence-only species distribution models based on distributional maps with varying coverage. *Scientific Reports*, 11(1), 1482.

Lembrechts, J. J., Lenoir, J., Roth, N., Hattab, T., Milbau, A., Haider, S., ... & Nijs, I. (2019a). Comparing temperature data sources for use in species distribution models: From in-situ logging to remote sensing. *Global Ecology and Biogeography*, 28(11), 1578-1596.

Lembrechts, J. J., Nijs, I., & Lenoir, J. (2019b). Incorporating microclimate into species distribution models. *Ecography*, 42(7), 1267-1279.

Liu, C., Ikeda, K., Rasmussen, R., Barlage, M., Newman, A. J., Prein, A. F., ... & Yates, D. (2017). Continental-scale convection-permitting modeling of the current and future climate of North America. *Climate Dynamics*, 49, 71-95.

Maréchaux, I., Langerwisch, F., Huth, A., Bugmann, H., Morin, X., Reyer, C. P., ... & Bohn, F. J. (2021). Tackling unresolved questions in forest ecology: The past and future role of simulation models. *Ecology and Evolution*, 11(9), 3746-3770.

Mateo, R. G., Gastón, A., Aroca-Fernández, M. J., Broennimann, O., Guisan, A., Saura, S., & García-Viñas, J. I. (2019). Hierarchical species distribution models in support of vegetation conservation at the landscape scale. *Journal of Vegetation Science*, 30(2), 386–396.

Mauri, A., Girardello, M., Strona, G., Beck, P. S. A., Forzieri, G., Caudullo, G., Manca, F., & Cescatti, A. (2022). EU-Trees4F, a dataset on the future distribution of European tree species. *Scientific Data*, 9(1), 37.

Mauri, A., Strona, G., & San-Miguel-Ayanz, J. (2017). EU-Forest, a high-resolution tree occurrence dataset for Europe. *Scientific Data*, 4(1).

McCune, B., J.B. Grace, & D.L. Urban. (2002). *Analysis of ecological communities*. OR: Gleneden Beach.

McDowell, N. G., Allen, C. D., Anderson-Teixeira, K., Aukema, B. H., Bond-Lamberty, B., Chini, L., Clark, J. S., Dietze, M., Grossiord, C., Hanbury-Brown, A., Hurtt, G. C., Jackson, R. B., Johnson, D. J., Kueppers, L., Lichstein, J. W., Ogle, K., Poulter, B., Pugh, T. A. M., Seidl, R., … Xu, C. (2020). Pervasive shifts in forest dynamics in a changing world. *Science*.

Mietkiewicz, N., Kulakowski, D., Rogan, J., & Bebi, P. (2017). Long-term change in sub-alpine forest cover, tree line and species composition in the Swiss Alps. *Journal of Vegetation Science*, 28(5), 951–964.

Mori, A. S., Lertzman, K. P., & Gustafsson, L. (2017). Biodiversity and ecosystem services in forest ecosystems: A research agenda for applied forest ecology. *Journal of Applied Ecology*, 54(1), 12–27.

Naimi, B., Hamm, N.A., Groen, T.A., Skidmore, A.K., & Toxopeus, A.G. (2014). Where is positional uncertainty a problem for species distribution modelling. *Ecography*, 37, 191-203.

Newbold, T. (2018). Future effects of climate and land-use change on terrestrial vertebrate community diversity under different scenarios. *Proceedings of the Royal Society B: Biological Sciences*, 285(1881), 20180792.

Patiño, J., Collart, F., Vanderpoorten, A., Martin-Esquivel, J. L., Naranjo-Cigala, A., Mirolo, S., & Karger, D. N. (2023). Spatial resolution impacts projected plant responses to climate change on topographically complex islands. *Diversity and Distributions*, 29(10), 1245-1262.

Pearson, R. G., Dawson, T. P., & Liu, C. (2004). Modelling species distributions in Britain: a hierarchical integration of climate and land-cover data. *Ecography*, 27(3), 285-298.

Pecchi, M., Marchi, M., Burton, V., Giannetti, F., Moriondo, M., Bernetti, I., Bindi, M., & Chirici, G. (2019). Species distribution modelling to support forest management. A literature review. *Ecological Modelling*, 411, 108817.

Plieninger, T., Draux, H., Fagerholm, N., Bieling, C., Bürgi, M., Kizos, T., Kuemmerle, T., Primdahl, J., & Verburg, P. H. (2016). The driving forces of landscape change in Europe: A systematic review of the evidence. *Land Use Policy*, 57, 204–214.

R Core Team (2023). *R: A language and environment for statistical computing*. R Foundation for Statistical Computing, Vienna, Austria.

Raffa, M., Adinolfi, M., Reder, A., Marras, G. F., Mancini, M., Scipione, G., ... & Mercogliano, P. (2023). Very High Resolution Projections over Italy under different CMIP5 IPCC scenarios. *Scientific Data*, 10(1), 238.

Raffa, M., & Mercogliano, P. (2022). Dynamical Downscaling with COSMO-CLM of historical (1989/2005) and future climate (2006/2050) data under scenario RCP8.5 at 2.2 km over Italy [*Data set*]. Fondazione CMCC. https://doi.org/10.25424/CMCC-J90A-5P12

Raffa, M., Reder, A., Marras, G.F., Mancini, M., Scipione, G., Santini, M., & Mercogliano, P. (2021). VHR-REA_IT Dataset: Very High Resolution Dynamical Downscaling of ERA5 Reanalysis over Italy by COSMO-CLM. *Scientific Data*, 6, 88.

Riley, S. J., DeGloria, S. D., & Elliot, R. (1999). Index that quantifies topographic heterogeneity. *Intermountain Journal of Sciences*, 5(1-4), 23-27.

Sánchez-Fernández, D., Lobo, J. M., & Hernández-Manrique, O. L. (2011). Species distribution models that do not incorporate global data misrepresent potential distributions: a case study using Iberian diving beetles. *Diversity and Distributions*, 17(1), 163-171.

Sanderson, B.M., Knutti, R. & Caldwell, P. (2015) A Representative Democracy to Reduce Interdependency in a Multimodel Ensemble. *Journal of Climate*, 28, 5171–5194.

SER (Society for Ecological Restoration Science and Policy Working Group) (2002) The SER primer on ecological restoration. *Society for Ecological Restoration*. www.ser.org/

Sharma, K., Walters, G., Metzger, M. J., & Ghazoul, J. (2023). Glocal woodlands–The rescaling of forest governance in Scotland. *Land Use Policy*, 126, 106524.

Simon, A., Katzensteiner, K., & Wallentin, G. (2023). The integration of hierarchical levels of scale in tree species distribution models of silver fir (Abies alba Mill.) and European beech (Fagus sylvatica L.) in mountain forests. *Ecological Modelling*, 485, 110499.

Smith, T., Traxl, D., & Boers, N. (2022). Empirical evidence for recent global shifts in vegetation resilience. *Nature Climate Change*, 12(5), 477–484.

Tinkham, W. T., Mahoney, P. R., Hudak, A. T., Domke, G. M., Falkowski, M. J., Woodall, C. W., & Smith, A. M. S. (2018). Applications of the United States Forest Inventory and Analysis dataset: A review and future directions. *Canadian Journal of Forest Research*, 48(11), 1251–1268.

Tomppo, E., Gschwantner, T., Lawrence, M., McRoberts, R. E., Gabler, K., Schadauer, K., ... & Cienciala, E. (2010). National forest inventories. Pathways for Common Reporting. *European Science Foundation*, 1, 541-553.

Twardek, W. M., Taylor, J. J., Rytwinski, T., Aitken, S. N., MacDonald, A. L., Van Bogaert, R., & Cooke, S. J. (2023). The application of assisted migration as a climate change adaptation tactic: An evidence map and synthesis. *Biological Conservation*, 280, 109932.

Valavi, R., Guillera-Arroita, G., Lahoz-Monfort, J. J., & Elith, J. (2022). Predictive performance of presence-only species distribution models: a benchmark study with reproducible code. *Ecological Monographs*, 92(1), e01486.

Vitasse, Y., Ursenbacher, S., Klein, G., Bohnenstengel, T., Chittaro, Y., Delestrade, A., Monnerat, C., Rebetez, M., Rixen, C., Strebel, N., Schmidt, B. R., Wipf, S., Wohlgemuth, T., Yoccoz, N. G., & Lenoir, J. (2021). Phenological and elevational shifts of plants, animals and fungi under climate change in the European Alps. *Biological Reviews*, 96, 1816–1835.

Waldock, C., Stuart-Smith, R. D., Albouy, C., Cheung, W. W., Edgar, G. J., Mouillot, D., ... & Pellissier, L. (2022). A quantitative review of abundance-based species distribution models. *Ecography*, 2022(1).

Wan, J. Z., Wang, C. J., & Yu, F. H. (2017). Spatial conservation prioritization for dominant tree species of Chinese forest communities under climate change. *Climatic Change*, 144, 303-316.

Watanabe, S., Kanae, S., Seto, S., Yeh, P. J. F., Hirabayashi, Y., & Oki, T. (2012). Intercomparison of bias-correction methods for monthly temperature and precipitation simulated by multiple climate models. *Journal of Geophysical Research: Atmospheres*, 117(D23).

Yamazaki D., D. Ikeshima, R. Tawatari, T. Yamaguchi, F. O'Loughlin, J.C. Neal, C.C. Sampson, S. Kanae & P.D. Bates. (2017) A high accuracy map of global terrain elevations. *Geophysical Research Letters*, 44, pp.5844-5853.

Zanon, M., Davis, B. A. S., Marquer, L., Brewer, S., & Kaplan, J. O. (2018). European Forest Cover During the Past 12,000 Years: A Palynological Reconstruction Based on Modern Analogs and Remote Sensing. *Frontiers in Plant Science*, 9, 253.

Zubler, E. M., Fischer, A. M., Fröb, F., & Liniger, M. A. (2016). Climate change signals of CMIP5 general circulation models over the Alps – impact of model selection. *International Journal of Climatology*, 36(8), 3088–3104.

Zurell, D., Franklin, J., König, C., Bouchet, P. J., Dormann, C. F., Elith, J., Fandos, G., Feng, X., Guillera-Arroita, G., Guisan, A., Lahoz-Monfort, J. J., Leitão, P. J., Park, D. S., Peterson, A. T., Rapacciuolo, G., Schmatz, D. R., Schröder, B., Serra-Diaz, J. M., Thuiller, W., … Merow, C. (2020). A standard protocol for reporting species distribution models. *Ecography*, 43(9), 1261–1277.

Zurell, D., König, C., Malchow, A. K., Kapitza, S., Bocedi, G., Travis, J., & Fandos, G. (2022). Spatially explicit models for decision-making in animal conservation and restoration. *Ecography*, 2022(4).

Supplementary Materials

Appendix A4 – Supplementary materials and methods

Table A4.1 shows relevant information for this study according to the ODMAP protocol suggested by Zurell et al. (2020). More details on R packages used and the meaning of bioclimatic variables can be found in Table A4.2 and Table A4.3, respectively.

TABLE A4.1. ODMAP protocol for the study (sensu Zurell et al., 2020).

ODMAP element	*Contents*
OVERVIEW	
Authorship	**Authors**: Nicolò Anselmetto*****, Donato Morresi, Simona Barbarino, Nicola Loglisci, Matthew G Betts, Matteo Garbarino **Contact email**: *****nicolo.anselmetto@unito.it **Title**: Fine-scale tree inventory data improve species distribution model predictions
Model objective	**Objective**: mapping/forecast/comparison of biodiversity and climate data. **Target outputs**: continuous occurrence probabilities, binary maps, and change in occurrence probability/range size.
Taxon	The 22 most common tree species in the alpine region of Piemonte, northwestern Italy.
Location	European Alps/Piedmont Region (NW Italy).
Scale of analysis	**Spatial extent** (Lon/Lat: Longitude 4.88° E - 16.47° E, Latitude 43.43° N - 48.37 ° N for the Alps; Longitude 6.63° E - 9.21° E, Latitude 44.06 ° N - 46.46 ° N for Piemonte Region). **Spatial resolution**: 250 m x 250 m. **Temporal resolution and extent**: we modelled current (1989-2013) and future (2051-2070) potential distribution. For the future, we selected two climate scenarios (RCP4.5 and RCP8.5). **Type of extent boundary**: rectangular (Alps) and political (Piedmont Region)**.**

Biodiversity data overview	**Observation type**: standardised monitoring (forest inventories, FIs) for calibration) and random observation for validation. **Response/Data type**: presence/absence data**.**
Type of predictors	Climate, topography, and soil.
Conceptual model/ Hypotheses	We modelled the potential distribution of species based on their climatic niche and we integrated topographic and soil variables to refine these predictions at 250 m. We considered the main abiotic drivers (climate, topography, soil) and we masked the unvegetated surfaces (urban, rocks, water) to constrain the distribution of species. We did not account for biotic drivers such as competition and facilitation and seed dispersal. We accounted for abundancy (i.e., relative basal area) of the local FI (LFI) led by IPLA for Piedmont by assigning weights to the machine learning model. We wanted to compare (i) different forest inventories and (ii) different climate datasets in species distribution models of trees at the local scale. The last aim was to forecast future change of distribution for the species.
Assumptions	We assumed that species were at pseudo-equilibrium with the environment. We assumed that climate drives most of the potential distribution of tree species. We assumed independence of species observations given the nature of the analyzed taxum. We assumed the climatic niches to be constant for future forecasting and that the correlation structure between predictors does not change between current and future time. We assumed neglectable observation bias issues both from an ecological and spatial point of view and we excluded imperfect detection because of the standardized and all encompassing monitoring approach of FIs. We masked unvegetated areas to further constrain species distribution but we intentionally included grasslands, meadows, prairies, and croplands to account for possible future forest gain due to post-abandonment or policy. We did not encompass the entire realised niche of the species when projecting into future time to account for population differences within a small region.

SDM algorithms	**Algorithms**: the final SDMs were fitted using Bayesian Additive Regression Trees (BARTs). We selected this particular machine learning algorithm because of its capability of providing model uncertainties based on posterior probabilities (Carlson, 2020), its flexibility, and its good accuracy/calibration. **Model complexity**: no parameters were chosen for SDMs tuning since BART proved to provide similar results than ensemble modeling and fine tuned machine learning algorithms (e.g., RF) with default settings, allowing for good accuracies while preventing excessive overfitting (e.g., Baquero et al., 2021).
Model workflow	For the local forest inventory, we used the abundance (i.e., relative basal area) as weights within the regression algorithm.
Software, codes and data	**Software**: all analyses were conducted using R version 4.2.3 (R Core Team, 2023) with packages in the Supplementary Material. **Code availability**: Codes are available upon request. **Data availability**: Data are available upon request.

DATA	

Biodiversity data	**Taxon names**: *Abies alba* Mill., *Acer campestre* L., *Acer pseudoplatanus* L., *Alnus glutinosa* (L.) Gaertn., *Betula pendula* Roth, *Carpinus betulus* L., *Castanea sativa* Mill., *Fagus sylvatica* L., *Fraxinus excelsior* L., *Fraxinus ornus* L., *Larix decidua* Mill., *Picea abies* (L.) H. Karst., *Pinus cembra* L., *Pinus nigra* J.F.Arnold, *Pinus sylvestris* L., *Populus tremula* L., *Prunus avium* L., *Quercus petraea* (Matt.) Liebl., *Quercus pubescens* Willd., *Quercus robur* L., *Robinia pseudoacacia* L., *Sorbus aucuparia* L. **Detalis on taxonomic reference system**: standard biologic taxonomy. **Ecological level**: species. **Biodiversity data source**: Piedmont Local Forest Inventory led by IPLA and EU-Forest (Mauri et al., 2017) for calibration, GBIF and LUCAS (EUROSTAT, 2017) for validation. **Sampling design**: uniform (IPLA LFI, EU-Forest AFI; LUCAS for validation) or unknown (GBIF for validation). We assumed the data position to be precise within the pixel dimension of 250 m. **Prevalence per taxon**: *Abies alba* Mill. (0.06/0.20), *Acer campestre* L. (0.02/0.04), *Acer pseudoplatanus* L. (0.09/0.09), *Alnus glutinosa* (L.) Gaertn. (0.02/0.02), *Betula pendula* Roth (0.03/0.04), *Carpinus betulus* L. (0.03/0.06), *Castanea sativa* Mill. (0.37/0.03), *Fagus sylvatica* L. (0.25/0.14), *Fraxinus excelsior* L. (0.14/0.02), *Fraxinus ornus* L. (0.05/0.01), *Larix decidua* Mill. (0.15/0.05), *Picea abies* (L.) H. Karst. (0.06/0.12), *Pinus cembra* L. (0.01/0.00), *Pinus nigra* J.F.Arnold (0.01/0.01), *Pinus sylvestris* L. (0.07/0.03), *Populus tremula* L. (0.04/0.00), *Prunus avium* L. (0.17/0.00), *Quercus petraea* (Matt.) Liebl. (0.13/0.01), *Quercus pubescens* Willd. (0.07/0.02), *Quercus robur* L. (0.09/0.00), *Robinia pseudoacacia* L. (0.20/0.00), *Sorbus aucuparia* L. (0.04/0.00). The first number indicates the prevalence in the LFI dataset, the second refers to the AFI (EU-Forest at the local extent).

	Country mask: rectangular bounding box for the Alpine Region (France, Italy, Switzerland, Luxembourg, Germany, Austria, Slovenia). Administrative box on Piedmont Region (Italy). **Data cleaning/filtering**: to overcome the uneven sampling intensity and point clustering, we thinned points using a custom function. A distance of 500 m was considered as the minimum distance between the points, to harmonize the sampling intensity between presence and absence data. **Potential biases**: spatial density of occurrence data varies within the study area and across different species for the EU-Forest dataset resulting in over- or under-represented areas. The spatial precision of point positioning could be low but we consider it to be <250m (pixel dimension).
Data partitioning	A 5-fold spatial cross validation was used to partition the data for model validation. Spatial partitioning of data followed a spatial blocking with a variable blocking factor based on the median of five ranges over which observations are independent. The ranges are determined by constructing empirical variograms for measuring spatial autocorrelation. When the range was > 15 000 m, we used 10 000 m as block-size dimension.

Predictor variables	**Predictor variables**: ▪ *Climate*: monthly mean, maximum, and minimum temperature and monthly precipitation and 19 bioclimatic variables. Monthly values were averaged over the time (1989-2013 for current, 2051-2070 for future). We compared two datasets; an Alpine Climate Dataset (ACD) from CHELSA v1.2 (Karger et al., 2017) for the Alpine space and a Local Climate Dataset (LCD) derived from the Very High Resolution (VHR) climate data derived from a dynamic downscaling through the Regional Circulation Model COSMO (Raffa et al., 2021) for Piedmont Region as part of the European project Highlander. ▪ *Topography*: mean and standard deviation of elevation, slope, heat load index, topographic position index, and topographic roughness index. ▪ *Soil*: pH and soil organic carbon between 0 and 15 cm depth. **Data sources**: ▪ *Climate*: time series of temperature and precipitation were downloaded from CHELSA v1.2 (https://chelsa-climate.org/downloads/). Bioclimatic variables were derived from these predictors. COSMO-CLM data are available in the Highlander project portal (https://dds-dev.highlander.cineca.it/app/datasets). ▪ *Topography*: elevation was downloaded from the spaceborn improved-terrain MERIT DEM (https://hydro.iis.u-tokyo.ac.jp/~yamadai/MERIT_DEM/). All the other topographic variables were derived from elevation (DEM). ▪ *Soil*: soil variables were downloaded from the SoilGrids250m v2.0 (https://soilgrids.org/). **Spatial resolution of raw data**: the original resolution of topography was 3" (~90 m at 45° of latitude). The original resolution of the ACD was 1 km. The original resolution of the LCD data was 0.02° (~1.8 km at 45° of latitude). Soil variables were available at 250-m resolution.

	Map projection: all layers were reprojected in EPSG:3035 coordinate reference system. **Temporal resolution and extent of raw data:** current climate referred to 1989-2013, future climate referred to 2051-2070. We used average monthly values and derived annual and seasonal bioclimatic variables. We considered topography and soil to be stable variables over long-term. **Data preprocessing:** all data were resampled to 250 m to match the spatial resolution of the LFI grid. **Dimension reduction:** we used variance inflation factor (VIF) and Pearson's correlation to reduce the number of variables and their multicollinearity.
Transfer data for projection	**Scenarios**: we projected future presence probability under two IPCC's scenarios; RCP4.5 and RCP8.5.
MODEL	
Variable pre-selection Multicollinearity	We reduced the number of initial variables through a variable pre-selection based on the correlation between variables and the variance inflation factor (VIF) through the function `vifcor` of the package `usdm` (Naimi et al., 2014). The function first pairs variables with a linear correlation higher than a pre-selected threshold and excludes the one with a greater VIF. The procedure is iterated until no pair of variables with a high correlation remains. We used Pearson's as correlation method and 0.9 as coefficient. Our aim was to avoid highly correlated variables and speed-up the computation time even if BART is considered to be robust against multicollinearity.
Model settings	We used BARTs with default settings of the `embarcadero` package; in particular, 200 trees, 1000 posterior draws, 100 Markov Chain Monte Carlo iterations, 100 possible values used in decision rules.
Model estimates	Variable importance (vimp) was calculated.
Non-indipendence correction/analyses	Spatial autocorrelation was considered when calculating the accuracy through the 5-fold spatial block cross validation procedure, using the mean range of spatial autocorrelation as block-size dimension. When the range was > 15 000 m, we used 10 000 m as block-size dimension. We assessed

	spatial autocorrelation using automatic variograms fitted through the R package automap (Hiemstra et al., 2009).
Threshold selection	We converted continuous probability maps into binary maps. We derived the binary maps using the value that maximized the TSS as threshold. We tested three different widely applied thresholds; minimum training presence (MTP, sometimes also called lowest presence threshold), 10th percentile of the predicted values (P10), and maximum of TSS (maxTSS). From an ecological perspective, we considered MTP to be too permissive, and presences were too widely distributed. Comparing the P10 and maxTSS approach, we observed a high degree of similarity between the two, and we selected the latter since it is considered the most conservative approach (Hintze et al., 2021).
ASSESSMENT	
Performance statistics	Performance was assessed by accuracy and calibration both on validation data using a 5-fold spatial block cross validation with the mean range of spatial autocorrelation as block-size dimension and on truly independent data derived from GBIF and LUCAS. We used a rectangular bounding box for the spatial extent of independent data to include points just outside the administrative Piemonte Region and evaluate the applicability and transferability of the models outside the calibration area. We analyzed and tested different accuracy metrics to compare biodiversity and climate data. We employed both threshold-dependent (TSS, Specificity, Sensitivity) and -independent (AUC) metrics. We used the threshold that maximized the TSS as threshold. We used Pearson's correlation (COR) to test for calibration and generalizability.
Plausibility check	We compared the maps resulting from our models with distribution maps from European Atlas of Forest Tree Species. We also used variable importance plots (vimps) to check the plausibility of the predictions.

PREDICTION	
Prediction output	**Prediction unit**: we derived continuous probability, uncertainty, and binary maps. **Post-processing steps**: we used Corine Land Cover (CLC) to mask unvegetated areas (i.e., urban areas, rocks and water).
Uncertainty quantification	Uncertainty maps derived based on the 5th and 95th percentile of the probability distribution obtained through the Bayesian approach.

TABLE A4.2. List of R packages used in the analysis with citations.

Package name	Version	Citation	Purpose
ade4	v1.7-22	Dray & Dufour, 2007	Perform PCA
automap	v1.1-9	Hiemstra et al., 2008	Creation of variograms
blockCV	v3.1-3	Valavi et al., 2019	Spatial block cross-validation
corrplot	v0.92	Wei et al., 2017	Creation of correlograms
doParallel	v1.0.17	Corporation & Weston, 2022	Parallelization of multiple tasks
embarcadero	v1.2.0	Carlson, 2020	Training of BART's SDMs
emmeans	v1.8.7	Lenth, 2023	Compute joint tests of models and perform *post-hoc*
fitdistrplus	v1.1-11	Delignette-Muller & Dutang, 2015	Test and assess distributions of models performance metrics
foreach	v1.5.2	Microsoft & Weston, 2022	Parallelization of multiple tasks
GenAlgo	v2.2.0	Coombes, 2020	Compute Mahalanobis distance between vectors
ggplot2	v3.4.3	Wickham, 2016	Creation of graphs
ggradar	v0.2	Bion, 2023	Creation of radar plots
ggridges	v0.5.4	Wilke, 2022	Creation of ridgeline plots
lme4	v1.1-34	Bates et al., 2014	Fit generalized linear mixed-effects model on models performance
modEvA	v3.82	Barbosa et al., 2013	Models accuracy assessment

overlap	v0.3.4	Ridout & Linkie, 2009	Calculate the coefficient of overlapping between two distributions
raster	v3.6-23	Hijmans, 2023	Manipulation of spatial raster data
sf	v1.0-8	Pebesma & Bivand, 2023	Manipulation of spatial vector data
terra	v1.7-39	Hijmans, 2023	Manipulation of spatial raster data
tidyverse	v1.3.1	Wickham et al., 2019	Manipulation of data
tmap	v3.3-2	Tennekes, 2018	Creation of maps
usdm	v2.1-6	Naimi et al., 2014	Variable selection based on VIF

TABLE A4.3. List of the 19 bioclimatic predictors calculated for the LCD and ACD.

Code	Meaning	Formula
bio_01	Annual mean temperature	-
bio_02	Mean diurnal range	Mean of monthly (max temp - min temp)
bio_03	Isothermality	(bio_02/bio_07) * 100
bio_04	Temperature seasonality	Standard deviation of monthly mean temp. * 100
bio_05	Maximum temperature of the warmest month	-
bio_06	Minimum temperature of the coldest month	-
bio_07	Temperature annual range	bio_05 – bio_06
bio_08	Mean temperature of the wettest quarter	-
bio_09	Mean temperature of the driest quarter	-
bio_10	Mean temperature of the warmest quarter	-
bio_11	Mean temperature of the coldest quarter	-
bio_12	Annual precipitation	-
bio_13	Precipitation of the wettest month	-
bio_14	Precipitation of the driest month	-

bio_15	Precipitation seasonality	Coefficient of variation of monthly precipitation
bio_16	Precipitation of the wettest quarter	-
bio_17	Precipitation of the driest quarter	-
bio_18	Precipitation of the warmest quarter	-
bio_19	Precipitation of the coldest quarter	-

Appendix A4 – References.

Baquero, R. A., Barbosa, A. M., Ayllón, D., Guerra, C., Sánchez, E., Araújo, M. B., & Nicola, G. (2021). Potential distributions of invasive vertebrates in the Iberian Peninsula under projected changes in climate extreme events. *Diversity and Distributions*, 27(11), 2262-2276.

Barbosa, A. M., Real, R., Muñoz, A. R., & Brown, J. A. (2013). New measures for assessing model equilibrium and prediction mismatch in species distribution models. *Diversity and Distributions*, 19(10), 1333-1338.

Barbosa, A. M., Brown, J., Jiménez-Valverde, A., & Real, R. (2016). `modEvA`: model evaluation and analysis.

Bates, D., Mächler, M., Bolker, B., & Walker, S. (2014). Fitting linear mixed-effects models using `lme4`. *arXiv preprint arXiv*:1406.5823.

Bion, R. (2023). `ggradar`: Create radar charts using ggplot2. R package version 0.2.

Carlson, C. J. (2020). `embarcadero`: Species distribution modelling with Bayesian additive regression trees in r. *Methods in Ecology and Evolution*, *11*(7), 850-858.

Coombes, K. R. (2020). `GenAlgo`: Classes and Methods to Use Genetic Algorithms for Feature Selection. R package version 2.2.0.

Corporation, M., & Weston, S. (2022). `doParallel`: Foreach Parallel Adaptor for the `parallel` Package. R package version 1.0.17.

Delignette-Muller, M. L., & Dutang, C. (2015). `fitdistrplus`: An R package for fitting distributions. *Journal of statistical software*, 64, 1-34.

Dray, S., Dufour, A. (2007). The `ade4` Package: Implementing the Duality Diagram for Ecologists. *Journal of Statistical Software*, 22(4), 1–20.

Hiemstra, P. H., Pebesma, E. J., Twenhöfel, C. J., & Heuvelink, G. B. (2009). Real-time automatic interpolation of ambient gamma dose rates from the Dutch radioactivity monitoring network. *Computers & Geosciences*, *35*(8), 1711-1721.

Hijmans, R. (2023). `raster`: Geographic Data Analysis and Modeling. R package version 3.6-23.

Hijmans R (2023). `terra`: Spatial Data Analysis. R package version 1.7-39.

Hintze, F., Machado, R. B., & Bernard, E. (2021). Bioacoustics for in situ validation of species distribution modelling: An example with bats in Brazil. *PLOS ONE*, *16*(10), e0248797.

Karger, D. N., Conrad, O., Böhner, J., Kawohl, T., Kreft, H., Soria-Auza, R. W., Zimmermann, N. E., Linder, H. P., & Kessler, M. (2017). Climatologies at high resolution for the earth's land surface areas. *Scientific Data*, 4(1).

Lenth, R. (2023). `emmeans`: Estimated Marginal Means, aka Least-Squares Means. R package version 1.8.7.

Mauri, A., Strona, G., & San-Miguel-Ayanz, J. (2017). EU-Forest, a high-resolution tree occurrence dataset for Europe. *Scientific Data*, 4(1).

Microsoft, & Weston, S. (2022). `foreach`: Provides Foreach Looping Construct. R package version 1.5.2.

Naimi, B., & Araújo, M. B. (2016). `sdm`: a reproducible and extensible R platform for species distribution modelling. *Ecography*, 39(4), 368-375.

Naimi, B., Hamm, N. A., Groen, T. A., Skidmore, A. K., & Toxopeus, A. G. (2014). Where is positional uncertainty a problem for species distribution modelling? *Ecography*, 37(2), 191-203.

Pebesma, E., & Bivand, R. (2023). *Spatial Data Science: With Applications in R*. Chapman and Hall/CRC.

Raffa, M., Reder, A., Marras, G.F., Mancini, M., Scipione, G., Santini, M., & Mercogliano, P. 2021. VHR-REA_IT Dataset: Very High Resolution Dynamical Downscaling of ERA5 Reanalysis over Italy by COSMO-CLM. *Scientific Data*, 6, 88.

R Core Team (2023). R: A language and environment for statistical computing. R Foundation for Statistical Computing, Vienna, Austria.

Ridout, M. S., & Linkie, M. (2009). Estimating overlap of daily activity patterns from camera trap data. *Journal of Agricultural, Biological, and Environmental Statistics*, 14, 322-337.

Valavi, R., Elith, J., Lahoz-Monfort, J. J., & Guillera-Arroita, G. (2018). `blockCV`: An r package for generating spatially or environmentally separated folds for k-fold cross-validation of species distribution models. *Biorxiv*, 357798.

Wei, T., Simko, V., Levy, M., Xie, Y., Jin, Y., & Zemla, J. (2017). Package `corrplot`. *Statistician*, 56(316), e24.

Wickham, H. (2016). `ggplot2`: Elegant Graphics for Data Analysis. *Springer-Verlag New York*.

Wickham, H., Averick, M., Bryan, J., Chang, W., McGowan, L. D., François, R., ... & Yutani, H. (2019). Welcome to the `tidyverse`. *Journal of Open Source Software*, 4 (43), 1686 (2019).

Wilke, C. (2022). `ggridges`: Ridgeline Plots in `ggplot2`. R package version 0.5.4.

Appendix B4 – Supplementary Results

The Appendix B4 contains information about predictors (Figures B4.1 and B4.2 about future climate, Figures B4.3 to B4.5 show variograms about the spatial autocorrelation of the selected predictors) and model outputs. Table B4.1 contains information about the GLMM outputs on cross-validation and independent model performance to assess differences among frameworks and species and climate data. Reliability is reported both in terms of visual comparison to different data sources (Figures B4.6 to B4.8) and relative variable importance (Figures B4.9 to B4.11). Figures B4.12 to B4.14 show current and future (RCP 4.5 and RCP 8.5) probability of occurrence for the species not reported in the main text. Finally, Figure B4.15 reports boxplots of change in probability of occurrence for the species not reported in the main text.

TABLE B4.1. Transformation, family, and p-values resulting from the GLMM models for the comparison of performance metrics (AUC, TSS, F1, and Pearson's correlation) according to species data (local vs broad inventory), climate data (local vs broad climate), and a combination of the two (frameworks, n = 5).

Cross-validation					
Metric	**Grouping factor**	**Transformation**	**Family**	***p-value***	
AUC	framework	none	Gamma	**0.004**	**
	species data	-	-	**0.002**	**
	climate data	-	-	0.900	ns
TSS	framework	none	Gaussian	0.998	ns
	species data	-	-	0.761	ns
	climate data	-	-	0.959	ns
F1	framework	logarithmic	Gamma	**<0.001**	***
	species data	-	-	**<0.001**	***
	climate data	-	-	0.299	ns
COR	framework	none	Gaussian	**<0.001**	***
	species data	-	-	**<0.001**	***
	climate data	-	-	0.397	ns
Independent validation					
Metric	**Grouping factor**	**Transformation**	**Family**	***p-value***	
AUC	framework	square root	Gaussian	**0.023**	*
	species data	-	-	**0.003**	**
	climate data	-	-	0.200	ns
TSS	framework	square root	Gaussian	0.451	ns
	species data	-	-	0.133	ns
	climate data	-	-	0.691	ns
F1	framework	logarithmic	Gaussian(log)	0.446	ns
	species data	-	-	0.121	ns
	climate data	-	-	0.962	ns
COR	framework	logarithmic	Gaussian	0.371	ns
	species data	-	-	0.050	ns
	climate data	-	-	0.781	ns

TABLE B4.2. Correlation between spatial predictions for current, RCP 4.5, and RCP 8.5 scenarios between the fine-scale and the coarse-scale models.

	Pearson correlation		
Species	**Current**	**RCP 4.5**	**RCP 8.5**
Silver fir	0.57	0.51	0.44
Black alder	0.55	0.61	0.53
Sycamore	0.50	0.24	0.21
Field maple	0.29	0.42	0.44
European birch	0.50	0.49	0.56
European hornbeam	0.73	0.63	0.60
Sweet chestnut	0.73	0.47	0.61
European ash	0.19	0.40	0.39
Manna ash	0.61	0.78	0.82
European beech	0.83	0.65	0.69
European larch	0.88	0.88	0.89
Norway spruce	0.64	0.50	0.49
Swiss stone pine	0.38	0.64	0.63
Black pine	0.18	0.31	0.39
Scots pine	0.51	0.29	0.22
Common aspen	0.23	0.08	0.12
Wild cherry	0.26	0.21	0.25
Pedunculate oak	0.67	0.60	0.70
Downy oak	0.27	0.36	0.31
Sessile oak	0.06	0.04	-0.01
Black locust	0.78	0.70	0.72
Rowan	0.24	0.39	0.48

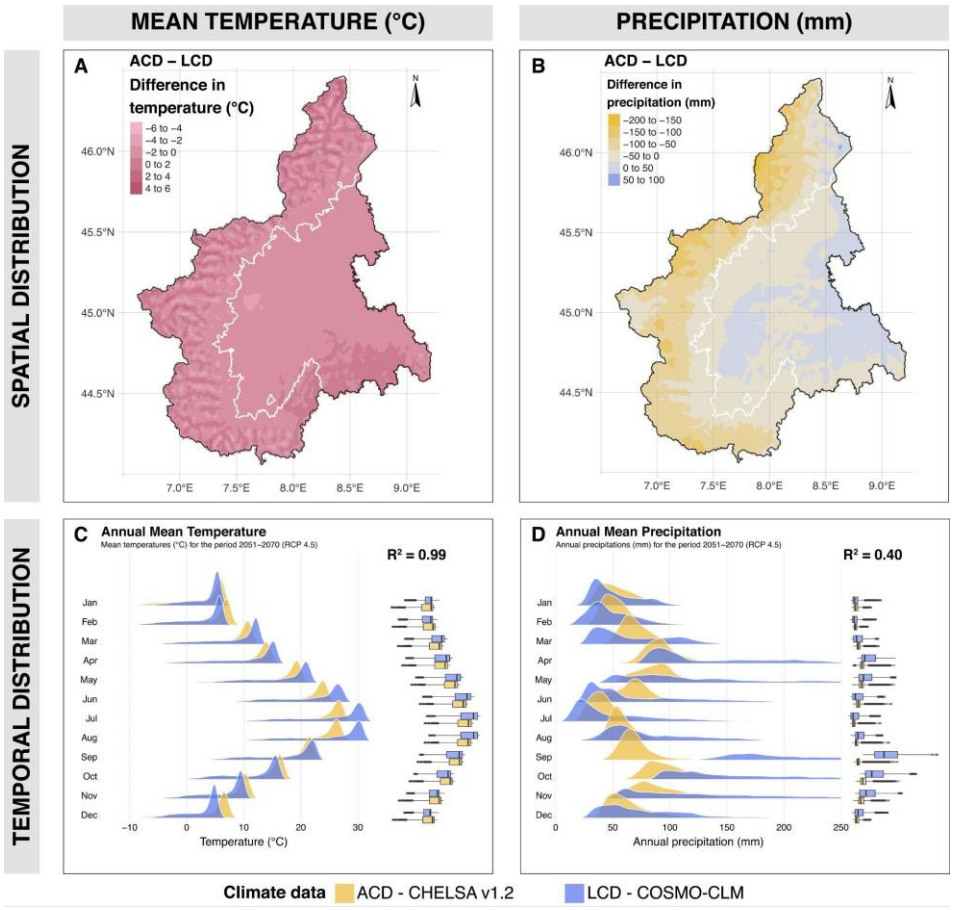

FIGURE B4.1. Spatial (a, b) and temporal (c, d) distribution of mean temperature (a, c) and precipitation (b, d) of the two climate datasets (LCD = COSMO-CLM and ACD = CHELSA v1.2) for the period 2051-2070 under the RCP4.5 scenario.

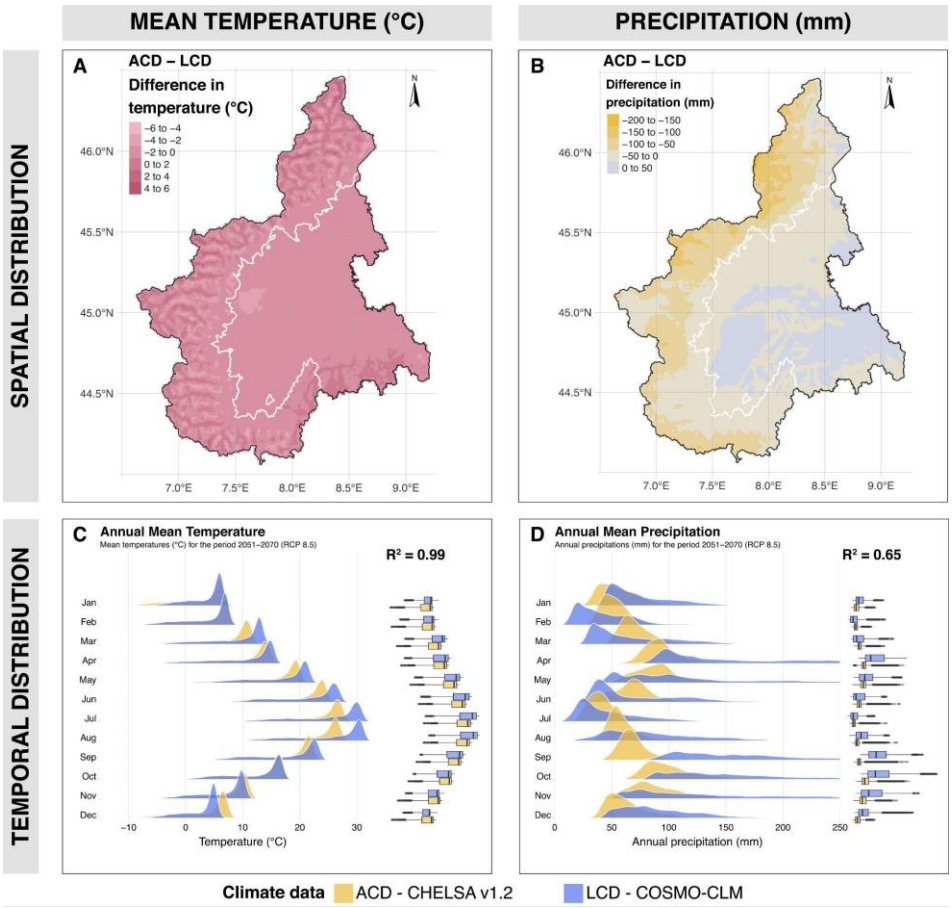

FIGURE B4.2. Spatial (a, b) and temporal (c, d) distribution of mean temperature (a, c) and precipitation (b, d) of the two climate datasets (LCD = COSMO-CLM and ACD = CHELSA v1.2) for the period 2051-2070 under the RCP8.5 scenario.

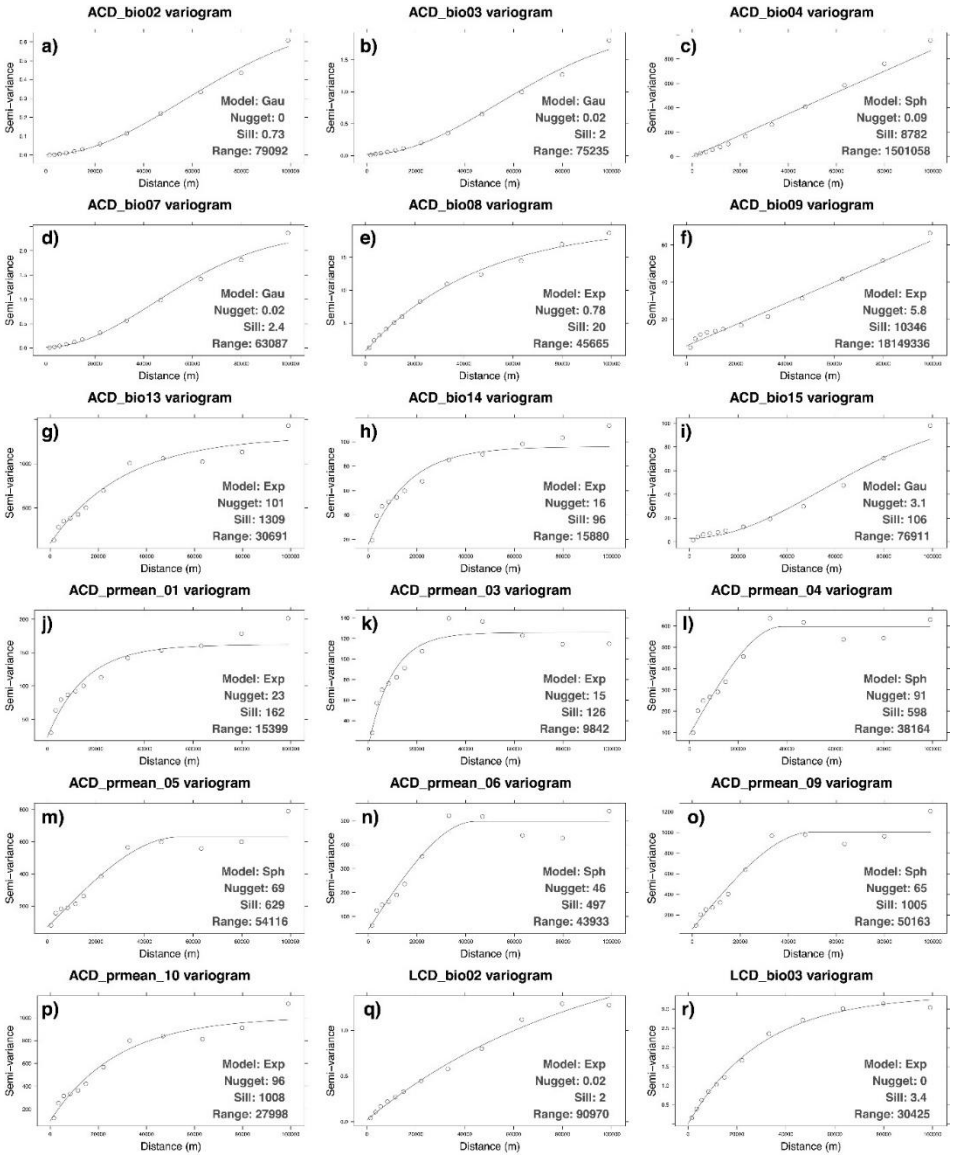

FIGURE B4.3. Experimental and fitted model variograms for 18 variables. a) to i) selected bioclimatic variables for the ACD; j) to p) precipitation for the selected months for the ACD; q) and r) the first two selected bioclimatic variables for the LCD.

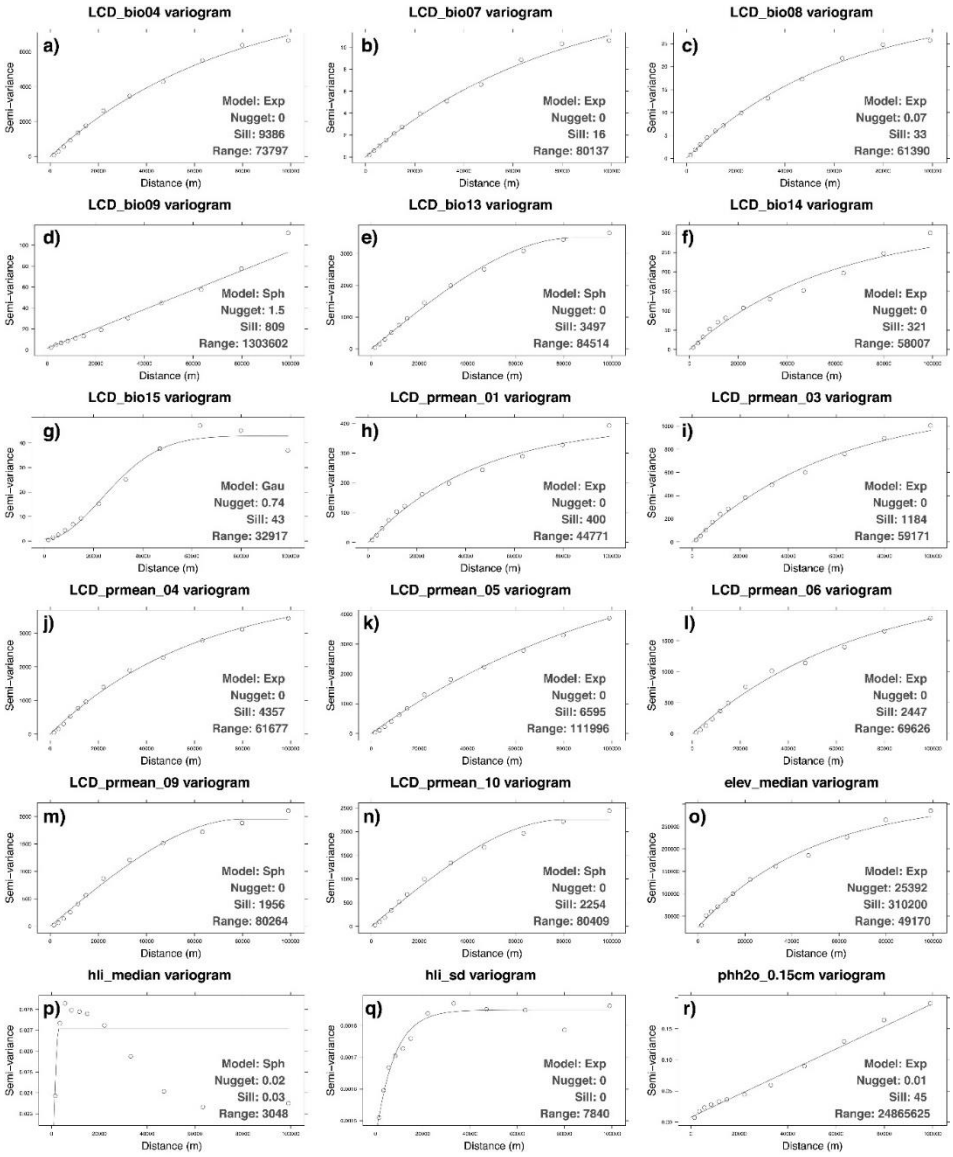

FIGURE B4.4. Experimental and fitted model variograms for 18 variables. a) to g) remaining selected bioclimatic variables for the ACD; h) to n) precipitation for the selected months for the ACD; o) median elevation; p) and q) median and standard deviation of the HLI; r) soil pH.

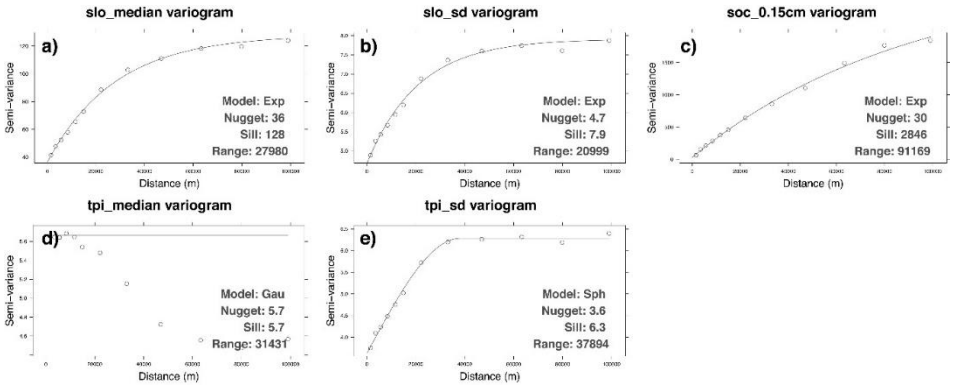

FIGURE B4.5. Experimental and fitted model variograms for 18 variables. a) and b) median and standard deviation of slope; c) soil organic Carbon; d) and e) median and standard deviation of TPI.

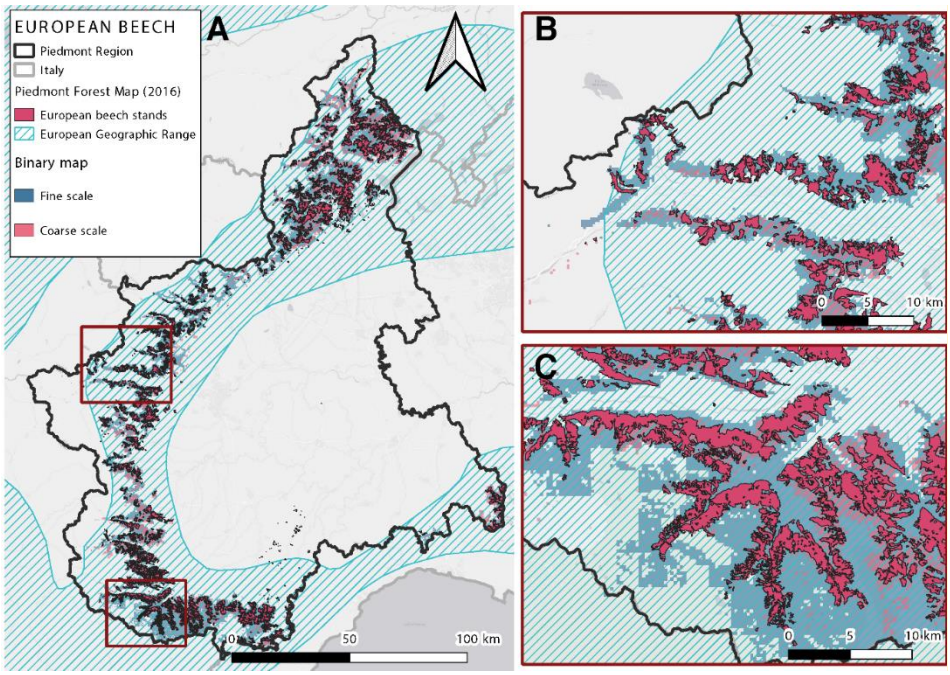

FIGURE B4.6. Comparison between the current potential suitable range of European beech Fagus sylvatica expressed by the two scales (Fine = local species data + local climate in blue and coarse scale = broad species data + broad climate at the extent of the Alpine region in red). The two outputs were compared to the Piedmont Forest Map of 2016 (filtered only for the selected forest type) and the geographic range for Europe derived from Caudullo et al. (2017). Panel (a) shows an overlook of the entire administrative area, panels (b) and (c) show two closeups corresponding to the (b) Northern and (c) rectangular red boxes in panel (a).

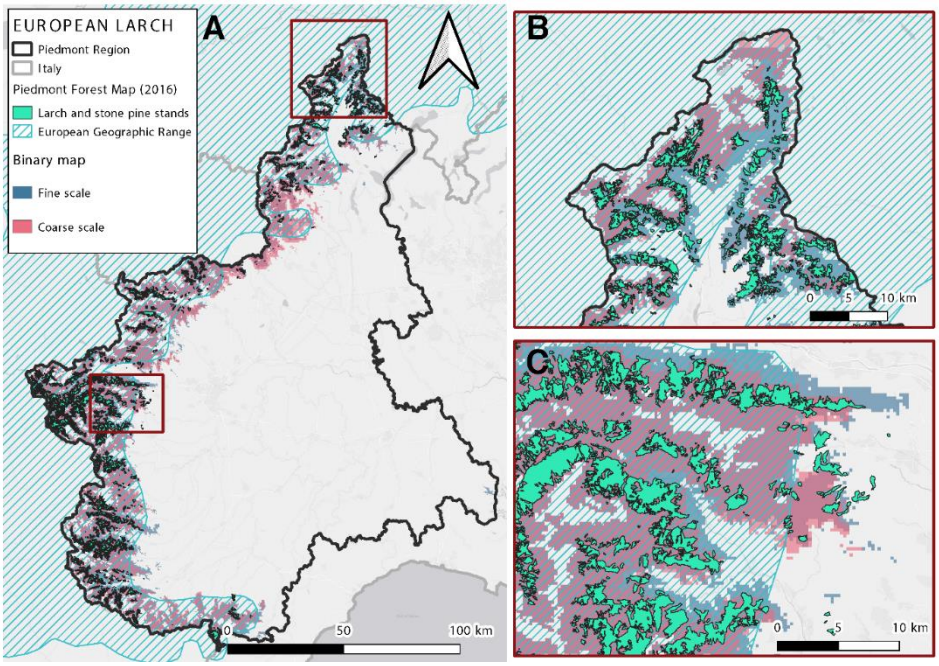

FIGURE B4.7. Comparison between the current potential suitable range of European larch Larix decidua expressed by the two scales (Fine = local species data + local climate in blue and coarse scale = broad species data + broad climate at the extent of the Alpine region in red). The two outputs were compared to the Piedmont Forest Map of 2016 (filtered only for the selected forest type) and the geographic range for Europe derived from Caudullo et al. (2017). Panel (a) shows an overlook of the entire administrative area, panels (b) and (c) show two closeups corresponding to the (b) Northern and (c) rectangular red boxes in panel (a).

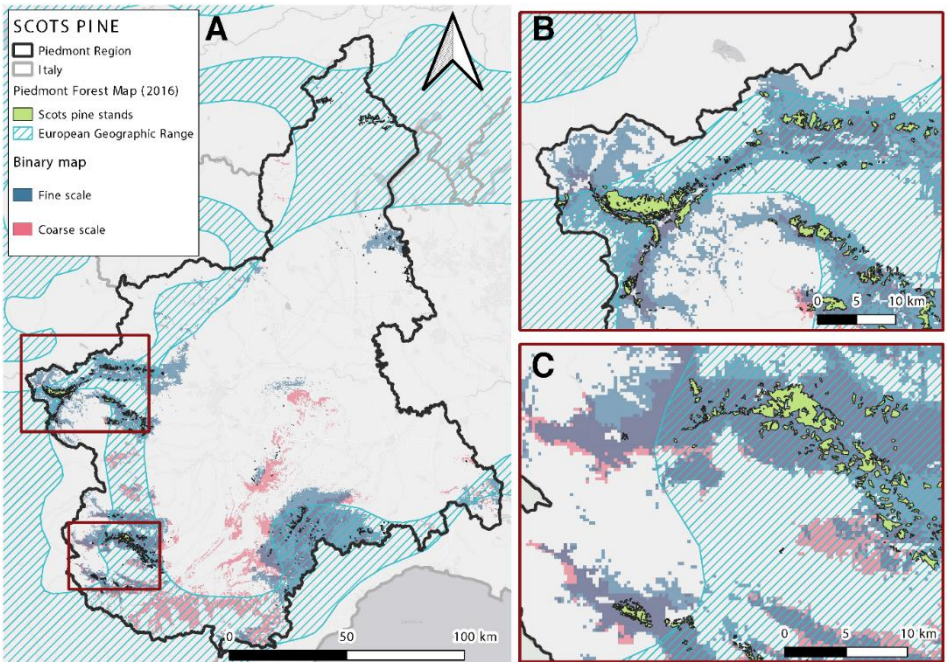

FIGURE B4.8. Comparison between the current potential suitable range of Scots pine Pinus sylvestris expressed by the two scales (Fine = local species data + local climate in blue and coarse scale = broad species data + broad climate at the extent of the Alpine region in red). The two outputs were compared to the Piedmont Forest Map of 2016 (filtered only for the selected forest type) and the geographic range for Europe derived from Caudullo et al. (2017). Panel (a) shows an overlook of the entire administrative area, panels (b) and (c) show two closeups corresponding to the (b) Northern and (c) rectangular red boxes in panel (a).

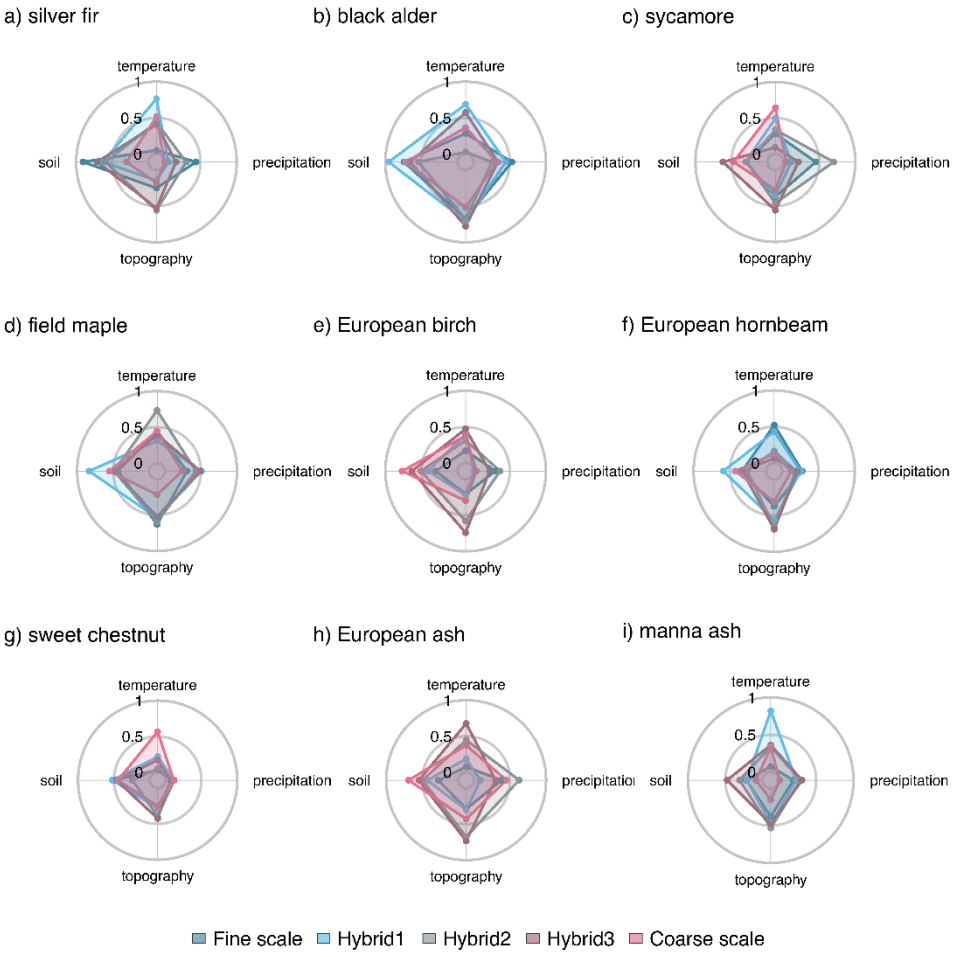

FIGURE B4.9. Radar plots of the relative variable importance for each species. Variables were grouped into four groups (Table 4.2) using the mean value of the relative importance of the different variables.

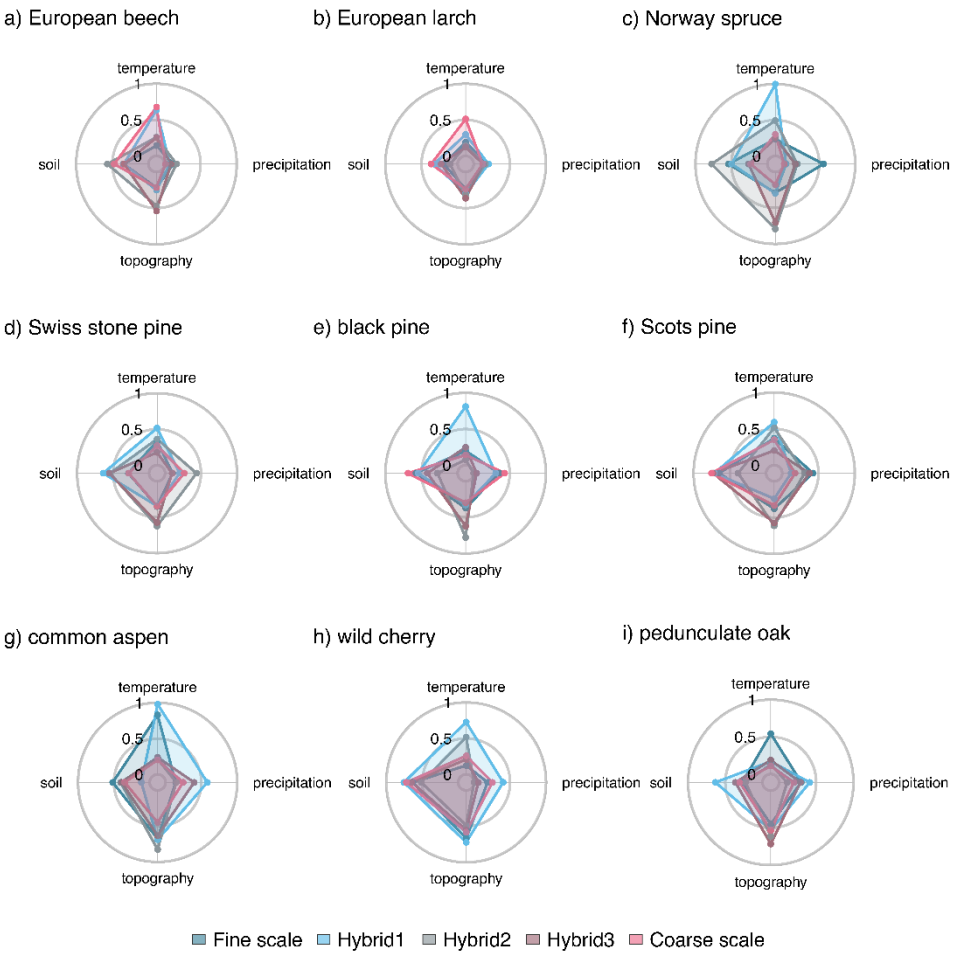

FIGURE B4.10. Radar plots of the relative variable importance for each species. Variables were grouped into four groups (Table 4.2) using the mean value of the relative importance of the different variables.

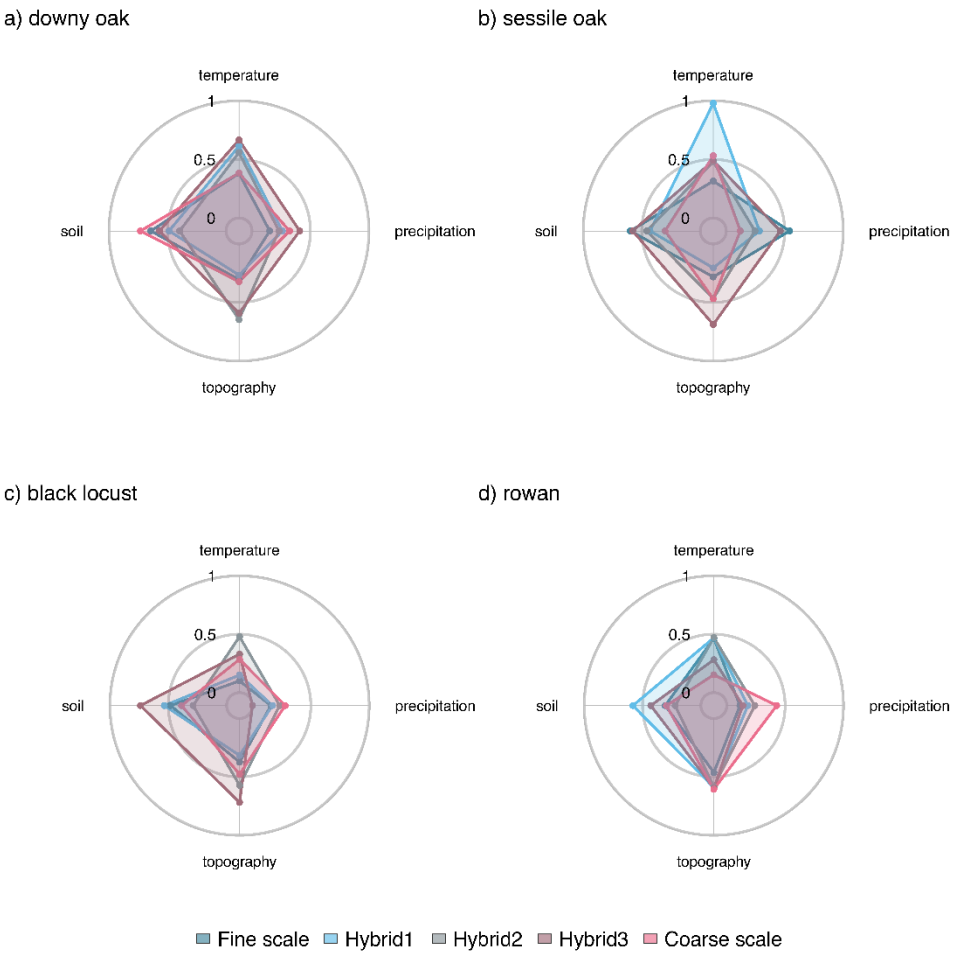

FIGURE B4.11. Radar plots of the relative variable importance for each species. Variables were grouped into four groups (Table 4.2) using the mean value of the relative importance of the different variables.

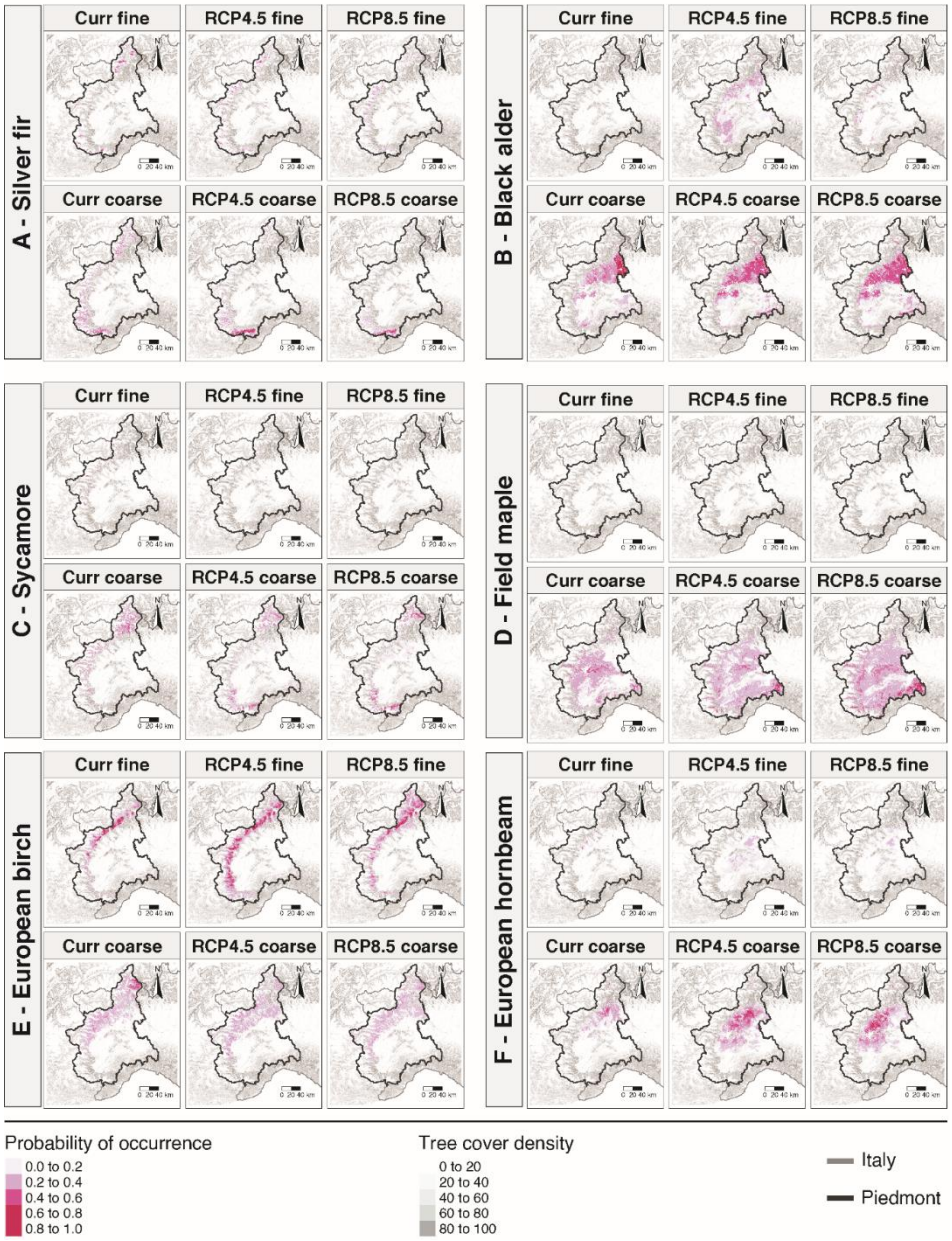

FIGURE B4.12. Probability of presence of six species (silver fir, black alder, sycamore, field maple, European birch, and European hornbeam) for current and future (RCP 4.5 and RCP 8.5) scenarios for fine-scale (local species data + local climate, upper rows) and coarse-scale (broad species data + broad climate at the alpine extent, lower rows) models.

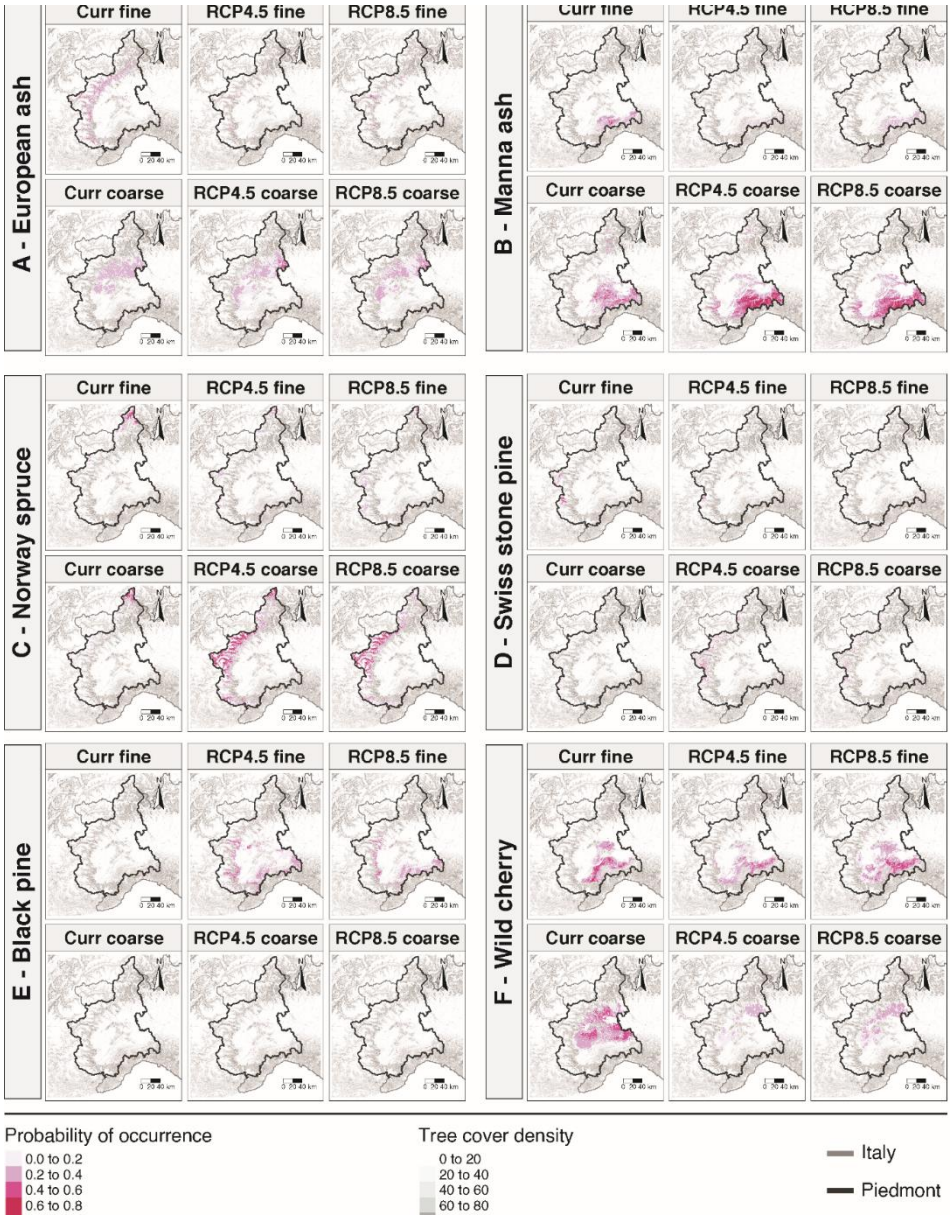

FIGURE B4.13. Probability of presence of six species (European ash, manna ash, Norway spruce, Swiss stone pine, black pine, and wild cherry) for current and future (RCP 4.5 and RCP 8.5) scenarios for fine-scale (local species data + local climate, upper rows) and coarse-scale (broad species data + broad climate at the alpine extent, lower rows) models.

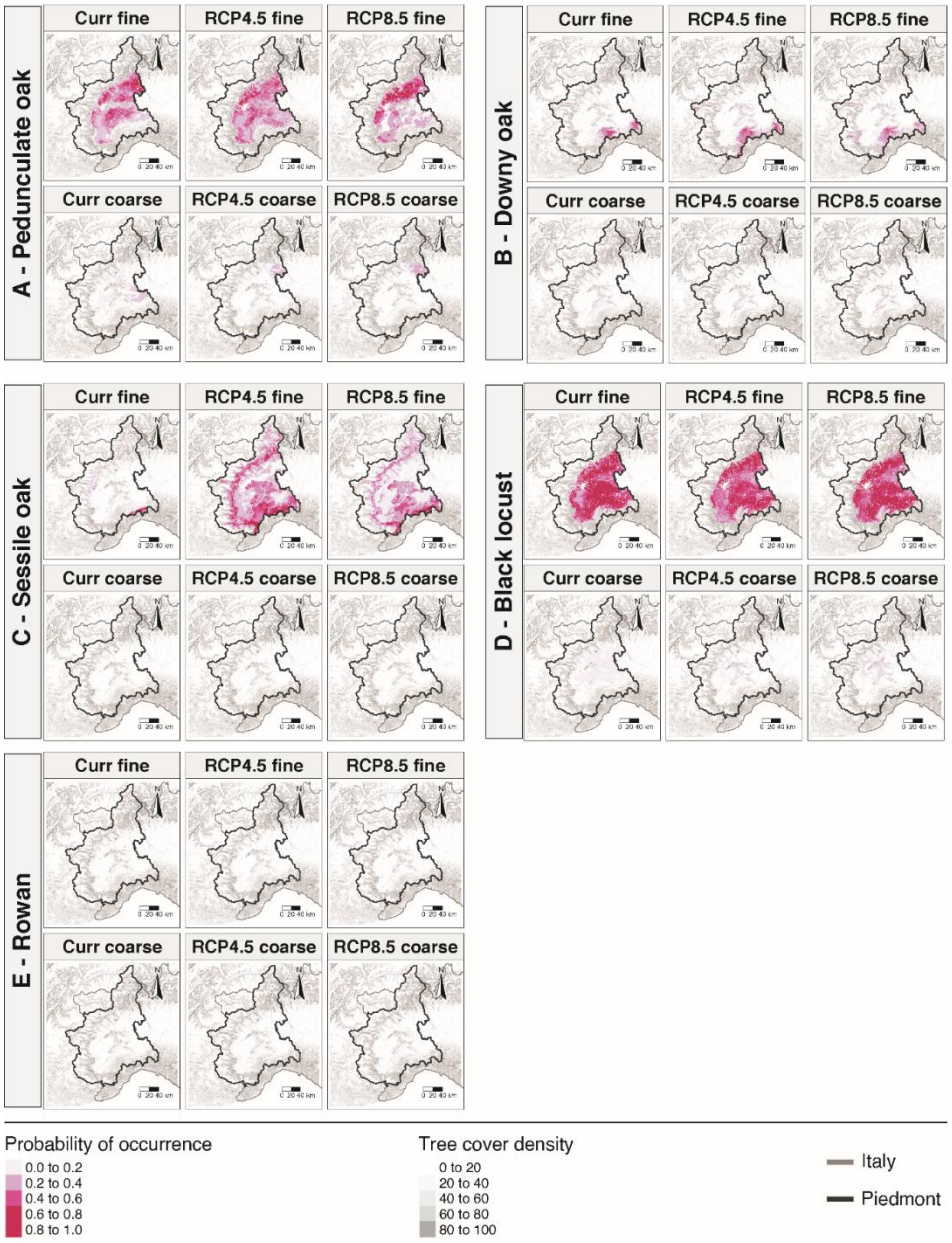

FIGURE B4.14. Probability of presence of five species (pedunculate, downy, and sessile oak, black locust, and rowan) for current and future (RCP 4.5 and RCP 8.5) scenarios for fine-scale (local species data + local climate, upper rows) and coarse-scale (broad species data + broad climate at the alpine extent, lower rows) models.

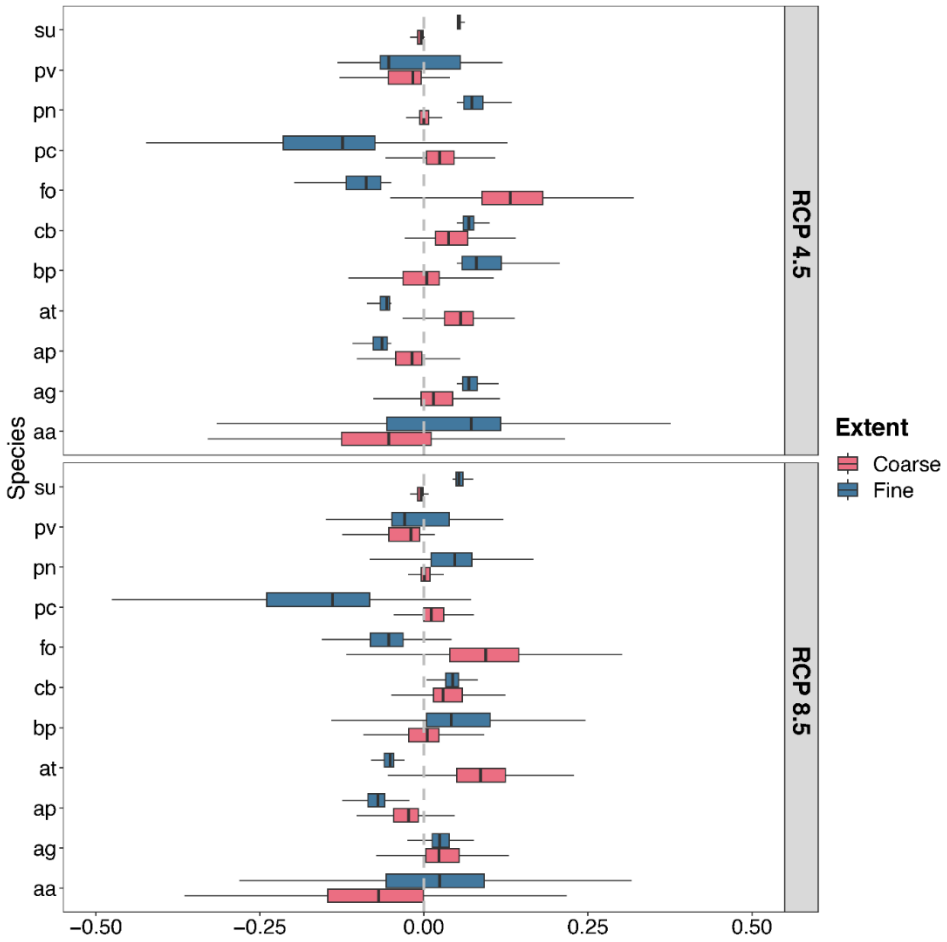

FIGURE B4.15. Boxplots representing the suitability change of nine species according to the two climate scenarios (RCP 4.5 and RCP 8.5) and the input dataset (fine = local species data + local climate, coarse = broad species data + broad climate at the extent of the Alps). aa = silver fir, ag = black alder, ap = sycamore, at = field maple, bp = European birch, cb = European hornbeam, fo = manna ash, pc = Swiss stone pine, pn = black pine, pt = Common aspen, pv = wild cherry, su = rowan.

Appendix B – References.

Caudullo, G., Welk, E., & San-Miguel-Ayanz, J. (2017). Chorological maps for the main European woody species. *Data in Brief*, 12, 662-666.

Chapter 5

Long-term data and temporal dynamic frameworks can improve landscape-scale species distribution models

Nicolò Anselmetto, Matteo Garbarino, David Bell, Christopher Daly, Clinton W. Epps, Hankyu Kim, Damon Lesmeister, Taal Levi, Joe LaManna, Brooke Penaluna, Mark Schulze, Marie I. Tosa, Matthew J. Weldy, Matthew G. Betts

This paper has been submitted to the *Ecography* journal.

Abstract

Species Distribution Models (SDMs) are among the most employed statistical models in conservation biology, global change assessment, and spatial prioritization. It is common to model heterogeneity in the data with coarse scale temporal macroclimate, which fails to represent conditions at an individual scale but neglects the thermal conditions experienced by most organisms. Further, most SDMs use occurrence data from short-term studies but make long-term predictions to future conditions implying stationarity in the environmental conditions. Our aim was to compare four modeling frameworks that varied the temporal extent (short term [1 year] versus long term [10 years]) and resolution of occurrence and microclimate data. We expected that long-term data and fine-resolution models should provide more accurate model predictions because they integrate variability in population sizes under varying conditions.

We used a 10-year (2010-2019) time series of annual bird observations across 184 plots in the H.J. Andrews Experimental Forest, Cascade Range, Oregon (USA) to construct response variables, and gridded maps of microclimate temperatures of below-canopy hourly data and LiDAR-derived vegetation variables as predictors. We evaluated each model through a temporal leave-one-

out cross-validation to assess model performance and tested for differences in model performance as function of the modeling scenarios and functional traits of the species.

Temporally dynamic (long-term) models with higher resolution outperformed short-term approaches both in terms of accuracy and calibration. Model performance and similarity between spatial predictions were higher for migratory species than for sedentary and partially migratory species. Models for small bird species performed better as the temporal resolution increased, whereas for long-lived species with larger body sizes dynamic approaches yielded no or little improvement. We advocate for increasing the temporal range of response and predictor variables in SDMs to boost accuracy and reliability of landscape-scale species distributions, especially when dealing with highly mobile and short-lived organisms.

Keywords: species distribution models, birds distribution, old-growth forests, long-term observations, microclimate, temporal resolution.

5.1 Introduction

Species Distribution Models (SDMs) have emerged as indispensable tools in ecological research, finding widespread applications in conservation biology (Guisan et al., 2013; Bai et al., 2020; Zurell et al., 2022), global change assessment (Bellard et al., 2013; Dyderski et al., 2018; Newbold et al., 2020), and spatial prioritization (Carroll et al., 2010; Adams et al., 2012; Bicknell et al., 2017), growing rapidly in popularity over the past two decades (Zurell et al., 2020, 2022). While SDMs have provided valuable insights into the potential impacts of climate change and the identification of critical conservation areas, they have mainly operated at a coarse spatiotemporal scale (Araújo et al., 2019). Most of SDMs are trained at broad spatial and temporal extent, primarily associated with free-air climatic datasets with a resolution of 30 arc seconds, such as the widely used WorldClim (Fick & Hijmans, 2017) and CHELSA (Karger et al., 2017). Indeed, these models have frequently overlooked the finer details of

ecological dynamics, particularly in terms of temporal and spatial resolution. From a spatial perspective, most SDMs operate at a broad scale. Global-scale models are usually used to delimitate and characterize biomes (e.g., Moonlight et al., 2020) or assess global patterns of species occurrence and abundance (e.g., Newbold et al., 2020), while regional-scale models focus on the climatic distribution of individual species (e.g., Hermosilla et al., 2022). However, conservation initiatives often necessitate a more nuanced approach that operates dynamically at the landscape scale (Guisan et al., 2013; Mateo et al., 2019). Indeed, since models may not match the scale of the problem, only 1-5% of correlative SDM studies produced clear management decisions (Guisan et al., 2013; Araújo et al., 2019).

Microclimate is an emerging topic with recently increasing popularity in ecological analyses. Recent studies have emphasized the need of including microclimatic data in SDMs, as neglecting this crucial factor can lead to overestimates of the effects of global changes across various spatial scales (Lenoir et al., 2017; Lembrechts et al., 2019; Haesen et al., 2023; Maclean & Early, 2023). Haesen et al. (2023) demonstrated the benefits of integrating microclimatic data into SDMs for plant species across Europe. Indeed, the effect of forest cover and topography can buffer or even decouple microclimates from free-air climate conditions (De Frenne et al., 2021; Lembrechts, 2023). In old-growth mountain forests, characterized by complex forest structures and topography, the abiotic conditions experienced by organisms can differ extremely from above-canopy conditions and can show strong gradients within a short distance (Frey et al., 2016; Wolf et al., 2021; Máliš et al., 2023). Distributions of long-living static organisms such as trees depend more on longer term patterns of air temperature, and adults can persist outside their optimal climatic niche for many years, but success during critical life history phases such as seedling establishment is strongly influenced by inter- and even intra-annual shifts in microclimate (Lembrechts et al., 2019). Conversely, animals have the potential to buffer their environment through movement. In general, larger organisms tend

to have broader environmental ranges and, consequently, a greater capacity to buffer their environment. This capacity is contingent on the conditions offered by their habitat (e.g., Pincebourde & Casas, 2019). Small animals, on the other hand, often operate within more confined ecological niches.

Conventional SDMs are typically static in time, integrating species occurrence and environmental variables that are either a single frame in time (low temporal extent) or an average of several annual or seasonal conditions (coarse temporal resolution) (Milanesi et al., 2020). By doing that, these models struggle to capture the temporal variability of ecological systems, such as inter- or intra-annual climate fluctuations or shifts in resource availability, assuming equilibrium and predicting stationarity (Milanesi et al., 2020; Zurell et al., 2022). Nevertheless, mobile species, particularly birds and mammals, often exhibit significant year-to-year variations in their distribution patterns because they can cope with those temporal fluctuations, especially at the landscape scale (Chávez-González et al., 2020). This dynamism necessitates a shift towards dynamic landscape-scale SDMs that incorporate temporal variability and microclimatic data, offering a more realistic representation of species distribution in the face of global change (Lembrechts et al., 2019).

Based on these gaps of knowledge, the aim of this study is to model the distribution of several bird species across ten years within an experimental forest in the Cascades Range of North-West USA, characterized by large patches of old-growth stands. Our general objectives were (i) to compare the accuracy, calibration, and predictions of different modeling frameworks based on a gradient of temporal resolutions to assess the reliability of dynamic models, (ii) to evaluate the transferability of these models to different years, and (iii) to examine the dissimilarities in spatial predictions. We did this by testing four different correlative SDM frameworks: (i) a framework based on a random year of species observations and environmental conditions, (ii) a framework based on average of microclimate conditions across ten years using presences in a plot where a species was recorded at least once and temporal abundance (number of occurrences/10

years) as weight within the models, (iii) a long-term ensemble of annual models through an average of probability of occurrence for each year, and (iv) a fully dynamic SDM approach accounting for spatiotemporal autocorrelation.

A central hypothesis guiding this research is that species with distinct functional traits may respond differently to modeling frameworks. We hypothesized that (i) migratory species would benefit more from dynamic models than sedentary species; and (ii) large birds with greater longevity should show worse results than smaller birds, and their accuracy should increase using a finer temporal resolution.

5.2 Material and methods

5.2.1 Study area

The study area is the H.J. Andrews Experimental Forest (HJA), situated within the Willamette National Forest of western Oregon, US (44.23°N, 122.188° W; Figure 5.1). Encompassing 6400 hectares in the Cascade Range, the forest's elevation spans from 407 to 1632 m a.s.l. Douglas fir (*Pseudotsuga menziesii* (Mirb.) Franco) and western hemlock (*Tsuga heterophylla* (Raf.) Sarg.) dominate the lower elevation, while the upper portion of the watershed features Pacific silver fir (*Abies amabilis* (Douglas ex Loudon) J. Forbes), noble fir (*Abies procera* Rehder), and mountain hemlock (*Tsuga mertensiana* (Bong.) Carr.). Most of the area consists of old-growth forest stands with complex vertical structure and age-class distributions and a smaller portion is covered by mountain meadow and shrubland. Approximately 25% of the HJA consists of closed-canopy second growth forest (25-70 years old) planted or naturally regenerated following clearcut, shelterwood or partial retention harvests (Kim et al., 2022). These second growth stands are characterized by distinct canopy and understory strata, the former dominated by Douglas fir (or noble fir at higher elevations) and the latter by shade-tolerant juvenile trees and shrubs (Figure 5.1b). The climate at HJA is marine temperate with an annual mean temperature of 9°C. Annual precipitation ranges from 1660 to 2810 mm and occurs especially from October

to April. Elevation, topography, and vegetation structure drive microclimate conditions within the area (Figure 5.1c; Frey et al., 2016; Wolf et al., 2021).

For this study, we used bird and microclimate sampling locations (n = 184) according to a systematic and stratified sampling design (Schulze et al., 2023), as previously described by Frey et al. (2016), Wolf et al. (2021), and Kim et al. (2022). The points were stratified across gradients in elevation (460–1558 m), vegetation structure (plantations, n = 66 vs. primary forest, n = 118) and distance from roads.

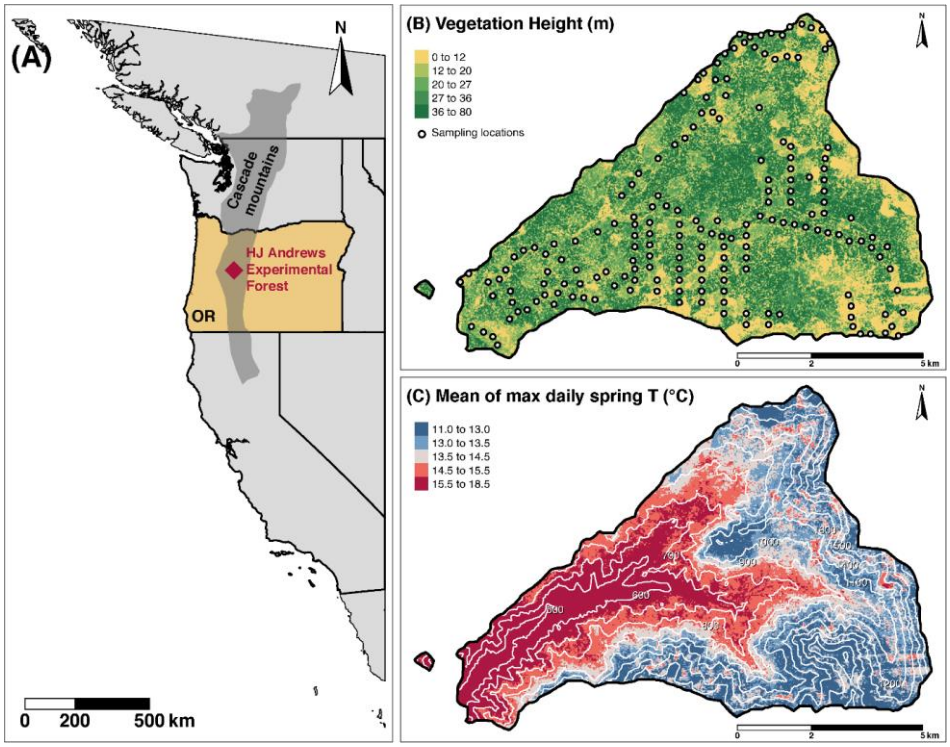

FIGURE 5.1. (a) Location of the study area (H.J. Andrews Experimental Forest) within the Northwestern US and the Cascade Range. (b) Map of the vegetation height (from CHM) and sampling locations for birds occurrence and temperature data loggers. (c) Mean of maximum daily spring temperatures and elevation belts.

5.2.2 SDM framework overview

In the next sections, we describe the SDM framework according to the ODMAP (Overview, Data, Model, Assessment, and Prediction) protocol for Species Distribution Models (Zurell et al., 2020) (refer to the Supplementary Materials for additional details). We operated under the following assumptions: (i) the distribution of our focal bird species within the landscape is mostly driven by microclimate conditions and forest structure (Kim et al., 2022); (ii) species are at (pseudo-) equilibrium with the environment (i.e., the species occupies all suitable habitats within the landscape); (iii) bird count sampling is both adequate and representative, with negligible detection errors, and unbiased species identification, (iv) vegetation and forest structure remain static over time (10 years).

All the analyses were conducted in R version 4.2.3 (R Core Team, 2023) (See Supplementary Materials for R packages used in the analyses).

5.2.3 Species data

We used a 10-year avian point count inventory spanning from 2010 to 2019 and based on the work of Kim et al. (2022). Avian point count surveys, each lasting 10 minutes, were conducted between 5:00 and 10:30 a.m. at 184 designated points during the breeding season from May to July (Figure 5.1b). Surveyors visited each point up to six times from 2010 to 2013 and up to 4 times from 2014 to 2019 (see Kim et al., 2022 for additional details). We considered 37 species (49% of the 75 species detected in total) for which model calibration and validation was possible. This exclusion was due to some species having only observed presences or absences for a limited number of years, rendering us unable to effectively calibrate and validate species distribution models at the landscape scale.

To complement our avian data, we obtained functional traits (i.e., morphological, ecological, and geographical traits) for each species from the AVONET dataset (Tobias et al., 2022). We applied a principal component analysis (PCA) as a data

reduction analysis to reduce the number of variables. Further information regarding species codes, names, and functional traits can be found in the Supplementary Materials.

5.2.4 Environmental predictors

5.2.4.1 Climate data

To assess the microclimate conditions of the landscape, we used data from 184 temperature and light data loggers placed at bird count stations. The sensors we used were HOBO Pendant® Temperature/Light Data Logger (Onset Computer Corporation), affixed to posts at 1.5 m above the ground, facing south, and shielded by a radiation shield made with PVC pipes (see Frey et al., 2016 for detailed specifications). Data loggers collected temperature and light intensity every 20 minutes. We filtered and cleaned temperature data to exclude errors.

For our analysis, we used undercanopy daily minimum, mean, and maximum temperatures from 2009 to 2019. We derived a set of temperature metrics (n = 56), including monthly and seasonal minimum, mean, maximum, and standard deviation, growing degree days (GDD), and cooling degree days (CDD). Notably, we calculated these metrics using monthly values from the month of July of the previous year to the month of June of the reference year to capture the microclimate of one year before species observation. For instance, when referring to the microclimate of 2015, we considered data from the 1st of July 2014 to the 30th of June 2015. To create comprehensive microclimate maps for the landscape, we followed the procedure outlined by Wolf et al. (2021). We used BRT models trained on the different microclimate variables as responses and vegetation, elevation, and microtopography (i.e., slope, aspect, topographic wetness index, and topographic position index) as predictors (Frey et al., 2016; Wolf et al., 2021). We generated these maps at 25-m resolution. Further details about vegetation variables can be found in Supplementary Materials.

5.2.4.2 Vegetation structure

We obtained several vegetation variables (n = 10) from a LiDAR flight (Oregon Lidar Consortium, 2016) operated between May and June 2016 using a Leica ALS80 sensor and capturing an average of 12.64 points per square meters (Oregon Lidar Consortium, 2016). The derived variables encompassed canopy cover, canopy point density, and several height metrics. We resampled vegetation structure raster data to 25-m resolution to ensure consistency.

5.2.4.3 Variable pre-selection

From an initial pool of 66 variables, we performed variable pre-selection by considering the correlation between variables (threshold = 0.90) and the variance inflation factor (VIF). This pre-selection was executed for each year (n = 10), and we retained variables occurring more than 5 times. Our aim was to speed-up the computation time and avoid highly correlated variables even if BRT is considered to be robust against multicollinearity. We obtained a final set of 41 variables (microclimate variables n = 32, vegetation structure variables n = 9) for our analysis (detailed information can be found in Supplementary Materials).

5.2.5 Species distribution modeling

We built species distribution models using boosted regression trees (BRTs) through the `dismo` R package v1.3-14 (Hijmans et al., 2023) and the dynamicSDM R package v1.3.2 (Dobson et al., 2023), both acting as wrappers for the `gbm` package (Greenwell et al., 2019). BRTs are machine learning models based on an ensemble of trees and are widely recognized as effective methods in species distribution modeling. Within a BRT framework, multiple decision trees sequentially predict residuals from the preceding tree. This boosting forward-fitting technique enhances the diversity of trees in an ensemble, improving predictive performance and resulting in an additive regression model (Elith et al., 2008). Several studies showed good to excellent predictive performance of BRTs in SDMs compared to other fine-tuned models or ensemble modeling methods (e.g., Elith et al., 2008; Valavi et al., 2022) We used BRTs optimization to

improve modeling performances of the different frameworks (refer to the Supplementary Materials).

We employed four distinct modeling frameworks based on their temporal extent and resolution, spanning from fully static to fully dynamic approaches to assess the interplay between species occurrence and environmental conditions.

5.2.5.1 Random year

We used the Random Year (RAY) approach to obtain the coarsest combination of temporal resolution and extent, capturing species response and environmental conditions within a single year of data collection (Figure 5.2a). We randomly selected one year from the 10 years of available data for calibration, creating a snapshot in time of species distribution. This accessible approach aligns with standard SDM applications, and we applied the RAY framework to 37 different species.

5.2.5.2 Temporal occupancy

We adapted our second modeling framework from the temporal occupancy framework described by Snell Taylor et al. (2021) (Figure 5.2b). The Temporal Occupancy (TOC) approach combines average environmental conditions (temporal extent = 10, temporal resolution = 1) with dynamic species responses (temporal extent = 10, temporal resolution = 10). By weighting BRT models with the proportion of times a species was observed over the 10 years (i.e., temporal abundance), this approach accounts for inter-annual variability. This approach is accessible for annual monitoring datasets. We applied the TOC framework to 32 different species.

5.2.5.3 Long-term ensemble

We built Long-term Ensemble (LTE) models by creating year-specific models correlating year-specific response to predictors, and then averaging them (Figure 5.2c). We paired response and predictors at the same temporal resolution (1 year), and an unweighted average produced the final prediction. This approach requires

both observations and predictor values to be collected at the same temporal resolution. This ensemble modeling strategy provides a nuanced understanding of temporal dynamics. We applied the LTE framework to 37 different species.

5.2.5.4 Dynamic model

For the last model, we applied a fully dynamic (DYN) model sensu Milanesi et al. (2020). To apply this framework, we used the R package `dynamicSDM` R package v. 1.3.2 (Dobson et al., 2023) (Figure 5.2d). First, we split the dynamic dataset into 5 spatiotemporal blocks accounting for both temporal and spatial autocorrelation, then we calibrated the models by using the default BRT settings. During calibration, each unique block is excluded through a jack-knife procedure (Bagchi et al., 2013). The model uses each spatiotemporal block as the testing dataset in numerical order and all the other blocks as training data. The calibration procedure returns a list of fitted BRT models equal to the length of blocks. We then derived both the mean and the uncertainty of the 5 resulting BRT models. As the previous approach, this approach works with fine temporal resolution (1 year) and long temporal extent (10 years). We considered DYN to be even more dynamic than LTE since it is not limited to annual dynamics but considers lagging effects through complex interactions and spatiotemporal autocorrelation. We applied the DYN framework to 37 different species.

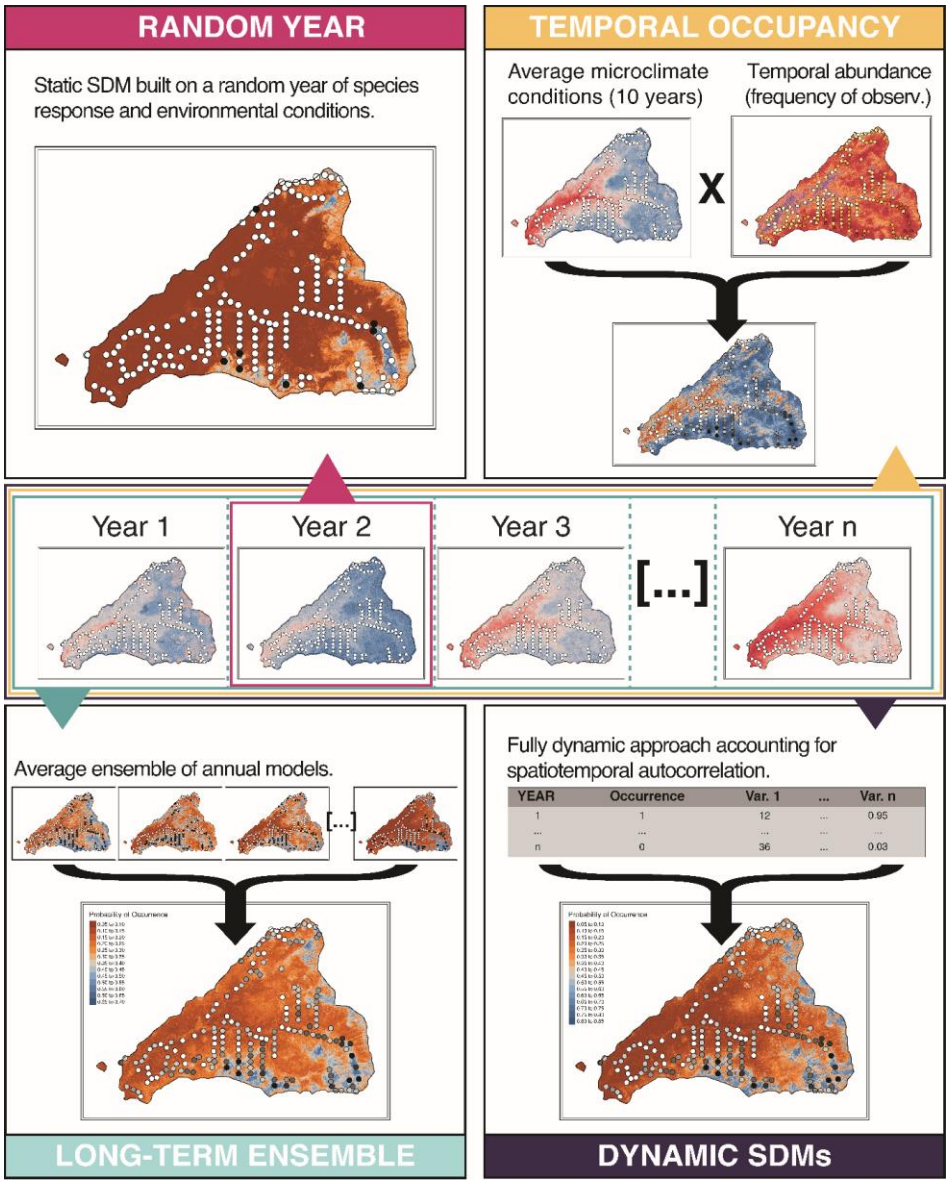

FIGURE 5.2 Workflow of the different temporal frameworks applied in the study. (A) Random Year = static SDM built using a random year of occurrences and environmental variables. (B) Temporal Occupancy = static SDM built using the temporal occupancy (n° annual observations/n° years) of a species for each sampling location as weight within the BRT model and the average of the environmental conditions as predictors. (C) Long-term ensemble = dynamic SDM built as an average of annual models. (D) Dynamic SDMs = fully dynamic model built using all the observations and environmental conditions accounting for spatiotemporal autocorrelation through modeling blocks.

5.2.6 Model performance and spatial predictions

To evaluate the accuracy and calibration of the models, we adopted a temporal leave-one-out cross-validation procedure (Wenger & Olden, 2012; Roberts et al., 2017), excluding in turn one year from the modeling process and using it as the testing sample. We retrieved three accuracy metrics: the Area Under the receiving operator Curve (AUC), True Skill Statistic (TSS), and F1 score. The AUC is a threshold-independent metric that illustrates the relationship between false-positive and true-positive rates. TSS and F1 score are threshold-dependent accuracy metrics that depend on the sensitivity and specificity of the models. In general, models with TSS > 0.6 and AUC > 0.8 are considered to be good to excellent. We assessed the calibration (i.e., the agreement between predicted probabilities of occurrence and observation of presence and absence) and generalizability of the models through Pearson's correlation coefficient (COR). We calculated the correlation between the observation (presence/absence dichotomous variable) and the predictions (range of probabilities). COR is therefore a threshold-independent metric similar to AUC, but it accounts for the distance between the prediction and the observation (Elith et al., 2006).

We tested accuracy and calibration against functional traits of bird species such as movement life history (sedentary, n = 11; partially migratory, n = 5; or migratory, n = 21) and body size (derived through principal component analysis of species' functional traits). We used linear mixed-effect models on accuracy (AUC, TSS, and F1) and calibration (COR) results to assess significant differences among modeling frameworks, movement life history, and body size. We incorporated nested random effects (species within families) to account for phylogenetic similarity between the species. We graphically checked assumptions of residuals' normality and homoscedasticity. We performed Tukey's post-hoc tests on significant effects ($p < 0.05$) with Bonferroni adjustment.

The primary output of the modeling consisted of predictions of relative probability of occurrence. For dynamic frameworks (i.e., LTE and DYN), we also

derived the uncertainty based on the 5th and 95th percentile of the probability distribution. We compared the wall-to-wall spatial predictions resulting from the different frameworks to assess Spearman's rank correlation between the modeling frameworks, and tested the correlation results against the movement life history and body size through linear mixed-effect models. We incorporated nested random effects (species within families) to account for phylogenetic similarity between species, and graphically checked assumptions of residuals' normality and homoscedasticity. We performed Tukey's post-hoc tests on significant effects ($p < 0.05$) with Bonferroni adjustment.

5.3 Results

5.3.1 Model performance and functional traits

Dynamic models (LTE and DYN) had better performance than static approaches (RAY and TOC) for all the metrics for the 37 species (Figures 5.3, 5.4). Migratory species had the highest accuracy and calibration, followed by sedentary ones. In general, model performance was acceptable to good for most of the species (26 species with AUC > 0.6 and TSS > 0.3), with five showing excellent accuracy results with dynamic frameworks (AUC > 0.8, TSS > 0.5, and COR > 0.4). Overall, models showed an average AUC of 0.69 ± 0.12 (mean ± standard deviation), an average TSS of 0.36 ± 0.18, an average F1 of 0.50 ± 0.23, and average COR (calibration) of 0.26 ± 0.17.

Predictions improved for 86.5% of the species when using dynamic models rather than static models. We observed an increasing performance trend in terms of mean, median, and extreme values through RAY to DYN both in terms of AUC (Figure 5.3a, b) and COR (Figure 5.3b, c). In particular, the drop-off of accuracy in calibrating fully dynamic versus random year (DYN – RAY) models was particularly evident for sedentary species, with an average drop-off in AUC of 0.097 (5^{th} percentile = -0.046, 95^{th} percentile = 0.159; Figure 5.3a) and in COR of 0.119 (-0.069, 0.268; Figure 5.3c). While validating partially migratory species, we observed the lowest drop-offs of AUC (0.073) and COR (0.067), but higher variability (standard deviation of 0.090 and 0.073, respectively). We compared AUC and COR to visualize the trade-offs between accuracy and calibration of the different models (Figure 5.3b). AUC and COR are correlated, and centroids of dynamic models (LTE, DYN) stood out from the others. In particular, three different clusters of accuracy appeared; dynamic models for migratory species, static models for migratory and dynamic models for sedentary species. We observed no statistical differences between the two dynamic frameworks for both AUC and COR in sedentary species. AUC, but not COR, of LTE models on partially migratory species was greater than DYN.

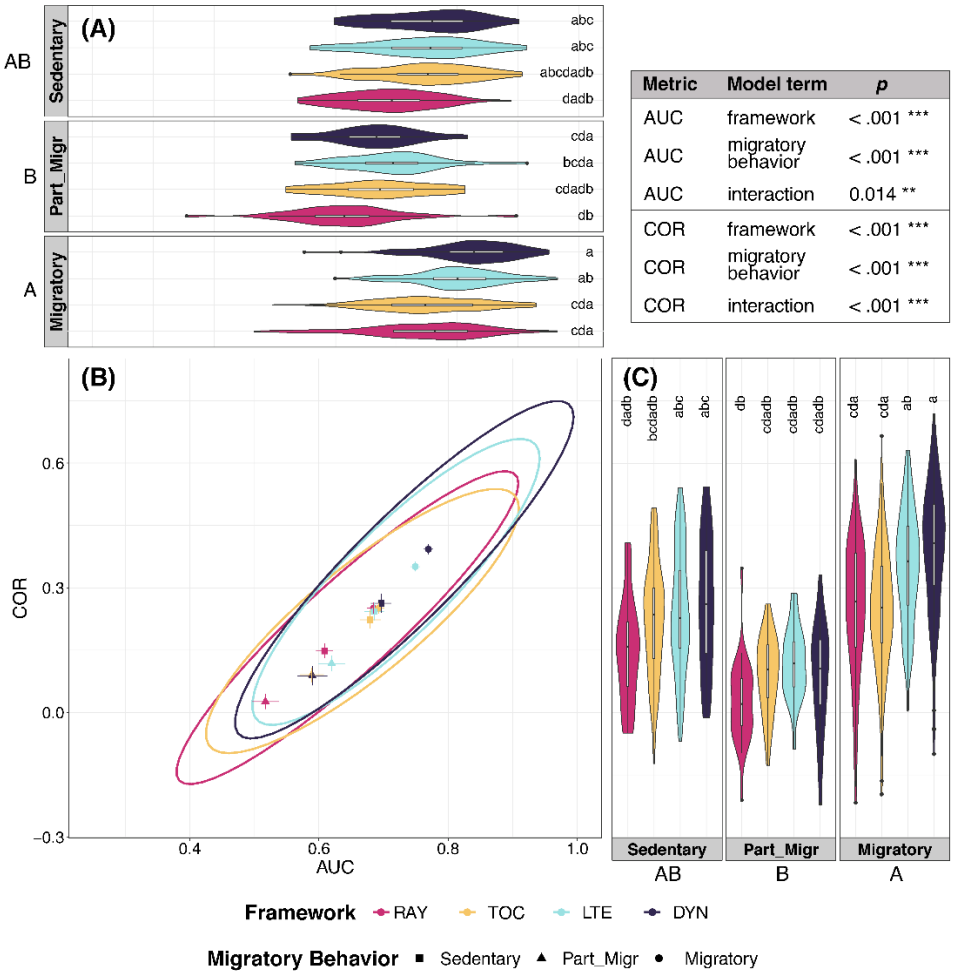

Metric	Model term	*p*
AUC	framework	< .001 ***
AUC	migratory behavior	< .001 ***
AUC	interaction	0.014 **
COR	framework	< .001 ***
COR	migratory behavior	< .001 ***
COR	interaction	< .001 ***

FIGURE 5.3 Results of temporal leave-one-out cross-validation of the different models according to the four modeling frameworks and three different movement behaviors (sedentary, partially migratory, and migratory) of birds. (A) violin plots of AUC results, (B) mean (centroids) and 95th-percentile ellipsoids of AUC and Pearson's correlation (COR), and (C) violin plots of COR results. Letters indicate post-hoc results on linear mixed-effect models. Gradients of improvement in model performance through an increase in the temporal complexity (dynamicity) of the models are visible for AUC and COR both in their mean and median values and in the upper and lower extremes.

Accuracy was negatively related to increasing body size. Large birds with low values of the PC1 showed significantly lower values of COR and F1 than smaller birds (greater PC1 values), but AUC and TSS were not significant (Figure 5.4). The interaction between body size and modeling framework was significant for

AUC, TSS, and COR. Larger birds showed similar COR and F1 between static and dynamic models, with temporal occupancy performing better than dynamic. Temporal occupancy models had the lowest slopes, meaning they mostly performed the same across the body size gradient.

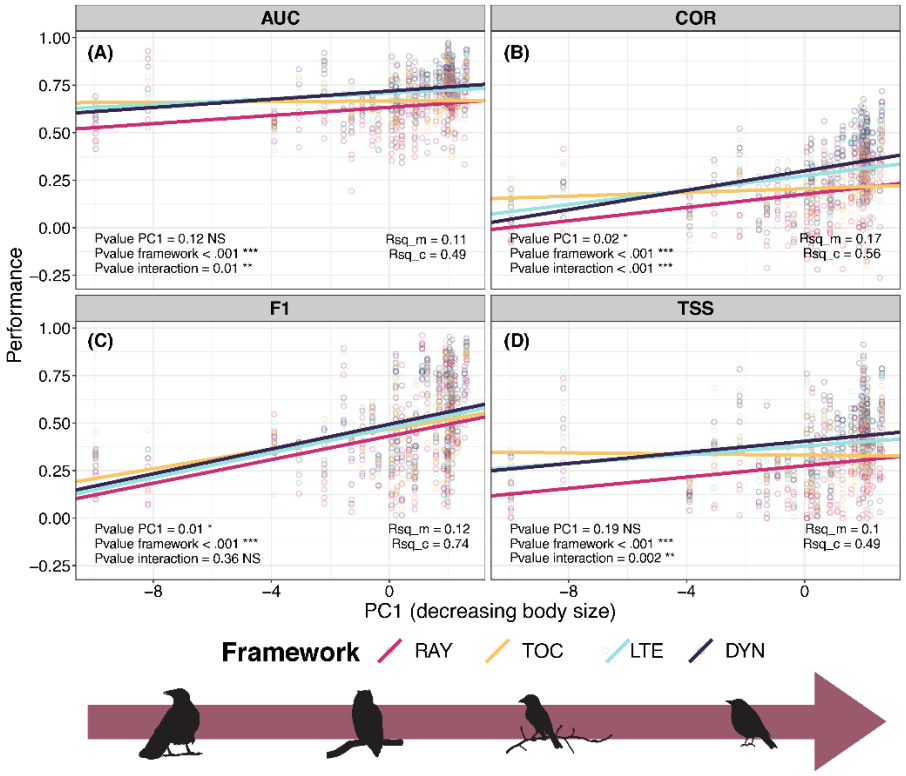

FIGURE 5.4 Relationship between models performance from temporal leave-one-out cross-validation according to the four modeling frameworks and species' body size (negatively correlated with the PC1 x axis). Panels indicate (a) AUC, (b) Pearson's correlation (COR), (c) F1 score, (d) True Skill Statistic. *P* values and R^2 are reported in the panels. The arrow below indicates the body size gradient across the x axis. The importance of dynamic models emerges especially for short-living smaller birds with a high PC1 value.

5.3.2 Spatial predictions

We compared the spatial predictions of continuous probability of occurrence across modeling frameworks, body size, and movement life history. Migratory species showed the greatest degree of similarity between modeling frameworks (mean = 0.70 ± 0.03), followed by sedentary (0.58 ± 0.04) and partially migratory

(0.43 ± 0.06) species. We observed the greatest similarity between model predictions of the two dynamic approaches for migratory species (0.78 ± 0.04) and the lowest between the two static models for partially migratory species (0.29 ± 0.09). The long-term ensemble framework showed most similarities to the other models (0.73 ± 0.04 with temporal occupancy and 0.63 ± 0.04 with both dynamic and random years). The Spearman's correlation of predicted probability of occurrence was not significantly correlated with body size (p = 0.23) and the interaction factor between body size and modeling framework (p = 0.06).

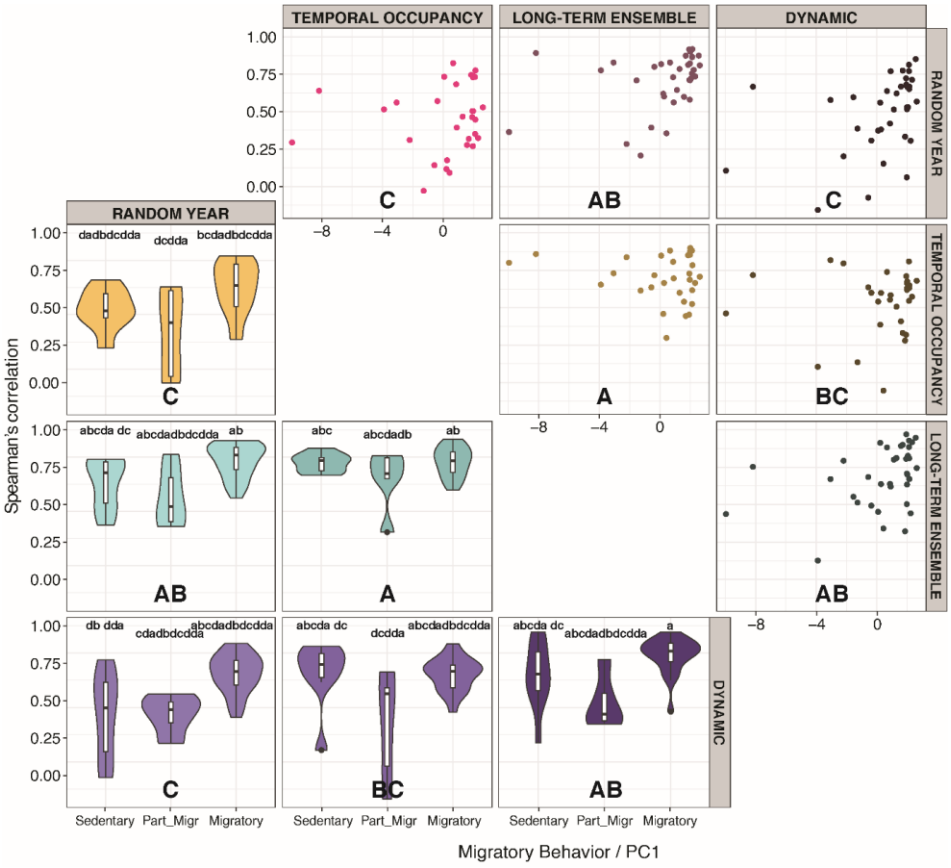

FIGURE 5.5 Spearman's rank correlation on spatial predictions of probability of occurrence between modeling frameworks based on body size (PC1) (upper right corner) and movement life history (lower left corner). Letters indicate post-hoc results on linear mixed-effect models. Migratory species had the greatest degree of similarity between modeling frameworks. Long-term ensemble framework was the most similar to all the other models.

Visual comparisons between the spatial predictions were performed for the 37 species (Figure 5.6 and Supplementary Materials). In general, the static frameworks showed smaller gradients of probability values, with random year returning low values of probability and temporal occupancy returning high values. We observed greater probability gradients across the landscape in dynamic models; their predictions also exhibited the highest degree of similarity.

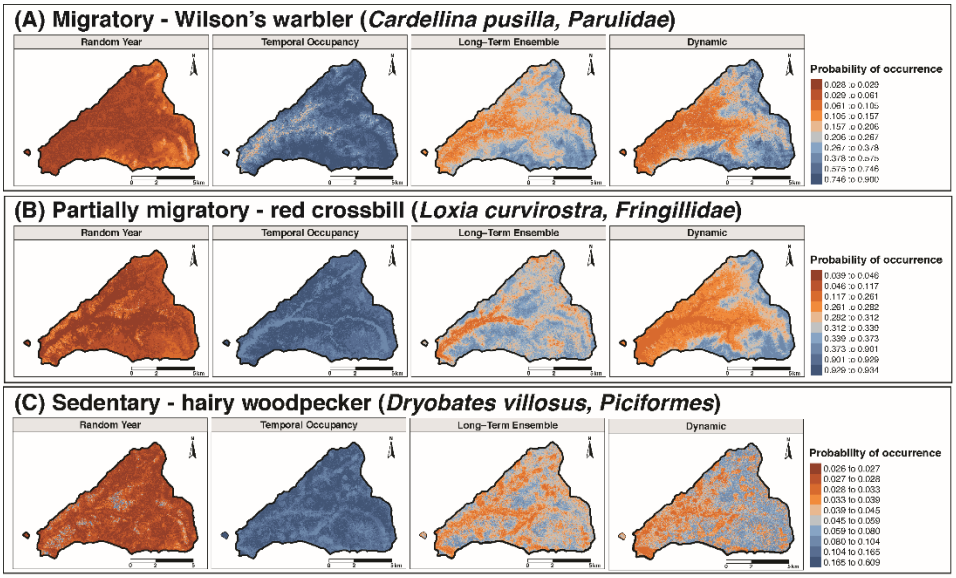

FIGURE 5.6 Spatial predictions of probability of occurrence for (a) Wilson's warbler (WIWA), (b) red crossbill (RECR), and (c) hairy woodpecker (HAWO) according to the four modeling frameworks. Maps for the other species can be found in the Supplementary Materials for both raw and normalized data.

5.4 Discussion

5.4.1 Temporal resolution in SDMs

In this study we compared four species distribution modeling (SDM) frameworks across a temporal scale gradient ranging from short to long temporal extent and from coarse to fine temporal resolution. Along this temporal gradient, we considered the random year (RAY) approach to be the simplest and most static and the fully dynamic (DYN) approach to be the most dynamic. In between, the temporal occupancy (TOC) framework is characterized by good temporal extent,

but coarser temporal resolution, and the long-term ensemble (LTE) approach is similar to DYN and can be considered as dynamic.

Our results showed that model accuracy and calibration were positively correlated with increasing temporal scale detail, with static models having the worst performance for every metric. AUC and COR did not show significant differences between LTE and DYN, but F1 and TSS did. Our results were in line with other papers showing better performance in dynamic SDMs than static SDMs (Reside et al., 2010; Elston et al., 2017; Milanesi et al., 2020; Briscoe et al., 2021; Bradter et al., 2022; Dobson et al., 2023). Reside et al. (2010) compared models trained on long temporal extent climate data (i.e., 30 years) against models trained with one month to one year data previous the birds observation highlighting the importance of the temporal match between predictors and species response. In our study, we showed how fully dynamic SDMs (DYN) proved to be even better than long-term ensemble since it is not limited to annual dynamics but considered lagging effects through complex interactions accounting for spatiotemporal autocorrelation.

Researchers are moving toward increasing spatiotemporal reliability of both response and predictive variables (Mannocci et al., 2017; Lembrechts, Lenoir, et al., 2019; Milanesi et al., 2020). Many applications have been developed for highly mobile marine animals (e.g., Mannocci et al., 2017; Pennino et al., 2019) but bird models benefitted from this approach too (Reside et al., 2010; Bradter et al., 2022; Conlisk et al., 2022). Our results support the hypothesis that models for highly mobile taxa such as birds show a clear and significant improvement in using fine temporal microclimate data that better represent real habitat conditions of these species (Lembrechts, Nijs, et al., 2019; Haesen et al., 2023). We observed that for most of the species, the two temporal dynamic approaches (i.e., LTE and DYN) provided similar results in terms of probability of occurrence. This result proves the similarity between these two frameworks and the difference between temporally static and dynamic models. Still, even if we assessed model temporal

transferability through temporal cross-validation, we believe that an independent validation would be useful to strengthen our considerations.

Regarding the models, since we used self-tuned models through cross-validation for all the frameworks, we expected the modeling results not to be biased due to parametrization efforts. Moreover, the DYN model was the least flexible, since it was not possible to implement cross-validation tuning of hyper-parameters as freely as the others. That said, this confirms that accounting for dynamic covariates and responses really boost modeling results.

5.4.2 Functional traits

We tested the accuracy and calibration performance of the modeling frameworks against several functional traits of the bird species. We observed significant differences among both movement life history and body size. As hypothesized, an increase in the temporal complexity of the frameworks resulted in increasing accuracy and calibration for migratory birds, but sedentary species benefitted more from the increasing temporal detail than the migratory ones.

For partially migratory species LTE slightly outperformed DYN in terms of AUC, but not Pearson's correlation while for sedentary species, LTE and DYN performance was similar. The increase of model performance in using DYN versus LTE was particularly evident for migratory species, probably because of the lagging effects these models account for. Migratory species are more heterogeneously present in time than sedentary species, that are supposed to show greater stationarity (MacLean & Beissinger, 2017). Indeed, migratory species might depend more on variations with a lagging effect longer than one year (Visser et al., 2015).

In general, large birds can move around more in response to microclimate variability. By doing that, these organisms have broader environmental ranges and are better in buffering their environment (Scheffers et al., 2014; Pincebourde et al., 2021). Smaller birds, instead, may have access to a larger spectrum of buffered microhabitats (Huey et al., 2012). Therefore, in any given snapshot a

survey might not find those species in portions of the landscape that they occupy sporadically over the longer term. Our results did not highlight this effect. There are many ecological and statistical reasons for that. First of all, by averaging seasonal bird observations, we might lose very detailed information at an intra-annual level. Site fidelity may be another important driver at the annual scale. Moreover, for some of those old-growth specialistic species, vegetation and forest structure might be more important than climatic variables.

Spatially, we should consider that, even if 25m can be considered a fine resolution, some of the bird dynamics and processes happen at a finer resolution. Indeed, also the temporal resolution we applied did not explicitly consider intra-annual variations, especially in the species data. For this reason, we expect that even finer spatiotemporal details might be required for SDMs at the landscape scale. For instance, Bradter et al., (2022) decomposed spatial, temporal, and spatiotemporal components revealing the importance of and intra-annual climate variability for bird species distribution and its modeling.

5.4.3 Implications for ecology and biological conservation

Quantitative and conservation ecology research is moving toward an increase of models reliability to better quantify the effects of global changes on ecosystem structure and species distribution (Navarro Cerrillo et al., 2021; Zurell et al., 2022; Garbarino et al., 2023). The rapid increase in data availability at different spatial (i.e., from microclimate to global circulation models) and temporal (i.e., from sub-hourly microclimate data collection to historical climate reconstruction) is pushing ecological models to promising frontiers, such as real-time accurate distribution modeling (e.g., Conlisk et al., 2022). However, the temporal scale in SDMs is still often underestimated (Milanesi et al., 2020; Zurell et al., 2022).

Our results highlight that long-term monitoring and data collection of fine-scale environmental predictors is crucial to build reliable models for practical applications. The concept of scale is the foundation of landscape ecology (Wiens, 1989). Body size has been considered as a proxy of several functional traits in

ecology for many years. It is true that small species with short life span and low mobility are more sensitive to fine-scale variations in both time and space, while long-living organisms react to longer and broader changes because of their higher mobility at the local extent (Huey et al., 2012; Scheffers et al., 2014). Therefore, we argue that landscape-scale prioritization and monitoring would benefit from models calibrated at a fine spatial and temporal scale. Microclimate is a trend topic in ecology nowadays and its data collection is very well suited to account for temporal dynamics within SDMs (Lembrechts et al., 2019; De Frenne et al., 2021). Dynamic approaches might be of particular interest in regions and landscapes with a greater mosaic complexity (e.g., mountain ranges, ecotones and transition zones; Milanesi et al., 2020; De Frenne et al., 2021) and when dealing with global change (Milanesi et al., 2020; Bradter et al., 2022). Indeed, recent and predicted future shifts in climate and land use are characterized by rapid dynamics and large intra- and interannual variations (Scheffers et al., 2014; Raymond et al., 2020).

Moreover, we think that integrating dynamic SDMs at various spatial and temporal scales would be important to build models that are both accurate and reliable in studying species response to global changes (Mateo et al., 2019; Zipkin et al., 2021; Banks-Leite et al., 2022). For instance, by further accounting for the macroecology of a species (e.g., distance from range borders or centroids, thermal stress, etc.) within landscape-scale models, we expect predictions to be more accurate and sound for conservation purposes.

5.5 Conclusions

Our results suggest that integrating dynamic covariates and species response should be preferred whenever possible. Particularly, models for highly mobile species (e.g., migratory species) had the highest accuracy and calibration when trained with data able to reflect the inter-annual variability of forest ecosystems.

We are aware that population and microclimate data needed to parameterize dynamic models at the landscape scale are scarce and that static species

distribution modeling applications will remain important because of their easier implementation. Nevertheless, we advocate for accounting for temporal resolution and population and climate variability whenever possible. Moreover, researchers should be aware of the different aims and objectives these tools have. If regional- to global-scale applications might be calibrated with data with coarse spatial and temporal scale, the reliability and soundness of landscape-scale applications would strongly benefit from fine variables in species distribution models. Indeed, this approach can be applied to different spatial extents and resolutions for many taxa such as birds, large mammals, and trees, for which the availability of fine data is usually good.

Acknowledgements

Data were provided by the H.J. Andrews Experimental Forest and Long-Term Ecological Research (LTER) program, administered cooperatively by Oregon State University, the USDA Forest Service Pacific Northwest Research Station, and the Willamette National Forest. This material is based upon work supported by the National Science Foundation under the grant LTER8 DEB-2025755. Opinions expressed in this study may not necessarily reflect the position of the U.S. Department of Agriculture or the Forest Service.

Indigenous peoples have been in relationship for thousands of years with the forests, streams, and meadows we now call the Blue River watershed. In the Kalapuya Treaty of 1855 (aka Treaty of Dayton, Willamette Valley Treaty), the Kalapuya were forced to cede this land to the US Government. We continue to learn about, recognize, and value the attributes of the Blue River watershed that reflect the enduring relationship between Indigenous people and the land. We strive to be mindful of this relationship and to integrate it in our research, our decision-making, and our actions.

Data availability

R code and species predictions will be available in a Figshare repository, predictors and response variable are available in the H.J. Andrews data catalog (https://andrewsforest.oregonstate.edu/data).

References

Adams, J., MacLeod, C., Suryan, R. M., David Hyrenbach, K., & Harvey, J. T. (2012). Summer-time use of west coast US National Marine Sanctuaries by migrating sooty shearwaters (Puffinus griseus). *Biological Conservation*, 156, 105–116.

Araújo, M. B., Anderson, R. P., Barbosa, A. M., Beale, C. M., Dormann, C. F., Early, R., Garcia, R. A., Guisan, A., Maiorano, L., Naimi, B., O'Hara, R. B., Zimmermann, N. E., & Rahbek, C. (2019). Standards for distribution models in biodiversity assessments. *Science Advances*, 5(1), eaat4858.

Bagchi, R., Crosby, M., Huntley, B., Hole, D. G., Butchart, S. H., Collingham, Y., ... & Willis, S. G. (2013). Evaluating the effectiveness of conservation site networks under climate change: accounting for uncertainty. *Global Change Biology*, 19(4), 1236-1248.

Bai, W., Huang, Q., Zhang, J., Stabach, J., Huang, J., Yang, H., Songer, M., Connor, T., Liu, J., Zhou, S., Zhang, H., Zhou, C., & Hull, V. (2020). Microhabitat selection by giant pandas. *Biological Conservation*, 247, 108615.

Banks-Leite, C., Betts, M. G., Ewers, R. M., Orme, C. D. L., & Pigot, A. L. (2022). The macroecology of landscape ecology. *Trends in Ecology & Evolution*.

Bellard, C., Thuiller, W., Leroy, B., Genovesi, P., Bakkenes, M., & Courchamp, F. (2013). Will climate change promote future invasions? *Global Change Biology*, 19(12), 3740–3748.

Bicknell, J. E., Collins, M. B., Pickles, R. S. A., McCann, N. P., Bernard, C. R., Fernandes, D. J., Miller, M. G. R., James, S. M., Williams, A. U., Struebig, M. J., Davies, Z. G., & Smith, R. J. (2017). Designing protected area networks that translate international conservation commitments into national action. *Biological Conservation*, 214, 168–175.

Bradter, U., Johnston, A., Hochachka, W. M., Soultan, A., Brommer, J. E., Gaget, E., Kålås, J. A., Lehikoinen, A., Lindström, Å., Piirainen, S., Pavón-Jordán, D., Pärt, T., Øien, I. J., & Sandercock, B. K. (2022). Decomposing the spatial and

temporal effects of climate on bird populations in northern European mountains. *Global Change Biology*, 28(21), 6209–6227.

Briscoe, N. J., Zurell, D., Elith, J., Koenig, C., Fandos, G., Malchow, A.-K., Kéry, M., Schmid, H., & Guillera-Arroita, G. (2021). Can dynamic occupancy models improve predictions of species' range dynamics? A test using Swiss birds. G*lobal Change Biology*, 27, 4269–4282.

Carroll, C., Dunk, J. R., & Moilanen, A. (2010). Optimizing resiliency of reserve networks to climate change: Multispecies conservation planning in the Pacific Northwest, USA. *Global Change Biology*, *16*(3), 891–904.

Chávez-González, E., Vizentin-Bugoni, J., Vázquez, D. P., MacGregor-Fors, I., Dáttilo, W., & Ortiz-Pulido, R. (2020). Drivers of the structure of plant–hummingbird interaction networks at multiple temporal scales. *Oecologia*, *193*(4), 913–924.

Conlisk, E. E., Golet, G. H., Reynolds, M. D., Barbaree, B. A., Sesser, K. A., Byrd, K. B., Veloz, S., & Reiter, M. E. (2022). Both real-time and long-term environmental data perform well in predicting shorebird distributions in managed habitat. *Ecological Applications*, 32(4). Scopus.

De Frenne, P., Lenoir, J., Luoto, M., Scheffers, B. R., Zellweger, F., Aalto, J., Ashcroft, M. B., Christiansen, D. M., Decocq, G., De Pauw, K., Govaert, S., Greiser, C., Gril, E., Hampe, A., Jucker, T., Klinges, D. H., Koelemeijer, I. A., Lembrechts, J. J., Marrec, R., … Hylander, K. (2021). Forest microclimates and climate change: Importance, drivers and future research agenda. *Global Change Biology*, *27*(11), 2279–2297.

Dobson, R., Challinor, A. J., Cheke, R. A., Jennings, S., Willis, S. G., & Dallimer, M. (2023). DYNAMICSDM: An R package for species geographical distribution and abundance modelling at high spatiotemporal resolution. *Methods in Ecology and Evolution*, 2041-210X.14101.

Dyderski, M. K., Paź, S., Frelich, L. E., & Jagodziński, A. M. (2018). How much does climate change threaten European forest tree species distributions? *Global Change Biology*, *24*(3), 1150–1163.

Elith, J., H. Graham, C., P. Anderson, R., Dudík, M., Ferrier, S., Guisan, A., ... & E. Zimmermann, N. (2006). Novel methods improve prediction of species' distributions from occurrence data. *Ecography*, 29(2), 129-151.

Elith, J., Leathwick, J. R., & Hastie, T. (2008). A working guide to boosted regression trees. *Journal of Animal Ecology*, *77*(4), 802–813.

Elston, D. A., Brewer, M. J., Martay, B., Johnston, A., Henrys, P. A., Bell, J. R., Harrington, R., Monteith, D., Brereton, T. M., Boughey, K. L., & Pearce-Higgins, J. W. (2017). A New Approach to Modelling the Relationship Between Annual Population Abundance Indices and Weather Data. *Journal of Agricultural, Biological and Environmental Statistics*, 22(4), 427–445.

Frey, S. J. K., Hadley, A. S., Johnson, S. L., Schulze, M., Jones, J. A., & Betts, M. G. (2016). Spatial models reveal the microclimatic buffering capacity of old-growth forests. *Science Advances*, 2(4), e1501392.

Garbarino, M., Morresi, D., Anselmetto, N., & Weisberg, P. J. (2023). Treeline remote sensing: From tracking treeline shifts to multi-dimensional monitoring of ecotonal change. *Remote Sensing in Ecology and Conservation*.

Guisan, A., Tingley, R., Baumgartner, J. B., Naujokaitis-Lewis, I., Sutcliffe, P. R., Tulloch, A. I. T., Regan, T. J., Brotons, L., McDonald-Madden, E., Mantyka-Pringle, C., Martin, T. G., Rhodes, J. R., Maggini, R., Setterfield, S. A., Elith, J., Schwartz, M. W., Wintle, B. A., Broennimann, O., Austin, M., … Buckley, Y. M. (2013). Predicting species distributions for conservation decisions. *Ecology Letters*, 16(12), 1424–1435.

Greenwell, B., Boehmke, B., Cunningham, J., & Developers, G. B. M. (2022). *gbm: Generalized boosted regression models*. R package version 2.1.8.1, 2(5), 37-40.

Haesen, S., Lenoir, J., Gril, E., De Frenne, P., Lembrechts, J. J., Kopecký, M., Macek, M., Man, M., Wild, J., & Van Meerbeek, K. (2023). Microclimate reveals the true thermal niche of forest plant species. *Ecology Letters*, ele.14312.

Hijmans, R. J., Phillips, S., Leathwick, J., & Elith, J. (2023). *dismo: Species Distribution Modeling*. R package version 1.3-14.

Huey, R. B., Kearney, M. R., Krockenberger, A., Holtum, J. A., Jess, M., & Williams, S. E. (2012). Predicting organismal vulnerability to climate warming: roles of behaviour, physiology and adaptation. *Philosophical Transactions of the Royal Society B: Biological Sciences*, 367(1596), 1665-1679.

Kim, H., McComb, B. C., Frey, S. J., Bell, D. M., & Betts, M. G. (2022). Forest microclimate and composition mediate long-term trends of breeding bird populations. *Global Change Biology*, 28(21), 6180-6193.

Lembrechts, J. J. (2023). Microclimate alters the picture. *Nature Climate Change*.

Lembrechts, J. J., Lenoir, J., Roth, N., Hattab, T., Milbau, A., Haider, S., Pellissier, L., Pauchard, A., Ratier Backes, A., Dimarco, R. D., Nuñez, M. A., Aalto, J., &

Nijs, I. (2019). Comparing temperature data sources for use in species distribution models: From in-situ logging to remote sensing. *Global Ecology and Biogeography*, 28(11), 1578–1596.

Lembrechts, J. J., Nijs, I., & Lenoir, J. (2019). Incorporating microclimate into species distribution models. *Ecography*, 42(7), 1267–1279.

Lenoir, J., Hattab, T., & Pierre, G. (2017). Climatic microrefugia under anthropogenic climate change: Implications for species redistribution. *Ecography*, 40(2), 253–266.

Maclean, I. M. D., & Early, R. (2023). Macroclimate data overestimate range shifts of plants in response to climate change. *Nature Climate Change*.

MacLean, S. A., & Beissinger, S. R. (2017). Species' traits as predictors of range shifts under contemporary climate change: A review and meta-analysis. *Global Change Biology*, 23(10), 4094–4105.

Máliš, F., Ujházy, K., Hederová, L., Ujházyová, M., Csölleová, L., Coomes, D. A., & Zellweger, F. (2023). Microclimate variation and recovery time in managed and old-growth temperate forests. *Agricultural and Forest Meteorology*, 342, 109722.

Mannocci, L., Boustany, A. M., Roberts, J. J., Palacios, D. M., Dunn, D. C., Halpin, P. N., Viehman, S., Moxley, J., Cleary, J., Bailey, H., Bograd, S. J., Becker, E. A., Gardner, B., Hartog, J. R., Hazen, E. L., Ferguson, M. C., Forney, K. A., Kinlan, B. P., Oliver, M. J., … Winship, A. J. (2017). Temporal resolutions in species distribution models of highly mobile marine animals: Recommendations for ecologists and managers. *Diversity and Distributions*, 23(10), 1098–1109.

Mateo, R. G., Gastón, A., Aroca-Fernández, M. J., Broennimann, O., Guisan, A., Saura, S., & García-Viñas, J. I. (2019). Hierarchical species distribution models in support of vegetation conservation at the landscape scale. *Journal of Vegetation Science*, 30(2), 386-396.

Milanesi, P., Della Rocca, F., & Robinson, R. A. (2020). Integrating dynamic environmental predictors and species occurrences: Toward true dynamic species distribution models. *Ecology and Evolution*, 10(2), 1087–1092.

Moonlight, P. W., Silva De Miranda, P. L., Cardoso, D., Dexter, K. G., Oliveira-Filho, A. T., Pennington, R. T., Ramos, G., & Särkinen, T. E. (2020). The strengths and weaknesses of species distribution models in biome delimitation. *Global Ecology and Biogeography*, 29(10), 1770–1784.

Navarro Cerrillo, R. M., Duque-Lazo, J., Ríos-Gil, N., Guerrero-Álvarez, J. J., López-Quintanilla, J., & Palacios-Rodríguez, G. (2021). Can habitat prediction models contribute to the restoration and conservation of the threatened tree Abies pinsapo Boiss. In Southern Spain? *New Forests*, 52(1), 89–112.

Newbold, T., Oppenheimer, P., Etard, A., & Williams, J. J. (2020). Tropical and Mediterranean biodiversity is disproportionately sensitive to land-use and climate change. *Nature Ecology & Evolution*, 4(12), Articolo 12.

Oregon Lidar Consortium. (2016). *2016 McKenzie River Lidar Project lidar QC acceptance report*. https://www.oregongeology.org/pubs/ldq/reports/2016_OLC_McKenzie_River_Acceptance_Report.pdf

Pennino, M. G., Vilela, R., & Bellido, J. M. (2019). Effects of environmental data temporal resolution on the performance of species distribution models. *Journal of Marine Systems*, 189, 78–86.

Pincebourde, S., & Casas, J. (2019). Narrow safety margin in the phyllosphere during thermal extremes. *Proceedings of the National Academy of Sciences*, 116(12), 5588-5596.

Pincebourde, S., Dillon, M. E., & Woods, H. A. (2021). Body size determines the thermal coupling between insects and plant surfaces. *Functional Ecology*, 35(7), 1424–1436.

Raymond, C., Horton, R. M., Zscheischler, J., Martius, O., AghaKouchak, A., Balch, J., Bowen, S. G., Camargo, S. J., Hess, J., Kornhuber, K., Oppenheimer, M., Ruane, A. C., Wahl, T., & White, K. (2020). Understanding and managing connected extreme events. *Nature Climate Change*, 10(7), 611–621.

Reside, A. E., VanDerWal, J. J., Kutt, A. S., & Perkins, G. C. (2010). Weather, Not Climate, Defines Distributions of Vagile Bird Species. *PLOS ONE*, *5*(10), e13569.

Roberts, D. R., Bahn, V., Ciuti, S., Boyce, M. S., Elith, J., Guillera-Arroita, G., Hauenstein, S., Lahoz-Monfort, J. J., Schröder, B., Thuiller, W., Warton, D. I., Wintle, B. A., Hartig, F., & Dormann, C. F. (2017). Cross-validation strategies for data with temporal, spatial, hierarchical, or phylogenetic structure. *Ecography*, *40*(8), 913–929.

Scheffers, B. R., Edwards, D. P., Diesmos, A., Williams, S. E., & Evans, T. A. (2014). Microhabitats reduce animal's exposure to climate extremes. *Global Change Biology*, 20(2), 495–503.

Schulze, M., Betts, M., Frey, S. (2023). *Air temperature at core phenology sites and additional bird monitoring sites in the Andrews Experimental Forest, 2009 to present. Long-Term Ecological Research*. Forest Science Data Bank, Corvallis, OR. [Database]. Available: http://andlter.forestry.oregonstate.edu/data/abstract.aspx?dbcode=MS045

Snell Taylor, S., Di Cecco, G., & Hurlbert, A. H. (2021). Using temporal occupancy to predict avian species distributions. *Diversity and Distributions*, 27(8), 1477–1488.

Tobias, J. A., Sheard, C., Pigot, A. L., Devenish, A. J. M., Yang, J., Sayol, F., Neate-Clegg, M. H. C., Alioravainen, N., Weeks, T. L., Barber, R. A., Walkden, P. A., MacGregor, H. E. A., Jones, S. E. I., Vincent, C., Phillips, A. G., Marples, N. M., Montaño-Centellas, F. A., Leandro-Silva, V., Claramunt, S., … Schleuning, M. (2022). AVONET: Morphological, ecological and geographical data for all birds. *Ecology Letters*, 25(3), 581–597.

Valavi, R., Guillera-Arroita, G., Lahoz-Monfort, J. J., & Elith, J. (2022). Predictive performance of presence-only species distribution models: A benchmark study with reproducible code. *Ecological Monographs*, 92(1), e01486.

Visser, M. E., Gienapp, P., Husby, A., Morrisey, M., Hera, I. de la, Pulido, F., & Both, C. (2015). Effects of Spring Temperatures on the Strength of Selection on Timing of Reproduction in a Long-Distance Migratory Bird. *PLOS Biology*, 13(4), e1002120.

Wenger, S. J., & Olden, J. D. (2012). Assessing transferability of ecological models: An underappreciated aspect of statistical validation. *Methods in Ecology and Evolution*, 3(2), 260–267.

Wiens, J. A. (1989). Spatial scaling in ecology. *Functional ecology*, 3(4), 385-397.

Wolf, C., Bell, D. M., Kim, H., Nelson, M. P., Schulze, M., & Betts, M. G. (2021). Temporal consistency of undercanopy thermal refugia in old-growth forest. *Agricultural and Forest Meteorology*, 307, 108520.

Zipkin, E. F., Zylstra, E. R., Wright, A. D., Saunders, S. P., Finley, A. O., Dietze, M. C., Itter, M. S., & Tingley, M. W. (2021). Addressing data integration challenges to

link ecological processes across scales. *Frontiers in Ecology and the Environment*, 19(1), 30–38.

Zurell, D., Franklin, J., König, C., Bouchet, P. J., Dormann, C. F., Elith, J., Fandos, G., Feng, X., Guillera-Arroita, G., Guisan, A., Lahoz-Monfort, J. J., Leitão, P. J., Park, D. S., Peterson, A. T., Rapacciuolo, G., Schmatz, D. R., Schröder, B., Serra-Diaz, J. M., Thuiller, W., … Merow, C. (2020). A standard protocol for reporting species distribution models. *Ecography*, 43(9), 1261–1277.

Zurell, D., König, C., Malchow, A., Kapitza, S., Bocedi, G., Travis, J., & Fandos, G. (2022). Spatially explicit models for decision-making in animal conservation and restoration. *Ecography*, 2022(4), ecog.05787.

Supplementary Materials

Appendix A5 – Supplementary Methods

TABLE A5.1. ODMAP protocol for the study (*sensu* Zurell et al., 2020).

ODMAP element	*Contents*
OVERVIEW	
Authorship	**Authors**: Nicolò Anselmetto*, Matteo Garbarino, David Bell, Christopher Daly, Clinton W. Epps, Hankyu Kim, Joseph A. LaManna, Damon B. Lesmeister, Taal Levi, Brooke Penaluna, Mark Schulze, Marie I. Tosa, Matthew J. Weldy, Matthew G. Betts **Contact email**: *****nicolo.anselmetto@unito.it **Title**: Long-term data and temporal dynamic frameworks can improve landscape-scale species distribution models
Model objective	**Objective**: mapping/interpolation. **Target outputs**: continuous occurrence probabilities.
Taxon	37 bird species.

Location	H.J. Andrews Experimental Forest, Cascade Mountains, Oregon (US).
Scale of analysis	**Spatial extent (Lon/Lat)**: Longitude ° 122.18 W, Latitude ° 44.24 N. **Spatial resolution**: 25 m x 25 m. **Temporal resolution and extent**: 2010-2019 with different temporal resolution for the different modeling frameworks. **Type of extent boundary**: administrative (perimeter of the H.J. Andrews Experimental Forest)**.**
Biodiversity data overview	**Observation type**: repeated observations (field surveys). **Response/Data type**: presence/absence data**.**
Type of predictors	Microclimate and vegetation.
Conceptual model/ Hypotheses	As forests (especially old-growth) strongly buffer temperatures, we hypothesized that bird species are particularly sensitive to the undercanopy microclimatic conditions derived from data loggers. We hypothesized that their response would vary according to their movement life history and their body size.
Assumptions	We assumed that the distribution of our focal bird species within the landscape is mostly driven by microclimate conditions and forest structure. We assumed that species are at (pseudo-) equilibrium with the environment (i.e., the species occupies all suitable habitats within the landscape). We assumed that bird count sampling is both adequate and representative, with negligible detection errors, and unbiased species identification. We also

	considered vegetation and forest structure to be static over the time of the analysis (10 years).
SDM algorithms	**Algorithms**: we fitted Boosted Regression Trees (BRTs) models. BRT proved to be robust against multicollinerity and is among the most reliable machine learning approaches in SDMs. **Model complexity**: We used BRTs optimization to improve modeling performances of the different frameworks.

Model workflow	We employed four distinct modeling frameworks based on their temporal extent and resolution, spanning from fully static to fully dynamic approaches to assess the interplay between species occurrence and environmental conditions. We used the Random Year (RAY) approach to obtain the coarsest combination of temporal resolution and extent, capturing species response and environmental conditions within a single year of data collection. We randomly selected one year from the 10 years of available data for calibration, creating a snapshot in time of species distribution. We adapted our second modeling framework from the temporal occupancy framework described by Snell Taylor et al. (2021). The Temporal Occupancy (TOC) approach combines average environmental conditions (temporal extent = 10, temporal resolution = 1) with dynamic species responses (temporal extent = 10, temporal resolution = 10). By weighting BRT models with the proportion of times a species was observed over the 10 years (i.e., temporal abundance), this approach accounts for inter-annual variability. We built Long-term Ensemble (LTE) models by creating year-specific models correlating year-specific response to predictors, and then averaging them. We paired response and predictors at the same temporal resolution (1 year), and an unweighted average produced the final prediction. We applied a fully dynamic (DYN) model using the R package dynamicSDM R package v. 1.3.2 (Dobson et al., 2023). First, we split the dynamic dataset into 5

	spatiotemporal blocks accounting for both temporal and spatial autocorrelation, then we calibrated the models by using the default BRT settings. During calibration, each unique block is excluded through a jack-knife procedure (Bagchi et al., 2013). The model uses each spatiotemporal block as the testing dataset in numerical order and all the other blocks as training data. The calibration procedure returns a list of fitted BRT models equal to the length of blocks. We then derived both the mean and the uncertainty of the 5 resulting BRT models.
Software, codes and data	**Software**: all analyses were conducted using R version 4.2.3 (R Core Team, 2023), packages are described in the Supplementary Materials. **Code availability**: code will be publicly available in Figshare. **Data availability**: species predictions will be available in Figshare, predictors and response variable are available in the H.J. Andrews data catalog (https://andrewsforest.oregonstate.edu/data).

DATA	
Biodiversity data	**Taxon names**: *Turdus migratorius, Pheucticus melanocephalus, Certhia americana, Setophaga nigrescens, Poecile rufescens, Corvus corax, Junco hyemalis, Hesperiphona vespertina, Regulus satrapa, Perisoreus canadensis, Empidonax hammondii, Dryobates villosus, Catharus guttatus, Setophaga occidentalis, Vireo huttoni, Geothlypis tolmiei, Colaptes auratus, Contopus cooperi, Pandion haliaetus, Troglodytes pacificus, Spinus pinus, Dryocopus pileatus, Empidonax difficilis, Sitta canadensis, Loxia curvirostra, Bonasa umbellus, Selasphorus rufus, Dendragapus fuliginosus, Cyanocitta stelleri, Catharus ustulatus, Myadestes townsendi, Chaetura vauxi, Ixoreus naevius, Vireo gilvus, Piranga ludoviciana, Cardellina pusilla, Setophaga coronata.* **Detalis on taxonomic reference system**: BirdLife International (2020). **Ecological level**: species. **Biodiversity data source**: avian point count inventory spanning from 2010 to 2019, based on the work of Kim et al. (2022). **Sampling design**: systematic and stratified sampling design (Schulze et al., 2023). The points were stratified across gradients in elevation (460–1558 m), vegetation structure (plantations, n = 66 vs. primary forest, n = 118) and distance from roads.

	Administrative mask: administrative box on the H.J. Andrews Experimental Forest (Oregon, US). **Data cleaning/filtering**: we considered as "present" when a species was observed at least once during the 4 to 6 annual visits. Surveyors visited each point up to six times from 2010 to 2013 and up to 4 times from 2014 to 2019 (see Kim et al., 2022 for additional details). We considered 37 species (49% of the 75 species detected in total) for which model calibration and validation was possible. **Potential biases**: by averaging the seasonal bird observations and considering it as the annual values, temporal mismatches might be introduced. Also, few bird observations were conducted at the beginning of July and annual microclimate conditions were calculated using monthly values from the month of July of the previous year to the month of June of the reference year to capture the microclimate of one year before species observation. By doing that, it is possible that July temperature of the point count year might be more relevant to distributions than July from the year prior. We did not consider that to matter at the annual scale.
Data partitioning	A 5-fold spatial cross validation was used to partition the data for dynamic SDMs model calibration. Spatial partitioning of data followed a spatial blocking with a variable blocking factor based on the median of five ranges over which observations are independent. The ranges are determined by constructing empirical variograms for measuring spatial autocorrelation. Temporal partitioning was used for both calibration

	(dynamic SDMs) and validation (all the modeling frameworks).
Predictor variables	**Predictor variables**: ▪ *Microclimate*: monthly and seasonal mean, maximum, and minimum undercanopy temperature, CDD, and GDD. Microclimate values were spanned 10 years (July 2009 - June 2019). Datasets derived from Schulze et al. (2023). ▪ *Vegetation*: we used 10 vegetation variables encompassing canopy cover, canopy point density, and several height metrics. See Supplementary Information for further details. **Data sources**: ▪ *Microlimate*: raw data derived from the 184 were HOBO Pendant® Temperature/Light Data Logger (Onset Computer Corporation) affixed to posts at 1.5 m above the ground, facing south, and shielded by a radiation shield made with PVC pipes. We derived gridded data using BRTs (Wolf et al., 2021). Data are available at https://andrewsforest.oregonstate.edu/data. ▪ *Vegetation*: LiDAR flight (Oregon Lidar Consortium, 2016) operating between May and June 2016 using a Leica ALS80 sensor and capturing an average of 12.64 points per square meters (Oregon Lidar Consortium, 2016). **Spatial resolution of raw data**: microclimate data derived from 184 data loggers. The original resolution of the vegetation data was at 5m.

	Map projection: all layers were reprojected in EPSG:26910 (NAD83 / UTM zone 10 N) coordinate reference system. **Temporal resolution and extent of raw data:** current microclimate data spanned from July 2009 to June 2019. We used average monthly and seasonal mean, minimum, and maximum values and also derived CDD and GDD for different temperatures and months. We considered vegetation variables to be stable variables over long-term. See the Supplementary Materials for details. **Data preprocessing:** all data were resampled to 25 m. **Dimension reduction:** we used variance inflation factor (VIF) and Pearson's correlation to reduce the number of variables and their multicollinearity.
Transfer data for projection	We transferred projection in time (across the 10 years) to validate model performance through a leave-one-out cross-validation procedure.
MODEL	
Variable pre-selection Multicollinearity	We reduced the number of initial variables through a variable pre-selection based on the correlation between variables and the variance inflation factor (VIF) through the function `vifcor` of the package `usdm` (Naimi et al., 2014). The function first pairs variables with a linear correlation higher than a pre-selected threshold and excludes the one with a greater VIF. The procedure is iterated until no pair of variables with a high correlation remains. We used Pearson's as correlation method and 0.9 as coefficient. Our aim was to avoid highly correlated

	variables and speed-up the computation time even if BRT is considered to be robust against multicollinearity.
Model settings	We used BRT and we perform an optimization to improve modeling performances of the different frameworks by varying the interaction depth, number of trees, shrinkage (also called learning rate), number of folds, and bag fraction. BRTs were built using dismo v1.3-14 (for RAY, TOC, and LTE frameworks) or dynamicSDM (for the DYN framework) v1.3.2 R packages.
Model estimates	Variable importance plots (vimps) were produced.
Non-indipendence correction/analyses	Spatial autocorrelation was considered when calibrating dynamic SDMs models.
Threshold selection	We did not produce binary maps.
ASSESSMENT	
Performance statistics	Performance was assessed by accuracy and calibration using a temporal leave-one-out cross-validation procedure. We used a rectangular bounding box for the spatial extent of independent data to include points just outside the administrative Piemonte Region and evaluate the applicability and transferability of the models outside the calibration area. We analyzed and tested different accuracy metrics to compare species' life history traits and

	modeling frameworks. We employed both threshold-dependent (TSS, F1) and -independent (AUC) metrics. We used the value that maximized the TSS as threshold for TSS and F1 calculation. We used Pearson's correlation (COR) to test for calibration and generalizability.
Plausibility check	Maps of modelled predictions were checked by experts for an ad-hoc subset of species. We also used variable importance plots (vimps) to check the plausibility of the predictions.
PREDICTION	
Prediction output	**Prediction unit**: we derived continuous probability (0-1). Uncertainty was produced for the dynamic approaches (LTE and DYN). **Post-processing steps**: none.
Uncertainty quantification	Uncertainty maps for LTE and DYN derived based on the 5th and 95th percentile of the probability distribution.

TABLE A5.2. List of the 37 species used in model calibration, validation, and prediction with their code, common and scientific name, family and order, migratory behavior, and information about models fitting. Taxonomic information derived from BirdLife International (2020).

Species code	Common Name	Scientific Name	Family	Order	Movem. life history	LTE #years	RAY cal.y	TOC Y/N	DYN Y/N
AMRO	American Robin	*Turdus migratorius*	*Turdidae*	*Passeriformes*	Migratory	9	2015	Yes	Yes
BHGR	Black-headed Grosbeak	*Pheucticus melanocephalus*	*Cardinalidae*	*Passeriformes*	Migratory	8	2011	Yes	Yes
BRCR	Brown Creeper	*Certhia americana*	*Certhiidae*	*Passeriformes*	Sedentary	10	2014	Yes	Yes
BTYW	Black-throated Warbler	*Setophaga nigrescens*	*Parulidae*	*Passeriformes*	Migratory	9	2010	Yes	Yes
CBCH	Chestnut-backed Chickadee	*Poecile rufescens*	*Paridae*	*Passeriformes*	Sedentary	6	2012	No	Yes
CORA	Common Raven	*Corvus corax*	*Corvidae*	*Passeriformes*	Partially Migratory	7	2010	Yes	Yes

DEJU	Dark-eyed Junco	*Junco hyemalis*	*Passerellidae*	*Passeriformes*	Migratory	10	2019	Yes	Yes
EVGR	Evening Grosbeak	*Hesperiphona vespertina*	*Fringillidae*	*Passeriformes*	Partially Migratory	5	2018	Yes	Yes
GCKI	Golden-crowned Kinglet	*Regulus satrapa*	*Regulidae*	*Passeriformes*	Migratory	9	2012	No	Yes
CAJA	Canada Jay	*Perisoreus canadensis*	*Corvidae*	*Passeriformes*	Sedentary	6	2011	Yes	Yes
HAFL	Hammond's Flycatcher	*Empidonax hammondii*	*Tyrannidae*	*Passeriformes*	Migratory	10	2011	Yes	Yes
HAWO	Hairy Woodpecker	*Dryobates villosus*	*Picidae*	*Piciformes*	Sedentary	7	2015	Yes	Yes
HETH	Hermit Thrush	*Catharus guttatus*	*Turdidae*	*Passeriformes*	Migratory	10	2016	Yes	Yes
HEWA	Hermit Warbler	*Setophaga occidentalis*	*Parulidae*	*Passeriformes*	Migratory	10	2019	No	Yes
HUVI	Hutton's Vireo	*Vireo huttoni*	*Vireonidae*	*Passeriformes*	Sedentary	4	2016	Yes	Yes

MGWA	MacGillivray's Warbler	*Geothlypis tolmiei*	*Parulidae*	*Passeriformes*	Migratory	10	2011	Yes	Yes
NOFL	Northern Flicker	*Colaptes auratus*	*Picidae*	*Piciformes*	Partially Migratory	7	2014	Yes	Yes
OSFL	Olive-sided Flycatcher	*Contopus cooperi*	*Tyrannidae*	*Passeriformes*	Migratory	9	2012	Yes	Yes
OSPR	Osprey	*Pandion haliaetus*	*Pandionidae*	*Accipitriformes*	Migratory	5	2012	Yes	Yes
PAWR	Pacific Wren	*Troglodytes pacificus*	*Troglodytidae*	*Passeriformes*	Migratory	10	2015	Yes	Yes
PISI	Pine Siskin	*Spinus pinus*	*Fringillidae*	*Passeriformes*	Sedentary	8	2016	Yes	Yes
PIWO	Pileated Woodpecker	*Dryocopus pileatus*	*Picidae*	*Piciformes*	Sedentary	7	2012	Yes	Yes
PSFL	Pacific-slope Flycatcher	*Empidonax difficilis*	*Tyrannidae*	*Passeriformes*	Migratory	10	2013	Yes	Yes

RBNU	Red-breasted Nuthatch	*Sitta canadensis*	*Sittidae*	*Passeriformes*	Migratory	10	2016	Yes	Yes
RECR	Red Crossbill	*Loxia curvirostra*	*Fringillidae*	*Passeriformes*	Partially Migratory	9	2018	Yes	Yes
RUGR	Ruffed Grouse	*Bonasa umbellus*	*Phasianidae*	*Galliformes*	Sedentary	7	2013	Yes	Yes
RUHU	Rufous Hummingbird	*Selasphorus rufus*	*Trochilidae*	*Caprimulgiformes*	Sedentary	4	2010	Yes	Yes
SOGR	Sooty Grouse	*Dendragapus fuliginosus*	*Phasianidae*	*Galliformes*	Sedentary	5	2013	Yes	Yes
STJA	Steller's Jay	*Cyanocitta stelleri*	*Corvidae*	*Passeriformes*	Sedentary	5	2019	No	Yes
SWTH	Swainson's Thrush	*Catharus ustulatus*	*Turdidae*	*Passeriformes*	Migratory	9	2019	No	Yes
TOSO	Townsend's Solitaire	*Myadestes townsendi*	*Turdidae*	*Passeriformes*	Partially Migratory	9	2011	Yes	Yes
VASW	Vaux's Swift	*Chaetura vauxi*	*Apodidae*	*Caprimulgiformes*	Migratory	5	2013	Yes	Yes

VATH	Varied Thrush	*Ixoreus naevius*	*Turdidae*	*Passeriformes*	Migratory	10	2015	Yes	Yes
WAVI	Warbling Vireo	*Vireo gilvus*	*Vireonidae*	*Passeriformes*	Migratory	7	2012	Yes	Yes
WETA	Western Tanager	*Piranga ludoviciana*	*Cardinalidae*	*Passeriformes*	Migratory	7	2010	Yes	Yes
WIWA	Wilson's Warbler	*Cardellina pusilla*	*Parulidae*	*Passeriformes*	Migratory	10	2016	Yes	Yes
YRWA	Yellow-rumped Warbler	*Setophaga coronata*	*Parulidae*	*Passeriformes*	Migratory	10	2014	Yes	Yes

TABLE A5.3. List of environmental variables used in the models with variable group (either microclimate or vegetation structure) and data source, unit, and brief description and ecological meaning.

Variable group and data source	Variable name	Unit	Description
Microclimate (spatial interpolation of sensors data)	CDD winter (0° C)	-	Cumulative cooling degree days (0° C threshold) between January and March; how much and for how long winter temperature were higher than 0° C
	CDD spring (0° C)	-	Cumulative cooling degree days (0° C threshold) between April and June; how much and for how long spring temperature were higher than 0° C
	CDD spring (10° C)	-	Cumulative cooling degree days (10° C threshold) between April and June; how much and for how long winter temperature were higher than 10° C
	GDD winter (5° C)	-	Cumulative growing degree days (5 °C threshold) between January and March; biologically relevant to plants and insects
	January max, mean, min T	°C	Mean daily minimum, mean, and maximum temperature of January
	February max T	°C	Mean daily maximum temperature of February
	March max and mean T	°C	Mean daily mean and maximum temperature of March
	April max T	°C	Mean daily maximum temperature of April
	May max T	°C	Mean daily maximum temperature of May

June max T	°C	Mean daily maximum temperature of June
July max, mean, min T	°C	Mean daily minimum, mean, and maximum temperature of July
August max, mean, min T	°C	Mean daily minimum, mean, and maximum temperature of August
September max and mean T	°C	Mean daily mean and maximum temperature of September
October max and mean T	°C	Mean daily mean and maximum temperature of October
November max T	°C	Mean daily maximum temperature of November
December max T	°C	Mean daily maximum temperature of December
Spring mean of max T	°C	Mean daily maximum temperature between April and June; spring max. temperatures are relevant to birds
Spring st.dev. of T	°C	Standard deviation of daily mean temperature between April and June; it reflects the T variability of the breeding season
Summer mean of max T	°C	Mean daily maximum temperature from July to September; extreme temperature metric – relevant to many taxa
Jan-Mar max and mean T	°C	Mean daily mean and maximum temperature between January and March
Jan-Mar st.dev. of T	°C	Standard deviation of daily mean temperature between January and March
Fall max T	°C	Mean daily maximum temperature between October and December; it

			reflects conditions of late animal activity before winter
Vegetation (LiDAR data)	Biomass	(Mg ha^{-1})	Aboveground live biomass
	Closure (>2 m)	%	Canopy closure of all returns above 2, 10, or 40 meters
	Closure (>10 m)	%	
	Closure (>40 m)	%	
	Density (0-2 m)	%	Canopy point density of returns from 0 to 2 and from 2 to 10 meters
	Density (2-10 m)	%	
	Height (mean)	m	Mean height of all 1st returns
	Height (st.dev.)	m	Standard deviation of height of all 1st returns
	Height (DEM)	m	Vegetation Height digital elevation model

TABLE A5.4. List of R packages used in the analysis with citations.

Package name	**Version**	**Citation**	**Purpose**
ade4	v1.7-22	Dray & Dufour, 2007	Perform PCA
data.table	v1.14.8	Dowle & Srinivasan, 2020	Data manipulation
dismo	v1.3-14	Hijmans et al., 2023c	Training of SDMs
doParallel	v1.0.17	Corporation & Weston, 2022	Parallelization of multiple tasks
dplyr	v1.1.3	Wickham et al., 2023	Data manipulation

dynamicSDM	v1.3.2	Dobson et al., 2023	Training of dynamic SDMs
emmeans	v1.8.8	Lenth, 2023	Compute joint tests of models and perform *post-hoc*
factoextra	v1.0.7	Kassambara & Mundt, 2020	Perform and assess PCA
fitdistrplus	v1.1-11	Delignette-Muller & Dutang, 2015	Test and assess distributions of models performance metrics
foreach	v1.5.2	Microsoft & Weston, 2022	Parallelization of multiple tasks
GGally	v2.1.2	Schloerke et al., 2021	Extension to ggplot2
ggplot2	v3.4.3	Wickham, 2016	Data visualization
lme4	v1.1-34	Bates et al., 2014	Linear mixed-effects model fitting
modEvA	v3.9.3	Barbosa et al., 2013	Models accuracy assessment
MuMIn	v1.47.5	Bartoń, 2023	Pseudo-R-squared for Linear mixed-effect model
PCAtest	v0.0.1	Camargo, 2023	PCA test
purrr	v1.0.2	Wickham & Henry, 2023	Data manipulation
raster	v3.6-23	Hijmans, 2023a	Spatial raster data manipulation
sf	v1.0-14	Pebesma, 2018	Spatial vector data manipulation

terra	v1.7-46	Hijmans, 2023b	Spatial raster and vector data manipulation
tmap	v3.3-2	Tennekes, 2018	Maps visualization
tidyverse	v2.0.0	Wickham et al., 2019	Data manipulation
usdm	v2.1-6	Naimi et al., 2014	Variable selection based on VIF

TABLE A5.5. List of default settings of BRTs for dismo and dynamicSDM packages used in the calibration.

Parameter	**Meaning**	**dismo**	**dynamicSDM**
Interaction depth	The maximum depth of each tree (i.e. highest level of variable interactions)	1 or 5 depending on species prevalence	Optimized 1-4
Number of trees	The number of trees in boosted regression tree models	Optimized 50-5000	5000
Shrinkage (learning rate)	Weight applied to individual trees	0.001	0.001
Number of folds	The number of different folds to split the dataset into training and testing samples	5	5
Bag fraction	The proportion of observations used in selecting variables	0.75	Based on spatiotemporal cross-validation

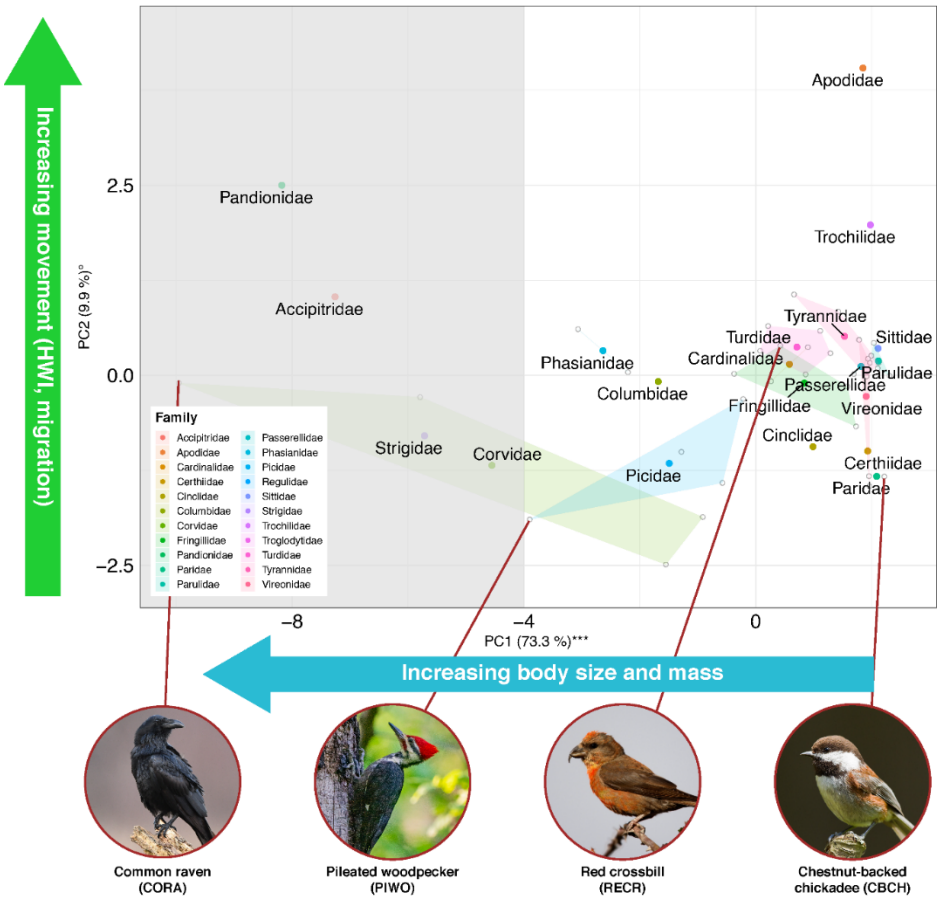

FIGURE A5.1. Principal component analysis on birds functional traits. The first PC axis is negatively associated to several body lengths measurements and body mass and explains the 73.3% of the total variance, being highly significant. The second axis is related to species movement and dispersal capacity (migratory behavior and hand-wing index, HWI) and shows no significance. Therefore, we only used PC1 and interpreted it as a proxy of body size.

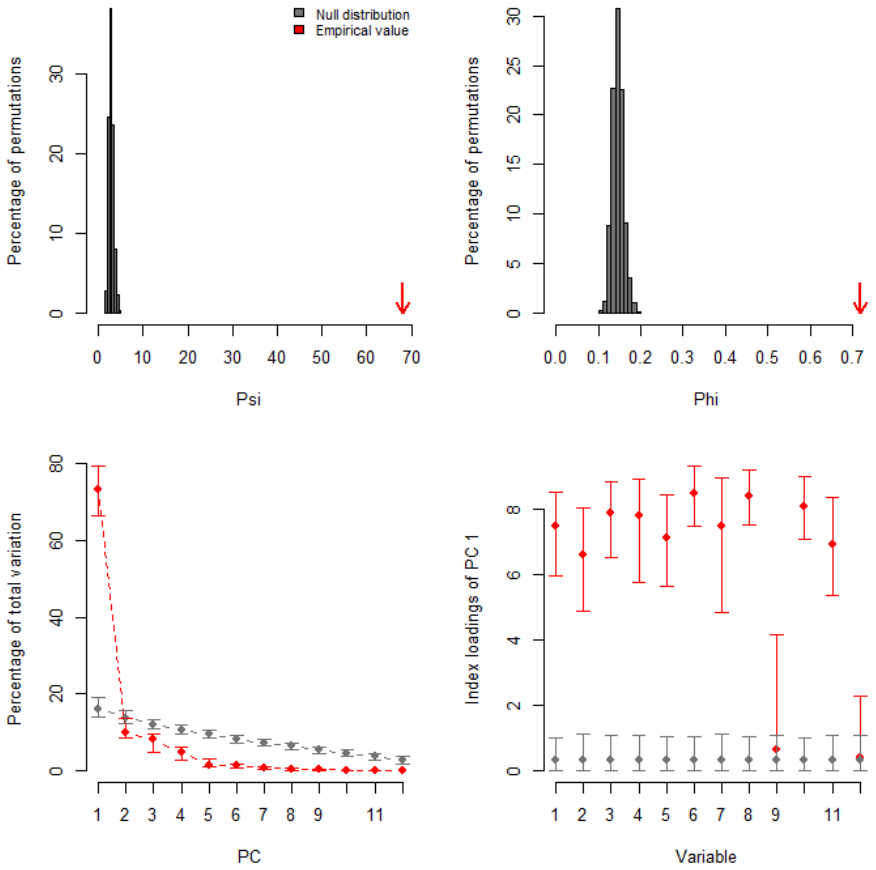

FIGURE A5.2. Results of the test on the principal component analysis on birds functional traits.

Appendix A5 – References.

Barbosa, A. M., Real, R., Muñoz, A. R., & Brown, J. A. (2013). New measures for assessing model equilibrium and prediction mismatch in species distribution models. *Diversity and Distributions*, 19(10), 1333-1338.

Barbosa, A. M., Brown, J., Jiménez-Valverde, A., & Real, R. (2016). modEvA: model evaluation and analysis.

Bartoń K (2023). `MuMIn`: Multi-Model Inference. R package version 1.47.5, <https://CRAN.R-project.org/package=MuMIn>.

Bates, D., Mächler, M., Bolker, B., & Walker, S. (2014). Fitting linear mixed-effects models using `lme4`. *arXiv preprint arXiv*:1406.5823.

Camargo A (2023). `PCAtest`: Statistical significance of PCA. R package version 0.0.1.

Corporation, M., & Weston, S. (2022). `doParallel`: Foreach Parallel Adaptor for the parallel Package. R package version 1.0.17.

Delignette-Muller, M. L., & Dutang, C. (2015). `fitdistrplus`: An R package for fitting distributions. *Journal of statistical software*, 64, 1-34.

Dobson, R., Challinor, A. J., Cheke, R. A., Jennings, S., Willis, S. G., & Dallimer, M. (2023). `dynamicSDM`: An R package for species geographical distribution and abundance modelling at high spatiotemporal resolution. *Methods in Ecology and Evolution*.

Dowle M, Srinivasan A (2023). `data.table`: Extension of `data.frame`. R package version 1.14.8, <https://CRAN.R-project.org/package=data.table>.

Dray, S., Dufour, A. (2007). The `ade4` Package: Implementing the Duality Diagram for Ecologists. *Journal of Statistical Software*, 22(4), 1–20.

Hijmans, R. (2023a). `raster`: Geographic Data Analysis and Modeling. R package version 3.6-23.

Hijmans R (2023b). `terra`: Spatial Data Analysis. R package version 1.7-39.

Hijmans RJ, Phillips S, Leathwick J, Elith J (2023c). `dismo`: Species Distribution Modeling. R package version 1.3-14, <https://CRAN.R-project.org/package=dismo>.

Kassambara A, Mundt F (2020). `factoextra`: Extract and Visualize the Results of Multivariate Data Analyses. R package version 1.0.7, <https://CRAN.R-project.org/package=factoextra>.

Kim, H., McComb, B. C., Frey, S. J., Bell, D. M., & Betts, M. G. (2022). Forest microclimate and composition mediate long-term trends of breeding bird populations. *Global Change Biology*, 28(21), 6180-6193.

Lenth, R. (2023). `emmeans`: Estimated Marginal Means, aka Least-Squares Means. R package version 1.8.7.

Microsoft, & Weston, S. (2022). `foreach`: Provides Foreach Looping Construct. R package version 1.5.2.

Oregon Lidar Consortium. (2016). 2016 McKenzie River Lidar Project lidar QC acceptance report. https://www.oregongeology.org/pubs/ldq/reports/2016_OLC_McKenzie_River_Acceptance_Report.pdf

Pebesma, E., 2018. Simple Features for R: Standardized Support for Spatial Vector Data. *The R Journal* 10 (1), 439-446, https://doi.org/10.32614/RJ-2018-009

R Core Team (2023). *R: A language and environment for statistical computing*. R Foundation for Statistical Computing, Vienna, Austria.

Schloerke B, Cook D, Larmarange J, Briatte F, Marbach M, Thoen E, Elberg A, Crowley J (2021). `GGally`: Extension to 'ggplot2'. R package version 2.1.2, <https://CRAN.R-project.org/package=GGally>.

Schulze, M., Betts, M., Frey, S. (2023). *Air temperature at core phenology sites and additional bird monitoring sites in the Andrews Experimental Forest, 2009 to present*. Long-Term Ecological Research. Forest Science Data Bank, Corvallis, OR. [Database]. Available: http://andlter.forestry.oregonstate.edu/data/abstract.aspx?dbcode=MS045

Snell Taylor, S., Di Cecco, G., & Hurlbert, A. H. (2021). Using temporal occupancy to predict avian species distributions. *Diversity and Distributions*, 27(8), 1477–1488.

Tennekes M (2018). "`tmap`: Thematic Maps in R." *Journal of Statistical Software*, *84*(6), 1-39. <https://doi.org/10.18637/jss.v084.i06>.

Wickham, H. (2016). `ggplot2`: Elegant Graphics for Data Analysis. Springer-Verlag New York.

Wickham, H., Averick, M., Bryan, J., Chang, W., McGowan, L. D., François, R., ... & Yutani, H. (2019). Welcome to the `tidyverse`. *Journal of Open Source Software*, 4 (43), 1686 (2019).

Wickham H, François R, Henry L, Müller K, Vaughan D (2023). `dplyr`: A Grammar of Data Manipulation. R package version 1.1.3, <https://CRAN.R-project.org/package=dplyr>.

Wickham H, Henry L (2023). `purrr`: Functional Programming Tools. R package version 1.0.2, <https://CRAN.R-project.org/package=purrr>.

Wolf, C., Bell, D. M., Kim, H., Nelson, M. P., Schulze, M., & Betts, M. G. (2021). Temporal consistency of undercanopy thermal refugia in old-growth forest. *Agricultural and Forest Meteorology*, 307, 108520.

Appendix B5 – Supplementary Results

TABLE B5.1. Drop-off of different validation metrics grouped by migratory behaviors. Drop-off was calculated as the performance of the dynamic model (DYN) – the performance of the most static approach (RAY).

Migratory behavior	Metric	5th percentile	Mean ± St. Dev	95th percentile
Migratory	AUC	-0.020	0.081 ± 0.054	0.159
	TSS	0.002	0.125 ± 0.077	0.217
	F1	-0.038	0.068 ± 0.073	0.136
	COR	-0.013	0.132 ± 0.089	0.271
Partially migratory	AUC	-0.033	0.073 ± 0.090	0.169
	TSS	-0.032	0.097 ± 0.103	0.199
	F1	-0.064	0.016 ± 0.060	0.070
	COR	-0.034	0.067 ± 0.073	0.117
Sedentary	AUC	-0.046	0.097 ± 0.094	0.199
	TSS	-0.047	0.143 ± 0.132	0.309
	F1	-0.059	0.068 ± 0.083	0.179
	COR	-0.069	0.119 ± 0.120	0.268

TABLE B5.2. Results of linear mixed models and post-hoc comparisons on accuracy against movement life history.

	p-values					Post-hoc comparisons			
Accuracy metric	**Framework**	**Migratory Behavior**	**Framework x Migratory Behavior**	**Movement life history**		**Random Year**	**Temporal Occupancy**	**Long-Term Ensemble**	**Dynamic SDMs**
AUC	<.0001***	0.0025**	0.0135*	Sedentary	AB	0.6±0.02^{DADB}	0.66±0.02^{ABCDADB}	0.68±0.02^{ABC}	0.69±0.02^{ABC}
				Partially Migratory	B	0.53±0.03^{DB}	0.6±0.03^{CDADB}	0.63±0.03B^{CDA}	0.61±0.03^{CDA}
				Migratory	A	0.68±0.02^{CDA}	0.68±0.02^{CDA}	0.75±0.02^{AB}	0.76±0.02^{A}
						C	B	A	A
TSS	<.0001***	0.0164*	0.0099**	Sedentary	AB	0.22±0.04^{DA}	0.33±0.04^{ABC}	0.33±0.04^{ABC}	0.35±0.04^{ABC}
				Partially Migratory	B	0.17±0.05^{CDA}	0.25±0.05^{BCDA}	0.26±0.05^{BCDA}	0.27±0.05^{ABCDA}
				Migratory	A	0.34±0.03^{CDA}	0.35±0.03^{CDA}	0.44±0.03^{AB}	0.47±0.03^{A}
						C	B	AB	A

F1				Sedentary	AB	0.39±0.06	0.44±0.06	0.43±0.06	0.46±0.06
	0.0016**	0.0404*	0.5747^{NS}	Partially Migratory	B	0.28±0.09	0.29±0.09	0.29±0.09	0.29±0.09
				Migratory	A	0.51±0.05	0.54±0.05	0.55±0.05	0.58±0.05
						B	AB	AB	A
COR				Sedentary	AB	0.13±0.04^{DADB}	0.2±0.04^{BCDADB}	0.23±0.04^{ABC}	0.25±0.04^{ABC}
	<.0001***	0.0014**	0.0001***	Partially Migratory	B	0.05±0.05^{DB}	0.11±0.05^{CDADB}	0.13±0.05^{CDADB}	0.11±0.05^{CDADB}
				Migratory	A	0.24±0.03^{CDA}	0.23±0.03^{CDA}	0.34±0.03^{AB}	0.38±0.03^{A}
						C	B	A	A

TABLE B5.3. Results of linear mixed models and post-hoc comparisons on accuracy against body size.

	p-values			*R^2*			Post-hoc comparisons			
Accuracy metric	**Framework**	**PC1**	**Framework x PC1**	**Marginal**	**Conditional**	**PC1**	**Random Year**	**Temporal Occupancy**	**Long-Term Ensemble**	**Dynamic SDMs**
AUC	<.0001***	0.1200^{NS}	0.0057**	0.11	0.49	Intercept	0.63	0.67	0.71	0.72
						Slope	0.011	0.001	0.008	0.011
							C	B	A	A
TSS	<.0001***	0.1906^{NS}	0.0016**	0.10	0.49	Intercept	0.28	0.33	0.38	0.40
						Slope	0.015	-0.001	0.011	0.014
							C	B	AB	A
F1	<.0001***	0.0139*	0.3591^{NS}	0.12	0.74	Intercept	0.43	0.47	0.47	0.49
						Slope	0.031	0.026	0.033	0.033
							B	AB	AB	A
COR	<.0001***	0.0197*	<.0001***	0.17	0.56	Intercept	0.18	0.21	0.27	0.30
						Slope	0.017	0.005	0.019	0.026
							C	B	A	A

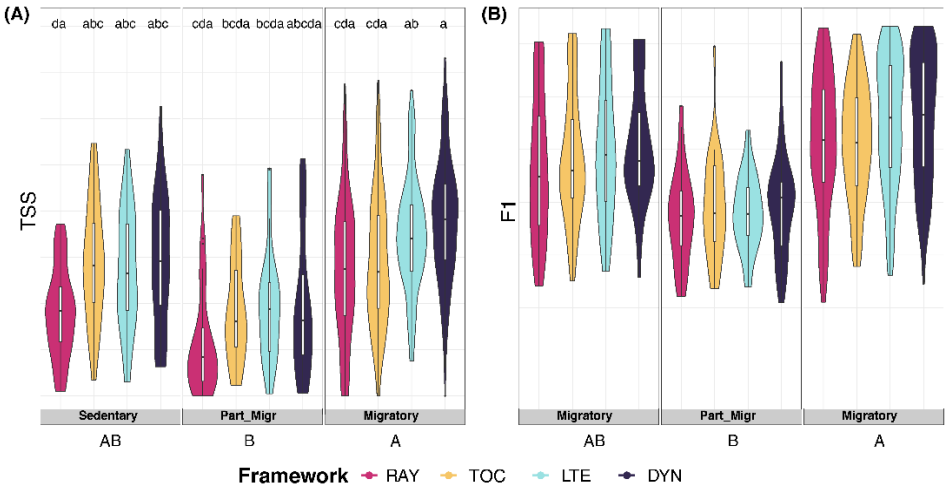

FIGURE B5.1. Results of temporal leave-one-out cross-validation of the different models according to the four modeling frameworks and three different movement behaviors (sedentary, partially migratory, and migratory) of birds. (A) violin plots of TSS results and (B) violin plots of F1 score results.

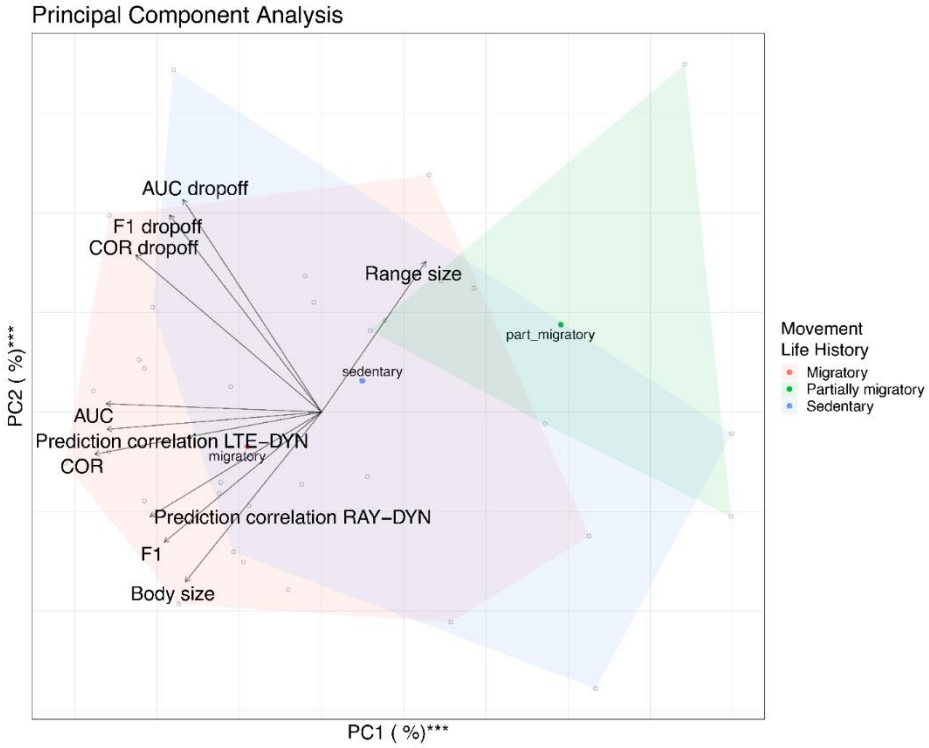

FIGURE B5.2. Principal component analysis on performance, Spearman's correlation between predictions, (decreasing) body size, and range size. Species were grouped into the three categories of movement life history. AUC, F1, and COR refer to performance of the dynamic SDMs, the drop-offs were calculated as RAY-DYN.

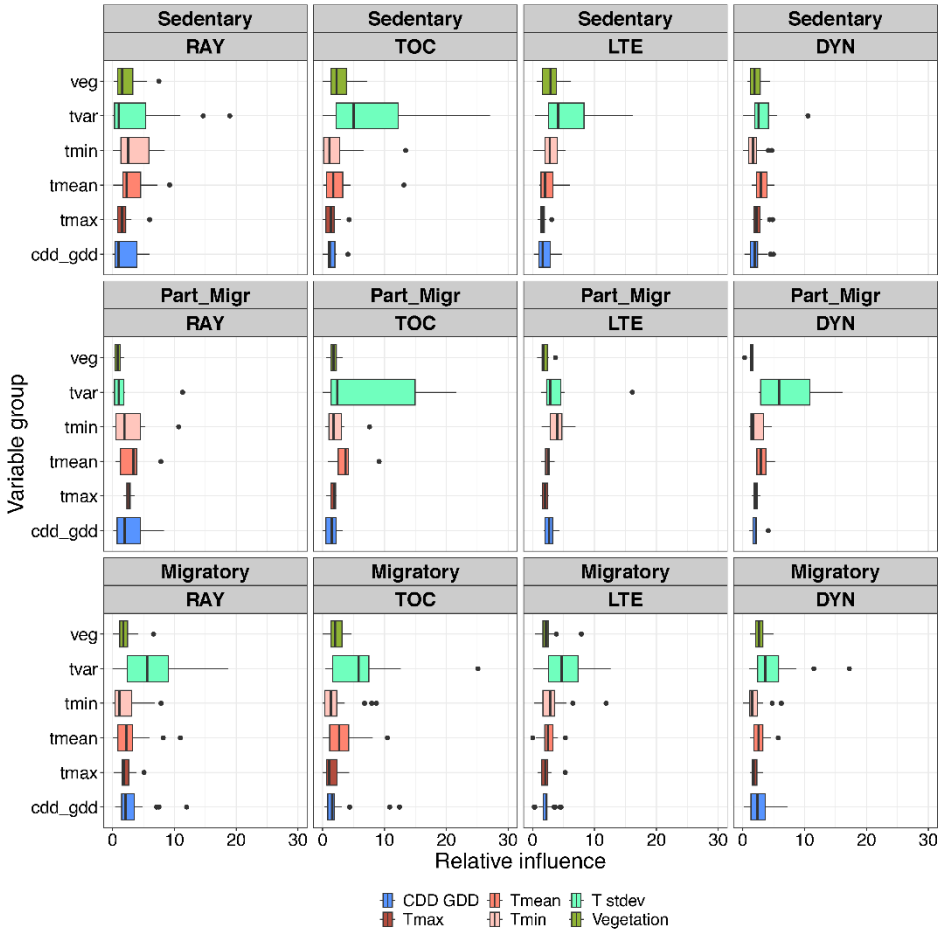

FIGURE B5.3. Variable importance according to movement life history (rows: sedentary, partially migratory, and migratory) and modeling framework (columns: random year, temporal occupancy, long-term ensemble, and dynamic SDMs). Variables were grouped into categories: CDD and GDD, Tmean = monthly or seasonal mean temperatures, T stdev = standard deviation of temperature, Tmax = monthly or seasonal maximum temperatures, Tmin = monthly or seasonal minimum temperatures, Vegetation = LiDAR-derived vegetation variables.

Appendix C5 – Probability Maps

Some examples of maps about probability of occurrence according to the different modeling scenarios for five additional species of birds.

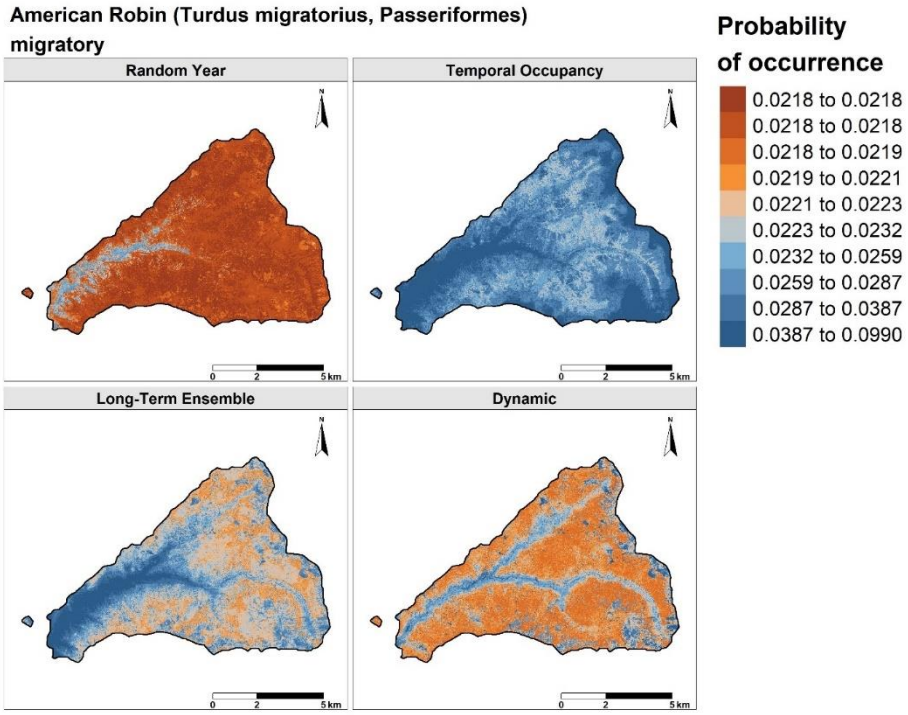

FIGURE C5.1. Spatial predictions of probability of occurrence for American robin (AMRO) according to the four modeling frameworks.

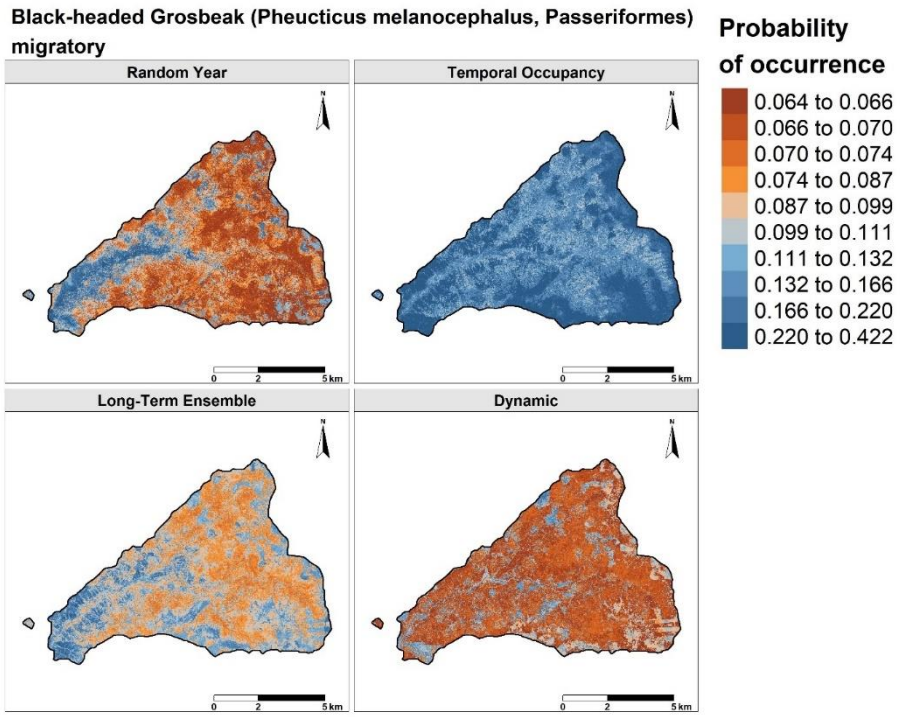

FIGURE C5.2. Spatial predictions of probability of occurrence for the Black-headed Grosbeak (BHGR) according to the four modeling frameworks.

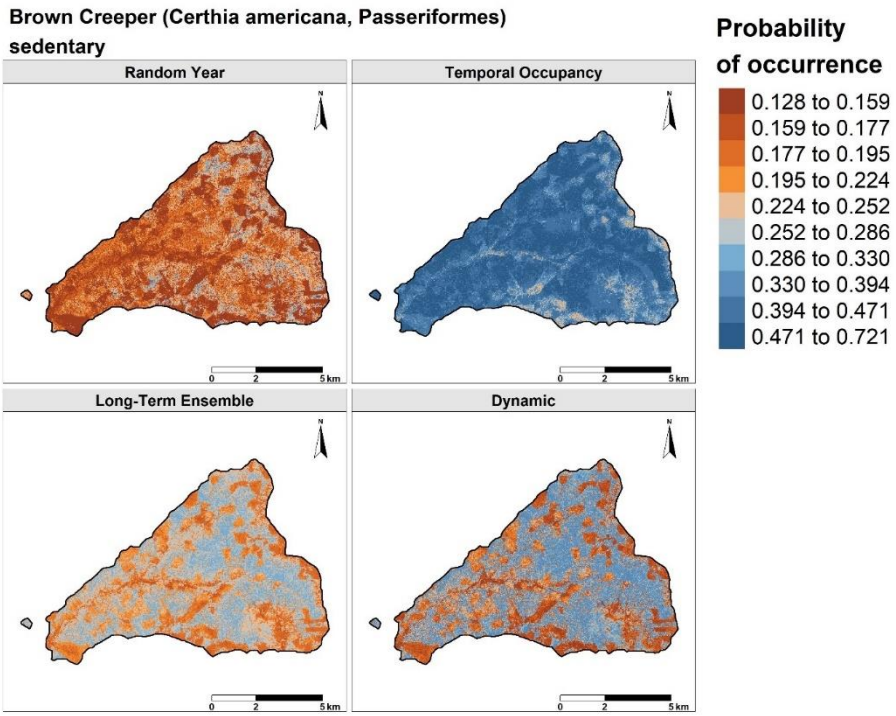

FIGURE C5.3. Spatial predictions of probability of occurrence for the brown creeper (BRCR) according to the four modeling frameworks.

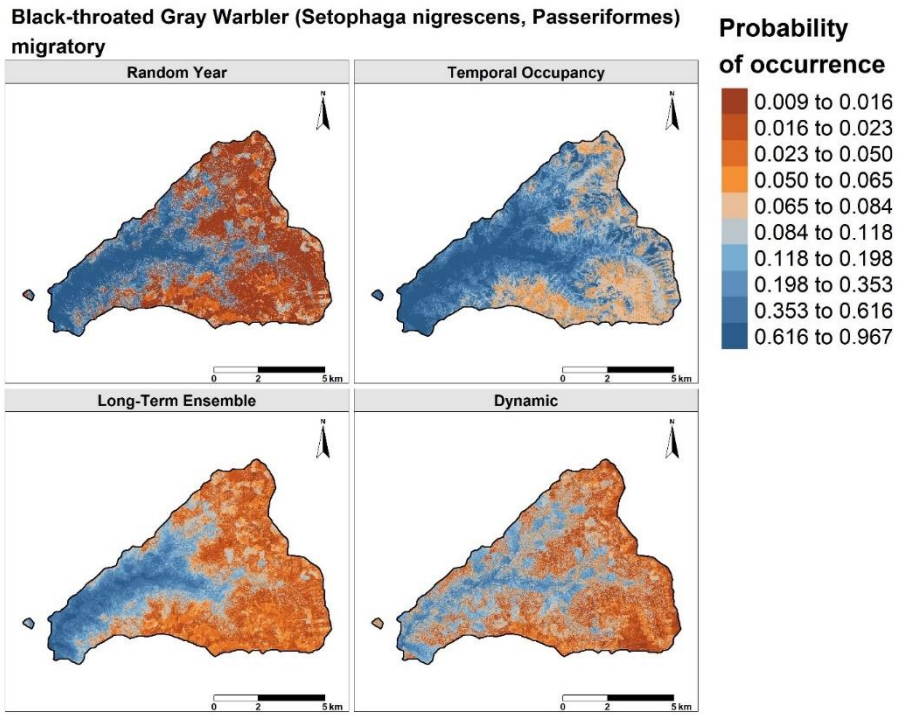

FIGURE C5.4. Spatial predictions of probability of occurrence for the black-throated gray warbler (BTYW) according to the four modeling frameworks.

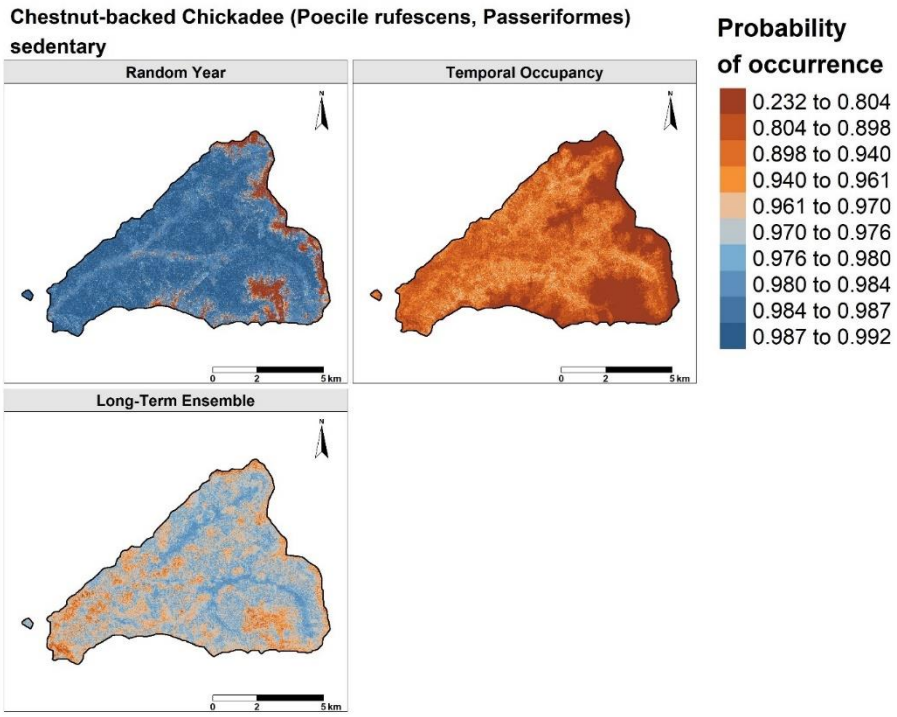

FIGURE C5.5. Spatial predictions of probability of occurrence for the chestnut-backed chickadee (CBCH) according to three modeling frameworks.

Chapter 6

General discussions

This thesis aims to analyze the main components of global environmental change on mountain forest ecosystems from a landscape ecology perspective (Figure 6.1). The four research chapters (Chapter 2 to Chapter 5) represent different spatiotemporal scale approaches to a complex and compelling global issue that can contribute to the growing literature on this compelling global issue. We have provided different perspectives on the role of landscape ecology for analyzing mountain forest dynamics in the light of land-use and climate changes. In analyzing the effects of climate and land-use change on mountain forests, we explored two main foundations of the discipline of landscape ecology: (i) ecological scale and (ii) spatial ecological models, which formed the common threads of this work.

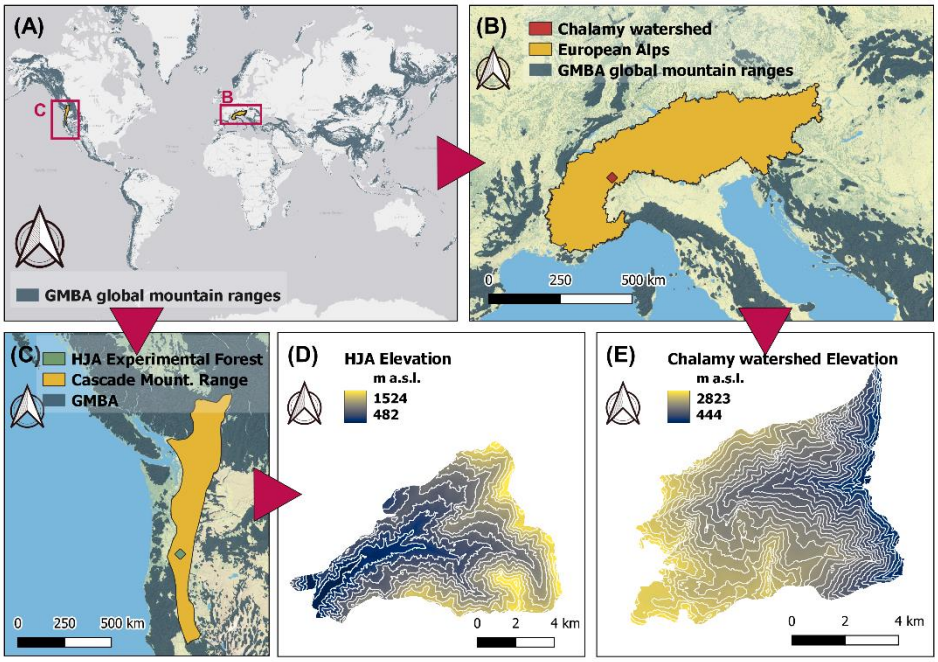

Figure 6.1. Locations of the different case studies included in the thesis. (a) global overview of mountain ranges according to the Global Mountain Biodiversity Assessment (GMBA v1.4;

Snethlage et al., 2022). The panels (b) and (c) represent at the regional scale the European Alps (Chapters 2, 3, 4) and the Cascade Range (Chapter 5) respectively. Panel (d): elevation and contour lines of the H.J. Andrews Experimental Forest in the Cascades (Chapter 5). Panel (e): elevation and contour lines of the Chalamy watershed in the European Alps (Chapter 3).

With Chapter 2 (Figure 6.1b) we aimed to assess the main drivers of post-abandonment reforestation in the European Alps and in Chapter 3 (Figure 6.1e) we quantified 50 years of changes in land-use and predicted future trajectories in a subalpine landscape of the Italian Alps. In Chapter 4 (Figure 6.1b) we constructed correlative species distribution models (SDMs) for tree species to compare fine- and coarse-calibration models and to predict the probability of occurrence under different climate scenarios in the Northwest Italy. In Chapter 5 (Figure 6.1c, d) we analyzed a different taxa – birds – and built long-term (10-year) landscape-scale SDMs to compare their performance and predictions with static and short-term SDMs in a forest matrix of the Cascade Range (USA).

A common thread discussed in the hole thesis was the emphasis on forest landscape planning and management. Although a global phenomenon, recent human-induced changes to natural resources have the potential to be managed locally or regionally in practice (Guisan et al., 2013). Therefore, the aim of three out of the four research chapters was to address changes in mountain forests at a scale which is finer than most of the global change studies but corresponding to the scale of management and decision-making.

This Chapter discusses the contribution of this thesis to mountain forest ecosystems (Section 6.1) and ecological modeling (Section 6.2). Finally, general and specific limitations and possible approaches to address them are presented in Section 6.3.

6.1 Mountain forest ecosystems: a global change research agenda

The global change research agenda has growing rapidly in recent years, not only because of the growing interest and awareness of these topics, but also because of the easy access to data, resources, and computational power (Ripple et al.,

2020; Pettorelli et al., 2021). Landscape ecology has the potential to provide useful tools for managers and planners (Stürck & Verburg, 2017). The climate and topography of a region not only directly influence ecosystem structure by providing the physical template for species to occur (i.e., the Grinnellian niche *sensu* Grinnell, 1924), but also indirectly by driving human actions and land use (e.g., MacDonald et al., 2000; Mietkiewicz et al., 2017). Although often neglected – or poorly incorporated – in global change ecology, the land use history of regions and landscapes is a critical step in integrating land use change into climate change ecology, and vice versa (Carlson et al., 2014; Garbarino & Weisberg, 2020). In particular, the magnitude and severity of global change on forests and communities is largely dependent on the number of concurrent global change drivers (Komatsu et al., 2019). The four case studies presented in this thesis are located in two different mountain ranges: the European Alps (Chapters 2, 3, and 4; Figure 6.1b) and the Cascade Range (Chapter 5; Figure 6.1c). These two mountain regions have a peculiar human history, that has shaped the forest landscape structure over time.

European Alps extend for 1200 km from east to west. They exhibit strong topographic variability, affecting temperatures and precipitation at different spatiotemporal scales (Isotta et al., 2014). These climatic gradients not only influence natural vegetation trajectories, but also the millennial history of land use of the region, especially after the Würm glaciation (Favilli et al., 2010; Mietkiewicz et al., 2017). While south-facing accessible slopes were mainly converted into pastures and crops (Kulakowski et al., 2011), steeper and cooler north-facing slopes were used for timber and charcoal production (Ludemann, 2010; Garbarino et al., 2022). The legacy of land use eventually changed the species composition of both tree and understory communities (e.g., Orlandi et al., 2016; Abadie et al., 2018). Beginning in the 19th century, the industrial revolution triggered an intense exodus from the marginal mountain valleys to urban and industrial centres in the lowlands (Batzing et al., 1996; MacDonald et al., 2000; Mietkiewicz et al., 2017). Following agricultural abandonment, secondary

succession has occurred in areas that had been converted to cropland and pasture for millennia (Gehrig-Fasel et al., 2007; Garbarino et al., 2020). The Chalamy watershed analyzed in Chapter 3 is a paradigmatic Alpine landscape. For centuries, it was heavily exploited for charcoal production (Garbarino et al., 2022), a common dynamic in many European mountain ranges (e.g., Apennines, Carrari et al., 2016; Pyrenees, Saulnier et al., 2018). This long-lasting activity left a pervasive legacy in the landscape structure and composition, leading to a large species turnover from Norway spruce-dominated forests to young stands of pioneer pines, such as Scots pine and mountain pine (*Pinus mugo* Turra subsp. *uncinata*). Most of the area is now part of the Mont Avic Natural Park.

The Cascade Range extends over 1,100 km from Lassen Peak, northern California (USA), through Oregon and Washington to the Fraser River in southern British Columbia (Canada). Although similar in size to the European Alps, its north-south orientation, parallel to the Pacific coast, generates a strong barrier to moist air coming from the ocean (Case & Peterson, 2005). Therefore, a strong climatic gradient exists between the western and eastern slopes. The west side is characterized by a wet maritime climate and highly productive temperate rainforests, while the east side, characterized by a continental climate, is dominated by dry grasslands and forests (Franklin & Dyrness, 1988). What history of land use is for the European Alps, fire is for the Cascades and other North American mountain ranges. Wildfire has historically shaped the spatial patterns and structure of forest ecosystems in the region (Hagmann et al., 2014; Larson et al., 2022). The disturbance regime in ponderosa pines *Pinus ponderosa* Douglas ex C. Lawson stands of the Eastern Cascades is one of the most studied fire regimes globally. It was characterized by frequent low-severity surface fires (Haugo et al., 2019; Littlefield et al., 2020; Larson et al., 2022). Traditional indigenous use of fire had contributed to maintain the natural spatial pattern of these ecosystems (Hessburg et al., 2005). Livestock and wild ungulate grazing, road and rail construction, grassland conversion to agriculture, urbanization, and rural development in the modern era have all contributed to the exclusion of fires

in the region (Hessburg et al., 2005; Parks et al., 2023). Since the 20th century, fire regimes have shifted towards high-severity crown fires, with hindered post-fire recovery (Littlefield et al., 2020). Therefore, fire-tolerant large-diameter trees that were historically abundant in forests with low and moderate severity fire regimes are now much less common, with cascading effects on ecosystem functioning and biodiversity conservation, and concerns about a potential transition to non-forest ecosystems (Hagmann et al., 2014; LeFevre et al., 2020; Larson et al., 2022). There is wide variability in historical fire regimes across the western side of the range, with mean fire return intervals ranging from 6 to 165 years (Johnston et al., 2023). Douglas-fir stands exhibited high- or mixed-severity infrequent events, mostly coupled with summer vapor pressure deficits. Increased dry conditions and a fuel build-up due to fire exclusion is currently leading to more frequent, larger, and severe wildfires in wetter parts of the Pacific Northwest (Reilly et al., 2017; Haugo et al., 2019; Merschel et al., 2021; Larson et al., 2022).

This thesis underlines the importance of analyzing the history of land use and its legacies in mountain forests. Reconstructing the impact of land-use legacies on forest landscapes requires a multidisciplinary and multiscale approach (Gimmi & Bugmann, 2013; Garbarino & Weisberg, 2020). Landscape history not only explains the current configuration of forests, but also guides and influences the future ecosystem resilience to disturbance, management, and global change (Garbarino & Weisberg, 2020). The goal should not be to restore historical conditions for their own sake, but to characterize and assess the historical patterns that have shaped these forests over centuries in order to foster adaptation to projected environmental changes in climate, land use, and disturbance regimes (Hagmann et al., 2014; Szabó, 2015; Garbarino et al., 2022). Integration between historical and current global change drivers is key. We attempted to explicitly consider interactive drivers in Chapter 2, where we showed that climate change is still a minor driver of forest gain in the European Alps. The issue was also partially discussed in Chapters 3 and 4, but without ad hoc analysis. We argue

that such explicit integration should take place at different spatiotemporal scales if the aim is to define best practices in landscape planning and restoration.

Past land uses play a strong role in shaping current mountain forest communities (Plue et al., 2008; Abadie et al., 2018). The time required for passive restoration to restore biogeochemical functions has been measured aa 35.5 ± 33.1 years, depending on ecosystem resilience, the type and intensity of land-use legacies, and local edaphic conditions (Meli et al., 2017). Even after centuries, current ecosystems reflect the past land uses in terms of soil conditions, species pool, or landscape structure (Flinn & Vellend, 2005; Dyer, 2010; Abadie et al., 2018). For instance, "recent" forests (i.e., forest stands originated from former croplands, pastures, or grasslands) often have lower organic matter, but higher nutrient content due to nutrient provision (Koerner et al., 1997; Flinn & Vellend, 2005). Moreover, forests that developed from former pasture had similar pattern and trajectories with "ancient" forests, whereas forests that originated from croplands had different species composition (Dyer, 2010). Given the rate of change induce by global change, high levels of biodiversity are essential to ensure rapid species turnover and avoid habitat loss (Allan et al., 2011).

By integrating some of the issues addressed in this thesis, there is the potential to address changes in understory communities by integrating land-cover maps and SDMs. For instance, Braziunas et al. (2024) recently built SDMs for understory species by accounting for both shifts in climate and in forest structure in a protected area of the German Alps. Carlson et al. (2014) accounted for glacier retreat and forest expansion in SDMs by explicitly modeling future land-use scenarios in the French Alps. These studies provide examples of how climate change, land use change and landscape structure can be combined to inform decision-making in the context of global change. Starting from the methodology adopted in the different chapters of this thesis, it would be advisable to develop a multi-scale and multi-model approach for different landscapes through hierarchical SDMs (e.g., Mateo et al., 2019). At a regional scale, Gelabert et al. (2022) applied an interesting framework to produce wall-to-wall maps of

probability of land abandonment in mountain regions, which can be developed for the European Alps by refining the approach we used in Chapter 2. Future trajectories of land use and land cover for the region can be derived from a Business-as-Usual perspective similarly to the MLP-MC procedure applied in Chapter 3. Then, SDMs can be built for different taxa including land use as predictor variable, using a dynamic (*sensu* Chapter 5) modeling strategy. The resulting outcomes of this exercise may provide interesting insights for different ecological questions or hypothesis in the study of protected areas, microrefugia, and treeline ecotones, that we try to anticipate.

Mountain forests are protected for the 14% of their area. The percentage of protected areas (PAs) in the Alps reaches 28% (53,000 km^2), while 13% (18,831 km^2) of the Cascade Range is protected. PAs provide high quality habitats that are protected from deforestation and agricultural and urban expansion (Andam et al., 2008; de Moraes et al., 2017). Protected forests have global cascading effects through carbon sequestration and biogeophysical climate feedbacks (Watson et al., 2014). Furthermore, we have already discussed the importance of considering microclimate into ecological research and SDMs. PAs were more effective than unprotected areas in buffering thermal increases due to climate change across several biomes (Xu et al., 2023). By simultaneously providing microclimate and habitat conservation, PAs can host many microrefugia, defined as small areas where populations can persist in favorable microclimate conditions during periods of unfavorable climate (Ashcroft et al., 2012; Hannah et al., 2014; Finocchiaro et al., 2023). We argue that quantifying the potential gain in undisturbed habitat and predicting future microrefugia inside and outside protected areas would be useful for implementing conservation and restoration strategies in different forest biomes and ecosystems. The Convention on Biological Diversity proposed to reach 30% of global land surface protection by 2030 (CBD, 2021). SDMs and land-use change models could be useful for spatial zonation and prioritization and may be integrated to assess the effectiveness of core areas, decide if and where to expand a PA, or outline important features to

protect (e.g., Guisan et al., 2013; Wan et al., 2017; Buenafe et al., 2023). Moreover, it is interesting to note that recent PAs (i.e., designated after the 60s) in the European Alps were mostly designated in marginal areas with predominant out-migration (Bender et al., 2017). This reinforces the strength of land abandonment and the resulting secondary succession in buffering thermal extremes caused by climate change.

Another possible playground for studying land-use legacies and predicting future trajectories of land use and climate is the treeline ecotone. Treelines are generally advancing worldwide, although there is local variability (Harsch et al., 2009; Hansson et al., 2021). The main driver of this elevational and latitudinal shift is global warming, but abandonment plays a pivotal role in European mountains (Ameztegui et al., 2016; Gehrig-Fasel et al., 2017). Treelines are an important environment to study the effects of climate change and its interactions with land abandonment (Ameztegui et al., 2016; Garbarino et al., 2023). Aerial images have been used to map forest cover over time and assess changes in land cover and habitat availability (Nguyen et al., 2022; Wang et al., 2022; Birre et al., 2023). They can generate not only land cover maps, but also landscape metrics that can inform correlative models such as SDMs in delineating potential distribution of several species (e.g., see Hu & Tong, 2022 for a similar application). For instance, an interesting application of SDM would be to assess seedling probability of occurrence and distribution at the treeline scale. Seedling niches have narrower climate envelopes than those of mature trees, and regeneration requirements can vary substantially among species at a very fine scales (Canham & Murphy, 2016). Little is known about the creation of novel habitats and microrefugia at higher elevations that manifest tree and shrub encroachment, and insights from this work may be helpful in this sense.

6.2 Ecological modeling: a mere academic exercise or a useful resource?

In the context of rapid and profound alterations to the Earth system, modeling is crucial to provide scenarios and anticipate expected shifts in ecological functioning. However, in a recent review, Zurell et al. (2022) found that only 1 to 5% of correlative SDMs studies published since 1995 produced clear management decisions for conservation and restoration of animals. A quantitative review of all ecological models in decision making is lacking, but the actual numbers are expected to be in this order of magnitude. A legitimate concern may therefore be: is spatial ecological modeling a mere academic exercise or can it be a useful resource for decision-making?

Several authors are confident that management decisions can be supported by models (Schuwirth et al., 2019; Dhyani et al., 2023) but decision-makers or managers sometimes perceive ecological models as useless or, even worse, as tools that can be misapplied to provide desired and incorrect predictions. Participatory modeling approaches with stakeholders and practitioners have been proposed as a way to overcome this problem (Parrott, 2017). Moreover, further challenges involve technical and ecological issues. For instance, many studies show a mismatch between the scale of application and the scale of management decisions (Guisan et al., 2013; Araújo et al., 2019). In Chapters 4 and 5, we tried to assess this issue in correlative models. We tried to increase the detail of the analysis at a local scale by incorporating finer resolution in space (Chapter 4) and time (Chapter 5). Local models for tree species better captured the current conditions at the extent of calibration, but it suffered from niche truncation when predicting future changes. We argued that different aims may be addressed using different scales, with current mapping better tackled through local inventories and fine-scale predictors and forecasting more suited to broad-scale patterns. Chapter 5 provides a reproducible and scalable application of SDMs using long-term observation and fine-scale predictors to build dynamic models accounting for

microclimate. We believe this approach can be applied to different ecosystems and spatiotemporal extents, as also highlighted by Milanesi et al. (2020).

As discussed in the previous section, modeling has the potential to account for interactions between land-use change, its legacies, and climate change (different drivers of global change) at different levels, from predictor variables to predicted outcomes. We believe that this thesis can provide a strong foundation for a comprehensive study of global change at the landscape to regional scale, incorporating multiple drivers and modeling tools. Nevertheless, it is hard to find the right balance between model complexity and the increase in model performance and reliability, given that adding detail beyond a certain threshold may result in a reduced payoff in model development (Loehle, 1990).

6.3 Limitations and future perspectives

Specific and general limitations are listed in this section, together with some possible solutions and future research to overcome them.

The main weakness of Chapter 2 "*Global change in the European Alps: a century of post-abandonment natural reforestation at the landscape scale*" is the lack of harmonization among different data sources. For example, there were inconsistencies in the rate of forest gain, with some studies covering almost 200 years and others only the last 40 or 50 years. Also, images, land cover classes and classification methods may have differed between studies or research groups. Nevertheless, we considered our results as the best approximation of the dynamics of forest gain across the European Alps, and further information can only be obtained through a systematic re-analysis based on classification sources. Producing a harmonized geodatabase of land-use changes at the landscape scale across the European Alps is one of the aims of future research. With this data, we aim to interpolate a wall-to-wall probabilistic occurrence of land abandonment and consequent reforestation to answer to research questions and address ecological hypotheses. Another interesting avenue for further investigation could involve examining land conversion and land-use legacies by exploring whether

the historical land use of the "recent" forests consists of unsuitable agricultural areas.

In Chapter 3 "*Land use modeling predicts divergent patterns of change between upper and lower elevations in a subalpine watershed of the Alps*" we assumed that recent successional dynamics in the upper elevations (i.e., primary successions from unvegetated – or sparsely vegetated – areas to grassland or sparse forest) were mainly related to climate change. However, we did not explicitly test for climate in the analysis. This could be done directly by using it as a predictor variable in the model or indirectly by assessing correlations between past climate and land uses. Our main concern would be that is difficult to infer these relationships on one site only, and possible future research may be use the past and future maps obtained from a harmonized geodatabase to test for the influences of climate in the past and future.

Chapter 4 "*Local forest inventory data improve species distribution model predictions*" and Chapter 5 "*Long-term data and temporal dynamic frameworks can improve landscape-scale species distribution models*" presented alternative applications of SDMs at local extent and compare this fine spatial (Chapter 4) and temporal (Chapter 5) scale to the common scale of SDM applications. Regarding Chapter 4, the higher performance from the local tree inventory may result from the precision of the data in terms of tree determination and plot location. The European inventory (i.e., EU-Forest) had a higher uncertainty of plot location that may have impacted the model performance. A possible way to overcome this issue would be to account for this uncertainty in predictor variables (e.g., Naimi et al., 2011, 2014).

Another issue in using local observations is niche truncation (Suárez-Seoane et al., 2013; Rousseau & Betts, 2022), which can affect the scaling and extrapolation of models to different spatiotemporal resolutions and extents. However, local and coarse models built in Chapter 4 did not show significant differences in performance when tested on independent datasets (Figure 4.4). This can be an indicator of limited niche truncation that can minimize problems in current

predictions. Nevertheless, when projecting probability of occurrence under future scenarios, we tend to rely more on coarse models that better represent the entire niche of a species. One possible implementation that we did not test for is to explicitly assess the niche truncation and the niche differences between modeling frameworks, where we could have assessed species-specific differences among models. As for Chapter 5, models should not suffer from niche truncation if the aim is to predict distribution of birds at the same limited scale for a short period of time. Nevertheless, other critical drivers of population dynamics, such as dispersal, mortality, and reproduction might be important to address at this scale (e.g., Singer et al., 2016 for a community-level mechanistic model). Acevedo et al. (2017) proposed the use of residuals of regression as a proxy of population growth rate and the use of upper limits of abundance as a proxy of the environmental carrying capacity. Braziunas et al. (2024) built SDMs using forest structure layers resulting from the landscape model iLand (Seidl et al., 2012) to assess the role of landscape structure versus climate change in understory communities. Further research at this scale might include these approaches as well as macroecology in terms of distance to the niche edges (e.g., Banks-Leite et al., 2022).

Generally, our models were calibrated at the species level but interest toward population and genetic levels is increasing, although 72% of ecological models still focus on species (Zurell et al., 2022). Future investigations may focus on populations or genetics, where the role of local observations and predictors may increase the reliability of the models by incorporating data that are at the appropriate scale for mechanisms operating at finer scale. Moreover, this thesis mainly presented correlative models, and no mechanistic approaches were developed. Nevertheless, given the increasing availability of observation and experimental data and computational resources, these two different worlds are more than ever easy to combine. Following up and learning from this work, multi- and cross-scale studies using multiple models and objectives are expected to increase the reliability and impact of ecological research, particularly ecological

modelling. The main highlights from this thesis are: (i) the integration of land use legacies and climate scenarios can help to unravel the drivers of change in mountain forest ecosystems; (ii) correlative SDMs and land use change models can act synergistically to link spatio-temporal patterns to ecological processes; (iii) fine-scale mechanistic models and population dynamics can be integrated into modelling frameworks to predict stages of landscape change; (iv) hierarchical SDMs can serve as a useful tool for policy makers and planners.

References

Abadie, J., Avon, C., Dupouey, J. L., Lopez, J. M., Tatoni, T., & Bergès, L. (2018). Land use legacies on forest understory vegetation and soils in the Mediterranean region: Should we use historical maps or in situ land use remnants?. *Forest Ecology and Management*, 427, 17-25.

Acevedo, P., Ferreres, J., Escudero, M. A., Jimenez, J., Boadella, M., & Marco, J. (2017). Population dynamics affect the capacity of species distribution models to predict species abundance on a local scale. *Diversity and Distributions*, 23(9), 1008-1017.

Allan, E., Weisser, W., Weigelt, A., Roscher, C., Fischer, M., & Hillebrand, H. (2011). More diverse plant communities have higher functioning over time due to turnover in complementary dominant species. *Proceedings of the National Academy of Sciences*, 108(41), 17034-17039.

Ameztegui, A., Coll, L., Brotons, L., & Ninot, J. M. (2016). Land-use legacies rather than climate change are driving the recent upward shift of the mountain tree line in the Pyrenees. *Global Ecology and Biogeography*, 25(3), 263-273.

Andam, K. S., Ferraro, P. J., Pfaff, A., Sanchez-Azofeifa, G. A., & Robalino, J. A. (2008). Measuring the effectiveness of protected area networks in reducing deforestation. *Proceedings of the national academy of sciences*, 105(42), 16089-16094.

Araújo, M. B., Anderson, R. P., Barbosa, A. M., Beale, C. M., Dormann, C. F., Early, R., Garcia, R. A., Guisan, A., Maiorano, L., Naimi, B., O'Hara, R. B., Zimmermann, N. E., & Rahbek, C. (2019). Standards for distribution models in biodiversity assessments. *Science Advances*, 5(1), eaat4858.

Ashcroft, M. B., Gollan, J. R., Warton, D. I., & Ramp, D. (2012). A novel approach to quantify and locate potential microrefugia using topoclimate, climate stability, and isolation from the matrix. *Global Change Biology*, 18(6), 1866-1879.

Banks-Leite, C., Betts, M. G., Ewers, R. M., Orme, C. D. L., & Pigot, A. L. (2022). The macroecology of landscape ecology. *Trends in Ecology & Evolution*.

Batzing, W., Perlik, M., & Dekleva, M. (1996). Urbanization and Depopulation in the Alps. *Mountain Research and Development*, 16(4), 335.

Bender, O., Roth, C. E., & Job, H. (2017). Protected areas and population development in the Alps. *Eco.mont*, 9, 5-16.

Birre, D., Feuillet, T., Lagalis, R., Milian, J., Alexandre, F., Sheeren, D., ... & Bader, M. Y. (2023). A new method for quantifying treeline-ecotone change based on multiple spatial pattern dimensions. *Landscape Ecology*, 38(3), 779-796.

Braziunas, K. H., Geres, L., Richter, T., Glasmann, F., Senf, C., Thom, D., ... & Seidl, R. (2024). Projected climate and canopy change lead to thermophilization and homogenization of forest floor vegetation in a hotspot of plant species richness. *Global Change Biology*, 30(1), e17121.

Buenafe, K. C. V., Dunn, D. C., Everett, J. D., Brito-Morales, I., Schoeman, D. S., Hanson, J. O., ... & Richardson, A. J. (2023). A metric-based framework for climate-smart conservation planning. *Ecological Applications*, 33(4), e2852.

Canham, C. D., & Murphy, L. (2016). The demography of tree species response to climate: seedling recruitment and survival. *Ecosphere*, 7(8), e01424.

Carrari, E., Ampoorter, E., Verheyen, K., Coppi, A., & Selvi, F. (2016). Former charcoal kiln platforms as microhabitats affecting understorey vegetation in Mediterranean forests. *Applied Vegetation Science*, 19(3), 486-497.

Carlson, B. Z., Georges, D., Rabatel, A., Randin, C. F., Renaud, J., Delestrade, A., ... & Thuiller, W. (2014). Accounting for tree line shift, glacier retreat and primary succession in mountain plant distribution models. *Diversity and Distributions*, 20(12), 1379-1391.

Case, M. J., & Peterson, D. L. (2005). Fine-scale variability in growth climate relationships of Douglas-fir, North Cascade Range, Washington. *Canadian Journal of Forest Research*, 35(11), 2743-2755.

CBD. (2021). *First draft of the post-2020 global biodiversity framework*. CBD/WG2020/3/3. Convention on Biological Diversity.

de Moraes, M. C. P., de Mello, K., & Toppa, R. H. (2017). Protected areas and agricultural expansion: Biodiversity conservation versus economic growth in the Southeast of Brazil. *Journal of Environmental Management*, 188, 73-84.

Dhyani, S., Adhikari, D., Dasgupta, R., & Kadaverugu, R. (2023). *Ecosystem and Species Habitat Modeling for Conservation and Restoration*.

Dyer, J. M. (2010). Land-use legacies in a central Appalachian forest: differential response of trees and herbs to historic agricultural practices. *Applied Vegetation Science*, 13(2), 195-206.

Favilli, F., Cherubini, P., Collenberg, M., Egli, M., Sartori, G., Schoch, W., & Haeberli, W. (2010). Charcoal fragments of Alpine soils as an indicator of landscape evolution during the Holocene in Val di Sole (Trentino, Italy). *The Holocene*, 20(1), 67-79.

Finocchiaro, M., Médail, F., Saatkamp, A., Diadema, K., Pavon, D., & Meineri, E. (2023). Bridging the gap between microclimate and microrefugia: A bottom-up approach reveals strong climatic and biological offsets. *Global Change Biology*, 29(4), 1024-1036.

Flinn, K. M., & Vellend, M. (2005). Recovery of forest plant communities in post-agricultural landscapes. *Frontiers in Ecology and the Environment*, 3(5), 243-250.

Franklin, J. F.,and C. T. Dyrness. 1988. *Natural vegetation of Oregon and Washington.* Second edition. Oregon State University Press, Corvallis, Oregon, USA.

Garbarino, M., Morresi, D., Anselmetto, N., & Weisberg, P. J. (2023). Treeline remote sensing: from tracking treeline shifts to multi-dimensional monitoring of ecotonal change. *Remote Sensing in Ecology and Conservation*.

Garbarino, M., Morresi, D., Meloni, F., Anselmetto, N., Ruffinatto, F., & Bocca, M. (2022). Legacy of wood charcoal production on subalpine forest structure and species composition. *Ambio*, 51(12), 2496-2507.

Garbarino, M., Morresi, D., Urbinati, C., Malandra, F., Motta, R., Sibona, E. M., … & Weisberg, P. J. (2020). Contrasting land use legacy effects on forest landscape dynamics in the Italian Alps and the Apennines. *Landscape Ecology*, 35, 2679-2694.

Garbarino, M., & Weisberg. P.J. (2020). Land-use legacies and forest change. *Landscape Ecology*, 35: 2641–2644.

Gehrig-Fasel, J., Guisan, A., & Zimmermann, N. E. (2007). Tree line shifts in the Swiss Alps: climate change or land abandonment? *Journal of vegetation science*, 18(4), 571-582.

Gelabert, P. J., Rodrigues, M., Vidal-Macua, J. J., Ameztegui, A., & Vega-Garcia, C. (2022). Spatially explicit modeling of the probability of land abandonment in the Spanish Pyrenees. *Landscape and Urban Planning*, 226, 104487.

Gimmi, U., & Bugmann, H. (2013). Preface: Integrating historical ecology and ecological modeling. *Landscape Ecology,* 28: 785–787.

Grinnell, J., 1924. Geography and evolution. *Ecology* 5, 225–229.

Guisan, A., Tingley, R., Baumgartner, J. B., Naujokaitis-Lewis, I., Sutcliffe, P. R., Tulloch, A. I. T., Regan, T. J., Brotons, L., McDonald-Madden, E., Mantyka-Pringle, C., Martin, T. G., Rhodes, J. R., Maggini, R., Setterfield, S. A., Elith, J., Schwartz, M. W., Wintle, B. A., Broennimann, O., Austin, M., … Buckley, Y. M. (2013). Predicting species distributions for conservation decisions. *Ecology Letters*, 16(12), 1424–1435.

Hagmann, R. K., Franklin, J. F., & Johnson, K. N. (2014). Historical conditions in mixed-conifer forests on the eastern slopes of the northern Oregon Cascade Range, USA. *Forest Ecology and Management*, 330, 158-170.

Hannah, L., Flint, L., Syphard, A. D., Moritz, M. A., Buckley, L. B., & McCullough, I. M. (2014). Fine-grain modeling of species' response to climate change: holdouts, stepping-stones, and microrefugia. *Trends in ecology & evolution*, 29(7), 390-397.

Hansson, A., Dargusch, P., & Shulmeister, J. (2021). A review of modern treeline migration, the factors controlling it and the implications for carbon storage. *Journal of Mountain Science*, 18(2), 291-306.

Harsch, M. A., Hulme, P. E., McGlone, M. S., & Duncan, R. P. (2009). Are treelines advancing? A global meta-analysis of treeline response to climate warming. *Ecology letters*, 12(10), 1040-1049.

Hessburg, P. F., Agee, J. K., & Franklin, J. F. (2005). Dry forests and wildland fires of the inland Northwest USA: contrasting the landscape ecology of the pre-settlement and modern eras. *Forest Ecology and Management*, 211(1-2), 117-139.

Haugo, R. D., Kellogg, B. S., Cansler, C. A., Kolden, C. A., Kemp, K. B., Robertson, J. C., ... & Restaino, C. M. (2019). The missing fire: quantifying human exclusion of wildfire in Pacific Northwest forests, USA. *Ecosphere*, 10(4), e02702.

Hu, R., & Tong, S. T. (2022). The use of remotely sensed data to model habitat selections of pileated woodpeckers (Dryocopus pileatus) in fragmented landscapes. *Forest Ecology and Management*, 521, 120433.

Isotta, F. A., Frei, C., Weilguni, V., Perčec Tadić, M., Lassègues, P., Rudolf, B., … & Vertačnik, G. (2014). The climate of daily precipitation in the Alps: Development and analysis of a high-resolution grid dataset from pan-Alpine rain-gauge data. *International Journal of Climatology*, 34(5), 1657–1675.

Johnston, J. D., Schmidt, M. R., Merschel, A. G., Downing, W. M., Coughlan, M. R., & Lewis, D. G. (2023). Exceptional variability in historical fire regimes across a western Cascades landscape, Oregon, USA. *Ecosphere*, 14(12), e4735.

Koerner, W., Dupouey, J. L., Dambrine, E., & Benoit, M. (1997). Influence of past land use on the vegetation and soils of present day forest in the Vosges mountains, France. *Journal of ecology*, 351-358.

Komatsu, K. J., Avolio, M. L., Lemoine, N. P., Isbell, F., Grman, E., Houseman, G. R., ... & Zhang, Y. (2019). Global change effects on plant communities are magnified by time and the number of global change factors imposed. *Proceedings of the National Academy of Sciences*, 116(36), 17867-17873.

Kulakowski, D., Bebi, P., & Rixen, C. (2011). The interacting effects of land use change, climate change and suppression of natural disturbances on landscape forest structure in the Swiss Alps. *Oikos*, 120(2), 216–225.

Larson, A. J., Jeronimo, S. M., Hessburg, P. F., Lutz, J. A., Povak, N. A., Cansler, C. A., ... & Churchill, D. J. (2022). Tamm Review: Ecological principles to guide post-fire forest landscape management in the Inland Pacific and Northern Rocky Mountain regions. *Forest Ecology and Management*, 504, 119680.

LeFevre, M. E., Churchill, D. J., Larson, A. J., Jeronimo, S. M., Bass, J., Franklin, J. F., & Kane, V. R. (2020). Evaluating restoration treatment effectiveness through a comparison of residual composition, structure, and spatial pattern with historical reference sites. *Forest Science*, 66(5), 578-588.

Littlefield, C. E., Dobrowski, S. Z., Abatzoglou, J. T., Parks, S. A., & Davis, K. T. (2020). A climatic dipole drives short-and long-term patterns of postfire forest recovery

in the western United States. *Proceedings of the National Academy of Sciences*, 117(47), 29730-29737.

Loehle, C. (1990). A guide to increased creativity in research - inspiration or perspiration? *Bioscience*, 40, 123-129.

Ludemann, T. (2010). Past fuel wood exploitation and natural forest vegetation in the Black Forest, the Vosges and neighbouring regions in western Central Europe. *Palaeogeography, Palaeoclimatology, Palaeoecology*, 291(1-2), 154-165.

MacDonald, D., Crabtree, J. R., Wiesinger, G., Dax, T., Stamou, N., Fleury, P ... & Gibon, A. (2000). Agricultural abandonment in mountain areas of Europe: Environmental consequences and policy response. *Journal of Environmental Management*, 59(1), 47–69.

Mateo, R. G., Gastón, A., Aroca-Fernández, M. J., Broennimann, O., Guisan, A., Saura, S., & García-Viñas, J. I. (2019). Hierarchical species distribution models in support of vegetation conservation at the landscape scale. *Journal of Vegetation Science*, 30(2), 386-396.

Meli, P., Holl, K. D., Benayas, J. M. R., Jones, H. P., Jones, P. C., Montoya, D., & Mateos, D. M. (2017). A global review of past land use, climate, and active vs. Passive restoration effects on forest recovery. *PLOS ONE*, 12(2), e0171368.

Merschel, A. G., Beedlow, P. A., Shaw, D. C., Woodruff, D. R., Lee, E. H., Cline, S. P., ... & Reilly, M. J. (2021). An ecological perspective on living with fire in ponderosa pine forests of Oregon and Washington: resistance, gone but not forgotten. *Trees, Forests and People*, 4, 100074.

Mietkiewicz, N., Kulakowski, D., Rogan, J., & Bebi, P. (2017). Long-term change in sub-alpine forest cover, tree line and species composition in the Swiss Alps. *Journal of Vegetation Science*, *28*(5), 951–964.

Milanesi, M., Runfola, A., & Guercini, S. (2020). Pharmaceutical industry riding the wave of sustainability: Review and opportunities for future research. *Journal of cleaner production*, 261, 121204.

Naimi, B., Hamm, N. A., Groen, T. A., Skidmore, A. K., & Toxopeus, A. G. (2014). Where is positional uncertainty a problem for species distribution modelling?. *Ecography*, 37(2), 191-203.

Naimi, B., Skidmore, A. K., Groen, T. A., & Hamm, N. A. (2011). Spatial autocorrelation in predictors reduces the impact of positional uncertainty in occurrence data on species distribution modelling. *Journal of biogeography*, 38(8), 1497-1509.

Nguyen, T. A., Kellenberger, B., & Tuia, D. (2022). Mapping forest in the Swiss Alps treeline ecotone with explainable deep learning. *Remote Sensing of Environment*, 281, 113217.

Orlandi, S., Probo, M., Sitzia, T., Trentanovi, G., Garbarino, M., Lombardi, G., & Lonati, M. (2016). Environmental and land use determinants of grassland patch diversity in the western and eastern Alps under agro-pastoral abandonment. *Biodiversity and Conservation*, 25(2), 275–293.

Parks, S. A., Holsinger, L. M., Blankenship, K., Dillon, G. K., Goeking, S. A., & Swaty, R. (2023). Contemporary wildfires are more severe compared to the historical reference period in western US dry conifer forests. *Forest Ecology and Management*, 544, 121232.

Parrott, L. (2017). The modelling spiral for solving 'wicked'environmental problems: Guidance for stakeholder involvement and collaborative model development. *Methods in Ecology and Evolution*, 8(8), 1005-1011

Plue, J., Hermy, M., Verheyen, K., Thuillier, P., Saguez, R., & Decocq, G. (2008). Persistent changes in forest vegetation and seed bank 1,600 years after human occupation. *Landscape Ecology*, 23, 673-688.

Reilly, M. J., Dunn, C. J., Meigs, G. W., Spies, T. A., Kennedy, R. E., Bailey, J. D., & Briggs, K. (2017). Contemporary patterns of fire extent and severity in forests of the Pacific Northwest, USA (1985–2010). *Ecosphere*, 8(3), e01695.

Ripple, W. J., Wolf, C., Newsome, T. M., Barnard, P., & Moomaw, W. R. (2020). World scientists' warning of a climate emergency. *BioScience*, 70, 8–12.

Rousseau, J. S., & Betts, M. G. (2022). Factors influencing transferability in species distribution models. *Ecography*, 2022(7), e06060.

Saulnier, M., Cunill Artigas, R., Foumou, L. F., Buscaino, S., Métailié, J. P., Galop, D., & Py-Saragaglia, V. (2020). A study of late Holocene local vegetation dynamics and responses to land use changes in an ancient charcoal making woodland in the central Pyrenees (Ariège, France), using pedoanthracology. *Vegetation History and Archaeobotany*, 29, 241-258.

Schuwirth, N., Borgwardt, F., Domisch, S., Friedrichs, M., Kattwinkel, M., Kneis, D., ... & Vermeiren, P. (2019). How to make ecological models useful for environmental management. *Ecological Modelling*, 411, 108784.

Seidl, R., Rammer, W., Scheller, R. M., & Spies, T. A. (2012). An individual-based process model to simulate landscape-scale forest ecosystem dynamics. *Ecological Modelling*, 231, 87-100.

Singer, A., Johst, K., Banitz, T., Fowler, M. S., Groeneveld, J., Gutiérrez, A. G., ... & Travis, J. M. (2016). Community dynamics under environmental change: How can next generation mechanistic models improve projections of species distributions?. *Ecological Modelling*, 326, 63-74.

Snethlage, M. A., Geschke, J., Ranipeta, A., Jetz, W., Yoccoz, N. G., Körner, C., ... & Urbach, D. (2022). A hierarchical inventory of the world's mountains for global comparative mountain science. *Scientific data*, 9(1), 149.

Stürck, J., & Verburg, P. H. (2017). Multifunctionality at what scale? A landscape multifunctionality assessment for the European Union under conditions of land use change. *Landscape Ecology*, 32, 481-500.

Suárez-Seoane, S., Virgós, E., Terroba, O., Pardavila, X., & Barea-Azcón, J. M. (2014). Scaling of species distribution models across spatial resolutions and extents along a biogeographic gradient. The case of the Iberian mole Talpa occidentalis. *Ecography*, 37(3), 279-292.

Szabó, P. (2015). Historical ecology: past, present and future. *Biological Reviews*, 90(4), 997-1014.

Wan, J. Z., Wang, C. J., & Yu, F. H. (2017). Spatial conservation prioritization for dominant tree species of Chinese forest communities under climate change. *Climatic Change*, 144, 303-316.

Wang, Z., Ginzler, C., Eben, B., Rehush, N., & Waser, L. T. (2022). Assessing Changes in Mountain Treeline Ecotones over 30 Years Using CNNs and Historical Aerial Images. *Remote Sensing*, 14(9), 2135.

Watson, J. E., Dudley, N., Segan, D. B., & Hockings, M. (2014). The performance and potential of protected areas. *Nature*, 515(7525), 67-73.

Xu, X., Huang, A., Belle, E., De Frenne, P., & Jia, G. (2022). Protected areas provide thermal buffer against climate change. *Science Advances*, 8(44), eabo0119.

Zurell, D., König, C., Malchow, A. K., Kapitza, S., Bocedi, G., Travis, J., & Fandos, G. (2022). Spatially explicit models for decision-making in animal conservation and restoration. *Ecography*, 2022(4).

Chapter 7

Conclusions

The consequences of global environmental changes in forest ecosystems have been observed worldwide at several spatial and temporal scales, from landscape to global assessments. Quantitative predictions are powerful tools for informed decision-making and management, anticipating ecological shifts and preparing for necessary interventions. Therefore, ecologists and practitioners need models that are reliable and informative at different spatial and temporal scales.

The four research papers presented in this thesis stress the essential role that models and scales play in ecological analysis. In particular, they emphasize the effects of different spatial and temporal scales in the accuracy and reliability of models predictions. This thesis calls for a reconsideration of the role of spatial and temporal scales into ecological models. In particular, the research papers emphasize the need for models with an appropriate scale both in terms of spatial and temporal resolution and extent. In long-lasting human-dominated mountain systems such as the Alps, long temporal extent (Chapter 2) and fine spatial resolution (Chapter 3) are needed to assess past and future patterns and consequences of post-abandonment natural reforestation. Moreover, we questioned the reliance on both (i) free-air climate variables with coarse spatial (Chapter 4) and temporal (Chapter 5) resolution as explanatory predictors and (ii) broad (Chapter 4) and static (Chapter 5) species data in species distribution modeling.

The contribution of this research has implications for forest landscape planning, biodiversity conservation, landscape restoration, and landscape change monitoring, particularly when assessing climate and land-use change scenarios. However, some limitations arose during the research. In Chapter 2 we were not able to train spatially explicit models to predict probability of land abandonment and post-abandonment natural reforestation (see for example Gelabert et al., 2022

for reference) because of a lack of metadata from the literature. Chapter 3 represents a single case study and, therefore, the generalizability is limited. Indeed, we expect interesting results from applying the same approach to bigger landscapes or to a set of multiple landscapes. Chapter 4 and 5 suffer from a lack of a cross-scale approach (i.e., hierarchical approaches). Indeed, this approach showed interesting and useful results in species distribution models, as showed by Mateo et al. (2019) and Banks-Leite et al. (2022). The same limitation is present in Chapters 2 and 3.

Several promising future applications arise from the four research papers and from the discussed limitations. Combining the insights and approaches we applied in the research process can provide a more holistic perspective on of ecological dynamics. In particular, dealing with land use in species distribution models and future scenarios is often neglected. Carlson et al. (2014) showed the role that this integration can achieve. Microclimate is another trend topic, and useful insights can be provided by the analysis of the buffering effect on climate extremes on post-abandonment natural reforestation. Indeed, land abandonment may be an opportunity for climate change mitigation in many ways that are still overlooked. In conclusion, the main future research that emerges from this thesis is how cross-scale hierarchical models can serve as powerful tools for landscape planning, conservation, and climate change impact assessment.

References

Banks-Leite, C., Betts, M. G., Ewers, R. M., Orme, C. D. L., & Pigot, A. L. (2022). The macroecology of landscape ecology. *Trends in Ecology & Evolution*.

Carlson, B. Z., Georges, D., Rabatel, A., Randin, C. F., Renaud, J., Delestrade, A., ... & Thuiller, W. (2014). Accounting for tree line shift, glacier retreat and primary succession in mountain plant distribution models. *Diversity and Distributions*, *20*(12), 1379-1391.

Gelabert, P. J., Rodrigues, M., Vidal-Macua, J. J., Ameztegui, A., & Vega-Garcia, C. (2022). Spatially explicit modeling of the probability of land abandonment in the Spanish Pyrenees. *Landscape and Urban Planning*, 226, 104487.

Mateo, R. G., Gastón, A., Aroca-Fernández, M. J., Broennimann, O., Guisan, A., Saura, S., & García-Viñas, J. I. (2019). Hierarchical species distribution models in support of vegetation conservation at the landscape scale. *Journal of Vegetation Science*, 30(2), 386-396.